

Investigation of PEPPSI precatalysts for controlled polymerization of π -conjugated polymers from cheap starting materials

Thesis submitted in partial fulfilment of the requirement for a degree of Doctor of Philosophy at the University of London

Benjamin John Groombridge



Acknowledgements

I would firstly like to thank my supervisors, Dr. Igor Larrosa and Dr. Stephen M. Goldup, for giving me the opportunity to carry out the research described in this thesis. Special gratitude to both of you, for the invaluable expert guidance and support during my PhD.

I would like to thank the following people for the words of wisdom and practical input during the course of my PhD: Prof. Mike Watkinson, Dr. Chris Bray, Dr. Joby Winn, Dr. Jamie Lewis, Dr. Catherine Fletcher, Dr. Saidul Islam, Dr. Xacobe Couso Cambeiro, Dr. Nanna Ahlsten, Dr. Paolo Ricci, Dr. Carlos Arróniz, Dr. Sara Preciado, Dr. Francisco Juliá-Hernández, Dr. Josep Cornella, Dr. Tanya Boorman, Dr. Saidul Islam, Robert Bordoli, Ed Neal, Jessica Pancholi, Katrina Krämer, Rachel Grainger, Marco Simonetti, Junfei Luo, Adam Johnston, Gregory Perry and Nicky Willis.

The research described would not have been possible without the fantastic support from both NMR and analytic services in particular Dr. Harold Toms and Dr. Ian Sanders.

Finally, I would like to thank my friends and family for their support and advice throughout my PhD and during the writing up period.

Declaration

I declare that the scientific work presented in this thesis is my own and was carried out in the School of Biological and Chemical Science at Queen Mary, University of London between September 2010 and September 2014. No part of this work has been submitted in support of an application for another degree or qualification at this University or any other institution of learning.

Signature:

Date:

Abstract

Since the discovery of catalyst-transfer polymerization in 2004 there has been significant research into expanding the scope from Kumada couplings of poly-thiophenes mediated by nickel initiators. This thesis presents an investigation toward the synthesis of π -conjugated polymers by the elusive pseudo-living polymerization of chloroarene monomers.

Chapter 1 sets the scene with an in-depth review of chain-growth polymerizations mediated by palladium catalysts. In chapter 2, we report the first examples of exhaustive substitution of poly-chloroarenes in the presence of a deficit of nucleophile in the sp^3 - sp^2 Negishi coupling mediated by PEPPSI-IPr. These experiments demonstrated intramolecular transfer of the active catalyst which is essential for catalyst-transfer polymerization.

Chapter 3 describes the synthesis of the highly active PEPPSI-IPent precatalyst from cheap commercially available starting materials with minimal purification. Subsequently in chapter 4, it was demonstrated that PEPPSI-IPent undergoes exhaustive substitution of poly-chloroarenes in the presence of a deficit of nucleophile in sp^2 - sp^2 Kumada, Negishi and Suzuki cross-couplings.

In chapter 5, optimization of current Kumada polymerization of bromo phenylene-based monomer mediated by PEPPSI-IPr is described. Direct comparison of model reactions and Kumada polycondensation confirmed high selectivity for exhaustive substitution is required to achieve polycondensation in a chain-growth manner. Initial research into catalyst-transfer polycondensation of chloroarene monomers did not achieve polymerization in a chain-growth manner using modified conditions from bromoarene monomers.

Table of Contents

Acknowledgements.....	2
Declaration.....	3
Abstract.....	4
List of abbreviations	11
<u>1.0 Chapter 1 - Introduction</u>	
1.1 Polymers	13
1.2 Statistical terms.....	13
1.3 Synthetic methods.....	15
1.3.1 Step growth polymerizations.....	15
1.3.2 Chain growth polymerizations	17
1.3.2.1 Radical chain growth polymerizations.....	18
1.3.3 Living polymerization.....	20
1.3.3.1 Ionic polymerizations.....	21
1.3.3.2 Chain growth polycondensation	22
1.3.3.3 Coordination polymerization	23
1.4 π -Conjugated polymers.....	24
1.4.1 Selected applications of conjugated polymers	26
1.4.2 Synthesis of conjugated polymers.....	27
1.4.3.1 Discovery of catalyst transfer polycondensation	28
1.4.3.2 Model reactions to identify intramolecular oxidative addition.....	29
1.4.3.3 Mechanism of catalyst transfer polymerization.....	30
1.4.3.4 Examples of Nickel Mediated Catalyst Transfer Polymerization.....	31
1.4.3.3 Scope and limitations of Nickel mediated chain transfer polymerization	33

1.4.4 Palladium and chain growth polymerization	34
1.4.4.1 Model reactions to identify intramolecular oxidative addition with palladium catalysts.....	34
1.4.4.2 Catalyst-transfer polymerizations mediated by palladium catalysts.....	37
1.4.4.3 Overview and outlook.....	42
1.5. Model reactions mediated by PEPPSI-IPr	43
1.6 Chain growth polymerization mediated by PEPPSI-IPr	47
1.7 Aims and Goals.....	48
1.8 References.....	49
<u>2.0 Chapter 2 - Model reactions mediated by PEPPSI-IPr</u>	
2.1 Introduction.....	55
2.2 Addition of functional groups to aryl dibromides.....	55
2.3 Addition of functional groups to aryl dichlorides.....	56
2.4 Competition between aryl chlorides	57
2.5 Poly-halogenated benzenes	59
2.6 Variation in reaction conditions.....	61
2.6.1 Solvent ratio	61
2.6.2 Temperature scan	62
2.6.3 Equivalents of 1,3-dichlorobenzene	63
2.6.4 Catalyst loading.....	64
2.6.5 Time Scan.....	64
2.7 Conclusions.....	65
2.8 References.....	66
<u>3.0 Chapter 3 - PEPPSI-IPent synthesis</u>	
3.1 Introduction.....	68

3.2 Negishi coupling of 3-pentylzinc bromide	70
3.3 Route 1: Synthesis of aniline 33d	72
3.4 Route 2: Synthesis of aniline 33d	74
3.5 PEPPSI-IPent synthesis	76
3.6 Conclusion	77
3.7 References.....	79
<u>4.0 Chapter 4 - Model reactions mediated by PEPPSI-IPent</u>	
4.1 Introduction.....	82
4.2 Comparison of PEPPSI-IPr and -IPent precatalysts	82
4.2.1 sp^3 - sp^2 Negishi couplings comparing PEPPSI-IPr v PEPPSI-IPent	82
4.2.2 sp^2 - sp^2 Kumada coupling PEPPSI catalyst scan of 1,4-dichlorobenzene	83
4.3 Electrophile scope.....	84
4.3.1 Regioisomers of dichlorobenzene	85
4.3.2 Substituted meta-dichlorobenzenes.....	85
4.3.3 Regioisomers of dichloroanisole.....	86
4.3.4 Polychlorobenzenes.....	87
4.4 Nucleophile scope.....	88
4.4.1 Grignard scope	88
4.4.2 Other sp^2 - sp^2 couplings	90
4.7 References.....	90
4.5 Monomer substrates	91
4.5.1 Kumada couplings.....	91
4.5.2 Suzuki and Negishi couplings of monomer derivatives.....	92
4.6 Conclusions.....	93

6.2.1 General remarks	115
6.2.2 General procedures.....	115
6.2.3 Starting material synthesis	117
6.2.4 Experimental Data.....	118
6.2.5 Variation in reaction conditions	141
6.3 Chapter 3 Experimental	142
6.3.1 Attempted synthesis of 33d	142
6.3.2 Route 1: Synthesis of aniline 33d.....	144
6.3.3 Route 2: Synthesis of aniline 33d.....	145
6.3.4 PEPPSI-IPent synthesis.....	148
6.3.5 Graphical NMR Data for all novel compounds	152
6.4 Chapter 4 Experimental	154
6.4.1 General Remarks	154
6.4.2 General Procedures	154
6.4.3 Synthesis of Starting Materials	155
6.4.4 Experimental Data.....	159
6.4.5 Graphical NMR Data for all novel compounds	184
6.5 Chapter 5 Experimental	198
6.5.1 General Remarks	198
6.5.2. Coupling of PhMgBr and di bromide 76 mediated by PEPPSI precatalysts	198
6.5.3 Kumada polymerization procedures.....	198
6.5.3.1. Monomer synthesis procedures.....	198

6.5.3.2. Polymerization procedure	199
6.5.3 Kumada polymerization experiments.....	200
6.5.3.1 Catalyst loading scan	200
6.5.3.2 Polymerization of different monomer synthesis procedures	200
6.5.4.3 Addition of additives.....	200
6.5.3.4 Polymerization of monomer 74 mediated by PEPPSI precatalysts	201
6.5.4.5 Block homo-polymerizations.....	202
6.5.4 Suzuki polymerization procedures	203
6.5.5 Negishi polymerization procedure	205
6.5.6 Synthesis of novel starting material	206
6.5.7 Chloride monomer polymerization procedure	208
6.6 References.....	209

List of abbreviations

δ	Chemical shift
DMF	N.N'-Dimethylformamide
Equiv.	Equivalents
GPC	Gel Permeation Chromatography
h	Hours
HRMS	High Resolution Mass Spectrometry
Hz	Hertz (frequency)
IR	Infrared
<i>J</i>	Coupling constant (¹ H NMR)
M	Molar
min	Minutes
mmol	Millimolar
M _n	Number average molecular weight
M _w	Weight average molecular weight
m/z	Mass-to-charge ratio
NMR	Nuclear Magnetic Resonance
PDI	Polydispersity index
rt	Room temperature
sat.	Saturated
THF	Tetrahydrofuran

Chapter 1 - Introduction

1.1 Polymers

Polymers are large molecules that consist of repeating units, called monomers. Their existence was first recognised in 1832 by Berzelius upon the discovery of compounds with the same proportionate composition but a different number of constituent atoms. Polymers include a broad range of macromolecules from biopolymers, such as DNA and proteins essential for life, to synthetic organic polymers such as Nylon and Kevlar which are used as functional materials.^{1,2}

Over the past century synthetic organic polymers have transformed the world we live in: they are used in everyday life by almost everyone on the planet. Their emergence has been driven by the economics and natural resources becoming scarcer and the discovery of oil for cheap starting materials. To put the importance of synthetic polymers into perspective there were 288 million tonnes of plastics produced worldwide in 2012 alone. The functional physical properties of polymers arise from their macromolecular structure which monomers and short oligomers do not possess.³

Synthetic organic polymers have not just replaced old materials but have led to advancements in a wide range of fields, from aerospace⁴ to medical applications.^{5,6} These novel technologies arose from improved materials, synthesized from new substrates or synthetic methods.

1.2 Statistical terms

There are numerous methods to synthesize polymeric materials with most polymerizations resulting in a molecular weight distribution, where not all polymer chains

have the same number of repeating units. Polymers of the same monomer but a different number of repeating units can have very different physical properties.

Instead of reporting the highest and lowest number of repeating units, statistical averages are used to report the molecular mass of the polymer sample. For this data the distribution of polymer chain lengths is calculated. The degree of polymerization (X_n) is used to describe the number of repeating units (n) in a polymer chain.

The number average molecular mass (M_n) and the mass average (M_w) are used to calculate the average molecular weight and mass distribution of polymer chain lengths, where N_i is the number of molecules with i repeating units and M_i is the molecular weight of the repeating unit (Figure 1, Eq. 1 and 2). The distribution of polymer chain lengths is quantified by the polydispersity index (PDI, Figure 1, Eq. 3). If all polymer chains are the same length then $M_w/M_n = 1.0$ and the number increases the broader the distribution of polymer chain lengths.

Figure 1. Statistical molecular weight of polymer samples and relative dispersity

$$M_n = \frac{\sum N_i \times M_i}{\sum N_i} \quad (\text{Eq. 1}) \quad M_w = \frac{\sum N_i \times M_i^2}{\sum N_i \times M_i} \quad (\text{Eq. 2}) \quad \text{PDI} = \frac{M_w}{M_n} \quad (\text{Eq. 3})$$

There are various methods of measuring both M_n and M_w , such as end group analysis, light scattering, sedimentation, viscosity and ultracentrifugation. The most convenient method for obtaining both M_n and M_w is using high performance gel permeation chromatography. This method uses size exclusion chromatography to separate polymer chains of different length and compares them to a standard. The standard is preferably monodisperse polymer chains of similar polymer architectures. The larger polymer chains have the weakest interaction with the solid phase and elute first, detected using an ultraviolet light or refractive index detector. The chromatogram is analysed in reference

to a standard to calculate the M_n and M_w , from which the polydispersity can be calculated.²

1.3 Synthetic methods

Typically, polymers in nature are synthesized by condensation polymerization where monomers are added to the end of a growing polymer chain, all stopping at an exact length, for example DNA synthesis mediated by DNA polymerase. The synthesis is extremely sophisticated and current synthetic methods need to be improved to match nature's complexity.⁷

The synthesis of organic polymers is divided into two distinct methods: step- and chain-growth polymerizations.

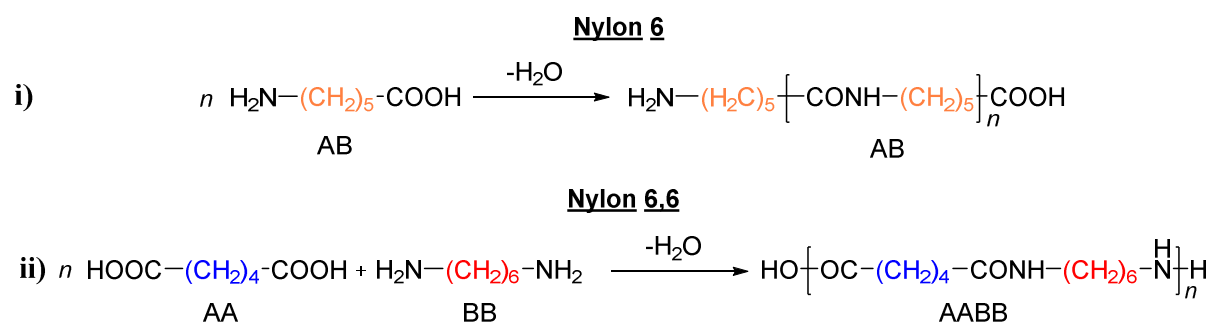
1.3.1 Step growth polymerizations

Step growth polymerizations are typically condensation reactions where monomers are covalently linked, for example by ester, amide and carbonate linkages. In step growth polymerizations there is only one reaction mechanism for polymer formation. Any monomer, oligomer or polymer present can react to grow a polymer chain.

Step growth polymerization of linear polymers can occur in two ways. Either from a monomer with both functional groups needed for polymerization at either end of a monomer (AB monomer), or with two different monomers with the same functional group needed for polymerization at both ends of the monomer (AA and BB monomers).⁸ For example, Nylon 6 is synthesized by polycondensation of a monomer with both amine and acid functional groups (AB polymerization, Scheme 1, i). Whereas, Nylon 6,6 is

synthesized by polycondensation of diacid (AA) and diamine (BB) monomers (AABB polymerization, Scheme 1, ii).²

Scheme 1. Step growth polymerization of Nylon 6,6 and Nylon 6.



First described by Carothers and Flory,⁹⁻¹¹ the assumption that the functional groups of a monomer and polymer show the same reactivity means that the synthesis of high molecular weight polymers requires excellent conversion. For example, a degree of polymerization (X_n) of 100 repeating units cannot be obtained unless the reaction exceeds a 99% conversion to polymer ($p = 0.99$, Figure 2).

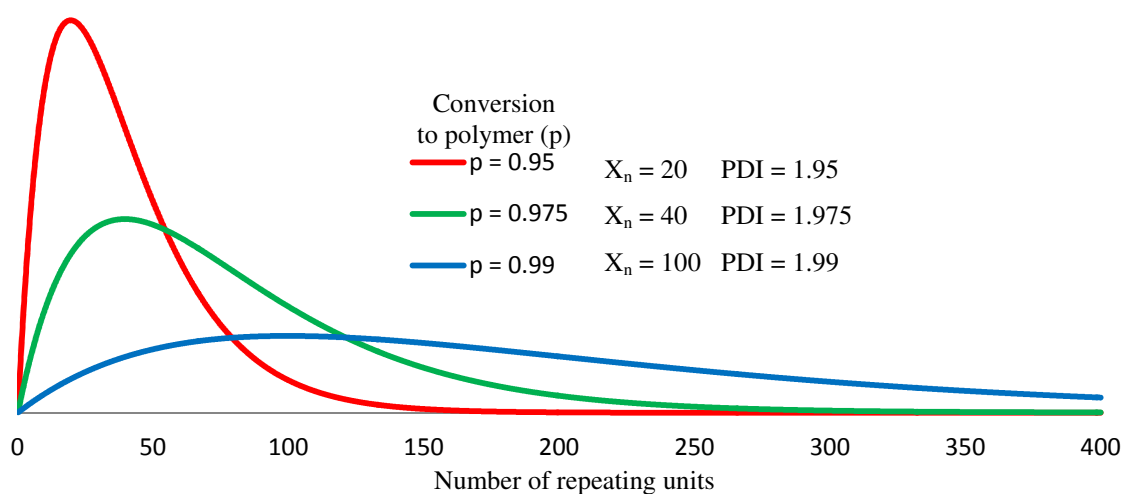
Figure 2. Statistical degree of polymerization and distribution with respect to conversion to polymer

$$X_n = \frac{1}{1-p} \text{ where } p = \frac{\text{number of functional groups that have reacted}}{\text{number of functional groups originally present}}$$

$$\text{and if } p = 0.99; X_n = \frac{1}{1-0.99} = 100; \frac{M_w}{M_n} = 1 + p = 1.99$$

Step growth polymerization methods result in a wide distribution of polymer lengths. Even at 99% conversion to polymer ($p = 0.99$) the PDI cannot be lower than 1.99. The distribution of polymer chain lengths is shown in Graph 1.

Graph 1. Distribution of polymer chain length with regard to conversion to polymer (p)



The statistical distributions described for AABB polymerizations are true only if both monomers are in an exact 1:1 ratio. A small excess of one monomer over the other reduces the maximum possible degree of polymerization dramatically. As little as 2% excess of one monomer limits the maximum possible degree of polymerization from infinity to 49 repeating units.¹²

Despite the uncontrolled nature of step growth polymerizations it has led to the synthesis of many important materials produced on multi-tonne scale and used worldwide, such as Nylon and Kevlar.

1.3.2 Chain growth polymerizations

Unlike step growth polymerizations there is more than one mechanism involved in chain growth polymerizations. There are four possible stages of polymerization: initiation, propagation, chain transfer and termination.

The initiation step generates a reactive species; this is followed by propagation where monomers sequentially extend a long polymer chain whilst retaining its reactive end

group. Subsequently the growing polymer chain undergoes chain transfer and/or termination, where the reactive end group is deactivated.

There are six main types of chain growth polymerization: radical, anionic, cationic, coordination, chain growth polycondensation and catalyst transfer polycondensation.

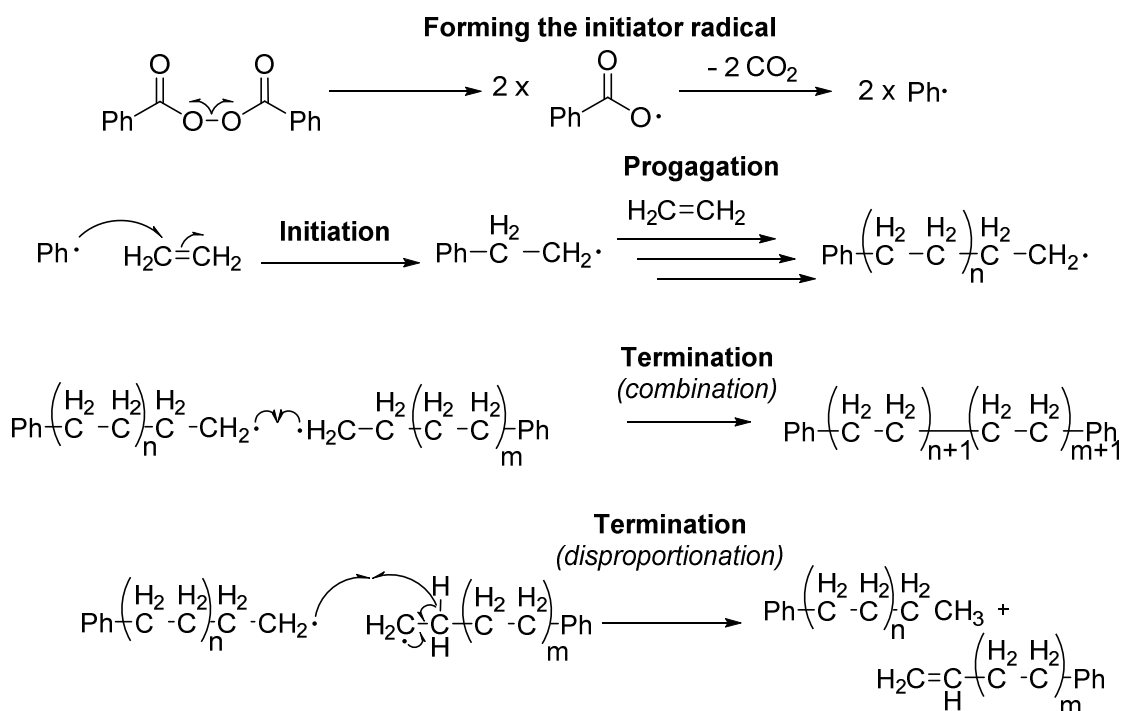
1.3.2.1 Radical chain growth polymerizations

1.3.2.1.1 Uncontrolled radical polymerization

Radical polymerizations form long polymer chains quickly as the rate of propagation is much faster than the rate of initiation and termination. In this short period of time a polymer chain will typically grow to 1000 repeating units, much higher than can feasibly be achieved *via* a step growth mechanism.

These steps are shown in the simplified synthesis of polyethylene from a benzoyl peroxide initiator (Scheme 2). The initiating radical, which is formed by the homolytic cleavage of the peroxide bond by heat or UV light, attacks the ethene monomer converting the C=C double bond into a single bond with the radical at the terminus. This radical attacks a further ethylene monomer and the process is repeated (propagation). This continues chain growth until termination by combination or disproportionation.

Scheme 2. Radical polymerization of polyethylene.



This type of radical polymerization results in a broad molecular weight distribution because of the uncontrolled nature of initiator formation and termination of growing polymer chains.

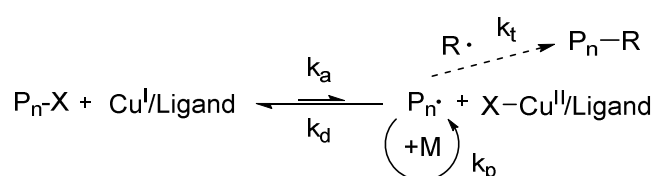
1.3.2.1.2 Controlled radical polymerization

Advancements in the field of radical polymerization have led to greater control of the polymer chain growth, resulting in a narrower distribution of chain lengths ($M_w/M_n < 1.5$). Controlled radical polymerization systems that have been developed are stable free radical polymerization (SFRP),¹³ atom transfer radical polymerization (ATRP)¹⁴ and reversible addition-fragmentation chain transfer polymerization (RAFT).¹⁵ Their control comes from creating a very low steady state concentration of radicals to reduce radical-radical interactions and therefore the rate of termination and other side reactions.

For example, ATRP exploits reversible halogen exchange between the propagating polymer radicals and an inorganic catalyst, typically a transition metal complex. This

equilibrium generates a low steady-state concentration of radical to help suppress the unwanted pathway of irreversible termination. The most commonly applied catalysts are Cu(I)X salts with bidentate or tridentate nitrogen ligands. The organo-halide initiator molecule undergoes homolytic cleavage of a carbon-halogen bond to generate a radical and a Cu(II)X₂ complex. This reaction is under equilibrium with the rate of radical formation (k_a) smaller than the rate of radical deactivation (k_d).

Figure 3. Mechanism for ATRP polymerization



This type of controlled polymerization yields a narrow distribution of molecular weight as well as the ability to influence the length of polymer chains by managing the concentration of monomer relative to initiator (feed ratio). The use of alkyl halides as initiators has created functional end groups on a polymer chain for the synthesis of copolymers and post synthetic polymer functionalization.

1.3.3 Living polymerization

In 1956 Szwarc¹⁶ coined the term ‘living polymerization’ as one that remained active until killed, essentially a system where initiation and propagation are the only two mechanistic steps involved in polymer growth.

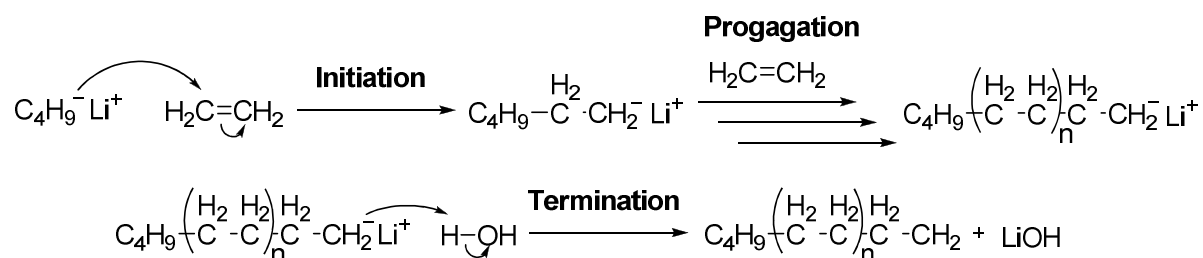
Living polymerizations allow the control over molecular weight of the polymer with a narrow distribution of polymer chain lengths and allow the synthesis of different architectures such as block copolymers. As the end of a polymer chain is still active until termination, end functionalization of the polymer is possible.

Well behaved living polymerizations only need an initiator and monomer; however, the employment of catalysts and chain-end stabilizers is not uncommon. The initiation step must be faster than or equal to the rate of chain propagation to control the molecular weight and ensure a narrow PDI.

1.3.3.1 Ionic polymerizations

The first living polymerization that led to the synthesis of well defined polymers was by Szwarc¹⁶ using anionic intermediates. In contrast to radical polymerization, electrostatic repulsion prevents a combination of two cationic or two anionic growing polymer chains. In the absence of a terminating agent, chain growth polymerization continues until all the monomer units are consumed. This allows the addition of another monomer to synthesize a block copolymer.

Scheme 3. Living polymerization of ethane to polyethane using butyl lithium initiator



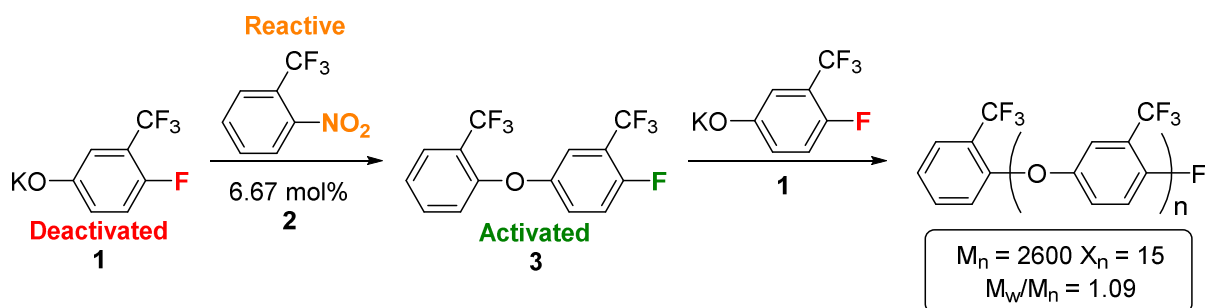
Although a great deal of control of the polymer length and distribution can be achieved, ionic polymerizations need demanding conditions for living conditions to occur. A small amount of air or water can result in unwanted termination steps affecting the polymer length and distribution of molecular weight. Unfortunately, this technique for controlling polymer synthesis has a limited scope in terms of polymer architectures.

1.3.3.2 Chain growth polycondensation

The statistical distributions associated with step growth polycondensations occur under the assumption that the reactivity of the monomer and polymer chains is identical. However, some polycondensations do not follow this rule and, similar to ionic polymerizations, result in controlled polymerization.¹⁷

Kim *et al.*¹⁸ demonstrated chain growth polycondensation of trifluoromethylated phenylene oxide monomer **1** initiated by nitrobenzene **2** (Scheme 4). The alkoxy anion donates electron density to the electrophilic fluorine through the aromatic ring, which deactivates it. The addition of initiator **2** to a much more reactive electrophile leads to the formation of **3**. Subsequently the fluoride on **3** increases in reactivity, due to the absence of an electron donating alkoxy anion and the polymer chain grows in a controlled manner.

Scheme 4. Chain growth polycondensation of monomer **1** initiated by **2**

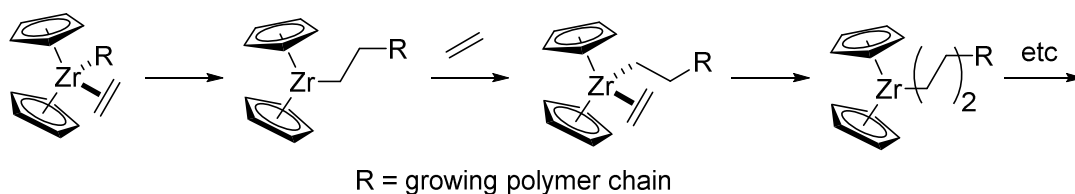


Without the initiator the polycondensation proceeded in a step-growth manner ($M_n = 2000$ Da, PDI = 2.0). The addition of the initiator **2** changed the polymerization to a chain-growth polycondensation showing a linear increase in molecular weight with respect to conversion.

1.3.3.3 Coordination polymerization

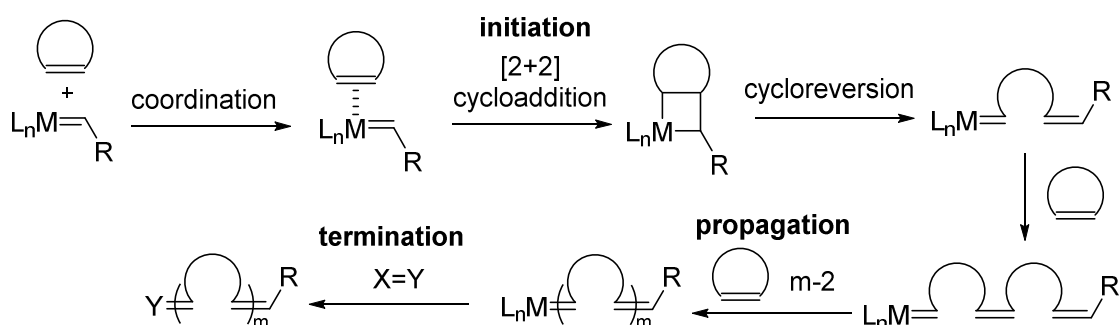
Coordination polymerizations were first developed in the 1950s by Ziegler and Natta who later won the Nobel Prize for chemistry in 1963. Using transition metal compounds (mainly Ti, Zr and V) 1-alkene monomers were polymerized via the Cossee-Arlman mechanism where an intermediate coordination complex contains the alkene monomer and growing polymer chain (Scheme 5). The resulting polymer has very high molecular weight.^{19,20}

Scheme 5. Example of the Cossee-Arlman mechanism for ethene polymerization by a Ziegler-Natta catalyst



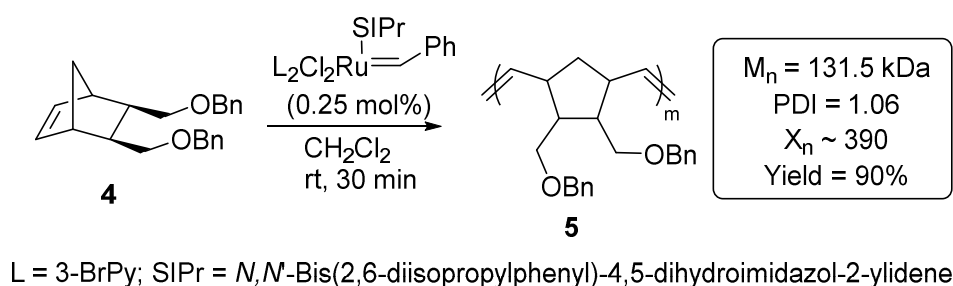
Another type of coordination polymerization is ring-opening metathesis polymerization (ROMP). ROMP converts strained cyclic monomers into linear polymers catalysed by metal alkylidene complexes. The polymerization proceeds in a living manner with the catalyst situated at the end of the growing polymer chain. After fast initiation relative to propagation, the cyclic monomer is added to the end of each growing polymer chain until consumed or the polymerization is quenched (Scheme 6).²¹

Scheme 6. Mechanism of ROMP²¹



In the absence of chain-transfer reactions and fast initiation of the catalyst, great control over the polymer length can be achieved with a narrow distribution of molecular weight ($PDI < 1.1$). Norbornene derivative **4** was successfully polymerized to yield the linear polymer with a long chain length ($M_n = 131.5$ kDa) and a narrow distribution of molecular weight ($PDI = 1.06$) under mild reaction conditions (Scheme 7).²²

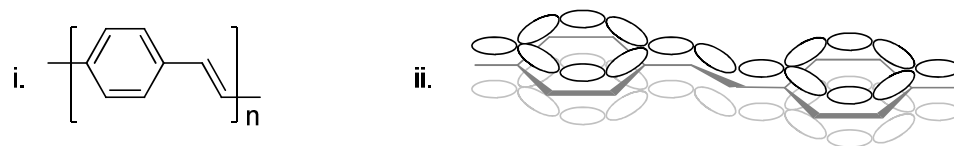
Scheme 7. ROMP of Norbonene **4**²²



1.4 π -Conjugated polymers

The majority of organic polymers, such as polypropylene or polystyrene, are insulators and do not conduct electricity or possess optical properties. Organic polymers that possess a delocalised π -orbital overlap along the polymer backbone are called π -conjugated polymers (Figure 4). They have the ability to conduct electricity acting as one-dimensional semiconductors and can interact with light. These characteristics arise from the energy band gap between the highest occupied molecular π orbital (HOMO) and the lowest unoccupied molecular π orbital (LUMO) which varies between 1.5 eV and 3 eV. Like most silicon and inorganic semi-conductors this energy gap is in the range of visible light and near infrared.^{23,24}

Figure 4: (i) Chemical structure of polyphenylene vinylene; (ii) π electron clouds above and below the carbon backbone.



The first conjugated polymers were unstable under atmospheric conditions. However, over the years chemical modifications have helped with stabilisation and their processibility for applications in electronic devices.

π -Conjugated polymers are used in organic light emitting diodes (OLEDs), organic field effect transistors (OFETs), solar cells and even chemo- and bio-sensing devices. π -Conjugated polymers are alternatives to commonly used inorganic electronic materials. Their ease of synthesis and processing are advantageous over their inorganic counterparts.^{25–27}

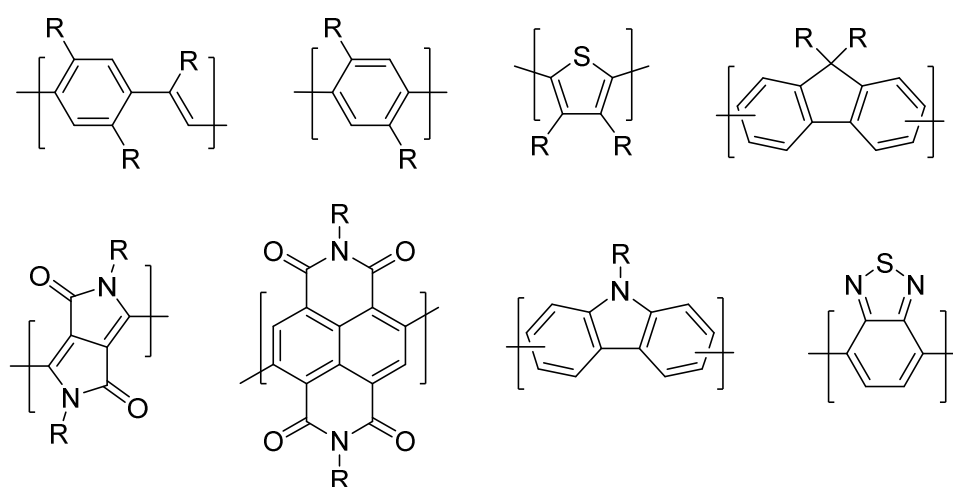
Another desirable property that conjugated polymers have compared to their inorganic equivalents is that they are lightweight and flexible. This creates the potential for the creation of electrical devices not possible from inorganic materials.²⁸

Figure 5. Examples showing the flexibility of polymer OLED^{29,30}



Over the years there has been a significant number of monomer units employed in the synthesis of polymers capable of expressing conductive or optical properties. The functional groups that have received most attention are thiophenes, phenylenes, fluorenes, carbazoles, benzothiazoles, naphthalenes (either as homo- or co-polymers) and graphene (Figure 6).

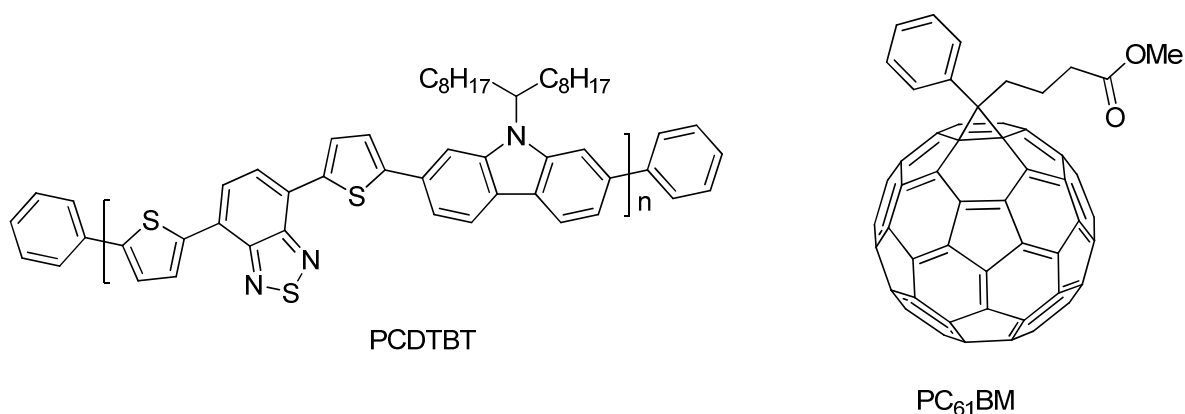
Figure 6. Examples of monomers used in conjugated polymers, where R represents various functional groups³¹



1.4.1 Selected applications of conjugated polymers

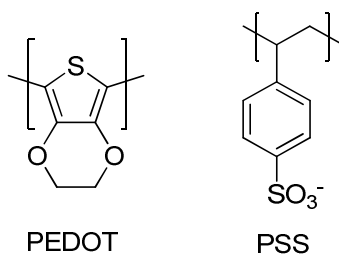
In 2007, Leclerc and co-workers³² constructed a photovoltaic cell based on the polymer poly[N-9'-heptadecanyl-2,7-carbazole-*alt*-5,5'-(4',7'-di-2-thienyl-2',1',3'-benzothiadiazole)] (PCDTBT) blended with [6,6]-phenyl-C₆₁ butyric acid methyl ester (PC₆₁BM) (Figure 7). The resulting solar cell had a power conversion efficiency of 3.6%, which was later improved to 6% by replacing PC₆₁BM with PC₇₁BM.³³ The most efficient organic solar cell has reached 10.6% PCE;³⁴ however this is some way off the world record of 44.7% report by Fraunhofer Institute for Solar Energy Systems ISE.³⁵

Figure 7. Chemical structure of PCDTBT and PC₆₁BM³²



Poly(3,4-ethylenedioxythiophene) (PEDOT) is mixed with poly(styrenesulfonate) (PSS) to form a macromolecular salt, used to create an antistatic layer for photographic films. It is a p-type polymer which undergoes partial oxidation, depopulating the HOMO to form a positive charge (Figure 8). This mixture is produced on multi-ton scale by Bayer and marketed as Baytron®.³⁶

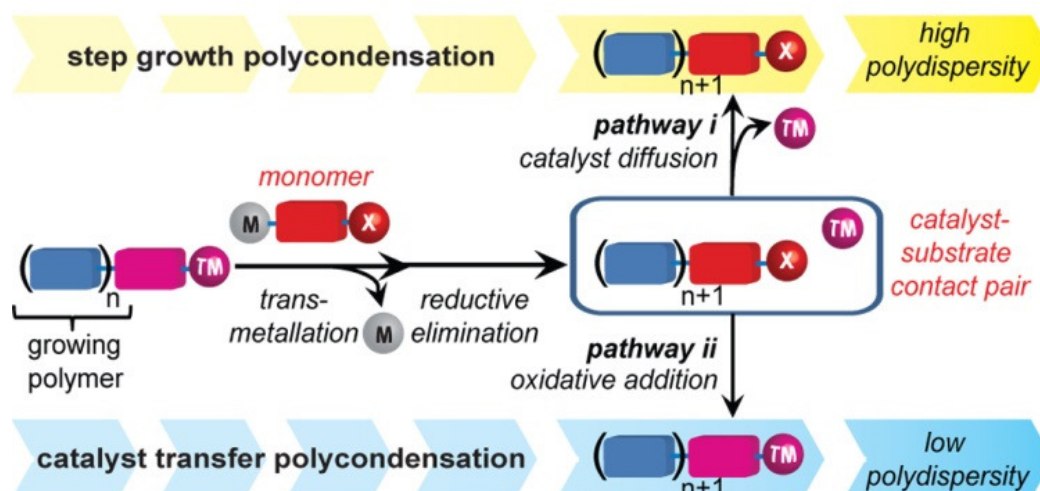
Figure 8. Macromolecular salt PEDOT:PSS



1.4.2 Synthesis of conjugated polymers

A key challenge in tailoring the properties of π -conjugated polymers is to control their detailed structure, in particular their molecular weight and polydispersity. However, transition metal-mediated cross-coupling reactions, the method of choice for the formation of the key Ar-Ar bond, typically result in step-growth polycondensations as the growing polymer chain and the catalyst do not remain associated throughout the catalytic cycle (Scheme 8, pathway i), leading to poor control of these important parameters.^{27,37}

Scheme 8. i) Step-growth and ii) chain-growth mechanisms of transition metal polycondensations

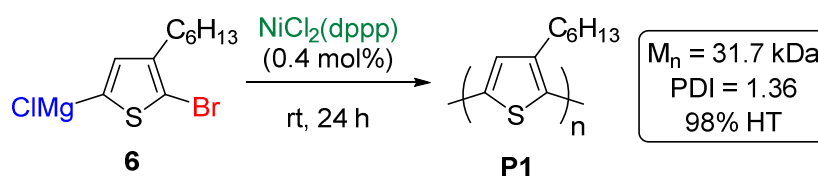


The ability of a transition metal catalyst to undergo oxidative addition to the C-X bond of the growing chain, after reductive elimination, faster than the catalyst and the nascent polymer separate (Scheme 8, pathway ii) leads to a chain growth mechanism and thus greater control over molecular weight and polydispersity. The pseudo-living nature of these systems also allows for the synthesis of conjugated homo- and block-copolymers.

1.4.3.1 Discovery of catalyst transfer polycondensation

Catalyst-transfer polycondensation was first identified independently by McCullough³⁸ and Yokozawa³⁹ in 2004 using a $\text{NiCl}_2(\text{dppp})$ to mediate the synthesis of poly(3-alkylthiophene)s **P1** from an AB monomer **6**.

Scheme 9. Catalyst transfer polycondensation of thiophene-based monomer **6**³⁹



Both reports achieved high molecular weight polymers with a narrow distribution of molecular weight. They demonstrated a linear relationship between the conversion of the

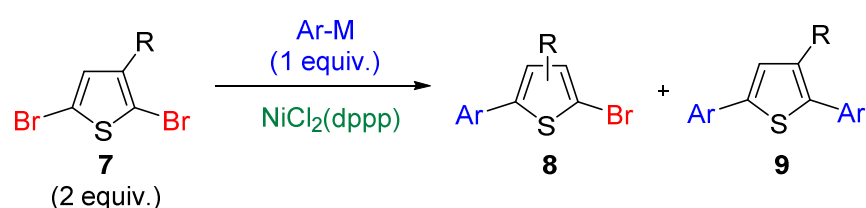
monomer and the M_n showing the polymer chains growing at an equal rate. Also, the PDI appeared independent of the conversion.

Control over the polymer length was achieved by varying the feed ratio ($[\text{Monomer}]/[\text{Catalyst}]$), with a linear change in M_n . The ability to control the feed ratio allowed for specific polymer lengths to be obtained, which was not easily obtainable for step-growth methods. Again, the distribution of molecular weight did not change when the feed ratio was varied.

1.4.3.2 Model reactions to identify intramolecular oxidative addition

McCullough and co-workers were the first to use model reactions to investigate the ability of a catalyst for chain-transfer polycondensation.³⁸ Using two equivalents of dibromothiophene relative to Grignard and organozinc coupling partners, excellent chemoselectivity was observed for di- over mono-substitution (Table 1). The excellent selectivity for **9** over **8** was suspected to be a result of intramolecular oxidative addition of the regenerated Ni(0) catalyst to the other C-Br bond on the same molecule.

Table 1. Model couplings of dibromothiophene **7** with different organometallics³⁸



Entry	R	Ar-M	8:9
1	H		~0:100
2	H		2:98
3	CH ₃		3:97

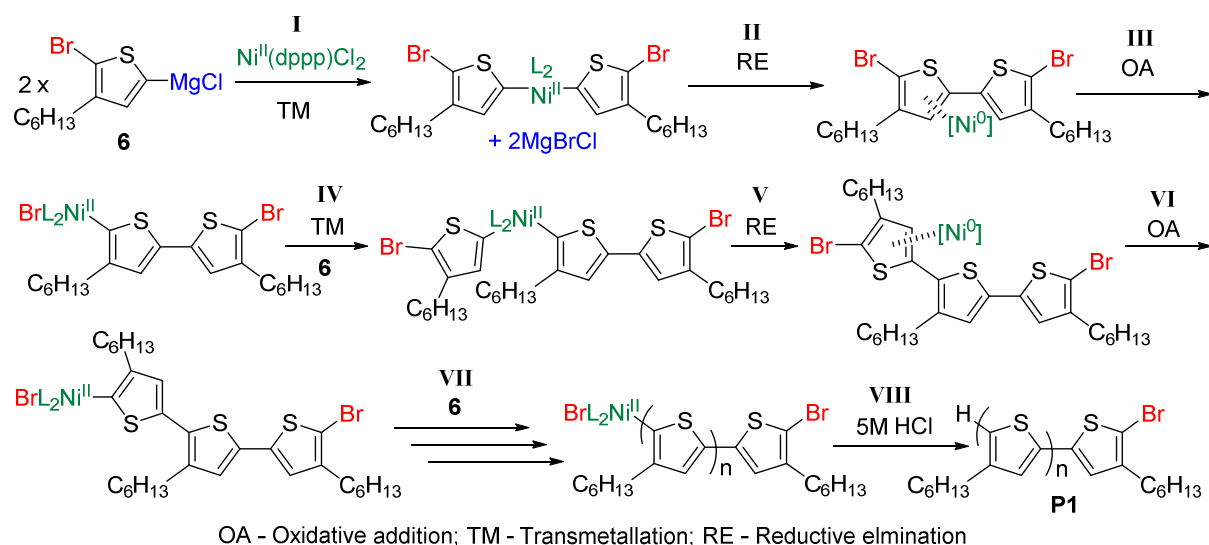
These model reactions helped support the proposed mechanism for catalyst transfer polycondensation whereby by the regenerated Ni(0) catalyst formed an ‘associative pair’ immediately after reductive elimination. This association pair enabled propagation of a single polymer chain as opposed to chain transfer of the catalyst to a different monomer of polymer chain.

1.4.3.3 Mechanism of catalyst transfer polymerization

After significant research there is not a definitive mechanism for the catalyst transfer polycondensation mediated by nickel-bidentate phosphine catalyst system. Both the precedence of π -complexes with nickel and studies by McCullough,⁴⁰ Yokozawa,⁴¹ McNeil,^{42–45} Kiriya^{46,47} and others⁴² provide compelling evidence the associative complex is a π -complex of nickel to the end of the growing polymer chain directing intramolecular oxidative addition.

The nickel catalyst acts as an initiator, where two equivalents of the monomer are consumed to form an ‘association pair’ between the nickel catalyst and start of the growing polymer chain (Scheme 10, i-ii). The Ni undergoes intramolecular oxidative addition to one of the two C-Br bonds (Scheme 10, iii), before transmetallation with a new monomer and reductive elimination, leading to the nickel again becoming coordinated to the aromatic system (Scheme 10, iv-v). This process repeats until all the monomer is consumed and the nickel is trapped at the end of the polymer chain before being cleaved with a strong acid (Scheme 10, vi-viii).

Scheme 10. Mechanism for catalyst transfer polymerization proposed by McCullough and co-workers

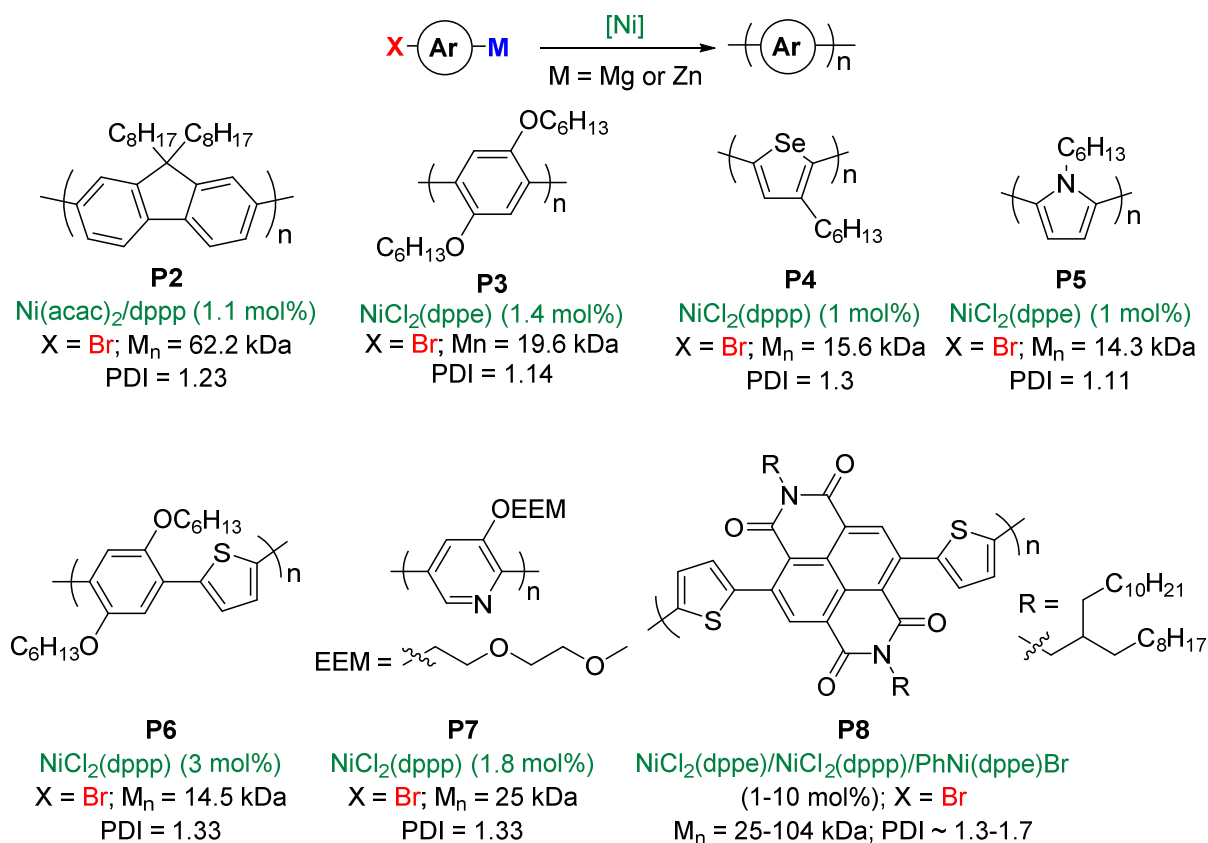


1.4.3.4 Examples of Nickel Mediated Catalyst Transfer Polymerization

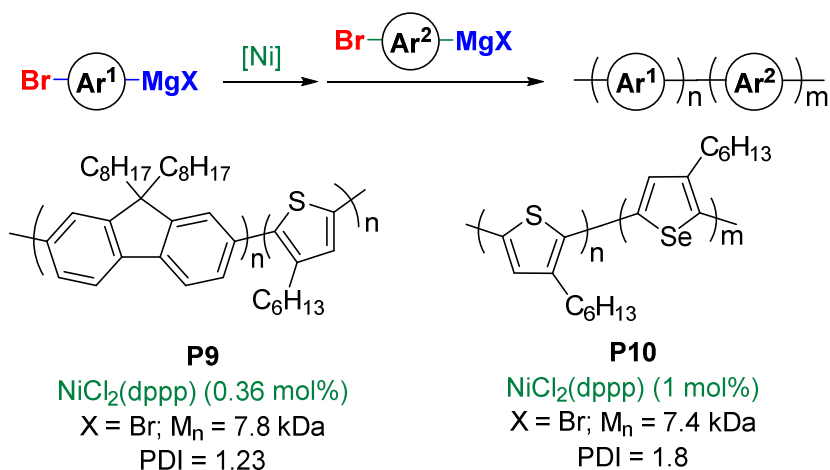
Catalyst transfer polymerizations were not limited to thiophene type monomers. Monomers with phenylene, fluorene, pyrrole, selenophene and other monomers showed polymerizations in a chain growth manner (Scheme 11).

All examples shown in Scheme 11 were synthesized with a low catalyst loading and preceded in a chain-growth manner. Block copolymers could be synthesized by taking advantage of the pseudo-living nature of the polymerizations, examples in Scheme 12. Typically the molecular weight of block copolymers was lower and distribution of polymer chain lengths higher compared to that of their respective homopolymers.

Scheme 11. Scope of nickel mediated chain-growth polycondensations⁴⁸⁻⁵⁴



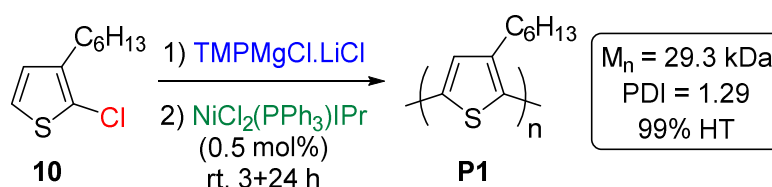
Scheme 12. Examples of block co-polymerizations mediated by nickel catalysts^{50,55}



All the examples above were synthesized from the dehalogenative polycondensation of Grignard monomers with C-Br or C-I bonds. Mori and co-workers demonstrated the significantly more atom efficient dehydrochlorinative polycondensation of thiophene

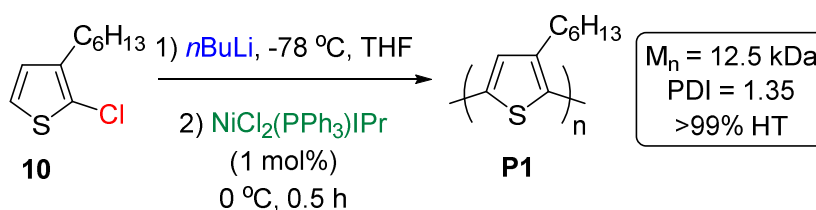
monomer **10** (Scheme 13).⁵⁶ Grignard formation with the Knochel-Hauser base and subsequent polymerization mediated by a nickel catalyst bearing an N-heterocyclic (NHC) ligand preceded in a chain-growth manner.

Scheme 13. Polycondensation of thiophene monomer **10**⁵⁶



Although the PDI was higher than that of previous polycondensations, this example shows a significant step toward the synthesis of conjugated polymers from cheap starting materials. Mori and co-workers showed this approach to work for the Murahashi coupling with lower M_n and higher PDI (Scheme 14).⁵⁷

Scheme 14. Murahashi coupling of thiophene monomer **10**⁵⁷



1.4.3.3 Scope and limitations of Nickel mediated chain transfer polymerization

The degree of control for thiophene-based monomers is very high for Nickel mediated chain transfer polymerisations, but could still benefit from further improvements when more complex monomers or initiators are to be used. Nickel initiators have yet to exhibit control for the polymerization of desirable n-type, low band-gap, and ambipolar conjugated polymers.⁴⁷

1.4.4 Palladium and chain growth polymerization

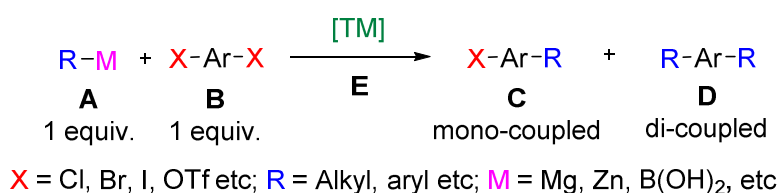
As with the C-C bond formation of aromatics catalysed by Nickel, there are other transition metals that can catalyse such transformations, preeminent among these is palladium.

1.4.4.1 Model reactions to identify intramolecular oxidative addition with transition metal catalysts

First used by McCullough and co-workers³⁸ model reactions can be used to investigate the ability of a catalyst for chain-transfer polycondensation (Table 1).

The model reaction consists of a cross-coupling between one or more equivalents of an aromatic compound with two carbon-halogen (C-X) bonds (Table 2, **B**) and one equivalent of organometallic (Table 2, **A**). Assuming a 100% conversion of the organometallic **A** there are two possible products, mono-coupled (Table 2, **C**) or di-coupled (Table 2, **D**).

Table 2. Simplified model reactions outcomes



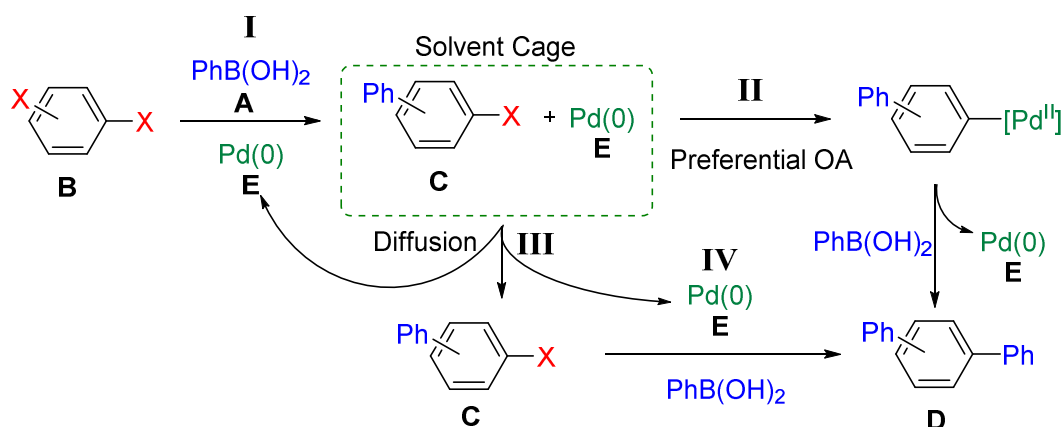
In a simplified model, we would expect a mixture of mono-coupled (**C**) and di-coupled (**D**) products favouring the mono-coupled product (**C**). At the start of the reaction the transition metal catalyst **E** is expected to undergo oxidative addition with another dihalide **B** molecule, because there is a greater concentration of dihalide **B** relative to that of the mono-coupled product (**C**). Also, the dihalide **B** is typically more reactive than the mono-

coupled product (**C**) due to electronic and/or steric effects of replacing an electron withdrawing bromide group with a more electron rich alkyl or aryl group (**R**).

Excellent selectivity for the di-coupled product (**D**) can be achieved by intramolecular oxidative addition of the regenerated transition metal catalyst (**E**) to the other C-X bond on the same molecule.

For example, to achieve di-substituted product selectively in a palladium catalysed Suzuki coupling, after the initial formation of 1-aryl-n-halobenzene ($n = 2, 3, 4$; Scheme 15, **I**) the regenerated Pd(0) catalyst undergoes intramolecular oxidative addition (Scheme 15, **II**). This happens preferentially to diffusion of the Pd(0) catalyst into the reaction solvent after reductive elimination (Scheme 15, **III**). When Pd(0) catalyst **E** diffuses into the reaction solvent it can react with either **B** or **C**. However **B** exhibits higher reactivity than **C**. Therefore if the reaction favours the formation of di-coupled product **D** the reaction di-selective and proceeds through a preferential oxidative addition mechanism (Scheme 15, **II**).

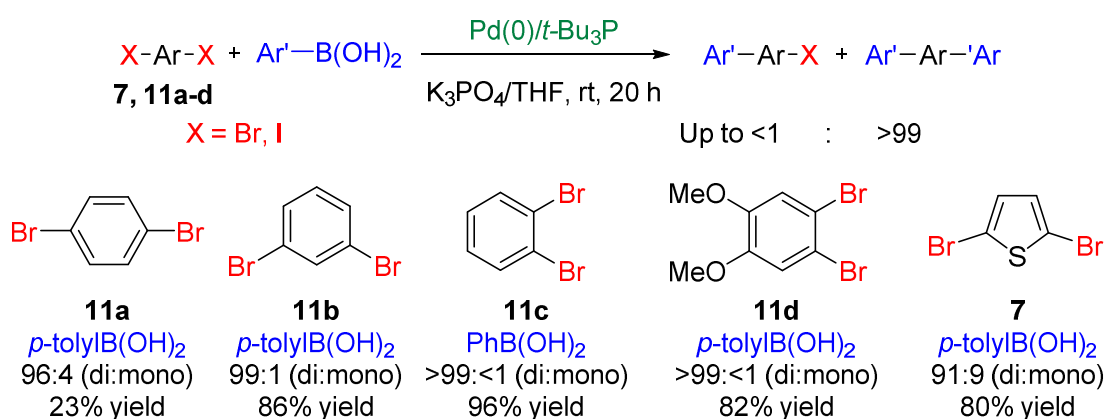
Scheme 15. Mechanism for preferential intramolecular oxidative addition



1.4.4.2 Model reactions to identify intramolecular oxidative addition with palladium catalysts

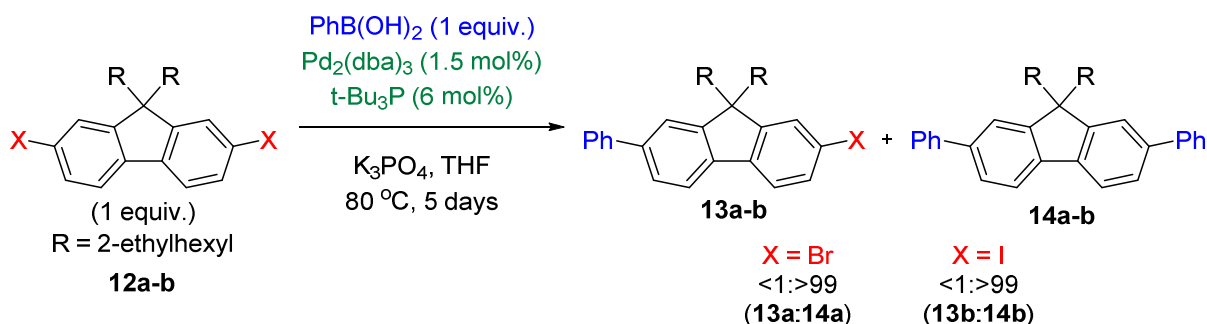
Hu and co-workers⁵⁸ reported excellent di-selective couplings of aryl dibromides and iodides in Suzuki couplings when a 1:1 ratio relative to an arylboronic acid is employed. The selectivity was only observed when the bulky, electron donating P(*t*-Bu)₃ ligand was used. With ligands such as P(Cy)₃, dppe, PPh₃ and Buchwald-type monophosphines either showing poor catalytic activity or a mixture of mono and di-products (Scheme 15).

Scheme 16. Model reactions mediated by Pd(0)/P(*t*-Bu)₃⁵⁸



Preferential oxidative addition was further expanded to from simple substrates to fluorene-based substrates by Scherf and co-workers⁵⁹. Utilizing the Pd(0)/P(*t*-Bu)₃ catalyst system exclusive formation of diarylated coupling product was achieved using model reactions using a 1:1 equivalents of both coupling partners (Scheme 17).

Scheme 17. Model reactions of Fluorene-based monomer⁵⁹



Excellent di-selectivity was obtained when X = Br or I, showing that this type of catalyst system could have been employed to a fluorene-based monomers. Interestingly, when 4-*t*-butylphenylboronic acid instead of phenylboronic acid was used as a coupling partner the majority of products were dehalogenated **12**, with no coupling products observed.

Hu and co-workers⁶⁰ demonstrated that preferential oxidative addition in model Suzuki couplings was not exclusive for the Pd(0)/P(*t*-Bu)₃ catalyst system. Ni(0)/PCy₃ showed excellent chemoselectivity for simple substrates, comparable to those obtained with the Pd(0)/P(*t*-Bu)₃ catalytic system. However, there have been no subsequent reports of Suzuki polycondensation in a chain-growth manner mediated by any nickel catalysts.

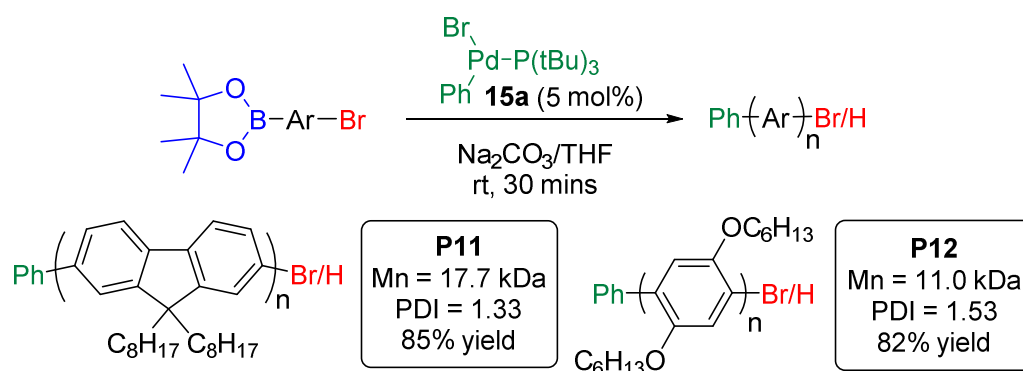
1.4.4.3 Catalyst-transfer polymerizations mediated by palladium catalysts

1.4.4.3.1 Suzuki catalyst- transfer polycondensation

Following the discovery of preferential oxidative addition with a Pd(0)/P(*t*-Bu)₃ catalyst system, Yokozawa and co-workers demonstrated the first polycondensation in a chain-growth manner using a palladium initiator.⁶¹ Using aryl(II)palladium catalyst **15a** as an initiator, fluorene- and phenylene-based monomers were successfully polymerized with a moderate degree of polymerization and a narrow distribution of polymer lengths (Scheme 18).

For the fluorene-based polycondensation, linear relationships in both conversion- M_n and feed ratio- M_n experiments were observed. The PDI remains low, independent of conversion or feed ratio, but increasing slightly at higher conversion and molecular weight (M_n = 20.7 kDa, PDI = 1.51). These experiments paired with MALDI-TOF end group analysis of the polymer chains proved the polymerizations proceeded in a chain-growth manner.

Scheme 18. Suzuki chain-growth polymerization of fluorene- and phenylene-based monomer⁶¹

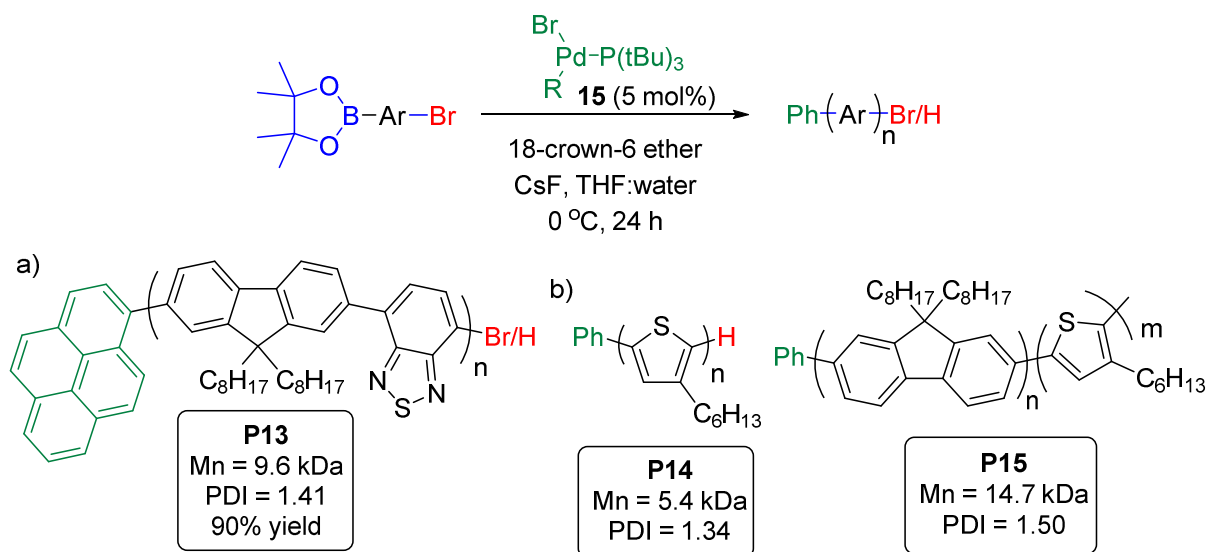


The CGP conditions were utilized by Kiriya and co-workers to graft polyfluorene by first synthesising the aryl(II)palladium initiator **15** bound to the surface before addition of the monomer.⁶²

Huck and co-workers expanded the scope of the Suzuki CGP utilizing *t*-Bu₃PPd(Ar)Br (**15**) initiators taking advantage of the complete incorporation of the aryl group on the initiator to add pyrene to the end of every polymer chain.⁶³ The scope was extended to fluorene *n*-type copolymers in a chain growth manner (Scheme 19, a).

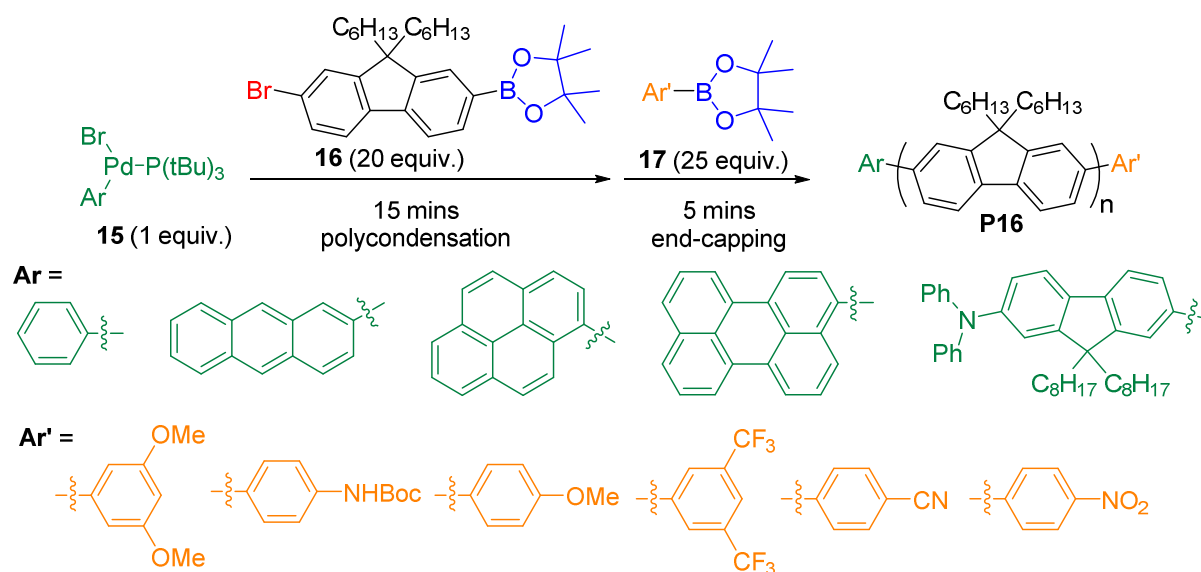
Using the same conditions, Yokowaza and co-workers demonstrated the first chain growth polymerization of thiophene-based monomers and subsequent block co-polymerization with a fluorene-based monomer (Scheme 19, b).⁶⁴ Similar to the first reported Suzuki polymerization, both molecular weights and their distribution were modest.

Scheme 19. Suzuki chain-growth polymerization of other monomers^{63,64}



Huck and co-workers utilized the chain-growth nature of the Suzuki polycondensation mediated by *t*-Bu₃PPd(Ar)Br initiators (**15**) to synthesize heterobis functionalised polyfluorene **P16**. They demonstrated excellent inclusion of the Ar group on the initiator and end-capping with additional boronic esters (Scheme 20).⁶⁵ This allowed for quick access to different functional materials in one pot.

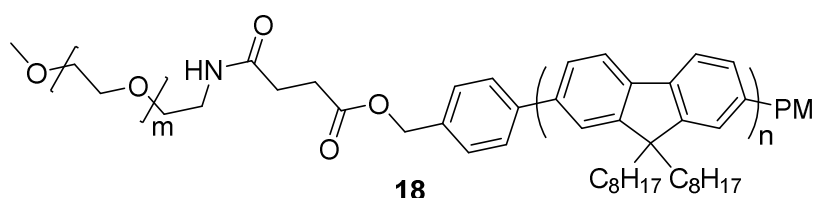
Scheme 20. Synthesis of heterobis functionalised polyfluorene⁶⁵



Although excellent control over end groups was observed conditions for the polymerization were far from optimal. To achieve a low PDI (1.20-1.40) the polymerizations were quenched at approximately 50% conversion as higher conversions led to a broader distribution of molecular weight. This limited the degree of polymerization to approximately 10. Additionally, a large excess of the end-capping reagent was needed to obtain >95% end-capping.

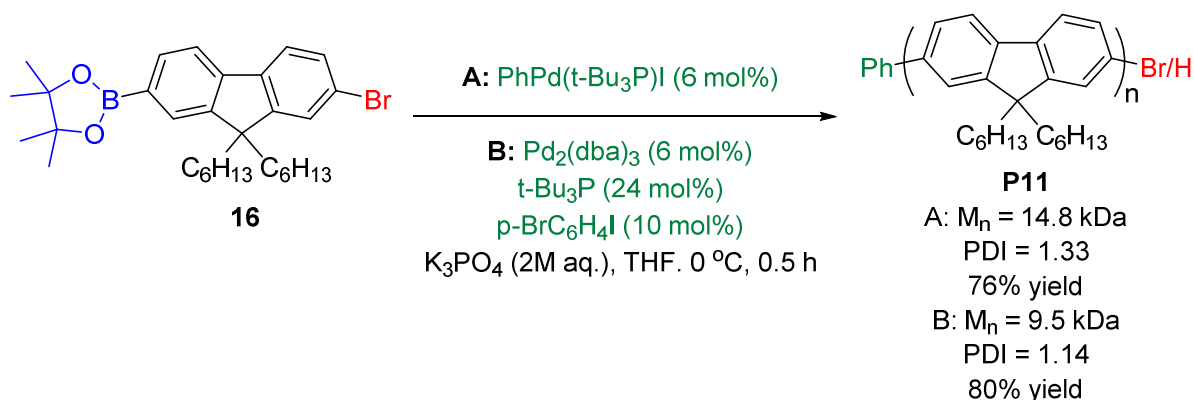
Mecking and co-workers utilized the control of polymer length and molecular weight shown for fluorene polycondensation for the synthesis of luminescent nanoparticles (Figure 9).⁶⁶ Their synthesis takes advantage of the living nature of the chain growth polymerization to end cap the fluorene monomer with a red-emitter. The aryl group on the initiator was subsequently modified to add a PEG group creating the block copolymer. This example shows the importance of CGP for the synthesis of new types of materials.

Figure 9. Nanoparticle synthesized from heterodifunctional Polyfluorene⁶⁶



Although the aryl(II)palladium initiator provides a narrow PDI and modest chain length (Scheme 21, method A), the *in situ* formation of the initiator led to a narrower distribution of molecular weight with the addition of 1-bromo-4-iodobenzene (Scheme 21, method B).⁶⁷ Using method B, the catalyst loading could be reduced to 2 mol% of Pd₂(dba)₃ for a longer chain length ($M_n = 31.4$ kDa) whilst retaining a narrow distribution of molecular weight (PDI = 1.20).

Scheme 21. Polymerization of polyfluorene initiated by in situ formation of aryl(II)palladium⁶⁷



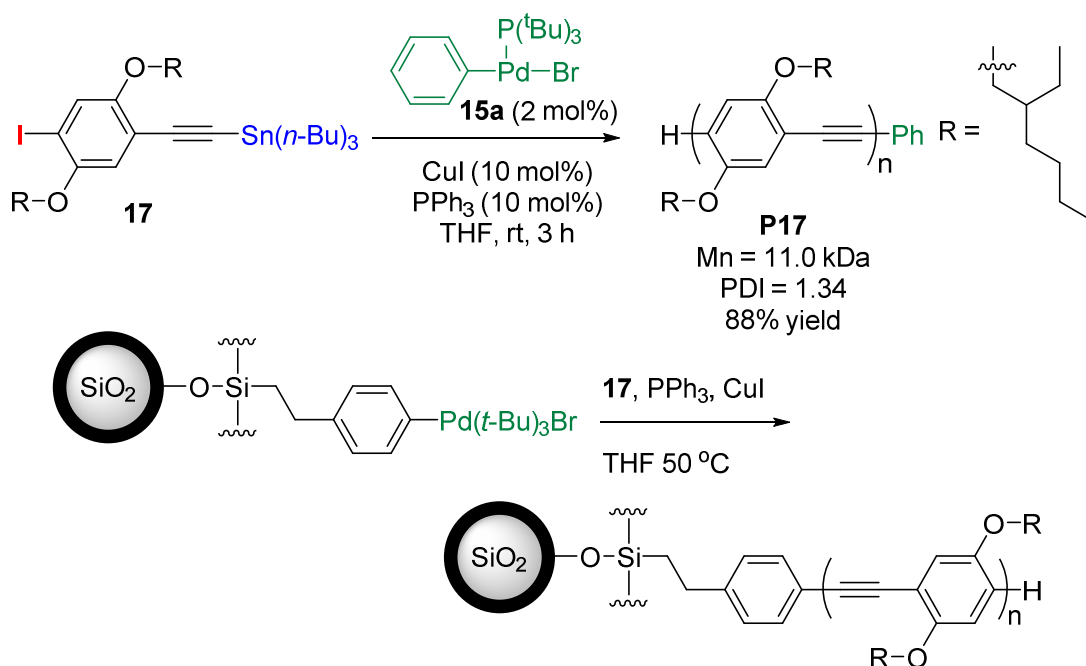
Similar studies into the in situ formation of the palladium initiator by Grisorio et al. resulted in an extremely fast polymerization of fluorene monomer (~1 min).⁶⁸ They demonstrated the importance of the addition of reagents with respect to control of the polymerization. Similar M_n (27.0 kDa) and PDI (1.19) were achieved for *in situ* formation of the Pd(II) initiator.

Both of these examples show the importance to the initiator with regards to control over the polymerization with the chain prorogation steps suspected to be the same.

1.4.4.3.2 Stille polycondensation

Chain growth polymerizations are not limited to sp²-sp² cross-couplings. Bielawski and co-workers demonstrated the polymerization of phenyleneethylene-based monomer **17** with *t*-Bu₃PPd(Ph)Br (**15a**).⁶⁹ The polymerization afforded poly(phenyleneethynylene) with a control over molecular weight and low polydispersity. The polymerization facilitated block co-polymerization with a fluorenyl-based monomer and chain growth from SiO₂ nanoparticles (Scheme 22). The mechanism of intramolecular transfer was not elucidated in this report.

Scheme 22. Synthesis of polyphenyleneethyne in a chain growth manner.⁶⁹



1.4.4.4 Overview and outlook

The initial observation that the $\text{Pd}(0)/\text{P}(t\text{-Bu})_3$ catalyst system undergoes preferential oxidative addition in model reactions was made by Hu and co-workers. Subsequently, Suzuki polycondensation were observed in a chain growth manner. Modest polymer lengths and molecular weight distribution were improved with subtle changes in initiator to yield longer polymer chain lengths and a narrow molecular weight distribution. Chain growth polycondensation mediated by $t\text{-Bu}_3\text{PPd}(\text{Ar})\text{Br}$ has led to examples of block copolymers and graft polymerizations.

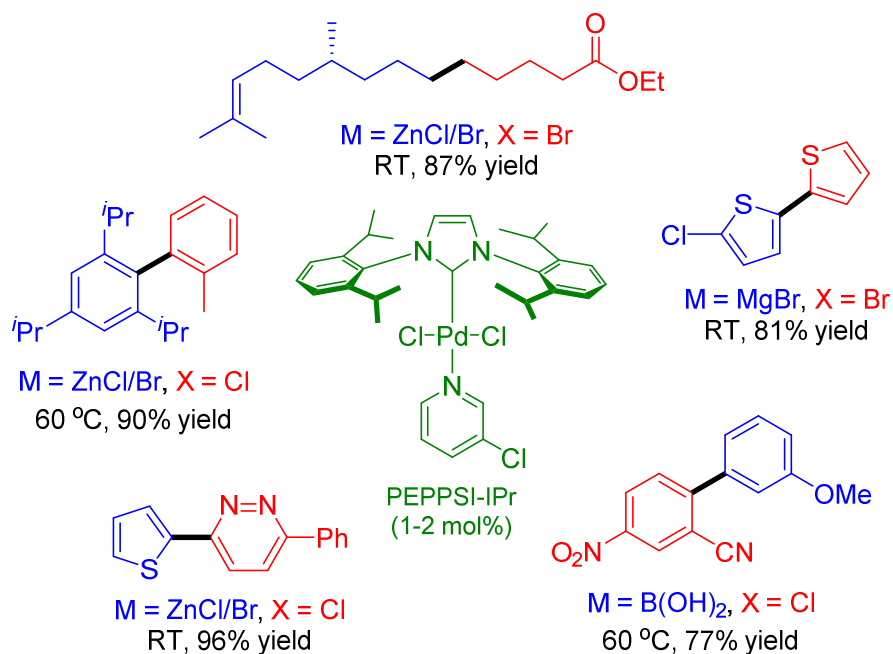
Although $t\text{-Bu}_3\text{PPd}(\text{Ph})\text{Br}$ is stable and easy to handle with control over both end groups of the polymer through different initiators and end capping, the best control over polymerization was obtained when the initiator was synthesized in situ. The $\text{P}(t\text{-Bu})_3$ ligand is difficult to handle as it spontaneously combusts in the presence of oxygen. Polymerization procedures have shown that palladium catalysts show comparable ability to undergo chain growth polymerizations to nickel catalysts in some cases. However, the

search for universal Pd catalyst for chain transfer polycondensation for the synthesis of conjugated polymers continues.

1.5. Model reactions mediated by PEPPSI-IPr

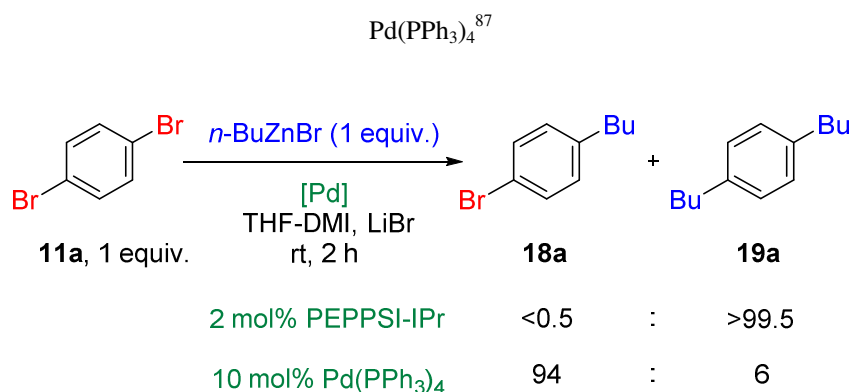
Since their use as spectator ligands for catalysis by Herrmann *et al.*⁷⁰ in 1995, NHCs have recently emerged as important ligands in transition metal catalyzed cross-coupling reactions.^{71–74} Their comparable reactivity to electron rich phosphine ligands has led to a growing number of well defined, isolable NHC-containing palladium complexes.^{75–84} Arguably preeminent among these is the PEPPSI (PEPPSI = pyridine, enhanced precatalyst, preparation, stabilization and initiation) series of catalysts synthesized by Organ *et al.*^{76,79} PEPPSI catalysts show exceptional stability to air and moisture in the solid state and in solution, unlike some commonly used phosphine ligated palladium complexes.⁸⁵ PEPPSI-IPr (IPr = N,N'-diisopropylphenyllimidazolium) was an efficient and versatile catalyst for mediating cross-coupling reactions at low catalyst loading and between challenging coupling partners, such as sterically encumbered biaryls under mild conditions.^{72,76,86}

Figure 10. PEPPSI-IPr and examples of possible cross-couplings



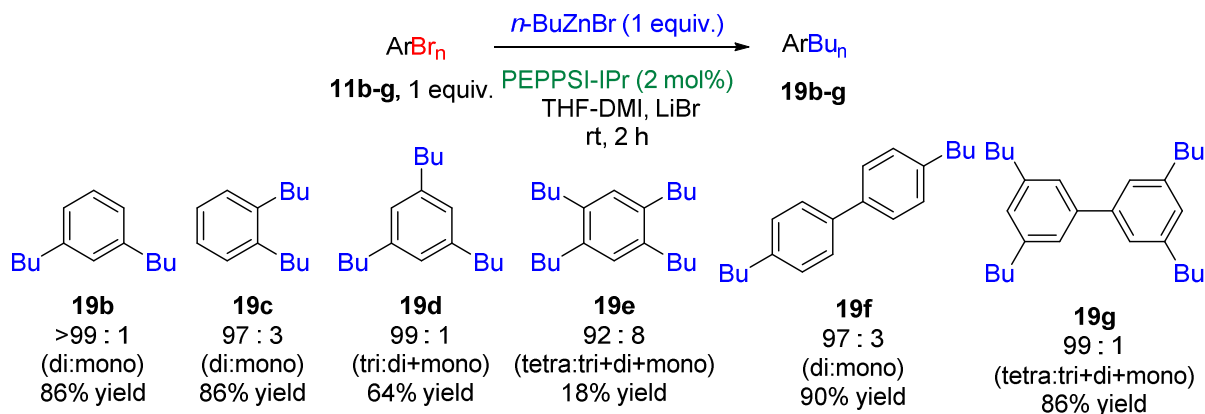
Previous work within the group attempted the monoalkylation of 1,4-dibromobenzene (**11a**) mediated by both PEPPSI-IPr and $\text{Pd(PPh}_3)_4$. One equivalent of n-butylzinc bromide relative to aryl bromide was employed replicating model reaction conditions for preferential oxidative addition (Scheme 23).⁸⁷

Scheme 23. Attempted monoalkylation of 1,4-dibromobenzene (**11a**) mediated by both PEPPSI-IPr and



Excellent selectivity for the di-alkylated product was observed in the Negishi coupling mediated by PEPPSI-IPr. The opposite selectivity was observed when $\text{Pd(PPh}_3)_4$ was used. The scope of this phenomenon was expanded to show excellent selectivity for polyfunctionalization of polybromo aromatic compounds mediated by PEPPSI-IPr (Scheme 24).

Scheme 24. Polyfunctionalization of polybromo aromatic compounds mediated by PEPPSI-IPr.^a

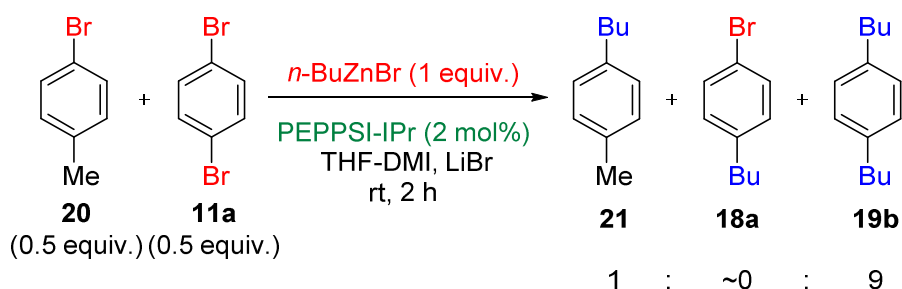


^aRatio of fully-alkylated product relative to other butylated products as determined by GC-MS.

Excellent chemoselectivity could have been obtained in two ways. Preferential intramolecular oxidative addition to the same molecule with the regenerated Pd(0) or the mono-alkylated product being more reactive than the dibromide starting material. To determine which pathway resulted in excellent chemoselectivity a competition reaction

between *p*-bromotoluene (**20**) and 1,4-dibromobenzene (**11a**) was run. *p*-Bromotoluene (**20**) was used to model the mono-alkylated product **18a** as the methyl group would show similar electronic donation to the phenyl ring as the *n*-butyl group on the mono-alkylated product **18a** (Scheme 25).

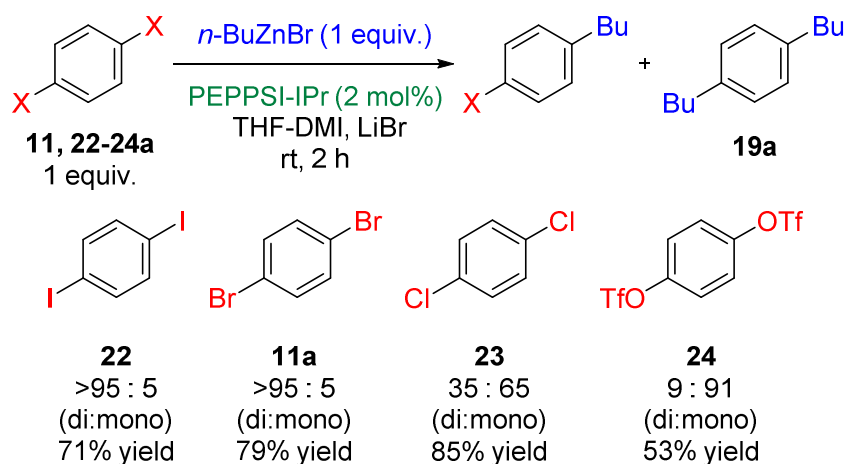
Scheme 25. Competition between **20** and **11a** mediated by PEPPSI-IPr



1,4-Dibromobenzene (**11a**) was more reactive than *p*-bromotoluene (**20**), proving that the preferential oxidative addition of the regenerated Pd(0) to the same molecule led to the selective formation of the di-alkylated product. This observation was rationalised by oxidative diffusion controlled reactivity of the active Pd⁰ species after reductive elimination on the same aromatic ring.⁸⁷ However, an associative pair similar to that for the nickel mediated chain transfer polycondensations could also be mediating excellent chemoselectivity.

The excellent selectivity for the di-alkylation was not limited to aryl bromides. 1,4-diiodobenzene (**22a**) showed excellent di-selectivity for the Negishi cross-coupling with *n*-BuZnBr. However, employment of 1,4-dichlorobenzene (**23a**) to the Negishi cross-coupling displayed low selectivity and 1,4-di(trifluoromethanesulfonyloxy)benzene (**24a**) showed mono-selectivity (Scheme 26).

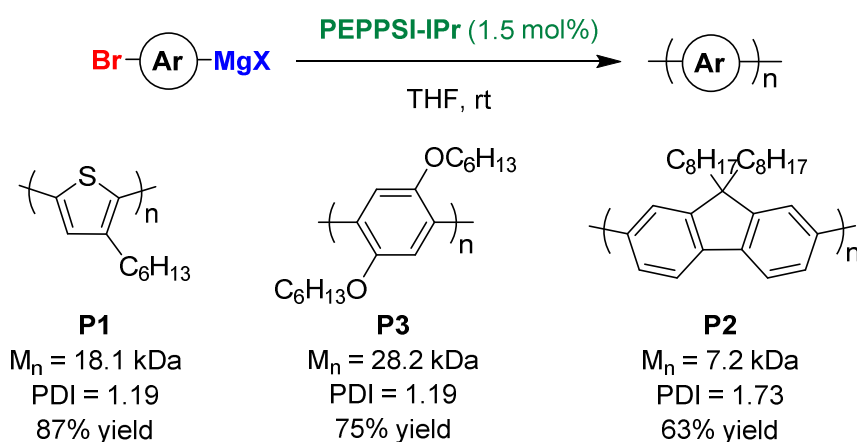
Scheme 26. PEPPSI-IPr Mediated Negishi Cross-Coupling of 1,4-Dihaloarenes



1.6 Chain growth polymerization mediated by PEPPSI-IPr

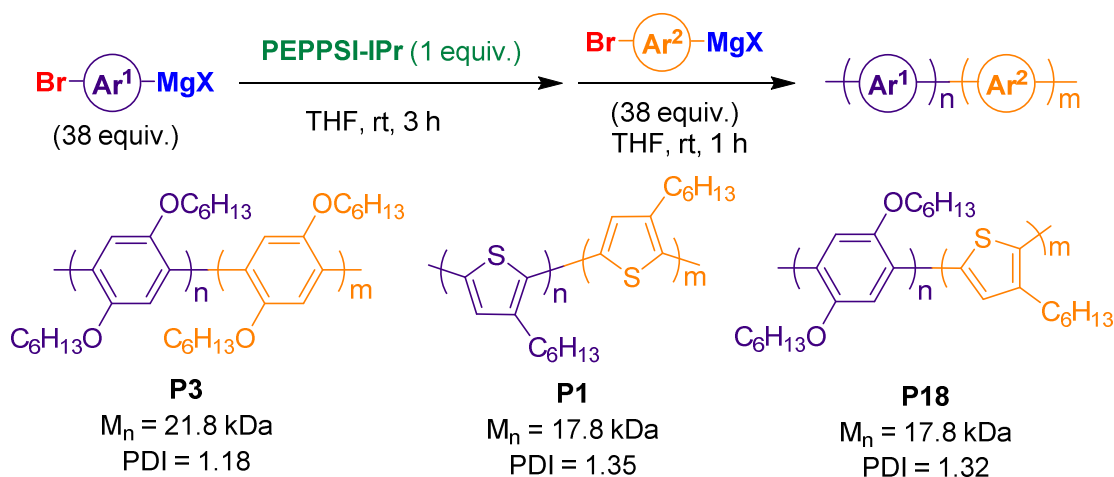
McNeil and co-workers⁸⁸ extended these results to PEPPSI-IPr mediated chain-growth polymerizations of Grignard monomers. The monomers used were both phenylene- and thiophene-based monomers. Unfortunately fluorene-based monomers did not proceed in a living manner (Scheme 27). To the best of our knowledge these results are the best chain growth polymerization conditions described for thiophene- and phenylene-based monomers by palladium catalysts in the literature to date.

Scheme 27. Chain growth polymerization mediated by PEPPSI-IPr



They further demonstrated the PEPPSI-IPr mediated block homo- and co-polymerizations of phenylene- and thiophene-based monomers (Scheme 28).

Scheme 28. Block homo- and co-polymerizations mediated by PEPPSI-IPr



Some chain termination was observed in the block co-polymerizations if the second monomer was not added shortly after the first monomer had been consumed. McNeil and co-workers suggest this is due to the catalyst resting-state at the end of the polymerization being unstable.

1.7 Aims and Goals

We aimed to expand the scope of substrates and conditions of model reactions to explore the limitations of intramolecular catalyst transfer. During these studies we hoped to gain mechanistic insight into the preferential oxidative addition of the regenerated palladium(0) species.

Subsequently, utilizing the lessons learnt from the model reactions we would synthesise relevant monomers and test the ability of PEPPSI-IPr to mediated catalyst-transfer polycondensations to form π -conjugated polymers in a controlled manner.

1.8 References

- (1) Morawetz, H. *Polymers: The Origins and Growth of a Science*; Wiley-Interscience: New York, 1985.
- (2) Walton, D.; Phillip, L. *Polymers*; Oxford University Press Inc.: New York, 2000.
- (3) http://www.plasticseurope.org/documents/document/20131014095824-final_plastics_the_facts_2013_published_october2013.pdf (accessed Sep 23, 2014).
- (4) Williams, J. C.; Starke, E. A. *Acta Mater.* **2003**, *51*, 5775.
- (5) Liechty, W. B.; Kryscio, D. R.; Slaughter, B. V; Peppas, N. A. *Annu. Rev. Chem. Biomol. Eng.* **2010**, *1*, 149.
- (6) Moro, T.; Takatori, Y.; Ishihara, K.; Konno, T.; Takigawa, Y.; Matsushita, T.; Chung, U.-I.; Nakamura, K.; Kawaguchi, H. *Nat. Mater.* **2004**, *3*, 829.
- (7) Alberts, B.; Johnson, A.; Lewis, J.; Raff, M.; Roberts, K.; Walter, P. *Molecular Biology of the Cell, 4th edition*; Garland Science: New York, 2002.
- (8) Stille, J. K. *J. Chem. Educ.* **1981**, *58*, 862.
- (9) Flory, P. J. *Chem. Rev.* **1946**, *39*, 137.
- (10) Carothers, W. H. *J. Am. Chem. Soc.* **1929**, *51*, 2548.
- (11) Flory, P. J. *J. Am. Chem. Soc.* **1936**, *58*, 1877.
- (12) Allcock, H.; Lampe, F.; Mark, J. *Contemporary Polymer Chemistry (3rd Edition)*; Prentice Hall: Englewood Cliffs, New Jersey, 2003.
- (13) Braunecker, W. A.; Matyjaszewski, K. *Prog. Polym. Sci.* **2007**, *32*, 93.
- (14) Patten, T. E.; Xia, J.; Abernathy, T.; Matyjaszewski, K. *Science.* **1996**, *272*, 866.
- (15) Chiefari, J.; Chong, Y. K.; Ercole, F.; Krstina, J.; Jeffery, J.; Le, T. P. T.; Mayadunne, R. T. A.; Meijs, G. F.; Moad, C. L.; Moad, G.; Rizzardo, E.; Thang, S. H. *Macromolecules* **1998**, *31*, 5559.
- (16) Szwarc M. *Nature* **1956**, *178*, 1168.
- (17) Yokozawa, T.; Ohta, Y. *Chem. Commun.* **2013**, *49*, 8281.
- (18) Kim, Y. J.; Seo, M.; Kim, S. Y. *J. Polym. Sci. Part A Polym. Chem.* **2010**, *48*, 1049.

- (19) Cossee, P. *J. Catal.* **1964**, 3, 80.
- (20) Arlman, E. *J. Catal.* **1964**, 3, 89.
- (21) Sutthasupa, S.; Shiotsuki, M.; Sanda, F. *Polym. J.* **2010**, 42, 905.
- (22) Choi, T.-L.; Grubbs, R. H. *Angew. Chemie Int. Ed.* **2003**, 42, 1743.
- (23) Müllen, K.; Reynolds, J. R.; Masuda, T. *Conjugated Polymers*; Royal Society of Chemistry: Cambridge, 2013.
- (24) Leclerc, M.; Morin, J.-F. *Design and Synthesis of Conjugated Polymers*; Wiley-VCH Verlag GmbH & Co. KGaA: Weinheim, Germany, 2010.
- (25) Holliday, S.; Donaghey, J. E.; McCulloch, I. *Chem. Mater.* **2014**, 26, 647.
- (26) Grimsdale, A. C.; Chan, K. L.; Martin, R. E.; Jokisz, P. G.; Holmes, A. B. *Chem. Rev.* **2009**, 109, 897.
- (27) Cheng, Y.-J.; Yang, S.-H.; Hsu, C.-S. *Chem. Rev.* **2009**, 109, 5868.
- (28) Strobl, G. *The Physics of Polymers*; Springer Berlin Heidelberg: Berlin, Heidelberg, 2007.
- (29) <http://www.sumitomo-chem.co.jp/english/pled/about.html> (accessed Sep 23, 2014).
- (30) <http://www.cdtltd.co.uk/technology/displays/> (accessed Sep 23, 2014).
- (31) Guo, X.; Baumgarten, M.; Müllen, K. *Prog. Polym. Sci.* **2013**, 38, 1832.
- (32) Blouin, N.; Michaud, A.; Leclerc, M. *Adv. Mater.* **2007**, 19, 2295.
- (33) Park, S. H.; Roy, A.; Beaupré, S.; Cho, S.; Coates, N.; Moon, J. S.; Moses, D.; Leclerc, M.; Lee, K.; Heeger, A. J. *Nat. Photonics* **2009**, 3, 297.
- (34) You, J.; Dou, L.; Yoshimura, K.; Kato, T.; Ohya, K.; Moriarty, T.; Emery, K.; Chen, C.-C.; Gao, J.; Li, G.; Yang, Y. *Nat. Commun.* **2013**, 4, 1446.
- (35) <http://www.ise.fraunhofer.de/en/press-and-media/pdfs-zu-presseinfos-englisch/2013/press-release-world-record-solar-cell-with-44-7-efficiency.pdf> (accessed Sep 23, 2014).
- (36) Groenendaal, L.; Jonas, F.; Freitag, D.; Pielartzik, H.; Reynolds, J. R. *Adv. Mater.* **2000**, 12, 481.
- (37) Carsten, B.; He, F.; Son, H. J.; Xu, T.; Yu, L. *Chem. Rev.* **2011**, 111, 1493.
- (38) Sheina, E. E.; Liu, J.; Iovu, M. C.; Laird, D. W.; McCullough, R. D. *Macromolecules* **2004**, 37, 3526.

- (39) Yokoyama, A.; Miyakoshi, R.; Yokozawa, T. *Macromolecules* **2004**, *37*, 1169.
- (40) Iovu, M. C.; Sheina, E. E.; Gil, R. R.; McCullough, R. D. *Macromolecules* **2005**, *38*, 8649.
- (41) Miyakoshi, R.; Yokoyama, A.; Yokozawa, T. *J. Am. Chem. Soc.* **2005**, *127*, 17542.
- (42) Bryan, Z. J.; McNeil, A. J. *Macromolecules* **2013**, *46*, 8395.
- (43) Lanni, E. L.; McNeil, A. J. *Macromolecules* **2010**, *43*, 8039.
- (44) Lanni, E. L.; McNeil, A. J. *J. Am. Chem. Soc.* **2009**, *131*, 16573.
- (45) Bryan, Z. J.; McNeil, A. J. *Chem. Sci.* **2013**, *4*, 1620.
- (46) Tkachov, R.; Senkovskyy, V.; Komber, H.; Sommer, J.-U.; Kiriy, A. *J. Am. Chem. Soc.* **2010**, *132*, 7803.
- (47) Kiriy, A.; Senkovskyy, V.; Sommer, M. *Macromol. Rapid Commun.* **2011**, *32*, 1503.
- (48) Sui, A.; Shi, X.; Wu, S.; Tian, H.; Geng, Y.; Wang, F. *Macromolecules* **2012**, *45*, 5436.
- (49) Miyakoshi, R.; Shimono, K.; Yokoyama, A.; Yokozawa, T. *J. Am. Chem. Soc.* **2006**, *128*, 16012.
- (50) Hollinger, J.; Jahnke, A. A.; Coombs, N.; Seferos, D. S. *J. Am. Chem. Soc.* **2010**, *132*, 8546.
- (51) Yokoyama, A.; Kato, A.; Miyakoshi, R.; Yokozawa, T. *Macromolecules* **2008**, *41*, 7271.
- (52) Ono, R. J.; Kang, S.; Bielawski, C. W. *Macromolecules* **2012**, *45*, 2321.
- (53) Nanashima, Y.; Yokoyama, A.; Yokozawa, T. *J. Polym. Sci. Part A Polym. Chem.* **2012**, *50*, 1054.
- (54) Senkovskyy, V.; Tkachov, R.; Komber, H.; Sommer, M.; Heuken, M.; Voit, B.; Huck, W. T. S.; Kataev, V.; Petr, A.; Kiriy, A. *J. Am. Chem. Soc.* **2011**, *133*, 19966.
- (55) Javier, A. E.; Varshney, S. R.; McCullough, R. D. *Macromolecules* **2010**, *43*, 3233.
- (56) Tamba, S.; Shono, K.; Sugie, A.; Mori, A. *J. Am. Chem. Soc.* **2011**, *133*, 9700.
- (57) Fuji, K.; Tamba, S.; Shono, K.; Sugie, A.; Mori, A. *J. Am. Chem. Soc.* **2013**, *135*, 12208.
- (58) Dong, C.-G.; Hu, Q.-S. *J. Am. Chem. Soc.* **2005**, *127*, 10006.

- (59) Weber, S. K.; Galbrecht, F.; Scherf, U. *Org. Lett.* **2006**, 8, 4039.
- (60) Dong, C.-G.; Hu, Q.-S. *Synlett* **2012**, 23, 2121.
- (61) Yokoyama, A.; Suzuki, H.; Kubota, Y.; Ohuchi, K.; Higashimura, H.; Yokozawa, T. *J. Am. Chem. Soc.* **2007**, 129, 7236.
- (62) Beryozkina, T.; Boyko, K.; Khanduyeva, N.; Senkovskyy, V.; Horecha, M.; Oertel, U.; Simon, F.; Stamm, M.; Kiriy, A. *Angew. Chemie Int. Ed.* **2009**, 48, 2695.
- (63) Elmalem, E.; Kiriy, A.; Huck, W. T. S. *Macromolecules* **2011**, 44, 9057.
- (64) Yokozawa, T.; Suzuki, R.; Nojima, M.; Ohta, Y.; Yokoyama, A. *Macromol. Rapid Commun.* **2011**, 32, 801.
- (65) Elmalem, E.; Biedermann, F.; Johnson, K.; Friend, R. H.; Huck, W. T. S. *J. Am. Chem. Soc.* **2012**, 134, 17769.
- (66) Fischer, C. S.; Baier, M. C.; Mecking, S. *J. Am. Chem. Soc.* **2013**, 135, 1148.
- (67) Zhang, H.-H.; Xing, C.-H.; Hu, Q.-S. *J. Am. Chem. Soc.* **2012**, 134, 13156.
- (68) Grisorio, R.; Mastroilli, P.; Suranna, G. P. *Polym. Chem.* **2014**, 5, 4304.
- (69) Kang, S.; Ono, R. J.; Bielawski, C. W. *J. Am. Chem. Soc.* **2013**, 135, 4984.
- (70) Herrmann, W. A.; Elison, M.; Fischer, J.; Köcher, C.; Artus, G. R. J. *Angew. Chemie Int. Ed.* **1995**, 34, 2371.
- (71) Díez-González, S.; Marion, N.; Nolan, S. P. *Chem. Rev.* **2009**, 109, 3612.
- (72) Kantchev, E. A. B.; O'Brien, C. J.; Organ, M. G. *Angew. Chemie Int. Ed.* **2007**, 46, 2768.
- (73) Glorius, F. *N-Heterocyclic Carbenes in Transition-Metal Catalysis*; Springer: Berlin, 2007.
- (74) Hopkinson, M. N.; Richter, C.; Schedler, M.; Glorius, F. *Nature* **2014**, 510, 485.
- (75) Navarro, O.; Kelly, R. A.; Nolan, S. P. *J. Am. Chem. Soc.* **2003**, 125, 16194.
- (76) Organ, M. G.; Abdel-Hadi, M.; Avola, S.; Hadei, N.; Nasielski, J.; O'Brien, C. J.; Valente, C. *Chem. Eur. J.* **2007**, 13, 150.
- (77) Marion, N.; Nolan, S. P. *Acc. Chem. Res.* **2008**, 41, 1440.
- (78) Würtz, S.; Glorius, F. *Acc. Chem. Res.* **2008**, 41, 1523.
- (79) Organ, M. G.; Calimsiz, S.; Sayah, M.; Hoi, K. H.; Lough, A. J. *Angew. Chemie Int. Ed.* **2009**, 48, 2383.

- (80) Fortman, G. C.; Nolan, S. P. *Chem. Soc. Rev.* **2011**, *40*, 5151.
- (81) Chartoire, A.; Lesieur, M.; Falivene, L.; Slawin, A. M. Z.; Cavallo, L.; Cazin, C. S. J.; Nolan, S. P. *Chem. Eur. J.* **2012**, *18*, 4517.
- (82) Sau, S. C.; Santra, S.; Sen, T. K.; Mandal, S. K.; Koley, D. *Chem. Commun.* **2012**, *48*, 555.
- (83) Zhang, Y.; César, V.; Storch, G.; Lugan, N.; Lavigne, G. *Angew. Chemie Int. Ed.* **2014**, *53*, 6482.
- (84) Pompeo, M.; Farmer, J. L.; Froese, R. D. J.; Organ, M. G. *Angew. Chemie Int. Ed.* **2014**, *53*, 3223.
- (85) Fu, G. C. *Acc. Chem. Res.* **2008**, *41*, 1555.
- (86) Organ, M. G.; Avola, S.; Dubovyk, I.; Hadei, N.; Kantchev, E. A. B.; O'Brien, C. J.; Valente, C. *Chem. Eur. J.* **2006**, *12*, 4749.
- (87) Larrosa, I.; Somoza, C.; Banquy, A.; Goldup, S. M. *Org. Lett.* **2011**, *13*, 146.
- (88) Bryan, Z. J.; Smith, M. L.; McNeil, A. J. *Macromol. Rapid Commun.* **2012**, *33*, 842.

Chapter 2 – Model reactions mediated by PEPPSI-IPr

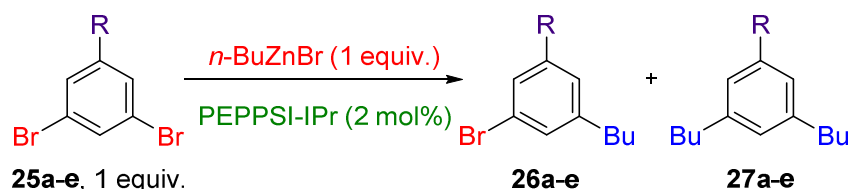
2.1 Introduction

Drawing on previous work in our group, the scope of the preferential intramolecular oxidative addition observed by PEPPSI-IPr was further explored in order to expand the substrate scope and potentially uncover the mechanism for this phenomenon.

2.2 Addition of functional groups to aryl dibromides

Excellent selectivity was previously observed for couplings of aryl bromides mediated by PEPPSI-IPr. However, no aryl bromides containing functional groups were subjected to the sp^3 - sp^2 Negishi coupling conditions. In a preliminary screening we examined the reactivity of *meta*-substituted 1,3-dibromobenzenes (**25a-e**), investigating the effect of functional groups on the chemoselectivity and yield (Table 2).

Table 2. PEPPSI-IPr mediated Negishi coupling reaction of *meta*-substituted aryl dibromides^a



Entry	R	25 : 27 ^b	Yield ^c
1	H (25a)	<1 : >99	98%
2	CH ₃ (25b)	<1 : >99	90% ^d
3	OMe (25c)	<1 : >99	94%
4	F (25d)	<1 : >99	92%
5	COOMe (25e)	<1 : >99	88%

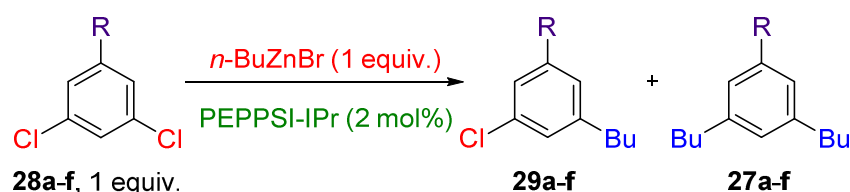
^a All reactions were performed on a 0.25 mmol scale of *n*-BuZnBr. LiBr (3 equiv.), THF-DMI (2 : 1), RT, 2 h. ^b Product ratio determined by ¹H NMR analysis of the crude reaction mixture. ^c Yield determined by ¹H NMR analysis of the crude reaction mixture relative to *n*-BuZnBr using mesitylene as an internal standard. ^d *p*-Xylene used as an internal standard.

Excellent di-selective couplings for both electron donating (Table 2, entries 2) and electron withdrawing groups (Table 2, entries 3-5) were obtained in excellent yields. Unfortunately, stronger electron-withdrawing nitrile and nitro groups led to the formation of impurities as a result of side reactions. Therefore, the ratio of products could not be accurately be obtained.

2.3 Addition of functional groups to aryl dichlorides

To better understand the effect of functional groups on the aromatic ring, similar *meta* substituted arenes were investigated replacing the C-Br bonds with C-Cl bonds. 1,4-Dichlorobenzene (mono : di, 65 : 35, 85%) showed a more equal ratio of mono- and di-substituted products in previous work. We hypothesised this would allow changes in product ratio to be observed more clearly as a result of the additional functional groups.

Table 3. PEPPSI-IPr mediated Negishi coupling reaction of *meta*-substituted dichloroarenes^a



Entry	R	29 : 27 ^b	Yield ^c
1	H (28a)	56 : 44	89%
2	F (28b)	3 : 97	78%
3	CF ₃ (28c)	6 : 94	80%
4	OMe (28e)	4 : 96	92%
5	CH ₃ (28d)	6 : 94	62%
6	CN (28f)	76 : 24	50%

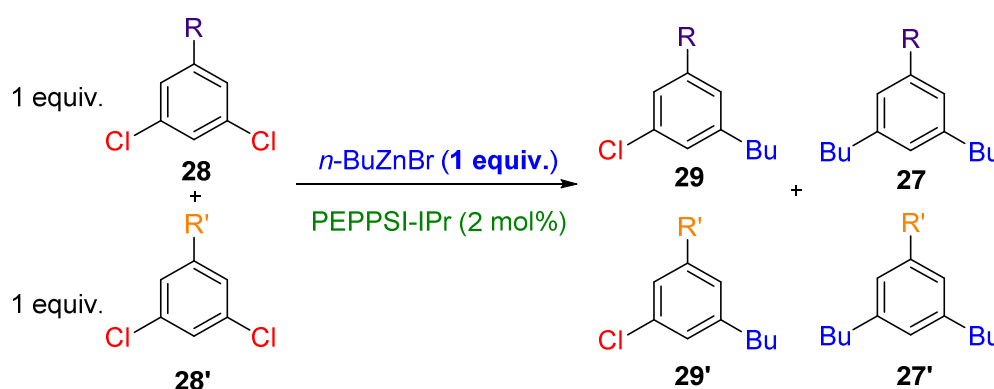
^a All reactions were performed on a 0.25 mmol scale of *n*-BuZnBr. LiBr (3 equiv.), THF-DMI (2 : 1), RT, 2 h. ^b Product ratio determined by GCMS analysis of the crude reaction mixture. ^c Yield determined by ¹H NMR analysis of the crude reaction mixture relative to *n*-BuZnBr using mesitylene as an internal standard. ^d See reference⁸⁹.

1,3-Dichlorobenzene (**28a**, Table 3, entry 1) showed comparable reactivity and selectivity relative to its regioisomer 1,4-dichlorobenzene. However, to our delight both electron withdrawing (Table 3, entries 2 - 4) and electron donating groups (Table 3, entry 5) facilitated excellent di-selective couplings in good to excellent yields, a dramatic contrast from 1,3-dichlorobenzene (**28a**, Table 3, entry 1). Selectivity towards the mono-alkylated product **29** was observed upon the addition of the strongly electron-withdrawing nitrile group with no impurities observed (**28f**, Table 3, entry 6).

2.4 Competition between aryl chlorides

There was no clear trend for excellent di-selectivity to account for why selectivity for di-alkylation was observed with the addition certain of the functional groups in Table 3. A competition experiment was performed between aryl dichlorides (**28a-c**, **e-f**) to identify if the chemoselectivity correlates with reactivity (Table 4).

Table 4. PEPPSI-IPr mediated Negishi competition experiment between dichlorobenzenes^a



Entry	R	R σ-meta ^f	R'	29 : 27 ^b	29' : 27' ^b	Relative reactivity R : R' ^c
1	CF ₃ (28c)	0.43	H (28a)	5 : 95 ^e	73 : 27	67 : 33
2	OMe (28e)	0.12	H (28a)	<5 : >95	57 : 43	14 : 86
3	F (28b)	0.34	H (28a)	<5 : >95	67 : 33	51 : 49
4	CN (28f)	0.56	H (28a)	85 : 15	NR ^d	>92 : <8
5	CN (28f)	0.56	F (28b)	88 : 12 ^e	NR ^d	>89 : <11

^a All reactions were performed on a 0.25 mmol scale of *n*-BuZnBr. LiBr (3 equiv.), THF-DMI (2 : 1), RT, 2 h. ^b Product ratio determined by ¹H NMR analysis of the crude reaction mixture. ^c Ratio of the yield of

both aryl dichlorides determined by ^1H NMR analysis of the crude reaction mixture relative to *n*-BuZnBr using mesitylene as an internal standard. ^dNo reaction detected by ^1H NMR. ^e Ratio obtained by GCMS due to overlapping peaks in the ^1H NMR. ^f See reference⁸⁹

When there was competition between aryl dichlorides **28c** and **28f** and 1,3-dichlorobenzene (**28a**, Table 4, entries 1 and 4) there was little or no conversion of 1,3-dichlorobenzene (**28a**). By comparison, dichloride **28e** (Table 4, entry 2) was less reactive than 1,3-dichlorobenzene (**28a**) and 1,3-dichloro-5-fluorobenzene (**28b**) showed equal reactivity with 1,3-dichlorobenzene (**28a**, Table 4, entry 4). Finally, 3,5-dichlorobenzonitrile (**28f**) was significantly more reactive than 1,3-dichloro-5-fluorobenzene (**28b**).

Whilst the combined yield for entries 1-3 were quantitative, when a nitrile group is present the reaction appears to stall at ~50% yield. The lower yield could be linked to its mono-selective coupling.

Interestingly, the product ratio between mono- and di-alkylated products in Table 4 varied only slightly in the competition reaction relative to the product ratios in Table 3. The ability for the regenerated Pd(0) catalyst to undergo intramolecular oxidative addition appears independent of the reactivity of the aryl dichloride.

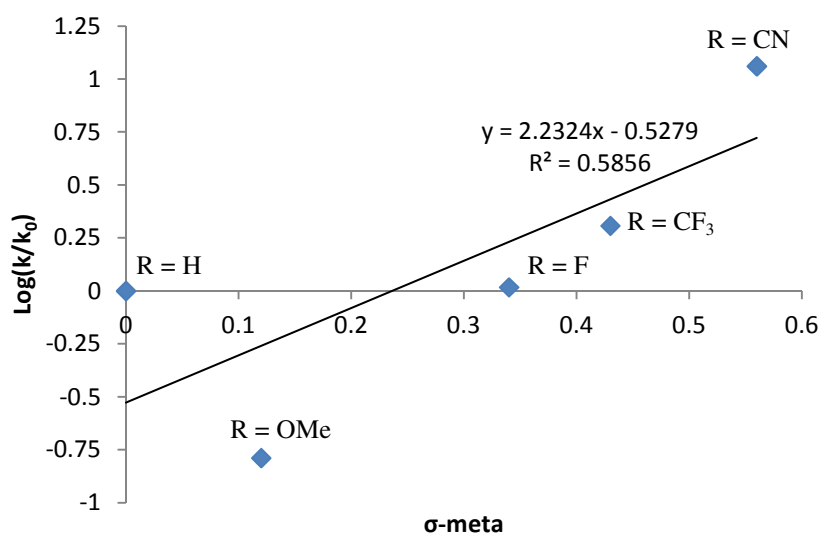
There appears to be a trend between relative reactivity of the dichloroarenes and the *meta*-Hammett constant for R, the more electron deficient the aromatic the more reactive it is. The competition reaction has given us the relative reactivities of *meta*-substituted dichlorobenzenes **28b,c,e** and **f** compared with 1,3-dichlorobenzene **28a**. These relative reactivities can be seen as the relative reaction rates. The Hammett equation (Equation 1) can be used to identify the influence of *meta*- and *para*- groups on a benzene ring.

Equation 1. Hammett equation

$$\log \frac{k}{k_0} = \sigma \rho; \quad \sigma = \text{Hammett constant}; \quad \rho = \text{Hammett reaction constant}$$

Unfortunately, the assumption that k as the rate of conversion for our *meta*-substituted dichlorobenzenes and k_0 is the rate of conversion of 1,3-dichlorobenzene does not fit the Hammett equation with the x,y intercept not 0,0 (Graph 2).

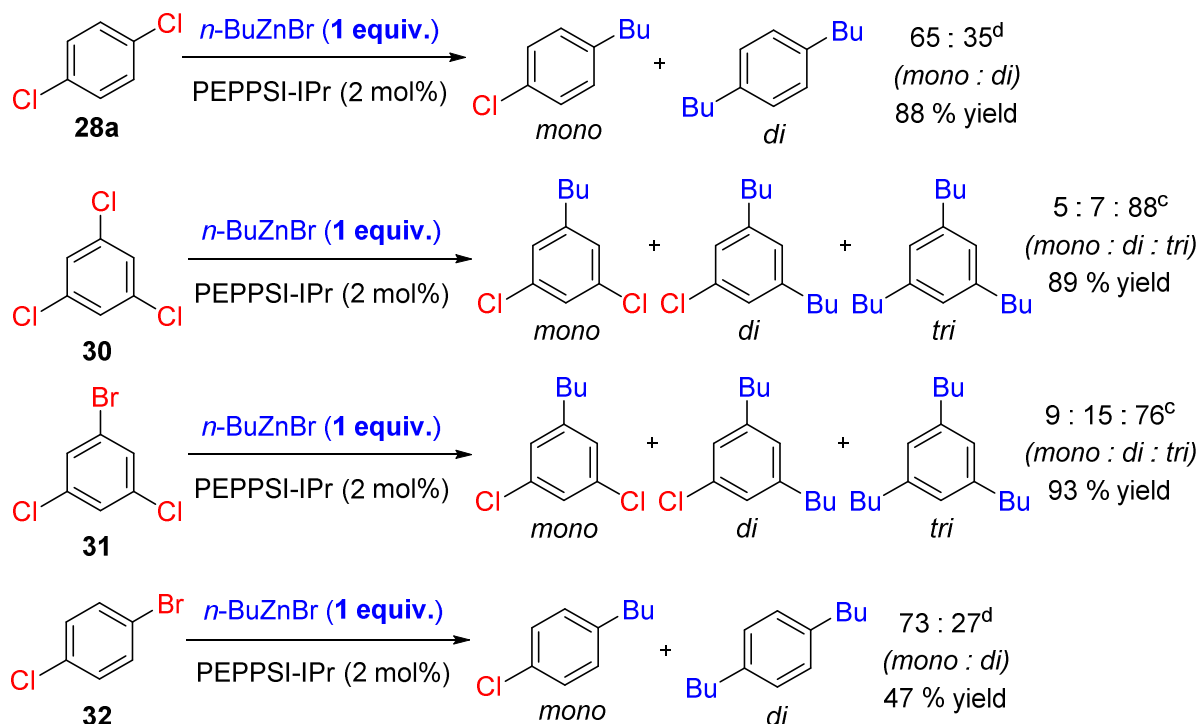
Graph 2. Hammett plot using the relative reactivities of meta-substituted dichlorobenzenes relative to 1,3-dichlorobenzene



2.5 Poly-Polyhalogenated benzenes

The addition of a functional group in the *meta* position to the two C-Cl bonds resulted in an increase in the di-selectivity of the coupling in most examples. We hypothesised that this would increase the selectivity for full-alkylation for the coupling of 1,3,5-trichlorobenzene (**30**) and 1-bromo-3,5-dichlorobenzene (**31**). These compounds' added functionality, however can themselves become alkylated.

Scheme 29. PEPPSI-IPr mediated Negishi coupling reaction of polyhalogenated benzenes^a



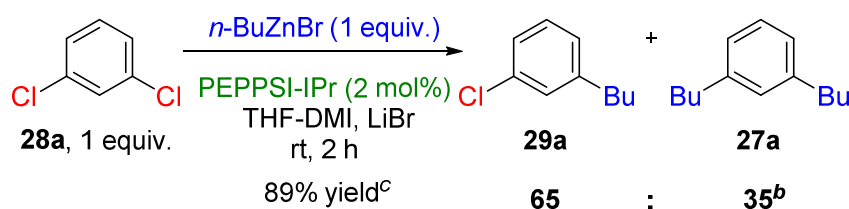
^a All reactions were performed on a 0.25 mmol scale of *n*-BuZnBr. LiBr (3 equiv.), THF-DMI (2 : 1), RT, 2 h. Product ratio determined by GCMS analysis of the crude reaction mixture. ^c Ratio of mono : di : tri substituted products; yield determined by ¹H NMR analysis of the crude reaction mixture relative to *n*-BuZnBr using *p*-Xylene as an internal standard. ^d Ratio of mono : di substituted products; Mesitylene used as an internal standard.

The addition of a halogen in the *meta* position showed a dramatic increase in selectivity for full-alkylation compared with 1,3-dichlorobenzene (Scheme 29, **30** and **31**). The tri-selective coupling of 1-bromo-3,5-dichlorobenzene (**31**) was surprising as not all of the more reactive C-Br bonds in the reaction coupled preferentially over the C-Cl bonds. This is a dramatic change compared to the previously reported selectivity with 1-bromo-4-chlorobenzene (**32**) which strongly favoured the coupling of the C-Br bond over the C-Cl bond (Scheme 29). This is further proof that the regenerated Pd(0) catalyst undergoes preferential intramolecular oxidative addition immediately after reductive elimination, as opposed to diffusing into the reaction solvent.

2.6 Variation in reaction conditions

After exploring changes in chemoselectivity with different aryl dichlorides, changes in the reaction conditions were investigated to further expand the scope and potentially gain some insight into the mechanism. The PEPPSI-IPr mediated $\text{sp}^3\text{-sp}^2$ Negishi coupling between 1,3-dichlorobenzene (**28a**) and *n*-BuZnBr (Scheme 30) was chosen as changes in chemoselectivity would be easily observed.

Scheme 30. PEPPSI-IPr mediated coupling of 1,3-dichlorobenzene (**28a**)^a



^a Performed on a 0.25 mmol scale of *n*-BuZnBr. LiBr (3 equiv.), THF-DMI (2 : 1), RT, 2 h. ^b Product ratio determined by ¹H NMR analysis of the crude reaction mixture. ^c Yield determined by ¹H NMR analysis of the crude reaction mixture relative to *n*-BuZnBr using mesitylene as an internal standard.

2.6.1 Solvent ratio

A solvent mixture of THF and DMI was used for the couplings described previously. In an attempt to probe the importance of the solvent mixture with respect to the product ratio, the ratio of solvents was varied. Keeping the concentration constant, the ratio was varied toward the more polar solvent DMI.

Table 5. Varying the solvent ratio of the Negishi coupling of 1,3-dichlorobenzene^a

Entry	Solvent Ratio (THF : DMI)	29a : 27a ^b	Yield ^c
1	2:1	63 : 37	85%
2	1:1	66 : 34	71%
3	1:2	68 : 32	45%
4	1:3	68 : 32	37%

^a 1,3-dichlorobenzene (**28a**, 0.25 mmol), *n*-BuZnBr (0.25 mmol), PEPPSI-IPr (2 mol%), LiBr (3 equiv.), THF-DMI, RT, 2 h. ^b Product ratio determined by ¹H NMR analysis of the crude reaction mixture. ^c Yield

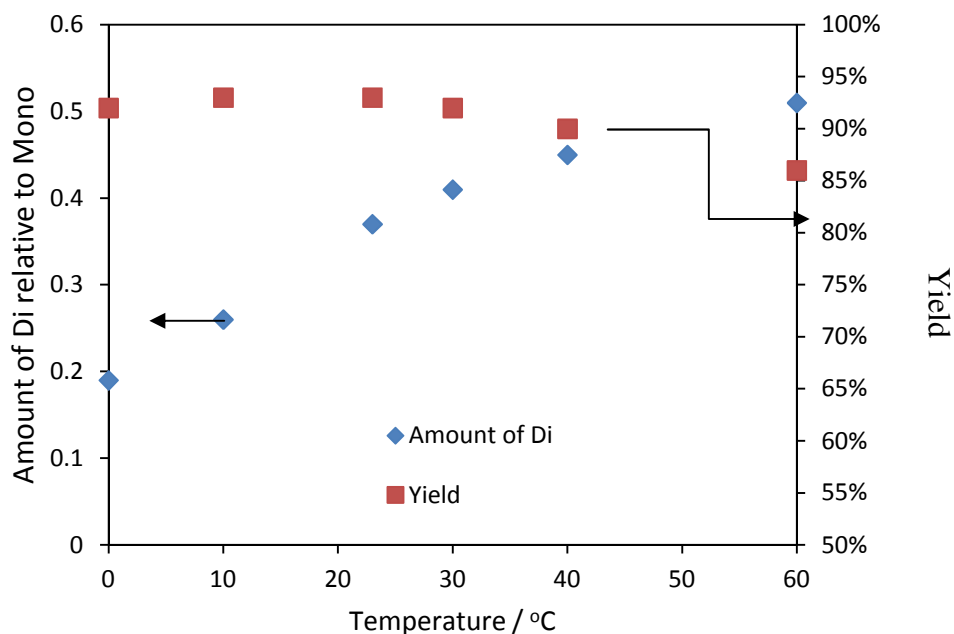
determined by ^1H NMR analysis of the crude reaction mixture relative to *n*-BuZnBr using mesitylene as an internal standard.

Increasing the amount of DMI relative to THF decreased the yield of the coupling by almost 50%. This is most likely due to the hygroscopic nature of DMI introducing more water into the coupling the higher the ratio of DMI:THF. The product ratio of the couplings remain consistent as the amount of DMI in the system increases. These results suggest conversion and solvent do not greatly affect the chemoselectivity of the coupling.

2.6.2 Temperature scan

Previously undertaken PEPPSI-IPr mediated Negishi couplings were run at room temperature. The temperature was varied to observe its effect on the product ratio and its implications for the chemoselectivity of the coupling.

Graph 3. Varying the temperature of the Negishi coupling of 1,3-dichlorobenzene^a



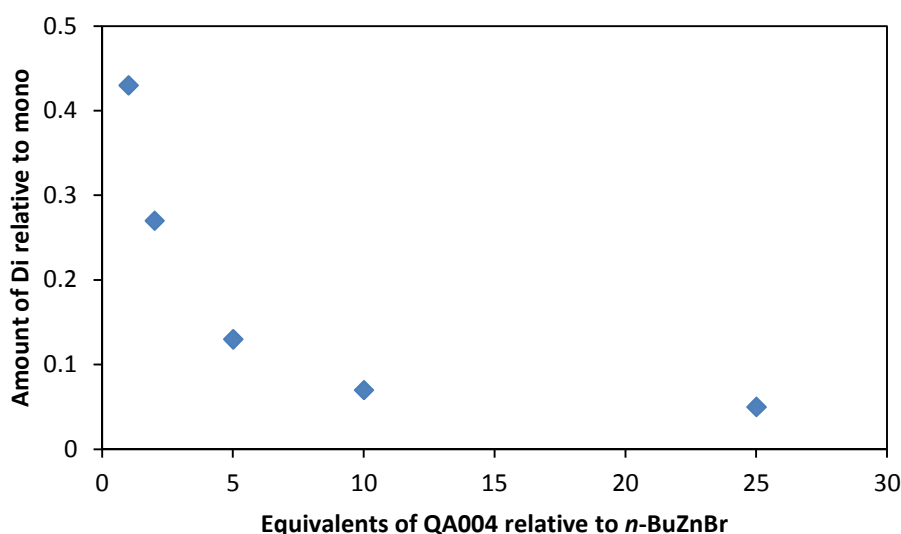
^a 1,3-dichlorobenzene (28a, 0.25 mmol), *n*-BuZnBr (0.25 mmol), PEPPSI-IPr (2 mol%), LiBr (3 equiv.), THF-DMI (2 : 1), 2 h. ^b Product ratio determined by ^1H NMR analysis of the crude reaction mixture. ^c Yield determined by ^1H NMR analysis of the crude reaction mixture relative to *n*-BuZnBr using mesitylene as an internal standard.

As the temperature increases the amount of di-alkylated product (**27a**) relative to mono-alkylated (**29a**) increases. The yield of the coupling remained approximately consistent at all temperatures.

2.6.3 Equivalents of 1,3-dichlorobenzene

Previous couplings were performed with an equal amount of aryl dichloride and *n*-BuZnBr compounds. Increasing the amount of the 1,3-dichloroarene (**28a**) relative to *n*-BuZnBr will lead to a higher probability of catalyst oxidative addition to a molecule of the dichloride **28a** rather than the mono-alkylated **29a** product. We hypothesised an increase in equivalents of **28a** relative to *n*-BuZnBr would have increase the relative amount of mono-alkylated product **29a**.

Graph 4. Varying the number of equivalents of 1,3-dichlorobenzene relative to *n*-BuZnBr^a



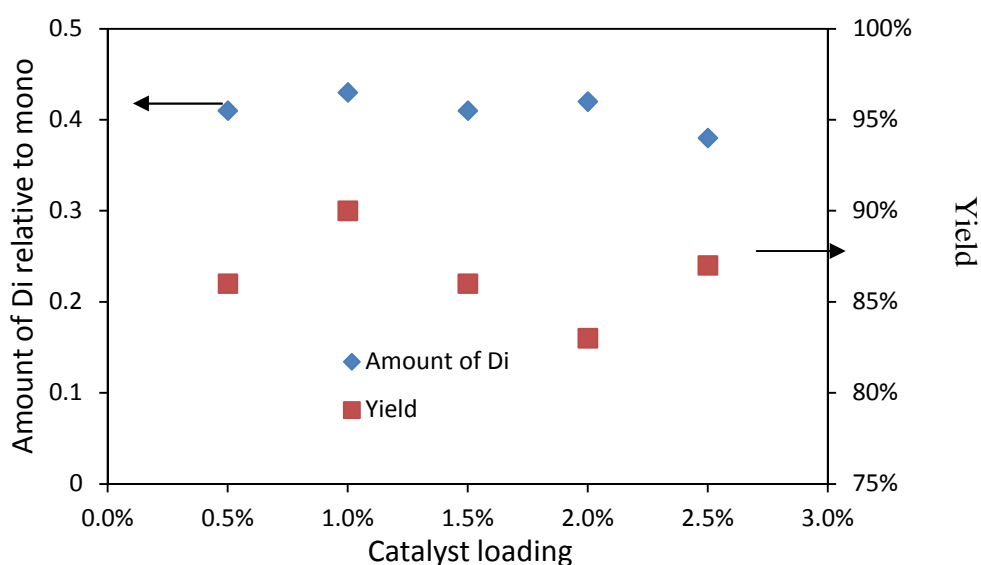
^a *n*-BuZnBr (0.25 mmol), PEPPSI-IPr (2 mol%), LiBr (3 equiv.), THF-DMI (2 : 1), 25 °C, 2 h. ^b Product ratio determined by ¹H NMR analysis of the crude reaction mixture. ^c Yield determined by ¹H NMR analysis of the crude reaction mixture relative to *n*-BuZnBr using mesitylene as an internal standard.

As predicted, the greater the number of equivalents of 1,3-dichloroarene relative to the *n*-BuZnBr, the higher the amount of mono-alkylated product **29a** relative to the di-alkylated arene **27a**. Unsurprisingly, yields were consistently excellent for all couplings.

2.6.4 Catalyst loading

Attempts to vary the concentration of the coupling led to a dramatic reduction in yield with no conversion observed when the concentration was halved. Instead, the concentration of PEPPSI-IPr was varied by changing the catalyst loading.

Graph 5. Varying the catalyst loading of PEPPSI-IPr^a



^a 1,3-dichlorobenzene (28a, 0.25 mmol), *n*-BuZnBr (0.25 mmol), LiBr (3 equiv.), THF-DMI (2 : 1), 25 °C, 2 h. ^b Product ratio determined by ¹H NMR analysis of the crude reaction mixture. ^c Yield determined by ¹H NMR analysis of the crude reaction mixture relative to *n*-BuZnBr using mesitylene as an internal standard.

Between a catalyst loading of 0.5-2.5 mol% the chemoselectivity and yield remained constant, independent of the catalyst loading.

2.6.5 Time Scan

A time scan was performed to investigate how the product distribution of the coupling changes over time and how long the reaction takes to go to completion.

Table 6. Time scan of the Negishi coupling of 1,3-dichlorobenzene^a

Entry	Time / mins	29a : 27a ^b	Yield ^c
1	5	59 : 41	89%
2	10	59 : 41	89%
3	30	58 : 42	81%

^a 1,3-dichlorobenzene (28a, 0.25 mmol), *n*-BuZnBr (0.25 mmol), PEPPSI-IPr (2 mol%), LiBr (3 equiv.), THF-DMI (2 : 1), 25 °C. ^b Product ratio determined by ¹H NMR analysis of the crude reaction mixture. ^c Yield determined by ¹H NMR analysis of the crude reaction mixture relative to *n*-BuZnBr using mesitylene as an internal standard.

The coupling appears to finish after just five minutes, therefore the variation in product distribution over time could not be followed. This demonstrates that PEPPSI-IPr is a very reactive catalyst.

2.7 Conclusions

The exploration into the scope of the selective di-alkylation for aryl dibromides was successfully expanded with the addition of a range of functional groups, with the exception of strongly electron withdrawing nitrile and nitro groups due to side reactions independent of the cross-coupling.

Subsequently the addition of most functional groups to aryl dichlorides switched on the preferential oxidative addition needed for chemoselective couplings. The trend in reactivity correlated with the Hammett constants, however did not fit the Hammett equation.

Variations on the reaction conditions with 1,3-dichlorobenzene (**28a**) demonstrated that variation in both temperature and relative equivalents of dichloride **28a** varied the product distribution.

To the best of our knowledge, at the time of research, these results were the first selective exhaustive substitution of poly-chloroarenes with an equal amount of nucleophile

observed. Although chain growth polycondensation has since been reported for nickel catalysts of thiophene-based monomers, these model reactions further suggest PEPPSI-IPr to be an ideal candidate to mediate chain-growth polymerizations from cheap chloride monomers.

Future research of the $\text{sp}^3\text{-sp}^2$ Negishi couplings mediated by PEPPSI-IPr would have focused on changing the reaction conditions with *meta*-substituted aryl dichlorides. However, research efforts moved towards a model reaction of $\text{sp}^2\text{-sp}^2$ cross-couplings mediated by PEPPSI precatalysts.

2.8 References

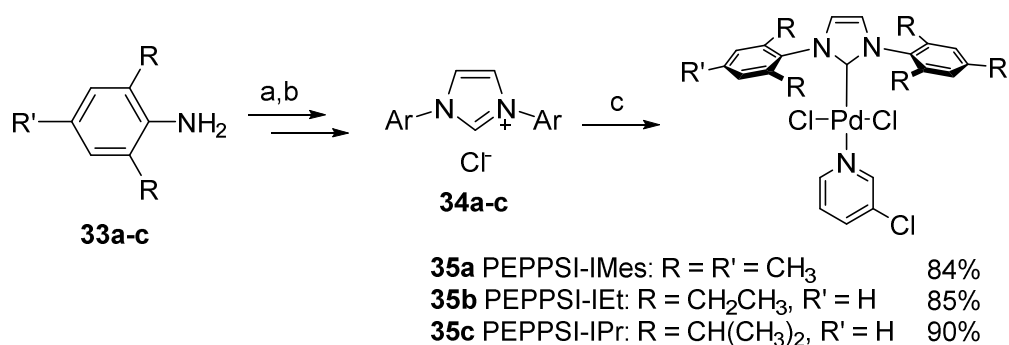
(89) Hansch, C.; Leo, A. *Substituent Constants for Correlation Analysis in Chemistry and Biology*; Wiley-Interscience: New York, 1979.

Chapter 3 – PEPPSI-IPent synthesis

3.1 Introduction

PEPPSI-IPr was one in a series of the pyridine stabilised palladium NHC complexes to be reported by Organ and co-workers, its efficacy and scope previously discussed.⁹⁰ It was the only commercially available PEPPSI catalyst available when our research into exploring chemoselective couplings began. Although commercially available, PEPPSI-IPr can easily be prepared from its corresponding NHC.⁹¹ We synthesized PEPPSI-IPr (**35c**) along with PEPPSI-IET (**35b**) and PEPPSI-IMes (**35a**) from their corresponding NHCs in excellent yields (Scheme 31). Due to difficult separation of 3-chloropyridine from the PEPPSI complexes the yields are slightly lower than reported. The NHCs in turn, were easily synthesized from commercially available anilines **33a-c** and provided in good yields.

Scheme 31. Synthetic route to PEPPSI complexes -IMes, -IET and -IPr

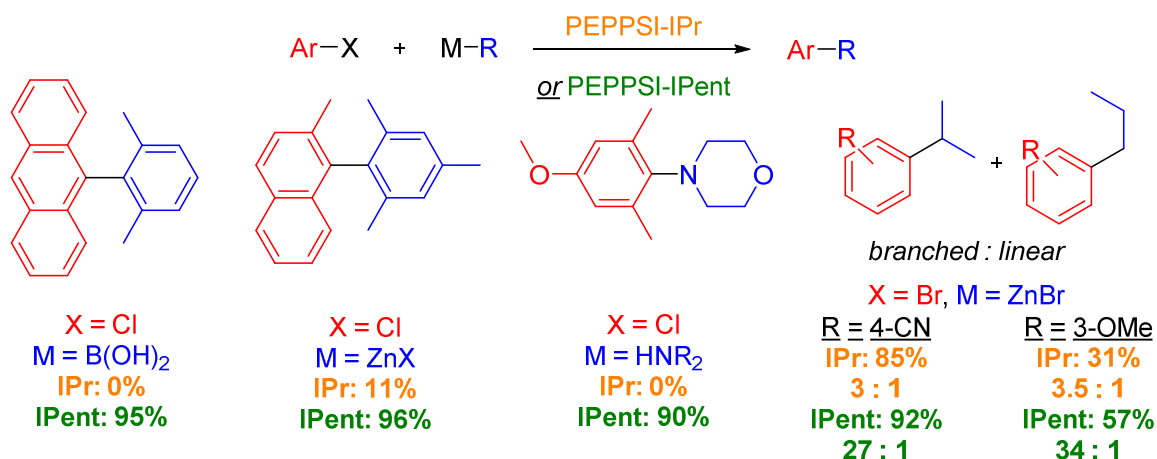


a. Glyoxal (1 equiv.), **33** (1.6 equiv.), formic acid (a few drops), methanol, RT, 4 h; b. Diimine (1 equiv.), ZnCl₂ (1 equiv.), paraformaldehyde (1.1 equiv.), HCl in dioxane (1.5 equiv.), THF, 70 °C, 16 h; c. PdCl₂ (1 mmol), **34** (1.1 mmol), K₂CO₃ (5 mmol), 3-chloropyridine, 80 °C, 16 - 20 h.

Organ and co-workers have shown that a second generation catalyst, PEPPSI-IPent (**35d**), is even more active than PEPPSI-IPr.⁹² PEPPSI-IPent follows the previous trend observed where increased steric bulk of the flexible alkyl chains led to increased activity. It outperforms PEPPSI-IPr in challenging cross-couplings, examples shown in Scheme 32. Scheme It is a more general catalyst for most C-C bond couplings as well as aminations and sulfonations.⁹² This made it an attractive catalyst to investigate as it could

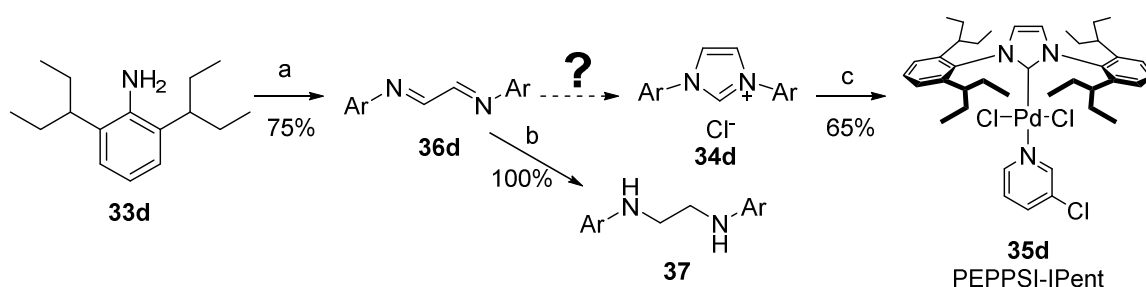
achieve a higher selectivity for intramolecular oxidative addition and expand the scope of potential monomers for chain transfer polymerization.

Scheme 32. Comparison of PEPPSI-IPr to -IPent⁹²



Unfortunately, it is an expensive catalyst at £416.50/g⁹³ with no reported synthetic route from commercially available materials. Starting from the non-commercial aniline **33d**, the synthesis of the diimine **36d** is reported in a separate publication⁹⁴ to that of the formation of the PEPPSI-IPent (**35d**) from the NHC (Scheme 33).⁷⁹

Scheme 33. Reported steps for the synthesis of PEPPSI-IPent

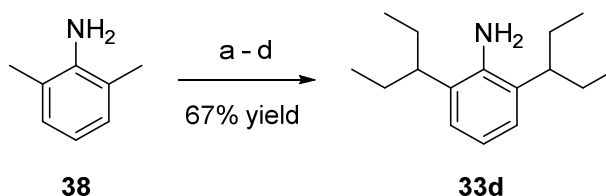


a. Glyoxal (0.5 equiv.), **33d** (1 equiv.), formic acid (0.12 equiv.), ethanol, 70 °C, 24 h; b. **36d** (1 equiv.), Na(CN)BH₃ (2 equiv.), AcOH, EtOH, Et₂O, RT, 4 h; c. PdCl₂ (1.38 mmol), IPent.HCl (0.93 mmol), K₂CO₃ (4.65 mmol), 3-chloropyridine (8 mL), 80 °C, 24 h.

To the best of our knowledge, there is one reported synthetic procedure to aniline **33d** by Steele *et al.* (Scheme 34).⁹⁵ The reaction can be performed on a multigram scale in one step with a good yield. Unfortunately the procedure has several drawbacks. It requires specialist equipment, the use of flammable ethene gas at high temperature, above

atmospheric pressure and the use of non commercial superbases. Additionally, the scope of this transformation lacks the ability to expand the library of the flexible alkyl chains on the aniline, with the possibility of synthesising a more active catalyst than PEPPSI-IPent.

Scheme 34. Synthesis of aniline **33d** by Steele *et al.*⁹⁵



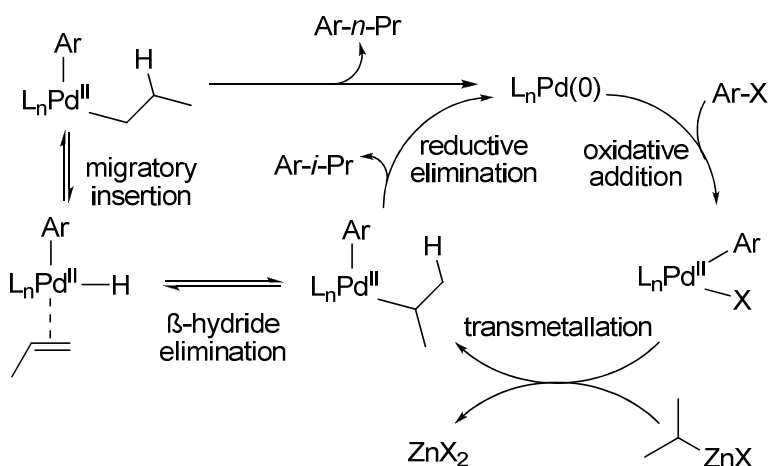
a. *n*BuLi (1 equiv.); b. *n*BuLi/LiK-(OCH₂CH₂NMe₂)₂; c. Mg(OCH₂CH₂OEt)₂, C₂H₄ (10 atm), 80 °C, 24 h; d. H₂O.

Consequently, we sought to improve on the synthesis of aniline **33d**. We looked for an alternative that can be performed under basic laboratory conditions, in the smallest number of steps, highest yield and with minimal purification.

3.2 Negishi coupling of 3-pentylzinc bromide

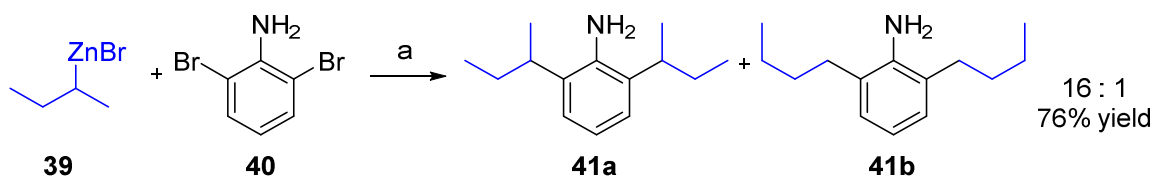
PEPPSI-IPent has been reported to show high selectivity for the direct coupling of secondary alkylzinc reagents.⁹⁶ The competing side reaction results in regioisomers of the alkyl chains. The ratio of secondary alkyl chains coupled directly compared with linear products is determined by the rate of β -hydride elimination followed by migratory insertion over the rate of reductive elimination after the transmetallation (Figure 11).

Figure 11. Catalytic cycle of *iso*-propylzinc halide



Organ and co-workers showed excellent selectivity for the coupling of *sec*-butylzinc bromide (**39**) with 2,6-dibromoaniline (**40**) mediated by PEPPSI-IPent (Scheme 35).⁹⁶

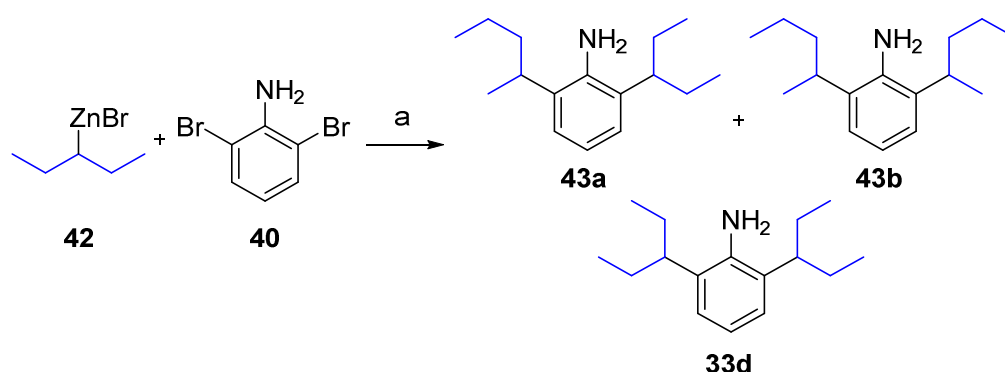
Scheme 35. PEPPSI-IPent mediated coupling of aniline **40** and *sec*-butylzinc bromides⁹⁶



a. **40** (1 equiv.), **39** in THF (3.4 equiv.), PEPPSI-IPent (2 mol%), toluene, RT, 20 h.

We envisaged using a catalytic amount of PEPPSI-IPent to synthesize the key aniline intermediate needed for the formation of PEPPSI-IPent. We proposed any minor isomers present would be removed by recrystallization at a later stage in the synthetic route. Therefore, we attempted the coupling of 3-pentylzinc bromide (**42**) and the same aniline **40** mediated by PEPPSI-IPent (Scheme 36).

Scheme 36. PEPPSI-IPent mediated coupling of aniline **40** and 3-pentylzinc bromides (**42**)



a. **40** (1 equiv.), **42** in THF (3.4 equiv.), PEPPSI-IPent (2 mol%), toluene, RT, 20 h.

The coupling was highly selective between branched and linear regioisomers; however there was a mixture of the desired regioisomer **33d** and *sec*-isomers **43a** and **b** (54: 46 respectively by ^1H NMR analysis) that proved inseparable *via* standard purification techniques. The intractable mixture of products made this route to PEPPSI-IPent look unworkable.⁹⁷

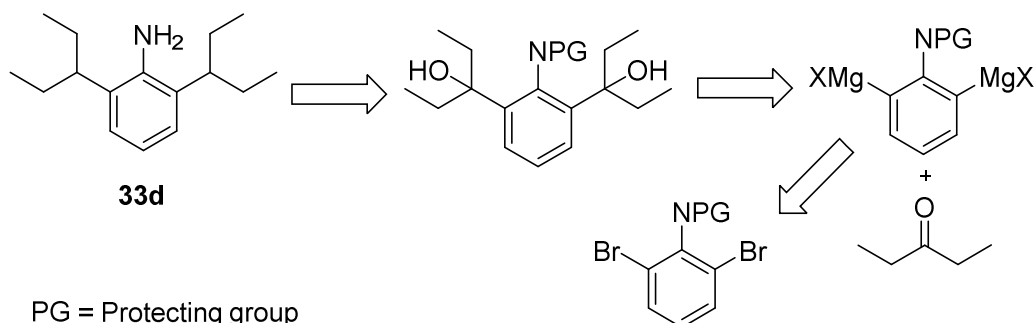
Organ and co-workers have reported that a third generation catalyst PEPPSI-IPent^{Cl} is even better at coupling secondary alkyl groups selectively.⁹⁸ Like PEPPSI-IPent, PEPPSI-IPent^{Cl} was not commercially available and had no synthetic route from commercially available starting materials. Even if it was viable to synthesize PEPPSI-IPent^{Cl}, it was unclear if the ratio of the desired product to its regioisomers would be enough to make the route viable. Therefore we turned our attention to alternative routes to synthesize aniline **33d**.

3.3 Route 1: Synthesis of aniline 33d

We proposed a retrosynthetic route to aniline **33d** utilising classical chemistry where by Grignard reagents would be used to add the flexible alkyl groups to the aniline. After the

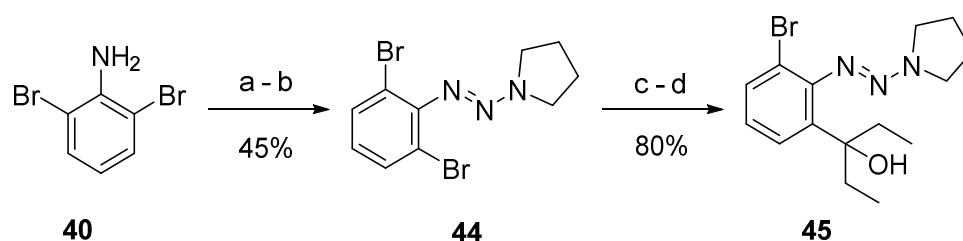
addition of alkyl groups, the routes required dehydration and alkene reduction to afford aniline **33d** (Scheme 37).

Scheme 37. Retrosynthetic routes to key aniline **33d**



Inspired by chemistry reported by Knochel and co-workers⁹⁹ we attempted the synthesis of aniline **33d** from 2,6-dibromoaniline (**40**). Using a triazene protecting group we formed a Grignard by halogen metal exchange from *i*-PrMgCl.LiCl. This was successfully quenched with pentanone to afford alcohol **45** in a good yield (Scheme 38).

Scheme 38. Synthesis of diol **45** from aniline **40**



a. **40** (1 equiv.), NaNO₂ (1.5 equiv.), conc. HCl (aq.), 0 °C, 30 mins; b. pyrrolidine (2 equiv.), K₂CO₃ (5 equiv.), acetonitrile : water (1 : 2), 0 °C, 30 mins; c. **44** (1 equiv.), *i*-PrMgCl.LiCl (1.1 equiv.), THF, -40 °C – -15 °C, 2.5 h; d. 3-Pentanone (2.2 equiv.), THF, -15 °C – RT, 30 mins.

With the successful installation of the alkyl groups for one C-Br bond, we attempted the same approach to the second C-Br bond. Unfortunately, the addition of 3 equivalents *i*-PrMgCl.LiCl to alcohol **45** did not yield any halogen metal exchange. Even when a large excess of *i*-PrMgCl.LiCl was added to dibromoarene **44** selective halogen metal exchange of only one C-Br bond was observed. Further attempts to form the Grignard at higher temperatures also failed (Scheme 39).

Chemical reaction scheme showing the conversion of compound **45** to compound **46** (labeled **a**) and then to compound **44** (labeled **b**). Compound **45** is a 2-bromo-1-(2-hydroxyethyl)-4-(pyrrolidin-1-ylazo)benzene derivative. Compound **46** is a 2-bromo-1-(2-hydroxyethyl)-4-(pyrrolidin-1-ylazo)benzene derivative. Compound **44** is a 2,6-dibromo-4-(pyrrolidin-1-ylazo)benzene derivative. The reaction **a** is marked with a red **X**, and reaction **b** is also marked with a red **X**.

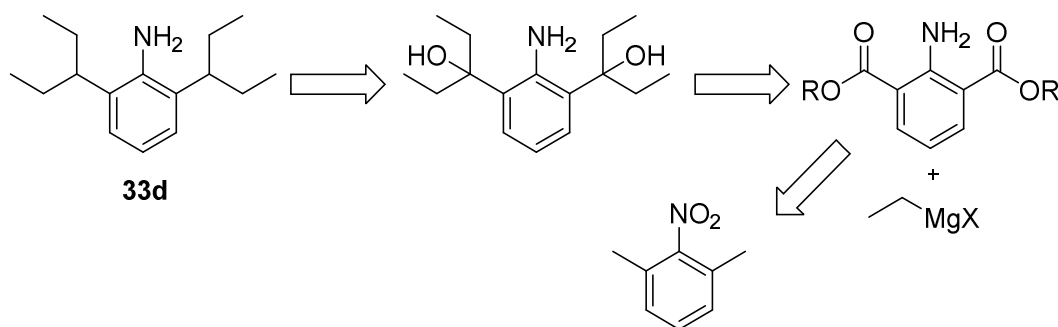
After attempts to form diol **46** failed, we hypothesized the alcohol functionality could be responsible for the failure to form the Grignard. Therefore, we attempted the dehydration with *p*-toluenesulfonic acid (*p*-TsOH). Unfortunately, this led to decomposition of the starting material involving the removal of the triazene with no product formed (Scheme 40).

As this route did not work we looked for another route to the desired aniline **33d**.

3.4 Route 2: Synthesis of aniline 33d

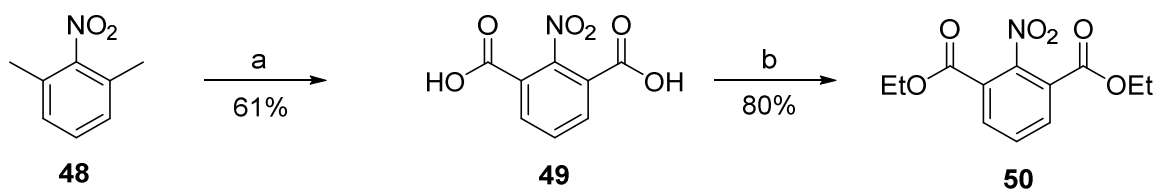
Page | 74

Scheme 41. Retrosynthetic routes to key aniline **33d**



Starting from 2-nitro-*m*-xylene we aimed to transform it into the desired aniline **33d** in just 6 steps. The double oxidation of 2-nitro-*m*-xylene (**48**) to 2-nitroisophthalic acid (**49**) was achieved in a good yield in accordance with the literature.¹⁰⁰ We found that an extra 10% KMnO_4 was needed to eliminate the intermediate 3-methyl-2-nitro-benzoic acid, which added an additional purification step. The diacid **49** was converted to the diester **50** in an excellent yield, with any unreacted diacid **49** easily recovered from the aqueous workup. Both reactions were easily performed on a multigram scale (Scheme 42).

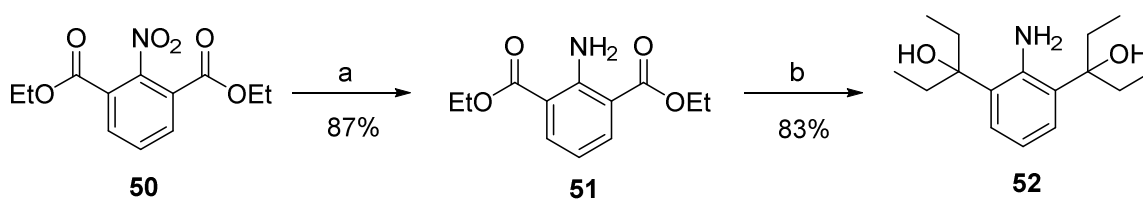
Scheme 42. Synthesis of diester **50** from 2-nitro-*m*-xylene (**48**)



a. **48** (1 equiv.), KMnO_4 (4.4 equiv.), NaOH (1.5 equiv.), water, reflux, 20 h; b. **49** (1 equiv.), SOCl_2 (4 equiv.), EtOH , 70 °C, 20 h.

Diethyl 2-nitroisophthalate was reduced to aniline **51** by hydrogenation catalysed by palladium on carbon. An alternative reduction with zinc and acetic acid was attempted but resulted in a lower yield. Utilising chemistry by Bowman *et al.*¹⁰¹ we added ethylmagnesium bromide to the diester **51** to afford diol **52** in an excellent yield (Scheme 43).

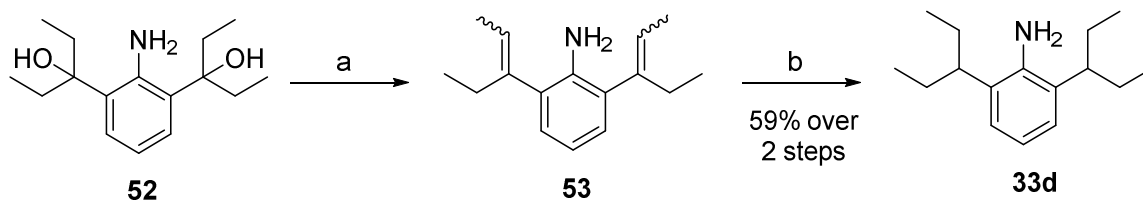
Scheme 43. Synthesis of diol **52** from diester **50**



a. **50** (1 equiv.), 10% Pd/C (2 mol%), H₂ (1 atm), EtOH, RT, 6 h; b. **51** (1 equiv.), EtMgCl (8 equiv.), THF, 0 °C - RT, 3 h.

Dehydration catalyzed by *p*-TsOH using Dean-Stark apparatus afforded dialkene **53** as a mixture of (*E*)- and (*Z*)-alkene isomers. Dialkenes **53** were taken forward crude to form the desired aniline **33d** by hydrogenation catalysed by palladium on carbon in a good yield over the two steps (Scheme 44). The 6 step synthesis of aniline **33d** was very scalable with only one flash column chromatography purification needed. This made the route very scalable and efficient.

Scheme 44. Synthesis of aniline **33d** from diol **52**

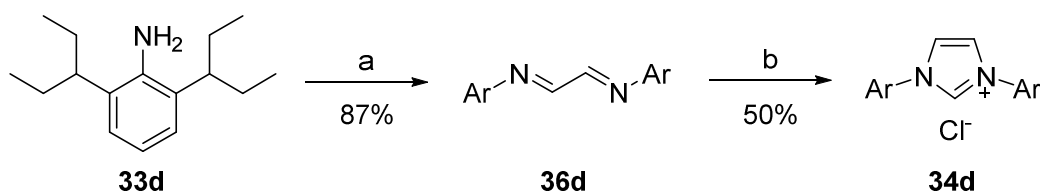


a. **52** (1 equiv.), *p*-TsOH (0.1 equiv.), toluene, reflux, 3 h; b. **53** (1 equiv.), 10% Pd/C (4 mol%), H₂ (1 atm), EtOH, RT, 12 h.

3.5 PEPPSI-IPent synthesis

With the aniline **33d** in hand we found we obtained a greater yield than the literature procedure for synthesis of the diimine by Organ and co-workers (75% yield).⁹⁴ This was achieved by using milder conditions and shorter reaction time used to synthesize the equivalent IPr diimine **36d**. The diimine **33d** was subsequently cyclised to form the NHC **34d** in a moderate yield (Scheme 45).

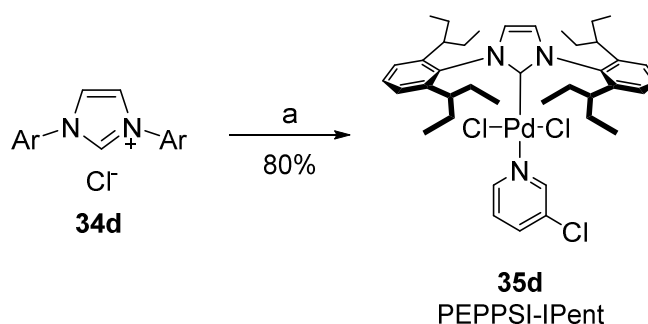
Scheme 45. Synthesis of IPent.HCl (QA003d) from aniline **33d**



a. Glyoxal (1 equiv.), **33d** (1.6 equiv.), formic acid (a few drops), methanol, RT, 4 h; b. **36d** (1 equiv.), ZnCl₂ (1 equiv.), paraformaldehyde (1.1 equiv.), HCl in dioxane (1.5 equiv.), THF, 70 °C, 16 h.

Subsequently, PEPPSI-IPent (**35d**) was synthesized in an excellent yield. In our hands, using the original conditions that were used to synthesize PEPPSI-IPr (**35c**) we achieved a better yield than that obtained by Organ and co-workers (65% yield).⁷⁹

Scheme 46. Synthesis of PEPPSI-IPent (**35d**) from NHC **34d**



a. PdCl₂ (1.0 mmol), IPent.HCl (**34d**, 1.1 mmol), K₂CO₃ (5.0 mmol), 3-chloropyridine (4.0 mL), 80 °C, 20 h.

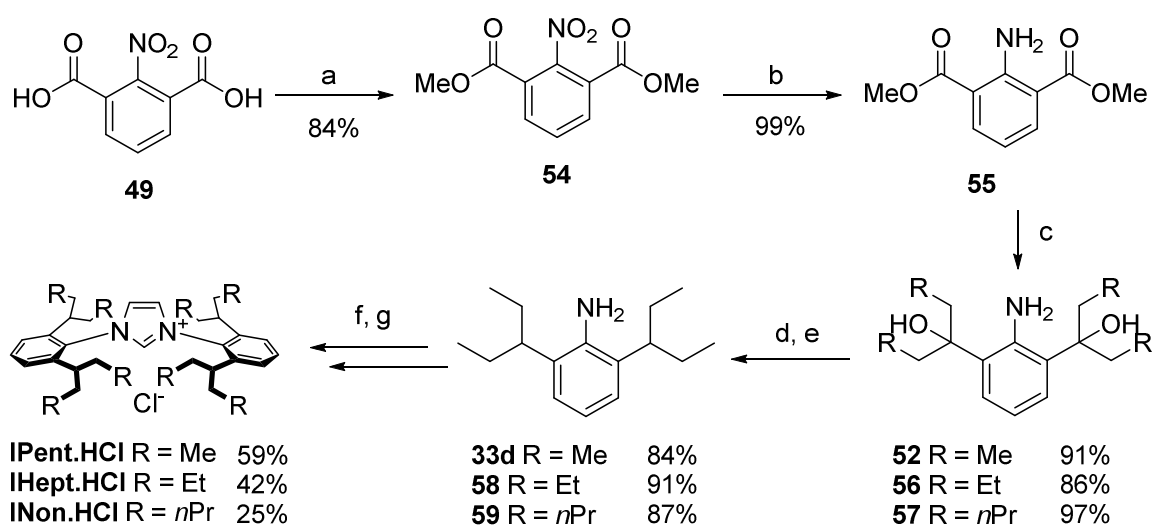
3.6 Conclusion

We successfully synthesized aniline **33d** in 6 steps from 2-nitro-*m*-xylene (**48**) in a 21% overall yield with minimal purification using standard laboratory equipment. This was successfully transformed to PEPPSI-IPent using procedures previously employed for the synthesis of PEPPSI-IPr. Utilising the PEPPSI-IPent synthesized, we can further explore the scope and limitations of chemoselective couplings.

Concurrently with our work, Nolan and co-workers published a very similar synthetic route to the IPent.HCl (**34d**, Scheme 47).¹⁰² Both routes utilize the addition of alkyl

Grignards to an ester to form tertiary alcohols, which was dehydrated and the resulting alkene reduced. All yields were comparable to our route apart from the last step where their dehydration appears cleaner, resulting in a higher yield. The scope of this route was successfully expanded to other NHCs with longer alkyl chains. Nolan and co-workers describe the NHCs with longer alkyl chains (IHept and INon) following the trend from IPent as part of the “ITent” family.

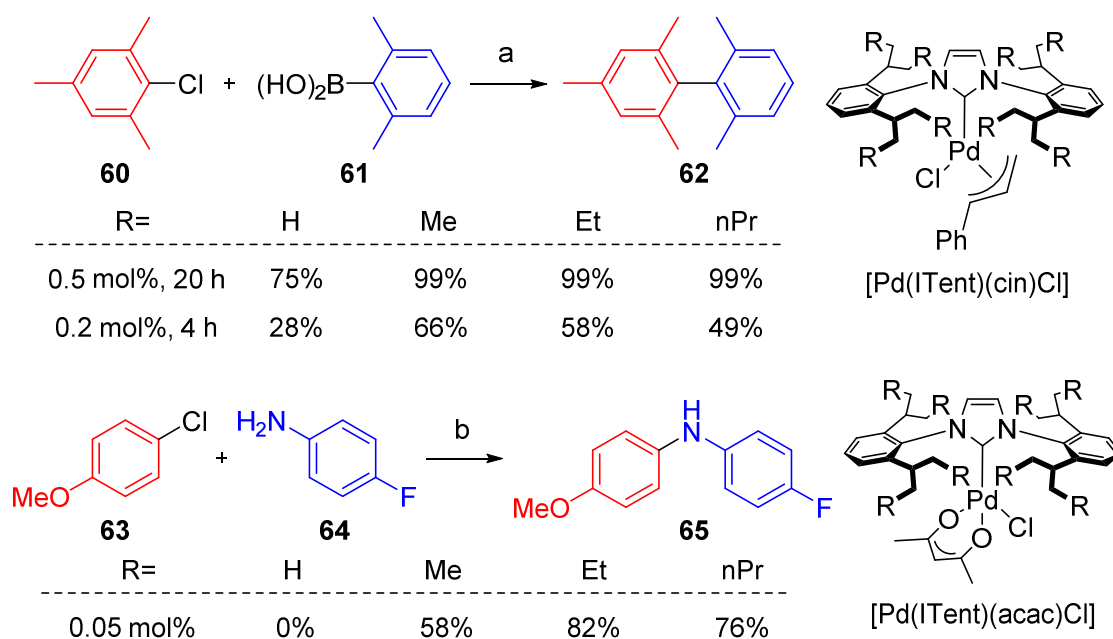
Scheme 47. Nolan and co-workers synthetic route to ITent.HCl salts¹⁰²



a) **49** (1 equiv.), H₂SO₄ (3.5 equiv.), MeOH, reflux, overnight; b) **54** (1 equiv.), 10% Pd/C (1.2 mol%), H₂, AcOEt, RT, 20 h; c) **55** (1 equiv.), alkylbromide RCH₂Br (R=Me, Et, *n*Pr, 8 equiv.), Mg (9 equiv.), THF, 0 °C to RT, 1 – 2 h; d) H₂SO₄ (10 equiv.), THF, 100 °C, 1 – 2 h; e) 10% Pd/C (10 mol%), H₂, EtOH, reflux, 6 – 48 h; f) Glyoxal (1 equiv.), **33d/58/59** (1.6 equiv.), formic acid (a few drops), methanol, RT, 3 - 4 h; g) diimine (1 equiv.), ZnCl₂ (1 equiv.), paraformaldehyde (1.1 equiv.), HCl in dioxane (1.5 equiv.), THF, 70 °C, 3 h.

Nolan and co-workers report similar activity for new palladium NHC complexes for the Suzuki coupling of **60** and **61** between [Pd(IPent)(cin)Cl], [Pd(IHept)(cin)Cl] and [Pd(INon)(cin)Cl]. A greater difference was observed with [Pd(IHept)(acac)Cl] and [Pd(INon)(acac)Cl] showing greater activity for Buchwald Hartwig aminations compared with [Pd(IPent)(acac)Cl] (Figure 12).

Figure 12. Comparison of ITent palladium complexes¹⁰²



a. 2-chloromesitylene (0.5 mmol), 2,6-dimethylbenzene boronic acid (1.0 mmol), KO^tBu (1.5 mmol), [Pd(ITent)(cin)Cl], toluene (2 mL), 65 °C; b. 4-chloroanisole (0.5 mmol), 4-fluoroaniline (0.55 mmol), KO^tBu (0.5 mmol), 0.05% [Pd(ITent)(acac)Cl], toluene (1.0 mL), 80 °C, 20 h; c. Conversion to coupling product based on starting aryl chloride by GC-MS.

3.7 References

- (79) Organ, M. G.; Calimsiz, S.; Sayah, M.; Hoi, K. H.; Lough, A. J. *Angew. Chemie Int. Ed.* **2009**, *48*, 2383.
- (90) Organ, M. G.; Chass, G.; Fang, D.-C.; Hopkinson, A.; Valente, C. *Synthesis* **2008**, 2776.
- (91) O'Brien, C. J.; Kantchev, E. A. B.; Valente, C.; Hadei, N.; Chass, G. A.; Lough, A.; Hopkinson, A. C.; Organ, M. G. *Chem. Eur. J.* **2006**, *12*, 4743.
- (92) Valente, C.; Calimsiz, S.; Hoi, K. H.; Mallik, D.; Sayah, M.; Organ, M. G. *Angew. Chemie Int. Ed.* **2012**, *51*, 3314.
- (93) *Sigma Aldrich* Cat. No. 732117.
- (94) Tsimmerman, M.; Mallik, D.; Matsuo, T.; Otani, T.; Tamao, K.; Organ, M. G. *Chem. Commun.* **2012**, 48, 10352.
- (95) Steele, B. R.; Georgakopoulos, S.; Micha-Screttas, M.; Screttas, C. G. *Euro. J. Org. Chem.* **2007**, 2007, 3091.
- (96) Çalimsiz, S.; Organ, M. G. *Chem. Commun.* **2011**, 47, 5181.

- (97) See experimental for details.
- (98) Pompeo, M.; Froese, R. D. J.; Hadei, N.; Organ, M. G. *Angew. Chemie Int. Ed.* **2012**, *51*, 11354.
- (99) Liu, C.-Y.; Knochel, P. *Org. Lett.* **2005**, *7*, 2543.
- (100) Wang, Q.; Qu, D.-H.; Ren, J.; Chen, K.; Tian, H. *Angew. Chemie Int. Ed.* **2004**, *43*, 2661.
- (101) Bowman, W. R.; Fletcher, A. J.; Pedersen, J. M.; Lovell, P. J.; Elsegood, M. R. J.; Hernández López, E.; McKee, V.; Potts, G. B. S. *Tetrahedron* **2007**, *63*, 191.
- (102) Meiries, S.; Le Duc, G.; Chartoire, A.; Collado, A.; Speck, K.; Athukorala Arachchige, K. S.; Slawin, A. M. Z.; Nolan, S. P. *Chem. Eur. J.* **2013**, *19*, 17358.

Chapter 4 – Model reactions mediated by PEPPSI-IPent

4.1 Introduction

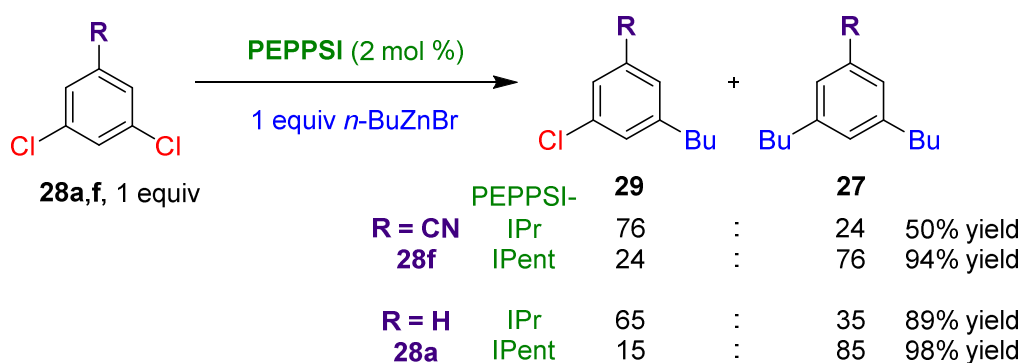
PEPPSI-IPent is a second generation catalyst which has been shown to be more active than PEPPSI-IPr for numerous cross couplings, as described in Chapter 3.⁹² Utilizing the new synthetic route, we tested PEPPSI-IPent in our exploration of chemoselective couplings towards controlled chain growth polymerization of conjugated polymers.

4.2 Comparison of PEPPSI-IPr and -IPent precatalysts

4.2.1 sp^3 - sp^2 Negishi couplings comparing PEPPSI-IPr v PEPPSI-IPent

In Chapter 2, PEPPSI-IPr showed excellent chemoselectivity for full substitution of all polybromo arenes and most substituted *meta*-dichlorobenzenes. Two aryl dichlorides **28a, f** that did not show high di-selectivity in the sp^3 - sp^2 Negishi coupling mediated by PEPPSI-IPr were compared with PEPPSI-IPent (Scheme 48).

Scheme 48. Negishi coupling of dichlorobenzenes and *n*-BuZnBr



^a All reactions were performed on a 0.25 mmol scale of *n*-BuZnBr. LiBr (3 equiv.), THF-DMI (2 : 1), RT, 2 h. Product ratio (**29**:**27**) determined by GCMS analysis of the crude reaction mixture. Yield determined by ¹H NMR analysis of the crude reaction mixture relative to *n*-BuZnBr using mesitylene as an internal standard.

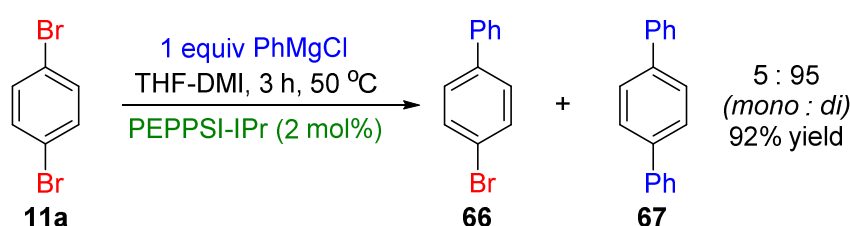
When mediated by PEPPSI-IPr, both 3,5-dichlorobenzonitrile (**28f**) and 1,3-dichlorobenzene (**28a**) showed a product ratio that favoured the formation of the mono-alkylated product **29a** or **29f** (Scheme 48). Conversely, when the coupling was mediated by PEPPSI-IPent the product ratio was dramatically reversed for both

compounds. PEPPSI-IPent showed a “switch on” for the preferential oxidative mechanism that was not observed with PEPPSI-IPr. Not only did the selectivity for the doubly substituted product increase but the yield in both couplings was also increased.

4.2.2 sp^2 - sp^2 Kumada coupling PEPPSI catalyst scan of 1,4-dichlorobenzene

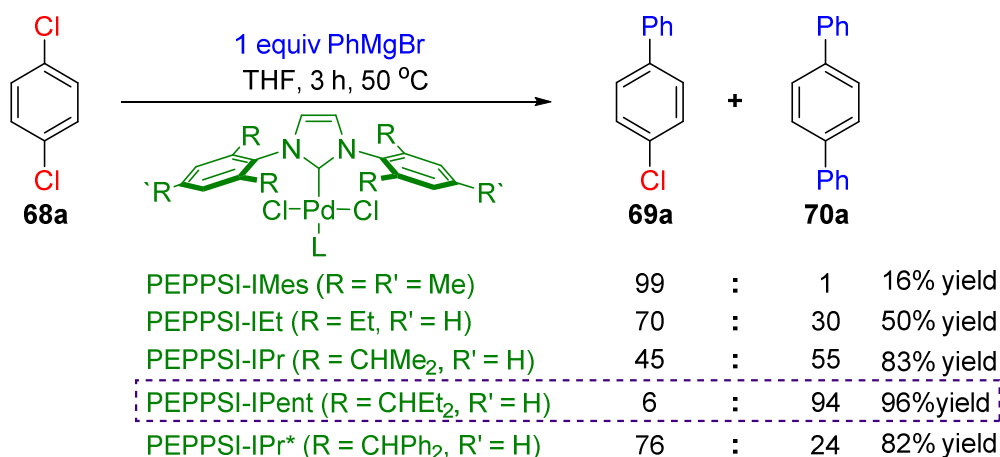
In our group's work, PEPPSI-IPr demonstrated excellent di-selectivity for the coupling of 1,4-dibromobenzene (**11a**) with one equivalent PhMgCl (Scheme 49).⁸⁷

Scheme 49. Kumada coupling of 1,4-dibromobenzene and PhMgCl mediated by PEPPSI-IPr⁸⁷



To explore the difference in reactivity between PEPPSI precatalysts further, we studied the sp^2 - sp^2 Kumada coupling between 1,4-dichlorobenzene (**11a**) and PhMgBr (Scheme 50). A variation in the structure of the NHC ligand was known to significantly alter the Pd-catalyst reactivity.⁹² This would give us an indication of how the steric bulk on the different NHC ligands affected the chemoselectivity of the coupling. Also, the catalyst scan would identify the best catalyst for further studies toward controlled polymerization of π -conjugated polymers.

Scheme 50. Catalyst scan of PEPPSI precatalysts coupling 1,4-dichlorobenzene (**68a**) and PhMgBr^a



^a All reactions were performed on a 0.25 mmol scale of PhMgBr. The catalyst loading was 2 mol%. Product ratio (**69a**:**70a**) determined by GCMS analysis of the crude reaction mixture. Yield determined by ¹H NMR analysis of the crude reaction mixture relative to PhMgBr using mesitylene as an internal standard. L = 3-chloropyridine.

Variation of the NHC ligand led to increasing selectivity for di-substitution in the order IMes < IEt < IPr* < IPr < IPent. When the side chains (R/R') were alkyl groups the chemoselectivity paralleled the trend in both ligand steric demand and catalyst activity. However, PEPPSI-IPr* showed a product ratio similar to PEPPSI-IEt, despite greater steric bulk than PEPPSI-IPent. This suggests that flexible alkyl groups are better than rigid aromatic groups for achieving high di-selectivity. Gratifyingly, PEPPSI-IPent displayed extremely high selectivity for the di-arylation of 1,4-dichlorobenzene (**68**) in an excellent yield (Scheme 50).

4.3 Electrophile scope

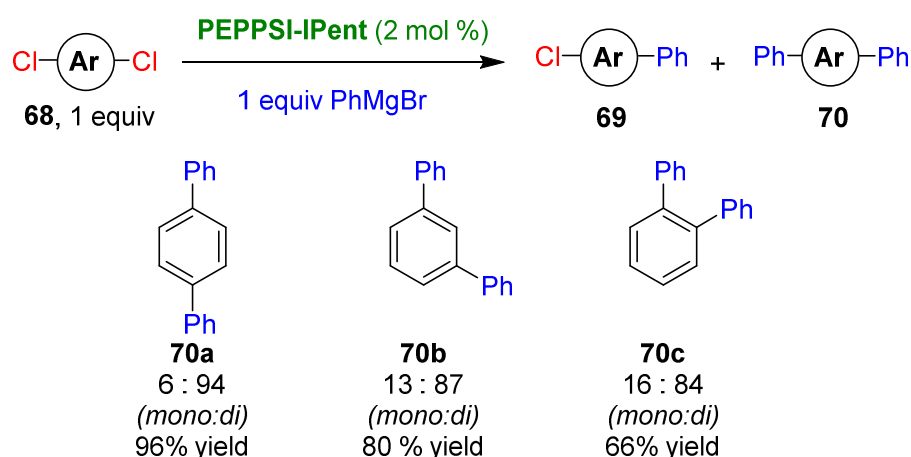
We set out to examine the substrate scope and limitations of the poly-substitution process mediated by PEPPSI-IPent. We tested numerous chloroarenes with multiple C-Cl bonds to expand the scope of the electrophilic coupling partner using PhMgBr as the Grignard reagent. This allowed us to directly compare the polychloroarenes to highlight strengths

and weaknesses in monomer structure with a view to examining polymerizations mediated by PEPPSI-IPent.

4.3.1 Regioisomers of dichlorobenzene

Firstly, the effect of the relative positions of the C-Cl bonds on the benzene ring on the chemoselectivity was explored (Scheme 51).

Scheme 51. Kumada coupling of regioisomers of dichlorobenzene mediated by PEPPSI-IPent



^a All reactions were performed on a 0.25 mmol scale of PhMgBr. THF, 50 °C, 3 h. Product ratio (**69**:**70**) determined by GCMS analysis of the crude reaction mixture. Yield determined by ¹H NMR analysis of the crude reaction mixture relative to PhMgBr using mesitylene as an internal standard.

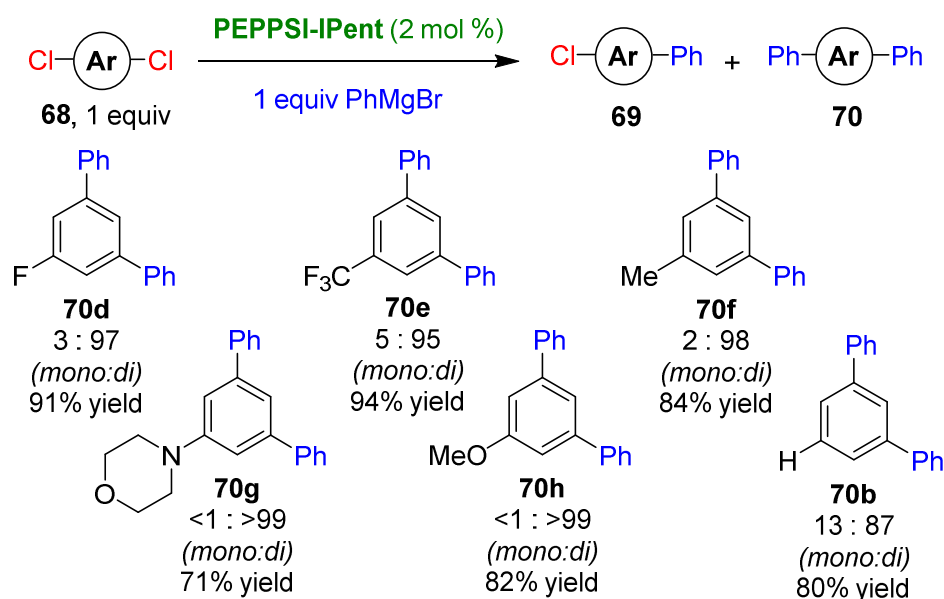
Variation in the relative orientation of the C-Cl moieties led to small changes in the reaction outcome with the selectivity falling from 6:94 for 1,4-dichlorobenzene (**70c**) to 16:84 in the case of sterically hindered 1,2-dichlorobenzene (**68c**). The yield of the coupling decreased as the C-Cl bonds were closer on the aromatic ring. Interestingly this trend is opposite to that observed by Dong and Hu for the model Suzuki couplings mediated by Pd(0)/P(*t*-Bu)₃, in which they found decrease in di-selectivity and yield as the bromines moved from *ortho* to *para*.⁵⁸

4.3.2 Substituted meta-dichlorobenzenes

In Chapter 2 the reactions with PEPPSI-IPr demonstrated the addition of most substituents (R) *meta* to two C-Cl bonds on a benzene ring increased dramatically the di-

selectivity for the sp^3 - sp^2 Negishi coupling ($R = CF_3, F, OMe, Me, <4: >96$ mono:di, Table 3). Therefore, *meta*-substituted dichlorobenzenes were subjected to the Kumada coupling mediated by PEPPSI-IPent in an attempt to increase the chemoselectivity relative to unsubstituted 1,3-dichlorobenzene (**70b**) which already showed high di-selectivity (Scheme 52).

Scheme 52. Kumada coupling of regioisomers of *meta*-substituted dichlorobenzene mediated by PEPPSI-IPent^a



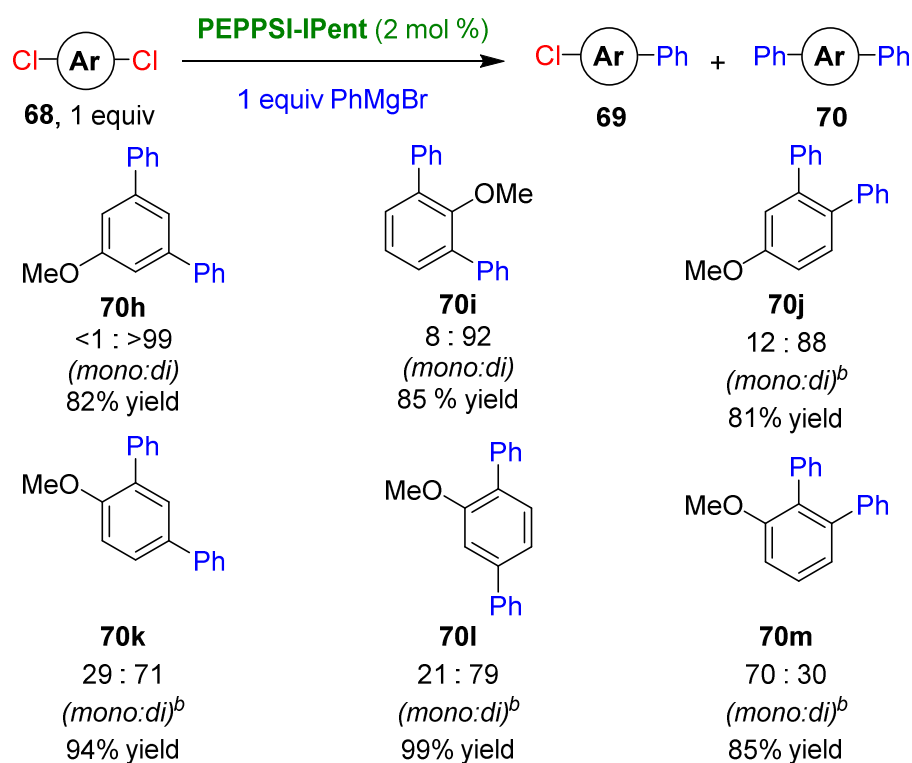
^a All reactions were performed on a 0.25 mmol scale of PhMgBr. THF, 50 °C, 3 h. Product ratio (**69**:**70**) determined by GCMS analysis of the crude reaction mixture. Yield determined by ¹H NMR analysis of the crude reaction mixture relative to PhMgBr using mesitylene as an internal standard.

As predicted, all substrates with either an electron withdrawing (**70d-e,h**) or electron donating (**70f-g**) displayed excellent di-selectivities, in good to excellent yields.

4.3.3 Regioisomers of dichloroanisole

Excellent di-selectivity was observed for the coupling of 3,5-dichloroanisole (**70h**). We sought to investigate the effect on the chemoselectivity of its regioisomers (Scheme 53). The regioisomers would show different electronic and steric affects on both C-Cl bonds which should have resulted in a lower di-selectivity.

Scheme 53. Kumada coupling of regioisomers of dichloroanisole mediated by PEPPSI-IPent^a



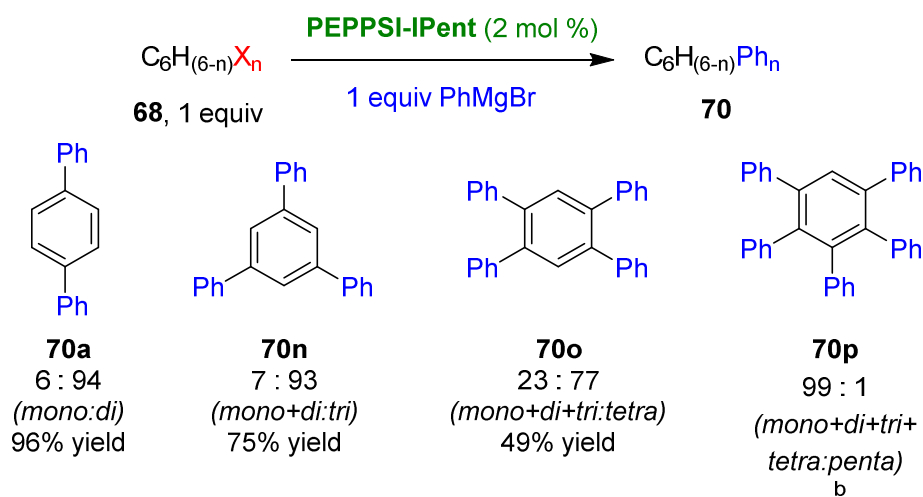
^a All reactions were performed on a 0.25 mmol scale of PhMgBr. THF, 50 °C, 3 h. Product ratio (**69:70**) determined by GCMS analysis of the crude reaction mixture. Yield determined by ¹H NMR analysis of the crude reaction mixture relative to PhMgBr using mesitylene as an internal standard.^b Ratio of both mono-coupled to di-coupled products.

Examination of a series of regioisomers of dichloroanisole (**60h-m**) demonstrated that the relative position of the substituents has an appreciable effect on the reaction selectivity; while highly symmetrical **70h** and **70i** were obtained with high selectivity, when the methoxy substituent was placed *ortho* to only one of the C-Cl bonds, di-selectivity was significantly reduced (**70k**, 29:71 and **70l**, 21:79) or even reversed (**70m**, 70:30).

4.3.4 Polychlorobenzenes

Subsequently we investigated the chemoselectivity of the Kumada coupling on substrates containing more than two C-Cl bonds.

Scheme 54. Kumada coupling of polychlorobenzenes mediated by PEPPSI-IPent^a



^a All reactions were performed on a 0.25 mmol scale of PhMgBr. THF, 50 °C, 3 h. Product ratio (other substituted products:exhaustive substitution **70**) determined by GCMS analysis of the crude reaction mixture. Yield determined by ¹H NMR analysis of the crude reaction mixture relative to PhMgBr using mesitylene as an internal standard. ^b Yield unable to be determined.

Benzenes substituted with 3 or 4 C-Cl bonds were found to lead to exhaustive substitution with high selectivities in favour of the fully-substituted products over other substituted products for aryl chlorides **68n** and **68o**. Interestingly, when 5 C-Cl bonds are present almost no penta-substitution was observed. This demonstrated that this effect is not limited to di-chloroarenes, however the selectivity for exhaustive substitution and yield decreased as more C-Cl bonds were on the benzene ring.

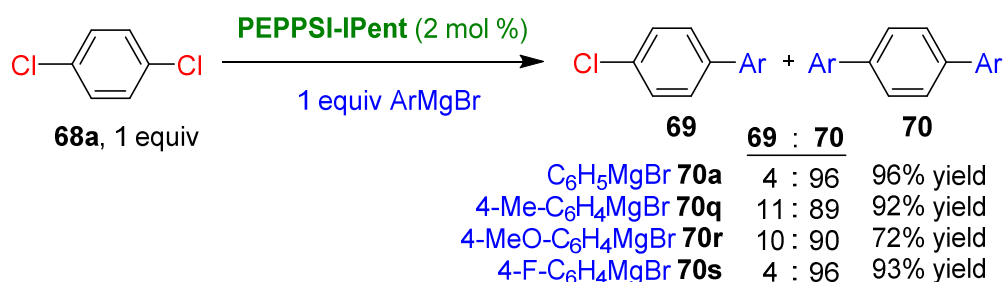
4.4 Nucleophile scope

In order to ascertain the effect of the nature of the nucleophile on the observed product selectivity we studied the reaction of 1,4-dichlorobenzene (**68a**) with a range of substituted Grignard reagents and other nucleophiles.

4.4.1 Grignard scope

With PhMgBr showing excellent di-selectivity, we investigated the effect of substituents *para* to the organometallic bond with other commercially available Grignard reagents .

Scheme 55. Kumada coupling of 1,4-dichlorobenzene and ArMgBr mediated by PEPPSI-IPent^a

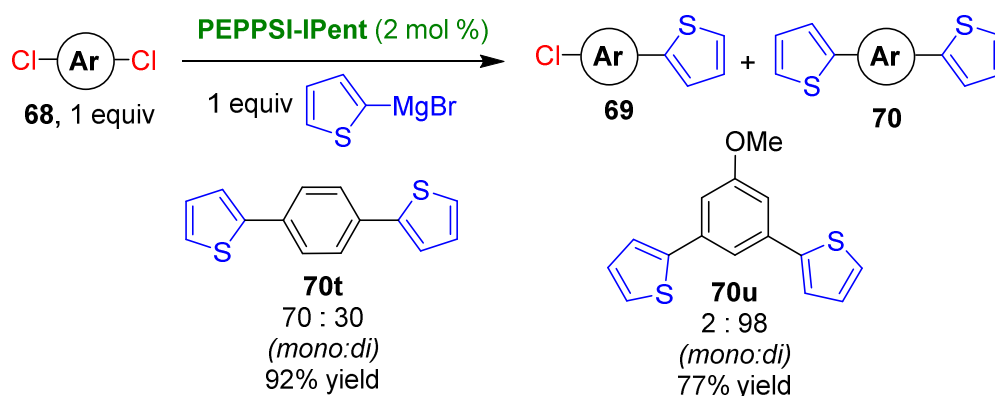


^a All reactions were performed on a 0.25 mmol scale of ArMgBr. THF, 50 °C, 3 h. Product ratio (**69**:**70**) determined by GCMS analysis of the crude reaction mixture. Yield determined by ¹H NMR analysis of the crude reaction mixture relative to ArMgBr using mesitylene as an internal standard.

Both electron-rich (**70q**, **r**) and electron-poor (**70s**) ArMgBr nucleophiles led to di-substituted adducts with high selectivities in good to excellent yields (Scheme 55). However, there was a small reduction in di-selectivity for the electron-rich Grignard reagents compared to PhMgBr.

With the addition of simple functional groups to the Grignard we subsequently tested 2-thienylmagnesium bromide with both 1,4-dichlorobenzene (**68a**) and 3,5-dichloroanisole (**68h**).

Scheme 56. Kumada coupling of dichloroarenes and 2-thienylmagnesium bromide^a



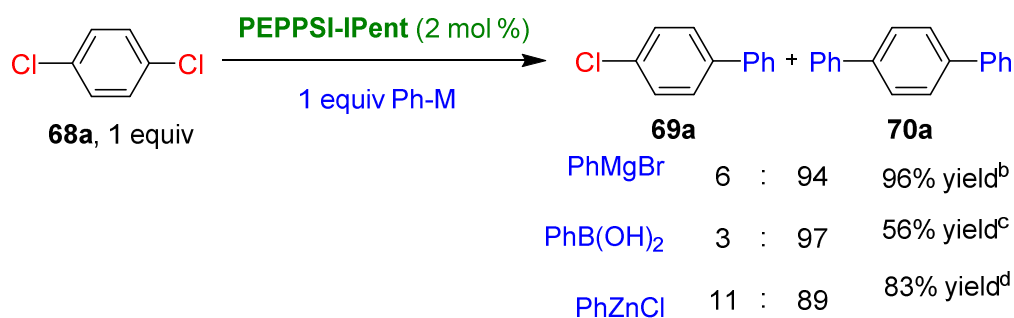
^a All reactions were performed on a 0.25 mmol scale of 2-thienylmagnesium bromide. THF, 50 °C, 3 h. Product ratio (**69**:**70**) determined by GCMS analysis of the crude reaction mixture. Yield determined by ¹H NMR analysis of the crude reaction mixture relative to ArMgBr using mesitylene as an internal standard.

For the coupling between this heteroaryl thienyl Grignard reagent and **68a**, a complete loss of selectivity was observed. Interestingly, excellent di-selectivity was found on coupling with 3,5-dichloroanisole (**68h**).

4.4.2 Other sp^2 - sp^2 couplings

All the sp^2 - sp^2 couplings described previously have been the Kumada coupling of Grignard reagents to aryl chlorides. There are many advantages to using other sp^2 - sp^2 C-C bond couplings including functional group tolerance. Suzuki and Negishi couplings mediated by PEPPSI catalysts have been described by Organ and co-workers.^{86,91}

Scheme 57. Suzuki and Negishi couplings of 1,4-dichlorobenzene mediated by PEPPSI-IPent^a



^a All reactions were performed on a 0.25 mmol scale of PhM. Product ratio (**69a**:**70a**) determined by GCMS analysis of the crude reaction mixture. Yield determined by ¹H NMR analysis of the crude reaction mixture relative to Ph-M using mesitylene as an internal standard. ^b THF, 50 °C, 3 h. ^c K₂CO₃ (3.0 equiv.), 1,4-dioxane, 60 °C, 12 h. ^d THF-NMP (1:1), 30 °C, 2 h.

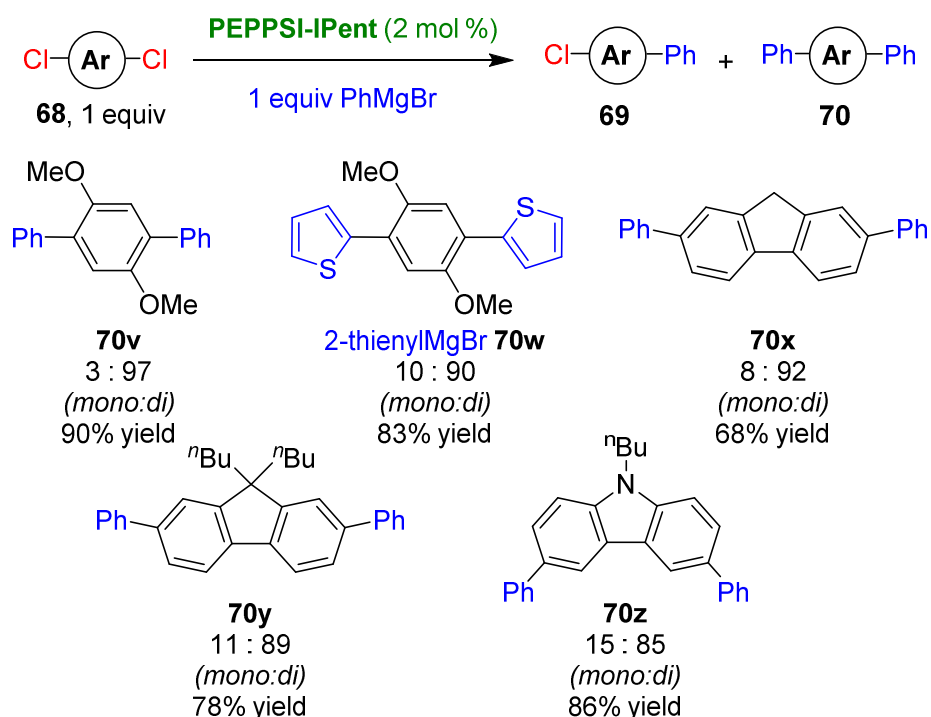
Remarkably, the observed di-selectivity is not limited to the Kumada coupling: the coupling of PhB(OH)₂ or PhZnCl with **68a** both proceeded with high di-selectivity (3:97 and 11:89, respectively). The yields are lower than for the Kumada coupling; however the conditions used were not fully optimized.

4.5 Monomer substrates

4.5.1 Kumada couplings

With numerous simple functionalized polychlorobenzenes and organometallics explored, we extended our study to a number of di-chloroarene derivatives of monomers commonly used in the synthesis of conjugated organic polymers (Scheme 58).

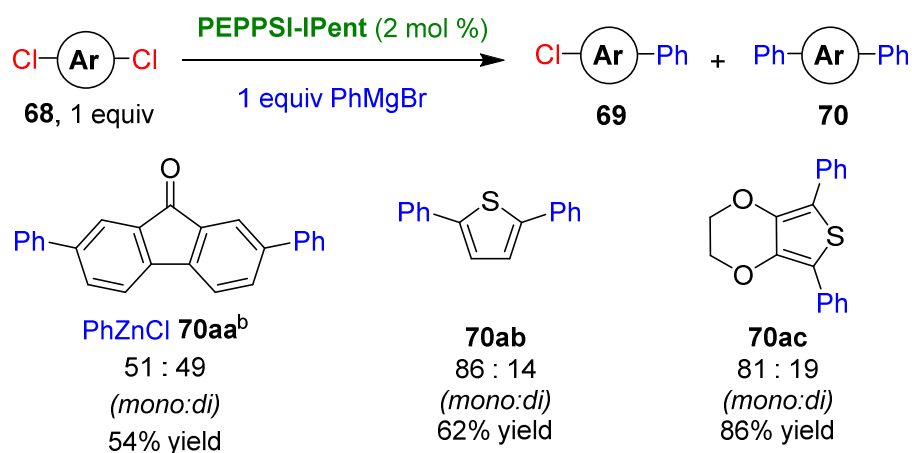
Scheme 58. Di-selective Kumada coupling of monomer derivatives mediated by PEPPSI-IPent



^a All reactions were performed on a 0.25 mmol scale of PhM. THF, 50 °C, 3 h. Product ratio (**69**:**70**) determined by GCMS analysis of the crude reaction mixture. Yield determined by ¹H NMR analysis of the crude reaction mixture relative to ArMgBr using mesitylene as an internal standard.

Gratifyingly, models of common p-type monomers including 1,4-dimethoxybenzene (**68v**), fluorene (**68x** and **68y**) and carbazole (**68z**) all displayed high selectivity for di-substitution when reacted with PhMgBr. This selectivity was maintained when 2-thienyl Grignard was used as the nucleophile (**68w**) all in good to excellent yields.

Scheme 59. Non-selective Kumada coupling of monomer derivatives mediated by PEPPSI-IPent



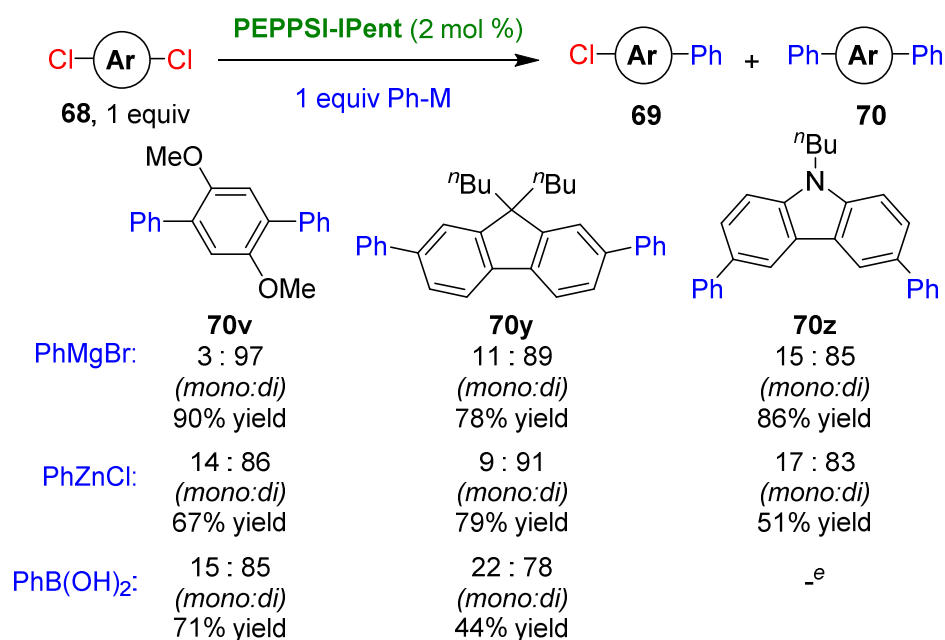
^a All reactions were performed on a 0.25 mmol scale of PhM. THF, 50 °C, 3 h. Product ratio (**69:70**) determined by GCMS analysis of the crude reaction mixture. Yield determined by ¹H NMR analysis of the crude reaction mixture relative to PhMgBr using mesitylene as an internal standard. ^b THF-NMP (1:1), 30 °C, 2 h.

Disappointingly, electron-deficient dichloro-fluorenone **68aa** and models of monomers dichlorothiophene, **68ab**, and dichloro-EDOT, **68ac**, were either non-selective (**68aa**) or gave rise to the product of mono-substitution (**68ab** and **68ac**). For the fluorenone derivative (**68aa**), PhZnCl was used instead of PhMgBr as the Grignard did not yield any mono- (**69aa**) or di-arylation (**70aa**) products.

4.5.2 Suzuki and Negishi couplings of monomer derivatives

The monomer substrates that showed high di-selectivity were subsequently tested for their chemoselectivities in the PEPPSI-IPent mediated $\text{sp}^2\text{-sp}^2$ Suzuki and Negishi couplings.

Scheme 60. sp^2 - sp^2 Couplings of monomer derivatives mediated by PEPPSI-IPent



^a All reactions were performed on a 0.25 mmol scale of PhM. Product ratio (**69**:**70**) determined by GCMS analysis of the crude reaction mixture. Yield determined by ¹H NMR analysis of the crude reaction mixture relative to Ph-M using mesitylene as an internal standard. ^b THF, 50 °C, 3 h. ^c K₂CO₃ (3.0 equiv.), 1,4-dioxane, 60 °C, 12 h. ^d THF-NMP (1:1), 30 °C, 2 h. ^e Not performed.

In all cases examined, Kumada couplings performed best, with Negishi and Suzuki couplings providing comparable or slightly lower selectivities, typically with lower yields.

4.6 Conclusions

The experiments covered in this chapter have demonstrated that PEPPSI-IPent is a better candidate than PEPPSI-IPr for our further studies on controlled polymerization of conjugated polymers from cheap chloroarenes.

PEPPSI-IPent showed a dramatic improvement in di-selectivity for sp^3 - sp^2 Negishi couplings compared to PEPPSI-IPr. This was further demonstrated in a PEPPSI precatalyst scan with 1,4-dichlorobenzene, where a trend in di-selectivity followed the size of flexible alkyl groups on the NHC ligand.

A large range of polychlorobenzenes were explored for their chemoselectivities with all functional groups showing high di-selectivity when the C-Cl bonds were *meta* to each other and even when 4 C-Cl bonds were on one benzene ring. However, di-selectivity was lost with regioisomers of dichloroanisole when one C-Cl bond is *ortho* to the methoxy group.

Based on these results we propose that PEPPSI-IPent will mediate chain-growth polymerizations of electron-rich chloro-fluorene-, chloro-carbazole- and chloro-1,4-dialkoxybenzene-type monomers. Further catalyst development is needed before this approach can be extended to thiophene and p-type monomers. Even more reactive catalysts with greater steric bulk will be required for the catalyst transfer polymerization of electron deficient or thiophene monomers.

4.7 References

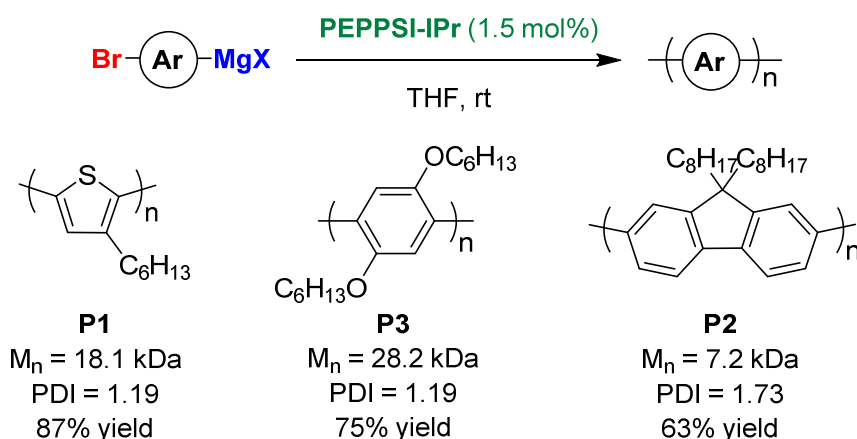
- (58) Dong, C.-G.; Hu, Q.-S. *J. Am. Chem. Soc.* **2005**, *127*, 10006.
- (86) Organ, M. G.; Avola, S.; Dubovyk, I.; Hadei, N.; Kantchev, E. A. B.; O'Brien, C. J.; Valente, C. *Chem. Eur. J.* **2006**, *12*, 4749.
- (87) Larrosa, I.; Somoza, C.; Banquy, A.; Goldup, S. M. *Org. Lett.* **2011**, *13*, 146.
- (91) O'Brien, C. J.; Kantchev, E. A. B.; Valente, C.; Hadei, N.; Chass, G. A.; Lough, A.; Hopkinson, A. C.; Organ, M. G. *Chem. Eur. J.* **2006**, *12*, 4743.
- (92) Valente, C.; Calimsiz, S.; Hoi, K. H.; Mallik, D.; Sayah, M.; Organ, M. G. *Angew. Chemie Int. Ed.* **2012**, *51*, 3314.

Chapter 5 – Polymerizations mediated by PEPPSI precatalysts

5.1. Introduction

Inspired by previous work in our group, McNeil and co-workers demonstrated the PEPPSI-IPr mediated living chain growth polymerizations of both phenylene- and thiophene-based Grignard monomers. However, fluorene-based monomers did not proceed in a living manner (Scheme 61).⁸⁸

Scheme 61. Chain growth polymerization mediated by PEPPSI-IPr



5.2. Aims

Our research has shown that the NHC ligand on PEPPSI precatalysts dramatically affects the chemoselectivity of couplings between aryl dihalides with one equivalent of an organometallic reagent. An increase in steric bulk of flexible alkyl groups on the flanking aromatics of the NHC ligand resulted in an increase in preferential oxidative addition of palladium to the other C-X bond on the same molecule.

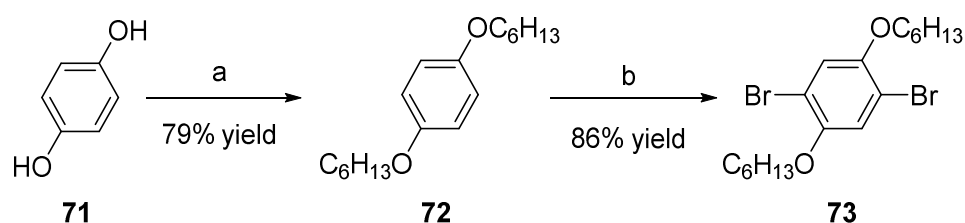
We attempted to explore the effect different PEPPSI precatalysts have on the polymerization of Grignard monomers as described by McNeil and co-workers.

5.3. Kumada polymerizations of phenylene-based monomer

5.3.1 Starting material synthesis

We attempted to replicate the results obtained by McNeil and co-workers with the phenylene-based monomer. We chose the phenylene-based monomer **74** as its precursor **73** was easily accessible from cheap commercial starting materials on multigram scale (Scheme 62).

Scheme 62. Synthesis of phenylene-based monomer precursor

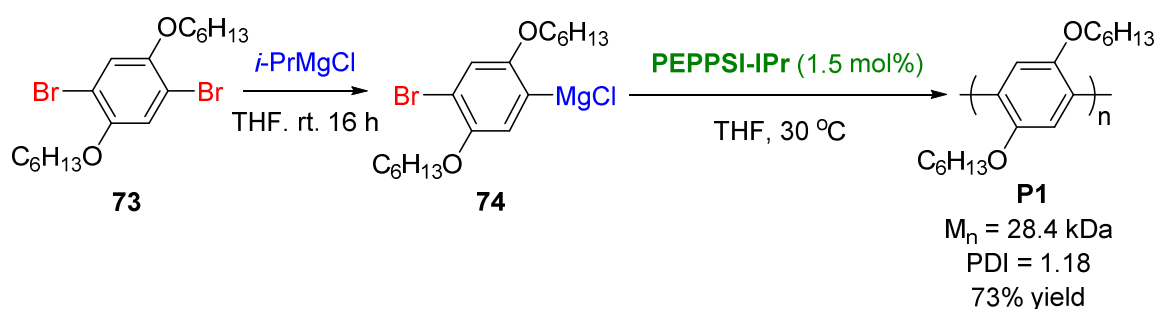


a. *n*-hexylbromide (2.5 equiv.), K_2CO_3 (2.5 equiv.), DMF, 110 °C, 24 h; b. Br_2 (2.5 equiv.), $CHCl_3$, 0 °C - rt, 1 h.

5.3.2 Replication of previous results

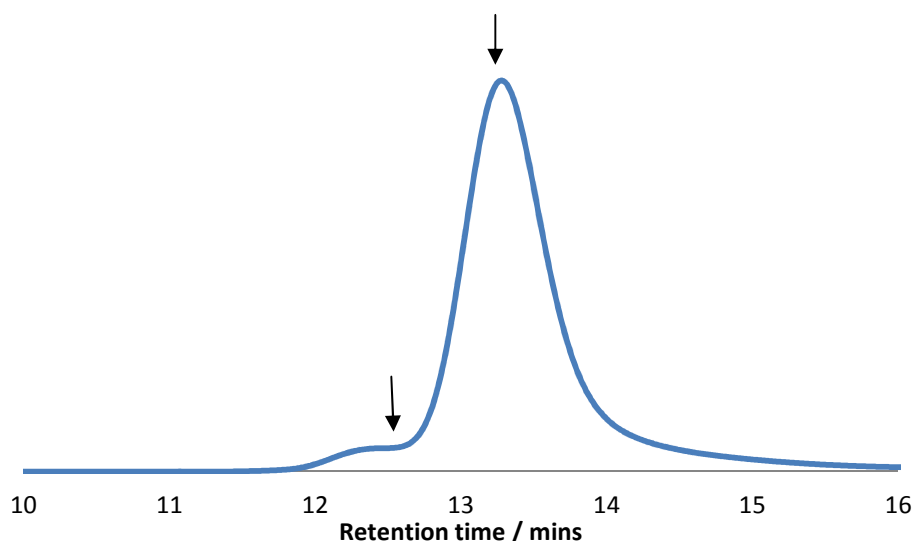
Following the literature procedure reported by McNeil and co-workers, we formed monomer **74** from halogen metal exchange with *i*-PrMgCl and initiated the polymerization with PEPPSI-IPr (Scheme 63). After an acidic work up, the organic phase was concentrated and washed with methanol to yield the polymer without purification.

Scheme 63. Replication of polymerization of monomer **74** mediated by PEPPSI-IPr



GPC analysis of the polymer showed similar chain length and distribution to the published data in a comparable yield. However, deeper analysis of the GPC spectra showed an additional peak at approximately double the molecular weight of the main peak (Graph 6).

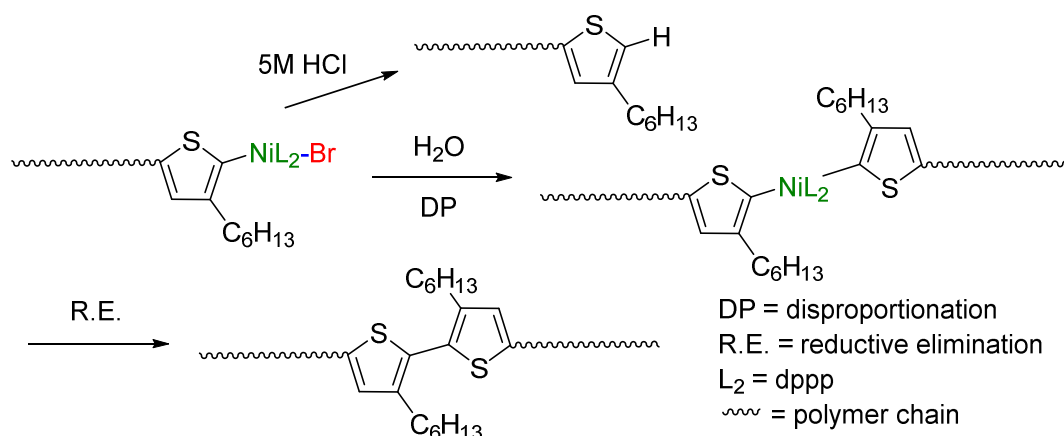
Graph 6. GPC spectrum of the **P1** ($M_n = 28.4$ kDa, PDI = 1.18)



McNeil and co-workers showed that this peak was not seen in their GPC spectra at 60% conversion ($M_n = 22.4$ kDa, PDI = 1.17). Unfortunately, no GPC spectra were reported at a higher conversion so a direct comparison could not be made.

This peak at higher molecular weight was not the first time a phenomenon similar to the one in Graph 6 has been observed. Miyakoshi *et al.*¹⁰³ described a double molecular weight peak that was a result of disproportionation of two living polymer chains for a similar polymerization mediated by a nickel catalyst (Scheme 64). They stopped this peak from forming by quenching the polymer with 5M HCl as opposed to water. However, McNeil and co-workers already used 5M HCl for the quench of the polymerization of monomer **74**.

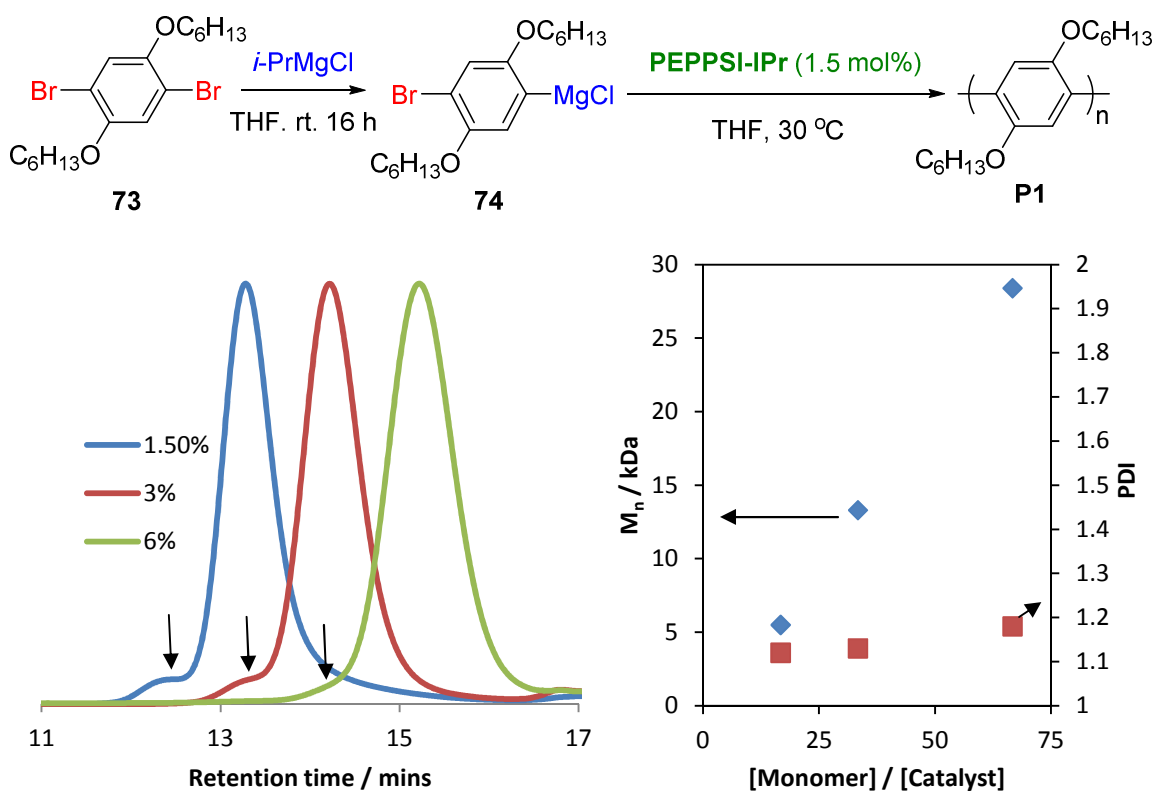
Scheme 64. Mechanism of disproportionation upon quenching with water



5.3.3 Investigation into extra peak

Before subjecting a range of PEPPSI precatalysts to the polymerization conditions, the extra peak in the GPC spectra was investigated. To gauge whether this peak formed at the end of the polymerization when the concentration of monomer was low, or as a result of the long chain length of the polymer, the catalyst loading was varied (Figure 13).

Figure 13. The effect of the catalyst loading on the polymerization of monomer **74**

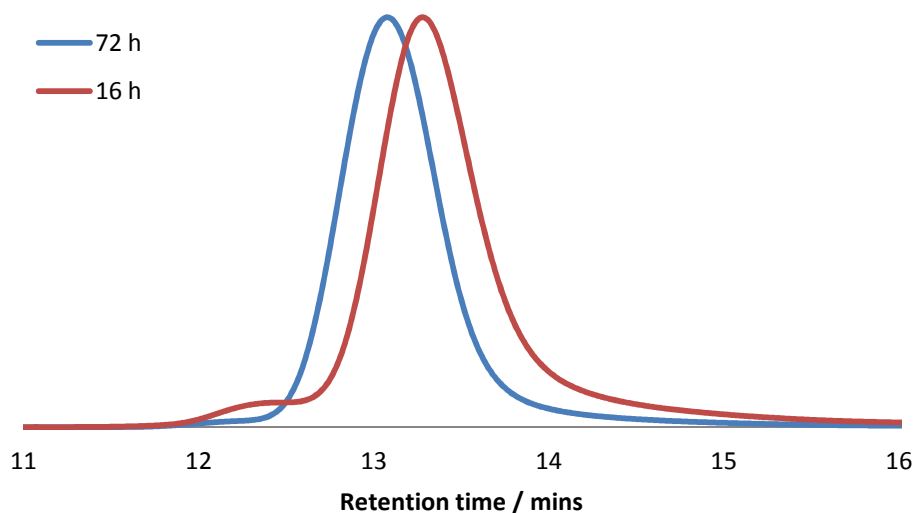


As the catalyst loading increased, the M_n and PDI decreased as expected. The prominence of the double molecular weight peak also decreased, but was still visible at 6% catalyst loading.

The higher molecular weight peak increased the distribution of polymer chain lengths. We sought to optimize the conditions for the polymerization of monomer **74** to stop this peak from forming, resulting in an even more controlled polymerization.

This was achieved serendipitously by leaving the halogen metal exchange to form monomer **74** for a longer period of time. Instead of allowing the monomer synthesis to be left overnight (16 hours), a batch of monomer **74** was left for 72 hours under an atmosphere of nitrogen. The polymerization with monomer **74** that had been left for longer led to a unimodal distribution of molecular weight. The M_n was higher (35.8 kDa) and the PDI reduced to just 1.11 (Graph 7).

Graph 7. Comparison of reported monomer synthesis for different lengths of time

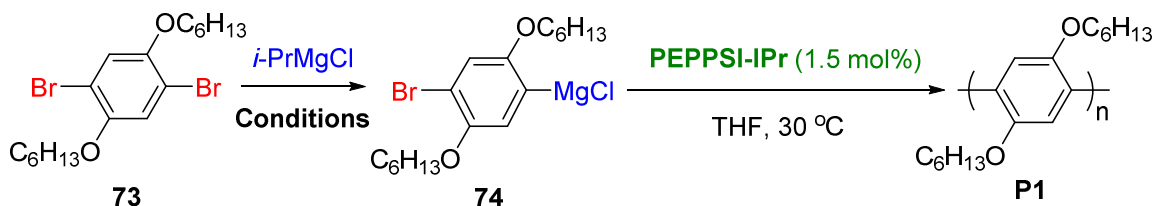


This result suggested that the source of the extra peak at higher molecular weight was a result of how monomer **74** was formed. Therefore, the halogen metal exchange procedure was modified to repeat this result.

5.3.4 Optimization of monomer synthesis

Extending the period of time the monomer was left stirring eliminated the extra peak at higher molecular weight. We optimized the monomer formation to obtain the best M_n and PDI (Table 7).

Table 7. Different conditions for the synthesis of monomer **74** and subsequent polymerization



Entry	Conditions	M_n / kDa	PDI	Yield
1	0.65 M $i\text{-PrMgCl}$ in THF, rt, 16 h	28.4	1.18	73%
2	1.8 M $i\text{-PrMgCl}$ in THF, rt, 16h then 0.65 M in THF, 4 h	37.7	1.10	95%

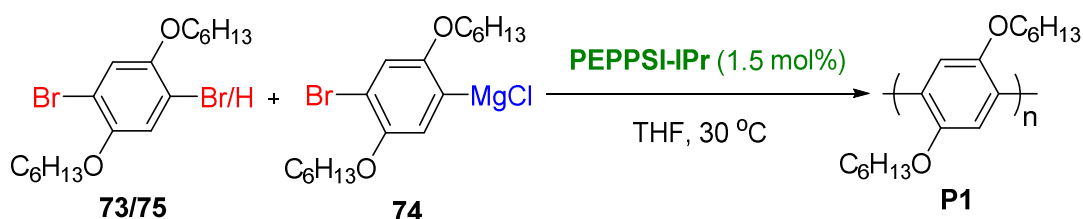
Performing the monomer synthesis in the minimum amount of THF for the addition of $i\text{-PrMgCl}$ followed by dilution gave the best polymer properties. The optimized conditions for the monomer synthesis not only eliminated the higher molecular weight peak but also increased the M_n (37.7 kDa) and lowered the PDI to just 1.10. Thus the properties of the polymer were dramatically improved with a small change in the monomer synthesis.

5.3.5 Addition of additives

The monomer synthesis used an excess of dibromide **73** (1 equiv.) relative to $i\text{-PrMgCl}$ (0.9 equiv.) and therefore dibromide **73** was present in the polymerization. McNeil and co-workers have already demonstrated that the excess dibromide does not greatly affect the polymerization by PEPPSI-IPr. However, ^1H NMR and GC-MS analysis of the monomer after a quench with iodine showed that there was some protodehalogenated monomer (**75**) present as well.

With the effect of impurity **75** on the polymerization unknown, an additional 0.5 equivalents of the additive, relative to the amount of monomer was added to observe if the impurity **75** had an effect on the polymerization.

Table 8. The effect of additives **73** and **75** in the polymerization



Entry	Additive	M_n / kDa	PDI
1	None	37.7	1.10
2	73	37.0	1.11
3	75	40.4	1.10

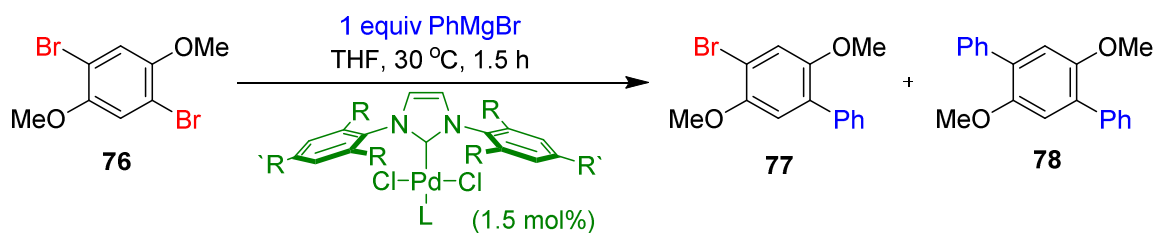
The addition of both dibromide **73** and impurity **75** had a minimal effect on the polymerization mediated by PEPPSI-IPr. The PDI remained constant and the M_n increased only slightly with the addition of impurity **75**.

5.4 Comparison of model reactions and polymerizations of PEPPSI precatalysts

5.4.1 Chemoselective couplings of dibromide monomer substrate

The conditions used for the Kumada couplings in the previous chapter were different to that used for the polymerization. The temperature, catalyst loading, concentration and reaction time were all variables that were different. Therefore the chemoselective coupling of the phenylene-based monomer substrate **76** was performed mediated by PEPPSI precatalysts under the previously described polymerization conditions (Table 9).

Table 9. Kumada coupling of dibromo phenylene-based substrate **76** mediated by PEPPSI precatalysts



Entry	PEPPSI-	77 : 78	Yield
1	IMes (R = R' = Me)	32 : 68	<5%
2	IEt (R = Et, R' = H)	10 : 90	18%
3	IPr (R = CHMe ₂ , R' = H)	2 : 98	68%
4	IPent (R = CHEt ₂ , R' = H)	3 : 97	98%

^a All reactions were performed on a 0.25 mmol scale of PhMgBr. THF, 50 °C, 3 h. Product ratio (77:78) determined by GCMS analysis of the crude reaction mixture. Yield determined by ¹H NMR analysis of the crude reaction mixture relative to PhMgBr using mesitylene as an internal standard. L = 3-chloropyridine.

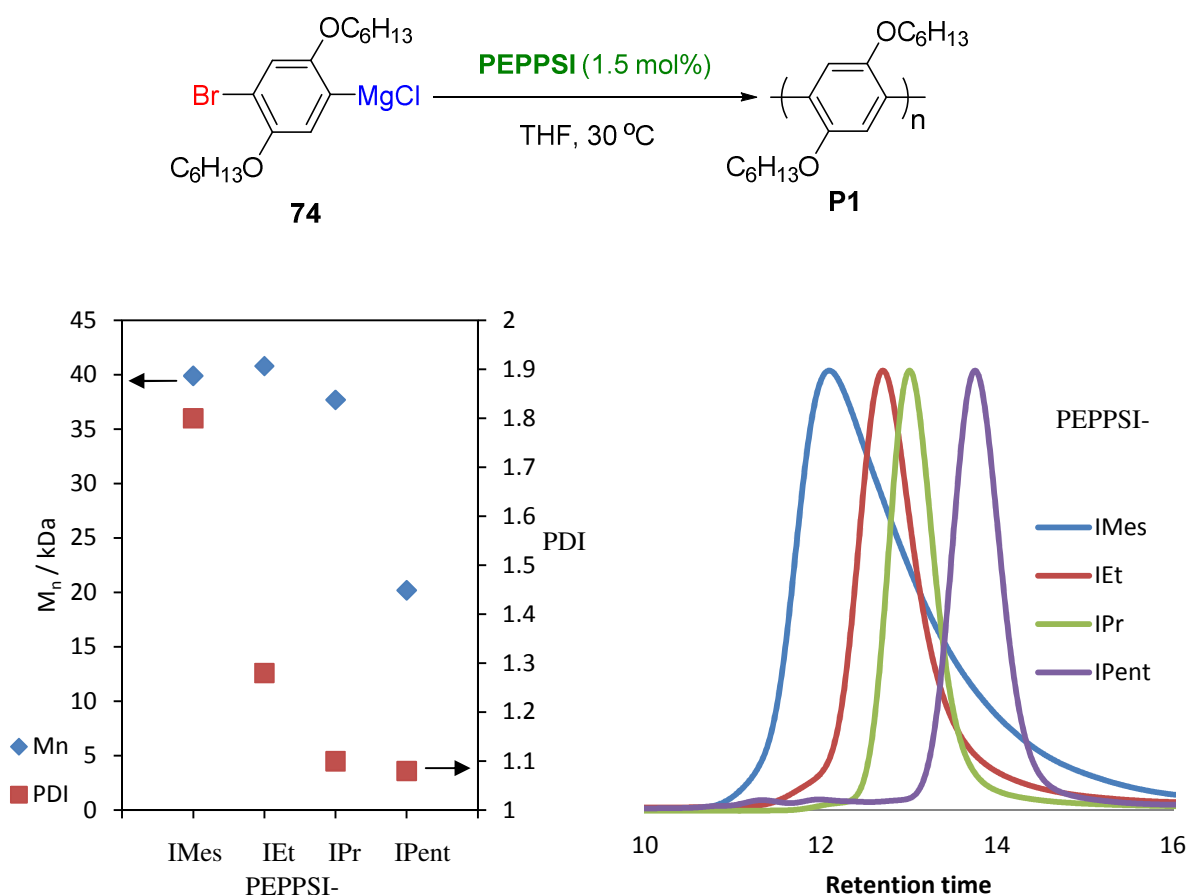
Unsurprisingly, the more steric bulk on the NHC ligand the greater the di-selectivity of the coupling and the greater the yield. Both, PEPPSI-IPr and -IPent both showed comparable selectivities for this coupling, suggesting a similar PDI should be observed with polymerization.

The results suggest that an excellent di-selectivity with a good yield is needed for a PEPPSI precatalyst to be a candidate to initiate chain growth polymerizations. This was encouraging as the selectivity for the dichloro phenylene-based derivative showed the same selectivity (3:97) when mediated by PEPPSI-IPent.

5.4.2 Polymerization of phenylene-based monomer mediated by PEPPSI precatalysts

With optimized conditions for the polymerization of the phenylene-based monomer mediated by PEPPSI-IPr, we looked to gauge the effect of the NHC ligand on the PEPPSI precatalysts with respect to the polymerization. The same four PEPPSI precatalysts were used as in Table 9 to compare the relative product ratios in the chemoselective couplings with dibromide **76** to the M_n and PDI of the polymers obtained.

Figure 14. Polymerization of monomer **74** mediated by PEPPSI precatalysts



PEPPSI-IMes, -IEt and -IPr all resulted in similar M_n , however, PEPPSI-IPent only showed polymer lengths approximately half of the others. There was a clear trend between the size of the steric bulk of the alkyl groups on the NHC and the polymer chain lengths. Surprisingly, the smaller the steric bulk on the NHC, the longer the polymer chains.

Although the M_n for the PEPPSI-IPent polymerization was lower than the others, it was still higher than the ideal living polymerization of 18.8 kDa. This result suggested that PEPPSI-IPent is more easily activated by the monomer than the other PEPPSI precatalysts at the start of the polymerization.

PEPPSI-IMes gave the highest PDI (1.80) which was reduced significantly when PEPPSI-IEt (PDI = 1.28) was used. Both PEPPSI-IPr and PEPPSI-IPent showed narrow

distributions of polymer lengths (PDI = 1.10 and 1.08, respectively). PEPPSI-IMes (95% yield), -IEt (96% yield) and -IPr (95% yield) showed excellent yields for the polymerization. Unfortunately, PEPPSI-IPent gave a much lower yield (59% yield) suggesting catalyst poisoning occurs during the reaction.

5.4.3 Comparison of polymerization properties to chemoselective couplings

There appeared to be a correlation between the di-selectivity of the coupling (Table 9) and the PDI of the polymer formed (Figure 14). A product ratio for the coupling of aryl dibromides of greater than 10:90 resulted in a low distribution of polymer chain lengths (PDI<1.28).

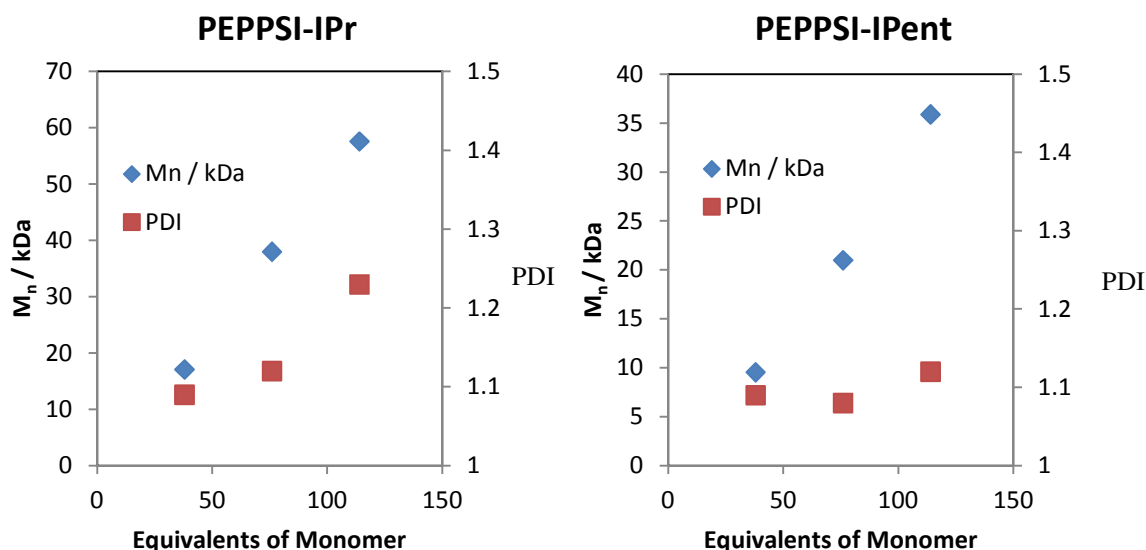
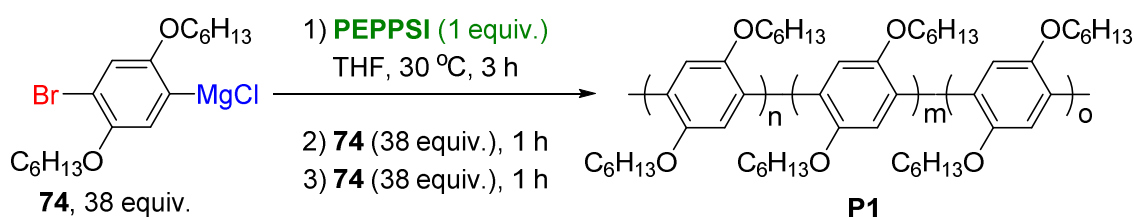
Interestingly the yield of the di-selective couplings appears not to give an indication of whether a PEPPSI precatalyst will mediate a polymerization in a high yield or give a high M_n . PEPPSI-IMes showed almost no yield in the chemoselective couplings, but an excellent yield for the polymerization of monomer **74** where $M_n = 39.9$ kDa.

The degree of polymerization appeared to be independent of how chemoselective a coupling was or its respective yield. It is more likely controlled by the amount of precatalyst activated at the start of the polymerization.

5.5 Block homo-polymerization

With PEPPSI-IPent showing a low M_n relative to PEPPSI-IPr and a lower yield, we investigated if PEPPSI-IPent was still 'living' by repeating the block homo-polymerization experiment described by McNeil and co-workers. Instead of adding one additional portion of 38 equivalents of monomer **74**, we added two lots of 38 equivalents for both PEPPSI-IPr and PEPPSI-IPent (Figure 15).

Figure 15. Block homo-polymerization of monomer **74** mediated by PEPPSI-IPr and -IPent



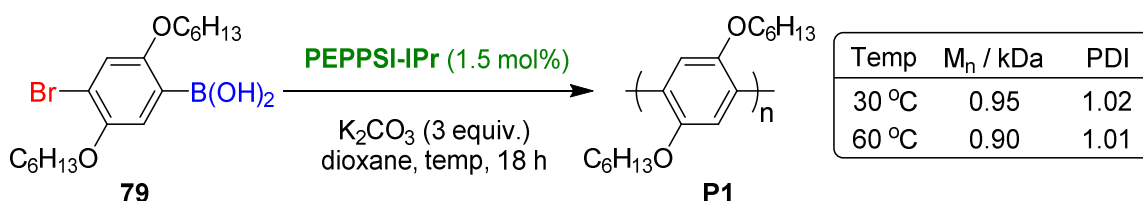
Both PEPPSI-IPr and -IPent gave a linear increase in the M_n , maintaining a low PDI showing both catalysts proceed in a chain growth manner. PEPPSI-IPr showed a slight increase in the PDI upon the third addition of monomer **74** suggesting some catalyst chain termination by catalyst decomposition occurred. In contrast, PEPPSI-IPent did not show an increase in the PDI even after the third addition of monomer.

5.6 Suzuki polymerizations

With the Kumada polymerization mediated by PEPPSI-IPr showing chain growth polymerization, we looked to expand the scope of the polymerizations mediated by PEPPSI-IPr to the Suzuki coupling. The conditions used for chemoselective couplings in Chapter 4 were modified to be similar to the polymerization procedure for the Kumada polymerizations. The concentration of monomer and catalyst were kept the same,

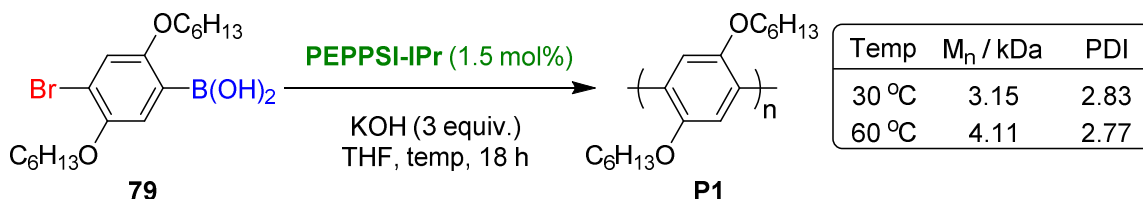
changing the solvent and the addition of potassium carbonate as a base was needed for the catalytic cycle (Scheme 65).

Scheme 65. Polymerization of monomer **79** mediated by PEPPSI-IPr (1)



The polymerization was performed at both 30 and 60 °C; unfortunately both failed to undergo significant polymerization. Subsequently, the conditions for the Suzuki polymerization were changed to convert the solvent back to THF and the base to KOH (Scheme 66).

Scheme 66. Polymerization of monomer **79** mediated by PEPPSI-IPr (2)



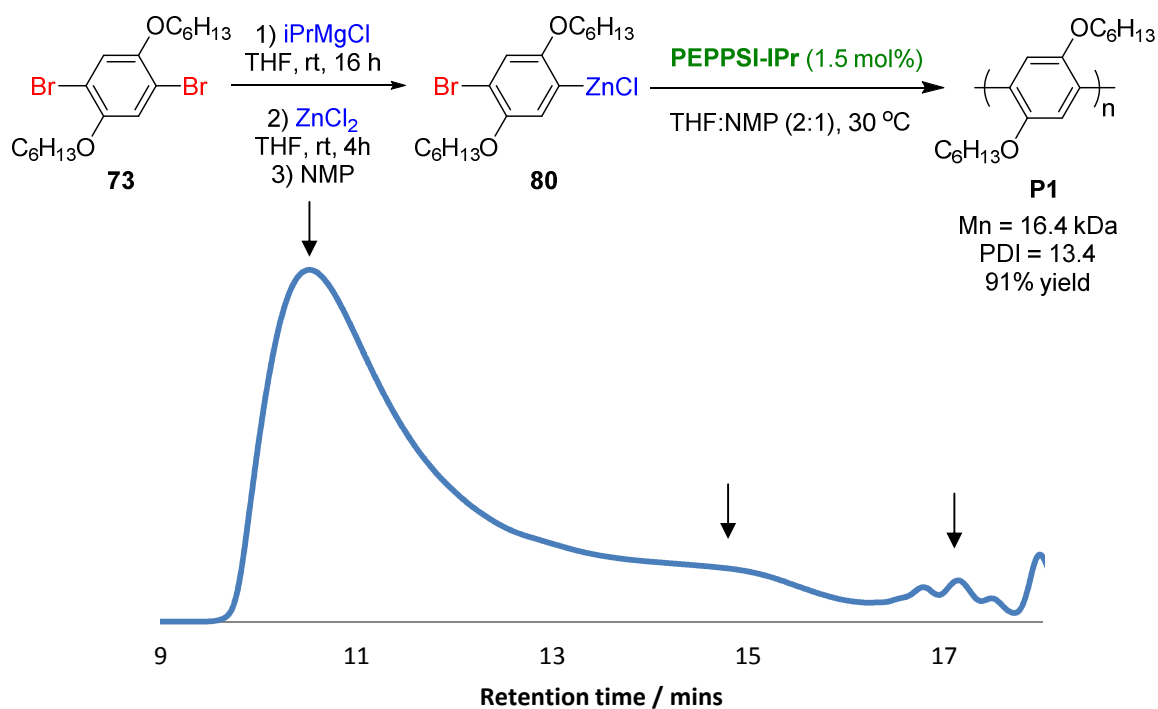
The change in conditions increased the M_n, however the PDI was large at both 30 and 60 °C and the polymer chain length was considerably shorter than the Kumada polymerization. The polymerization at 60 °C showed a higher M_n and lower PDI. The Suzuki polymerization appeared to need significant optimization to assess if PEPPSI-IPr can undergo chain growth polymerization which could open the path to new monomer substrates that can undergo chain growth polymerization.

5.7 Negishi polymerization

Similar to the initial work on the Suzuki coupling, the Kumada conditions were modified to the conditions for di-selective Negishi couplings described in Chapter 4. The optimized

conditions for monomer **74** were modified to add a THF solution of ZnCl_2 instead of THF for the transmetallation to form monomer **80**. NMP was added at the end of the monomer synthesis to limit the effect the water content would have on quenching the organozinc **80** during the polymerization.

Figure 16. Polymerization of monomer QA012 mediated by PEPPSI-IPr



The polymerization resulted in a polymer with very long chain lengths, but also a large distribution of polymer chain lengths. Unfortunately the polymerization was polymodal in the GPC spectrum significantly increasing the PDI and lowering the M_n . The polymer lengths and distribution suggested a PEPPSI-IPr was not being activated by the monomer at the start of the reaction or underwent a catalyst poisoning side reaction.

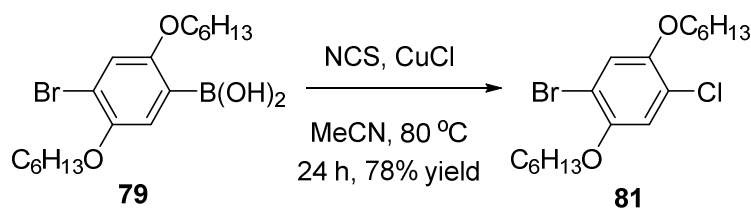
The initial work on both the Negishi and Suzuki polymerizations mediated by PEPPSI-IPr suggested that the Kumada coupling was the best for chain growth polymerization. For this reason, researched focused on the Kumada polymerization of Grignard monomers with C-Cl bonds.

5.8 First attempt at Kumada polymerization of ClArMgCl monomer

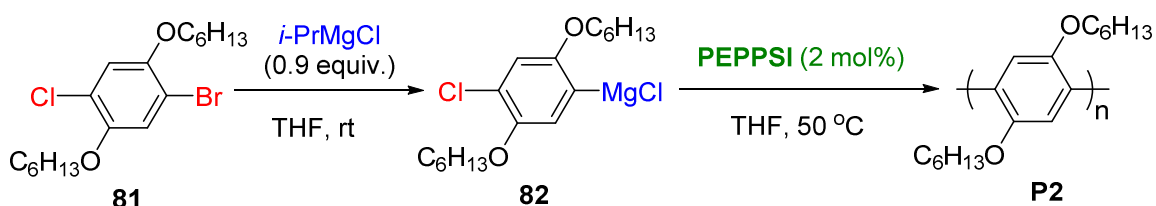
Both PEPPSI-IPr and PEPPSI-IPent showed excellent control over the distribution of polymer chain lengths in the polymerization of phenylene-based monomer **74**. Excellent di-selectivity (3:97 \leq) in chemoselective couplings with dihalides appeared to be needed for chain growth polymerization to occur. High di-selective couplings with the phenylene-based dichloride substrate mediated by PEPPSI-IPent were already obtained (3:97, Chapter 4). Therefore we aimed to synthesize a phenylene-based monomer for the polymerization by C-Cl coupling mediated by PEPPSI-IPent.

Using the transformation of an arylboronic acid to an aryl chloride described by Wu *et al.*¹⁰⁴ the monomer precursor **81** was synthesized in good yield (Scheme 9).

Scheme 67. Synthesis of monomer precursor **81**



Monomer precursor **81** was subsequently submitted to the optimized conditions for halogen metal exchange to synthesize monomer **82**. The monomer was subsequently polymerized by a series of PEPPSI precatalysts using the conditions for the bromide polymerization (Table 10).

Table 10. Polymerization of monomer **82** mediated by PEPPSI precatalysts

Entry	PEPPSI	Time	M _n / kDa	PDI
1	IMes	1.5 h	1.10	1.15
2	IEt	1.5 h	1.34	1.35
3	IPr	1.5 h	4.72	1.89
4	IPr	18 h	4.79	1.80
5	IPent	1.5 h	4.65	1.67
6	IPent	18 h	4.98	1.77

Unfortunately, the series of PEPPSI precatalysts tested did not show the expected control of polymer chain lengths or a large degree of polymerization. PEPPSI-IMes and PEPPSI-IEt showed lower M_n after 1.5 hours compared to both PEPPSI-IPr and -IPent. The polymerization mediated by PEPPSI-IPr and -IPent showed minimal change in the polymer properties between 1.5 and 18 hours. PEPPSI-IPent appears to show a smaller distribution of polymer chain lengths than PEPPSI-IPr, however not significantly.

Overall the polymerizations of monomer **82** did not achieve the expected control over the polymerization. The monomer precursor **81** was taken forward to the polymerization from the Grignard monomer synthesis. This is thought to have dramatically affected the polymerization. The presence of the C-Br bond in the polymerization would have allowed for preferential oxidative addition to aryl bromide **81** over monomer **82**, hindering the polymerization. The formation of monomer **82** without the presence of C-Br bond appears necessary to test if it is a living polymerization with PEPPSI precatalysts.

5.9 Conclusions

Repetition of the reported polymerization of monomer **74** mediated by PEPPSI-IPr resulted in the discovery of an additional peak at higher molecular weight than the main peak in the GPC spectra. This peak was broadening the PDI and was found to be coming from the monomer synthesis procedure. Optimization of the monomer procedure resulted in the suppression of the higher molecular weight peak, an increase in M_n and lowering of PDI.

Comparison of the chemoselective couplings between dibromide **76** and PhMgBr and the polymerization of monomer **74** mediated by PEPPSI precatalysts showed promising results. PEPPSI-IEt showed a di-selectivity of 1:9 which resulted in large M_n (40.8 kDa) with a low PDI (1.28). Although PEPPSI-IPent gave a lower M_n than PEPPSI-IPr, block homo-polymerization showed the polymerization to still be living.

Initial attempts to expand the scope of the chain growth polymerizations mediated by PEPPSI-IPr to other cross couplings were unsuccessful. The Suzuki polymerizations achieved a high degree of polymerization and the Negishi polymerization gave a very high distribution. Both need significant optimization to ascertain if chain growth polymerization is achievable.

Finally the polymerization of ClArMgCl monomer **82** was attempted mediated by PEPPSI precatalysts. Unfortunately a low degree of polymerization was obtained with a broad distribution of polymer lengths. Aryl bromide **81** was thought to be the underlying factor for why the polymerizations failed to proceed in a chain growth manner.

5.10 Future work

Our polymerization studies have focused on the easily accessible PEPPSI precatalysts discovered by Organ and co-workers. Different Pd-NHC precatalysts could be tested in model reactions and under the polymerization conditions to identify the key structural traits needed for controlled synthesis of π -conjugated polymers. For example PEPPSI-IPent^{Cl},⁹⁸ [Pd(ITent)(acac)Cl] or [Pd(ITent)(cinnamyl)Cl].¹⁰²

Our first attempts at Suzuki and Negishi polycondensations in a chain-growth manner were not successful. Further optimisation of reaction conditions is needed to better identify if PEPPSI-IPr will be able to polymerize monomers not accessible by nickel complexes in the Kumada catalyst transfer polymerizations.

With regard to the PEPPSI mediated polymerization of chloroarene monomers, polymerization of Grignard monomer **82** with the addition of extra precursor **81** is needed to confirm if it is detrimental to the polymerizations as suspected. If so, a new synthetic route to the Grignard monomer **82** is needed to potentially enable catalyst-transfer polycondensation as model reactions predicted.

5.11 References

- (88) Bryan, Z. J.; Smith, M. L.; McNeil, A. J. *Macromol. Rapid Commun.* **2012**, *33*, 842.
- (98) Pompeo, M.; Froese, R. D. J.; Hadei, N.; Organ, M. G. *Angew. Chemie Int. Ed.* **2012**, *51*, 11354.
- (102) Meiries, S.; Le Duc, G.; Chartoire, A.; Collado, A.; Speck, K.; Athukorala Arachchige, K. S.; Slawin, A. M. Z.; Nolan, S. P. *Chem. Eur. J.* **2013**, *19*, 17358.
- (103) Miyakoshi, R. *Macromol. Rapid Commun.* **2004**, 1663.

Chapter 6 – Experimental

6.1 General Experimental

All reagents were purchased from Sigma Aldrich, Alfa Aesar, Matrix Scientific or Fluka, and were used without further purification unless otherwise stated. THF, DMF, CH₂Cl₂, diethyl ether and toluene were obtained anhydrous from an MBraun MB SPS-800 solvent purification rig. Nitrogen used for inert atmosphere was oxygen-free grade. Thin layer chromatography was performed on either silica gel 60F₂₅₄ plates (Merck). Manual flash chromatography was performed on silica gel (VWR, 40-63 µm). Automated flash chromatography was performed using Varian Intelliflash, or Biotage Isolera-4 automated chromatography systems, employing Varian Superflash, or Biotage SNAP or ZIP cartridges.

Melting points were measured on a Stuart SMP3 melting point apparatus and are uncorrected. ¹H NMR and ¹³C NMR were recorded using a Bruker AV400 or a Bruker AMX400 and normalized on the signal of tetramethylsilane (TMS). Coupling constants (J) are reported in hertz (Hz). The multiplicities are expressed as follows: s = singlet, d = doublet, t = triplet, q = quartet, m = multiplet and combinations of the above for more complex patterns. Gel Permeation Chromatography: Polymer molecular weights were determined by comparison with polystyrene standards (Varian, EasiCal PS-2 MW 580-377,400) on a Agilent Infinity 1290 HPLC instrument equipped with 2 Agilent Plgel (5 µm, Mixed D) columns in sequence and analyzed with Agilent Infinity 1260 Refractive Index Detector eluted in THF. Samples were dissolved in THF (with mild heating) and passed through a 0.2 µm PTFE filter prior to analysis. IR spectra were recorded on a Perkin Elmer Spectrum 65 IR spectrometer equipped with ATR accessory. Low resolution mass spectrometry was carried out by the mass spectrometry services at the Queen Mary University of London. High resolution mass spectrometry was carried out by

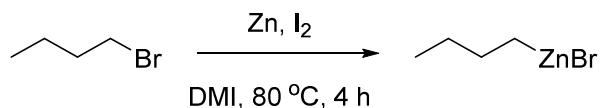
the EPSRC National Mass Spectrometry Centre in Swansea. Water is always intended as distilled water and was obtained from an Elga Purelab Option distillation system.

6.2 Chapter 2 Experimental

6.2.1 General remarks

All PEPPSI-IPr mediated cross-couplings were performed with equal amounts of aryl halide and organometallic, unless otherwise stated. The crude reaction mixture was analysed by ^1H NMR and GC-MS relative to an internal standard unless otherwise stated. Due to the intractable nature of the starting material and products they were not isolated to give a gravimetric yield. Instead the crude ^1H NMR was analysed relative to similar products published in the literature along with GC-MS spectra.

6.2.2 General procedures



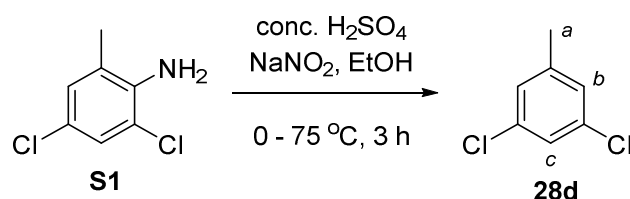
Preparation of *n*-BuZnBr:¹⁰⁵ A Schlenk flask was charged with zinc powder (2.45 g, 37.5 mmol) and iodine (320 mg, 1.25 mmol), sealed, purged with N_2 and anhydrous DMI (25 mL) was added. 1-Bromobutane (2.7 mL, 25 mmol) was added to the suspension and the mixture stirred vigorously at 80 $^\circ\text{C}$ for 4 h. The mixture was allowed to cool to rt and the molarity of the *n*-BuZnBr solution produced determined (*vide infra*).

Titration of organometallics:¹⁰⁶ A CEM microwave vial was charged with iodine (0.127 g, 0.50 mmol), sealed, purged with N_2 and anhydrous LiCl (0.5 M in THF, 2.0 mL, 1.0 mmol) was added. The resulting brown solution was cooled to 0 $^\circ\text{C}$ and organometallic was added dropwise until the solution became colourless which indicated consumption of one equivalent (0.50 mmol) of organometallic.

General procedure $\text{sp}^3\text{-sp}^2$ Negishi coupling: In air, a CEM microwave vial equipped with a stirrer bar was charged with PEPPSI-IPr (3.5 mg, 5.0 μmol), and if solid at rt, the aryl halide (0.25 mmol) was added. The vial was sealed and flushed with N_2 and anhydrous LiBr (0.33 M in THF, 0.75 mL, 0.50 mmol) was added via syringe and the solution was stirred at 25 $^\circ\text{C}$. If the aryl halide was a liquid at room temperature, it was added right after the addition of LiBr. *n*-BuZnBr (0.66 M in DMI, 350 μL , 0.25 mmol) was then added via syringe and the solution was stirred for 2 h at which time an internal standard was added, mesitylene or *p*-xylene (0.5 M in CDCl_3 , 0.50 mL, 0.25 mmol) and the crude reaction mixture was analysed by GC-MS and ^1H NMR.

General procedure for $\text{sp}^3\text{-sp}^2$ Negishi competition coupling: Following the Negishi coupling procedure, 0.25 mmol of the competing aryl chlorides was added before the addition of the *n*-BuZnBr.

6.2.3 Starting material synthesis

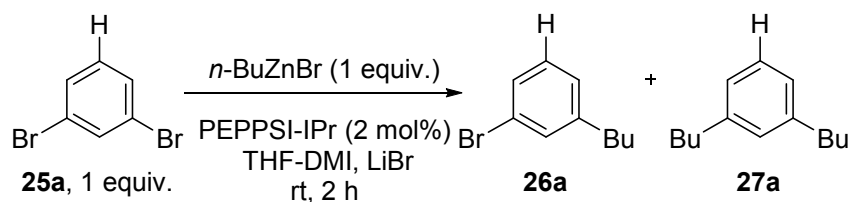


2,4-Dichloro-6-methylaniline (**S1**, 880 mg, 5.0 mmol) was dissolved in EtOH (20 mL) and the solution cooled to 0 °C. Conc. H₂SO₄ (1.8 mL) was added drop-wise and the mixture allowed to warm to rt. NaNO₂ (1.06 g, 12.5 mmol) was added portion-wise and the reaction mixture stirred at 75 °C for 3 h. The reaction mixture was cooled to rt and poured onto ice (20 g). The precipitate was collected by suction filtration, washed with H₂O (10 mL), dissolved in CH₂Cl₂, dried over MgSO₄, and concentrated *in vacuo*. The residue was dissolved in petrol, filtered through a SiO₂ plug and concentrated *in vacuo* to give **28d** as a low melting colourless solid (679 mg, 84%): **Melting point** 26 °C (lit.¹⁰⁷ 24.5 °C); ¹H NMR (400 MHz, CDCl₃) δ 7.20 – 7.12 (m, 1H, H_c), 7.09 – 7.02 (m, 2H, H_b) 2.32 (s, 3H, H_a); ¹³C NMR (101 MHz, CDCl₃) δ 141.3, 134.7, 127.7, 125.8, 21.2.

6.2.4 Experimental Data

Table 2

Table 2, Entry 1:



Using the general procedure for $\text{sp}^3\text{-sp}^2$ Negishi couplings employing 1,3-dibromobenzene (59 mg, 0.25 mmol) a product mixture of **26a** and **27a** is obtained in a <1 : >99 ratio by GC-MS analysis and in a <5 : >95 ratio by ^1H NMR analysis. ^1H NMR analysis using mesitylene as internal standard indicated a 98% yield of **26a+27a** based on *n*-BuZnBr. Product ^1H NMR signals in the crude were assigned by analogy with 1-bromo-3-*n*-butylbenzene **26a**¹⁰⁸ and 1,3-di(*n*-butyl)benzene **27a**.¹⁰⁹

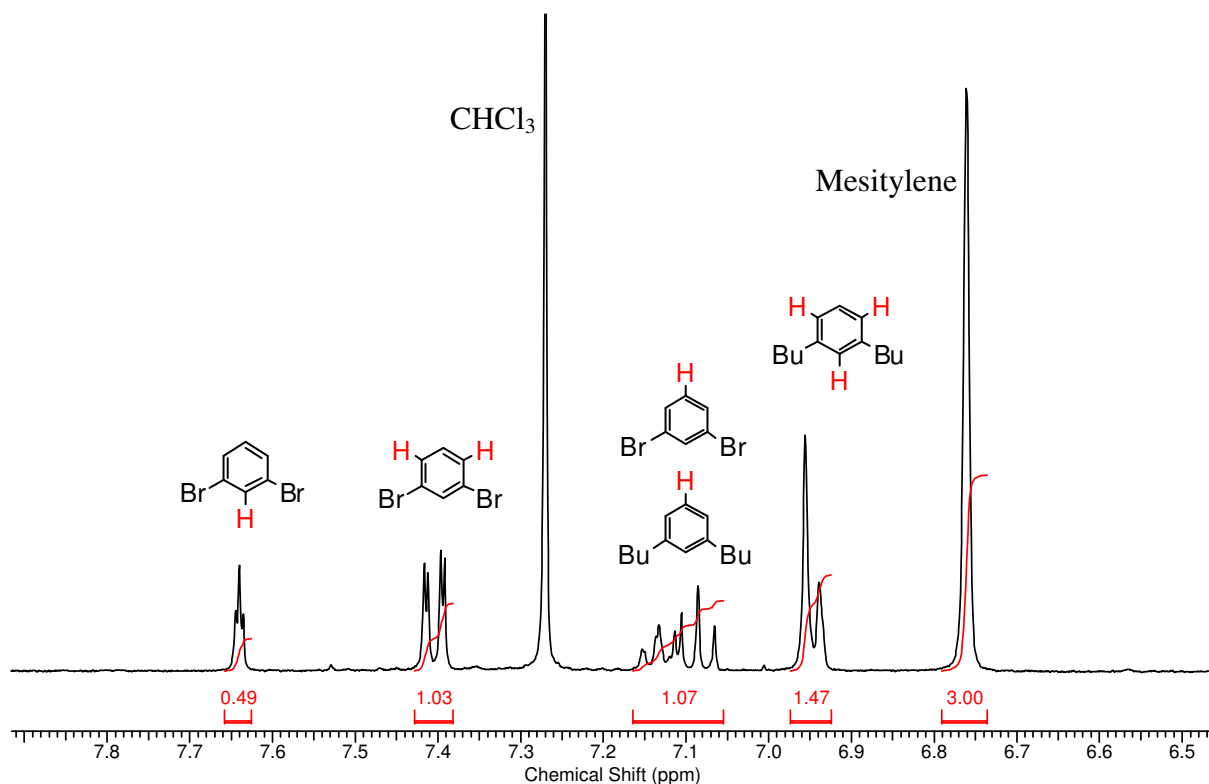
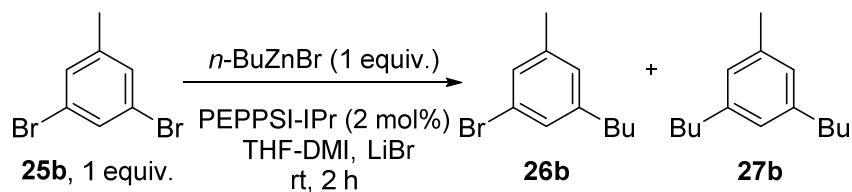


Table 2, Entry 2:



Using the general procedure for $\text{sp}^3\text{-sp}^2$ Negishi couplings employing 3,5-dibromotoluene (63 mg, 0.25 mmol) a product mixture of **26b** and **27b** is obtained in a <1 : >99 ratio by GC-MS analysis and in a <5 : >95 ratio by ^1H NMR analysis. ^1H NMR analysis using mesitylene as internal standard indicated a 90% yield of **26b+27b** based on $n\text{-BuZnBr}$. ^1H NMR signals in the crude were assigned by analogy with 5-bromo-*m*-xylene¹¹⁰ and 3,5-di(*n*-butyl)toluene **27b**.¹¹¹

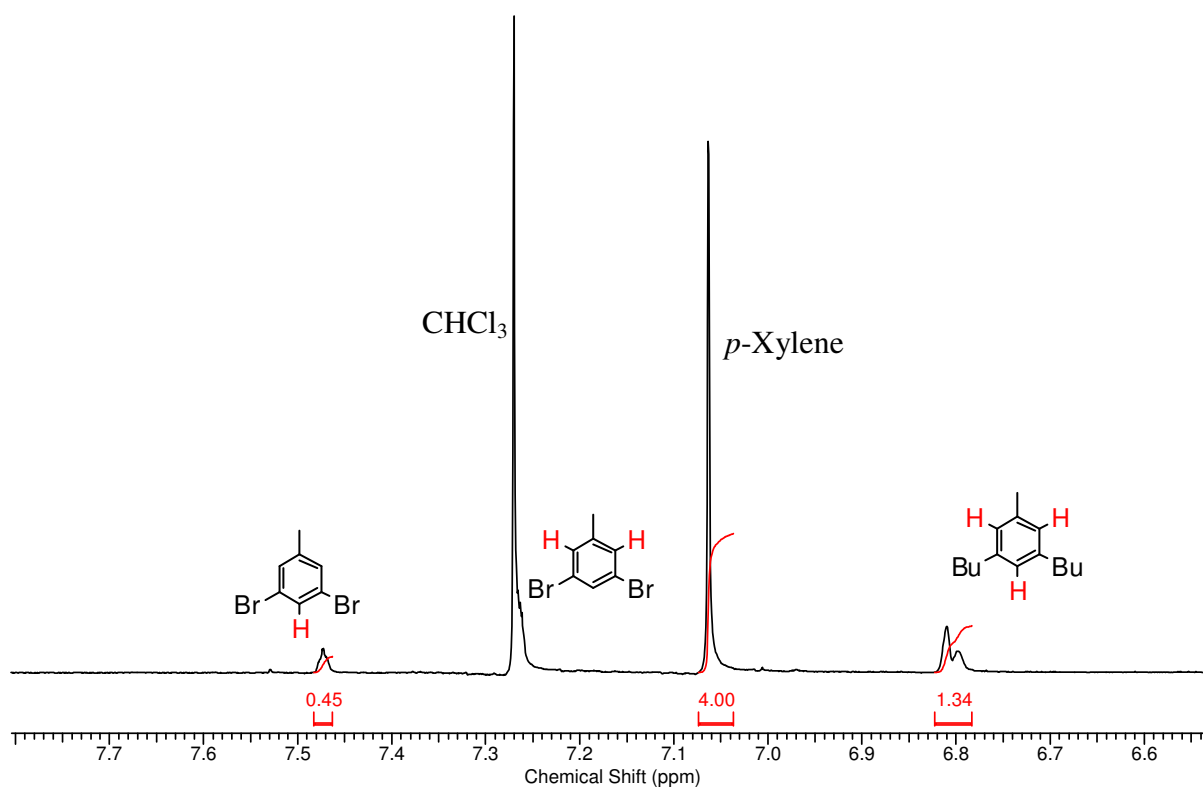
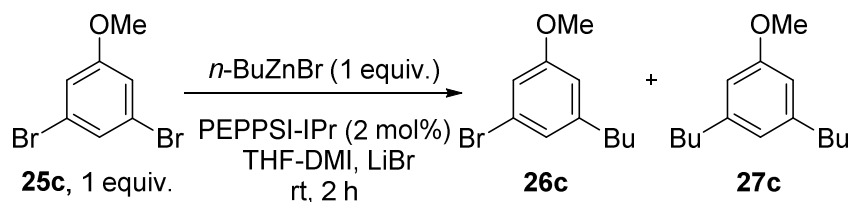


Table 2, Entry 3:



Using the general procedure for $\text{sp}^3\text{-sp}^2$ Negishi couplings employing 3,5-dibromoanisole (67 mg, 0.25 mmol) a product mixture of **26c** and **27c** is obtained in a <1 : >99 ratio by GC-MS analysis and in a <5 : >95 ratio by ^1H NMR analysis. ^1H NMR analysis using p -xylene as internal standard indicated a 94% yield of **26c+27c** based on $n\text{-BuZnBr}$. ^1H NMR signals in the crude were assigned by analogy with 3-bromo-5-methylanisole¹¹² and 3,5-dimethylanisole.¹¹³

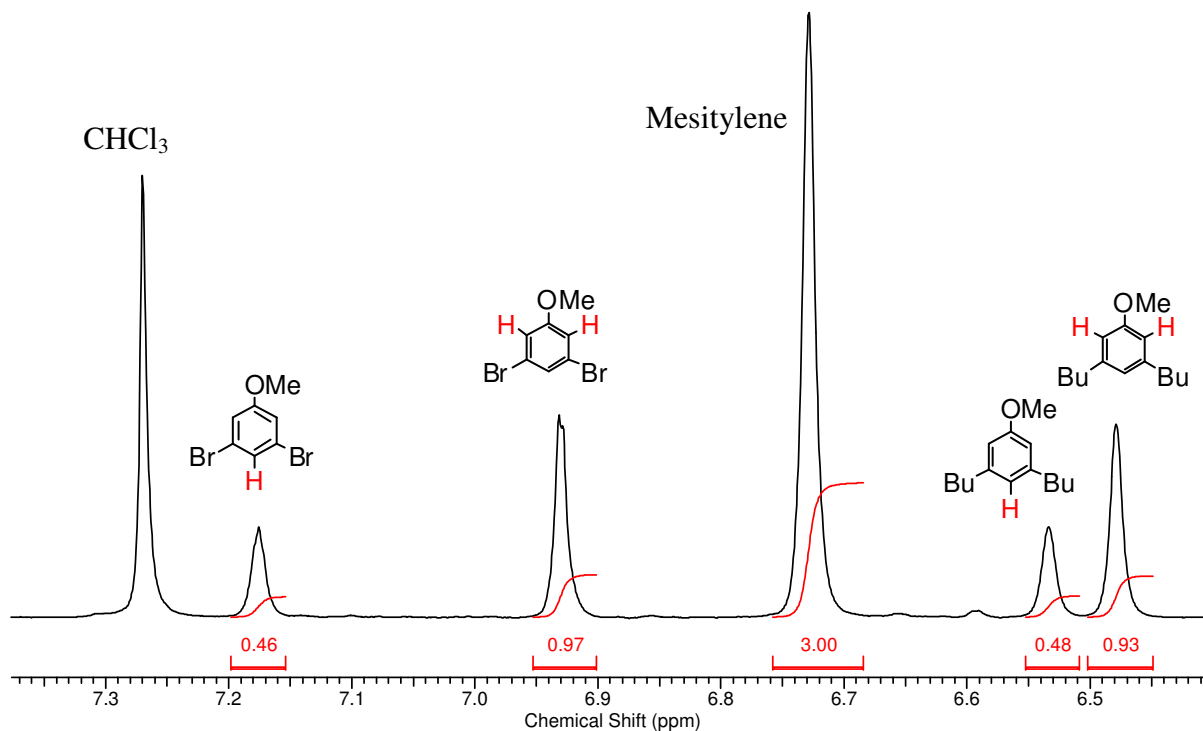
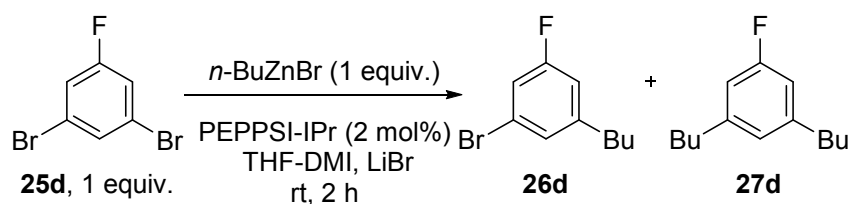


Table 2, Entry 4:



Using the general procedure for $\text{sp}^3\text{-sp}^2$ Negishi couplings employing 1,3-dibromo-5-fluorobenzene (64 mg, 0.25 mmol) a product mixture of **26d** and **27d** is obtained in a <1 : >99 ratio by GC-MS analysis and in a <5 : >95 ratio by ^1H NMR analysis. ^1H NMR analysis using mesitylene as internal standard indicated a 92% yield of **26d+27d** based on $n\text{ BuZnBr}$. ^1H NMR signals in the crude were assigned by analogy with 5-fluoro-*m*-xylene.¹¹⁴

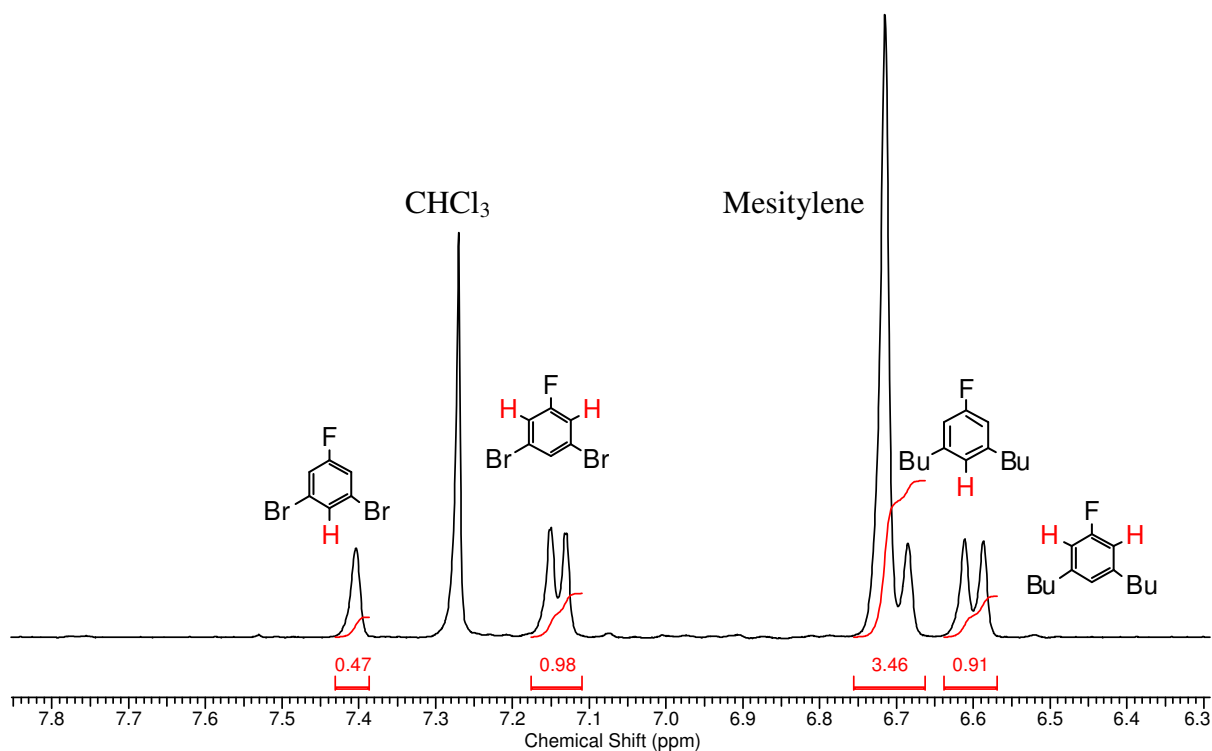
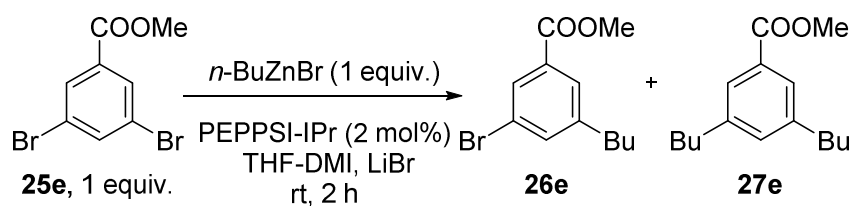


Table 2, Entry 5:



Using the general procedure for $\text{sp}^3\text{-sp}^2$ Negishi couplings employing 1-methyl-3,5-dibromobenzoate (74 mg, 0.25 mmol) a product mixture of **26e** and **27e** is obtained in a <1 : >99 ratio by GC-MS analysis and in a <5 : >95 ratio by ^1H NMR analysis. ^1H NMR analysis using mesitylene as internal standard indicated a 88% yield of **26e+27e** based on *n*-BuZnBr. ^1H NMR signals in the crude were assigned by analogy with 3-bromo-5-methylbenzoate¹¹⁰ and methyl 3,5-di(*n*-butyl)benzoate **27e**.¹¹⁵

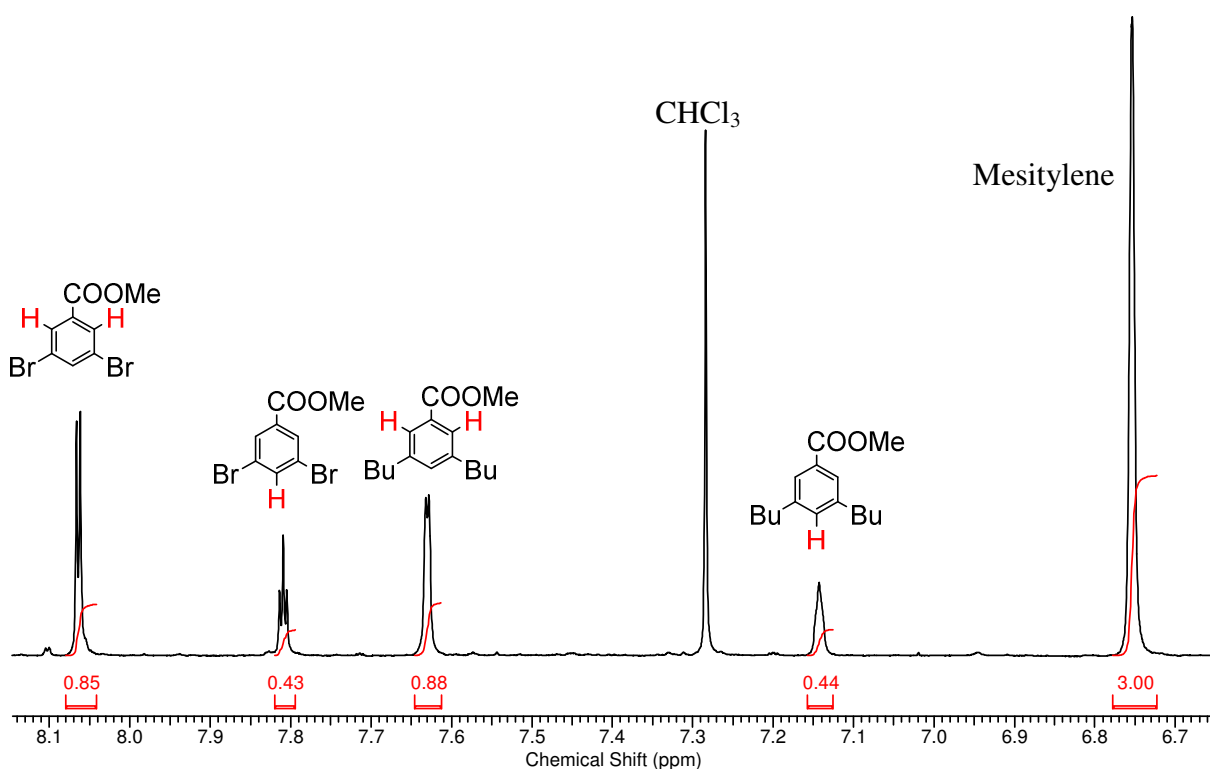
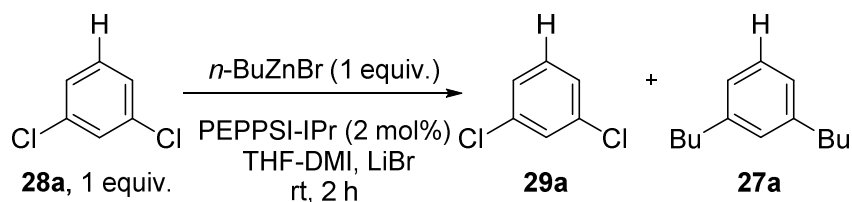


Table 3Table 3, Entry 1:

Using the general procedure for $\text{sp}^3\text{-sp}^2$ Negishi couplings employing 1,3-dichlorobenzene (29 μL , 0.25 mmol) a product mixture of **29a** and **27a** is obtained in a 56 : 44 ratio by GC MS analysis and in a 65 : 35 ratio by ^1H NMR analysis. ^1H NMR analysis using mesitylene as internal standard indicated a 89% yield of **29a+27a** based on *n* BuZnBr. ^1H NMR signals in the crude were assigned by analogy with 1-chloro-3-*n*-butylbenzene **29a**¹⁰⁹ and 1,3-di(*n*-butyl)benzene **27a**.¹⁰⁹

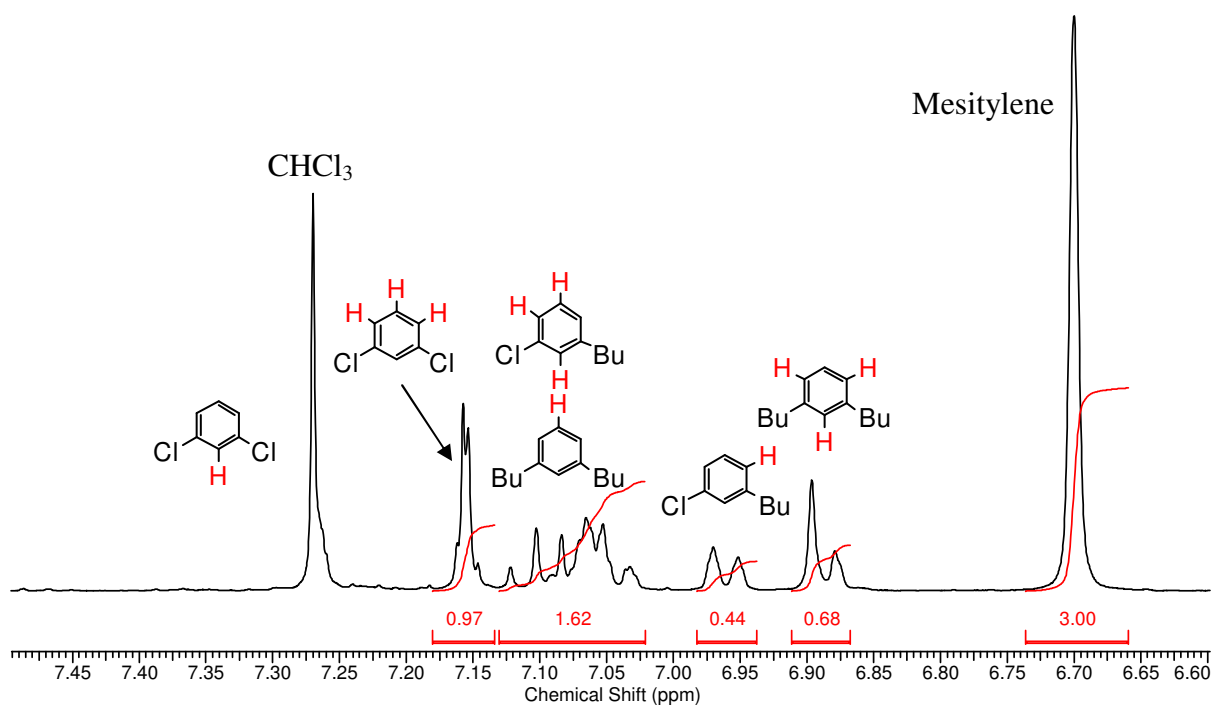
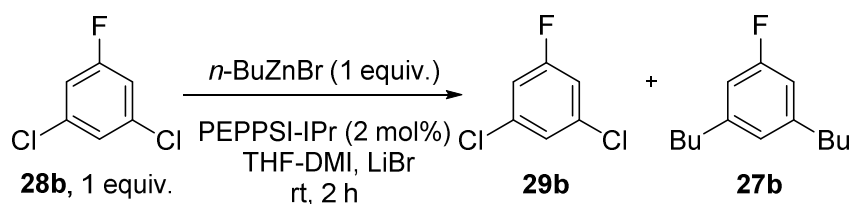


Table 3, Entry 2:



Using the general procedure for $\text{sp}^3\text{-sp}^2$ Negishi couplings employing 1,3-dichloro-5-fluorobenzene (30 μL , 0.25 mmol) a product mixture of **29b** and **27b** is obtained in a 3 : 97 ratio by GC-MS analysis and in a <5 : >95 ratio by ^1H NMR analysis. ^1H NMR analysis using mesitylene as internal standard indicated a 78% yield of **29b+27b** based on $n\text{BuZnBr}$. ^1H NMR signals in the crude were assigned by analogy with 5-fluoro-*m*-xylene.¹¹⁴

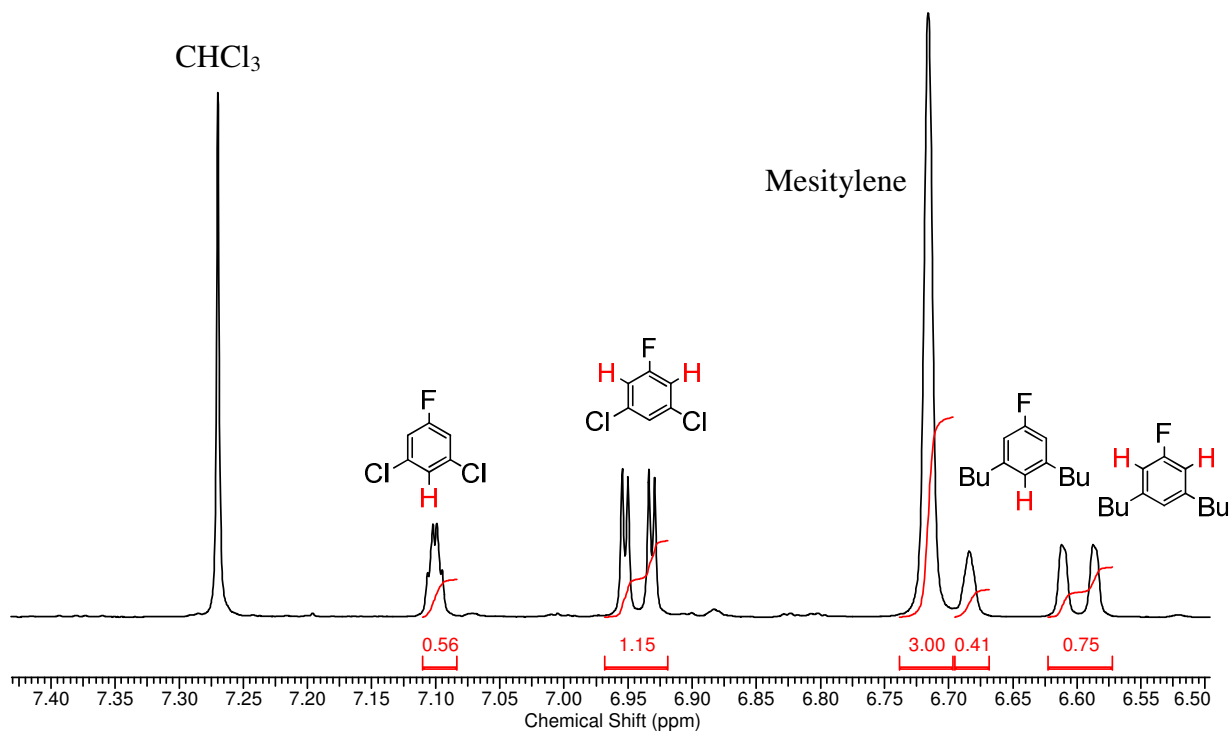
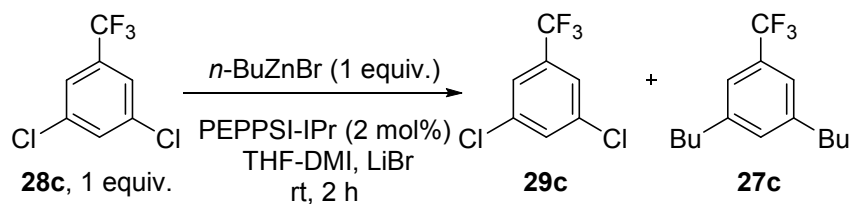


Table 3, Entry 3:



Using the general procedure for $\text{sp}^3\text{-sp}^2$ Negishi couplings employing 1,3-dichloro-5-(trifluoromethyl)benzene (37 μL , 0.25 mmol) a product mixture of **29c** and **27c** is obtained in a 6 : 94 ratio by GC-MS analysis and in a <5 : >95 ratio by ^1H NMR analysis. ^1H NMR analysis using mesitylene as internal standard indicated a 80% yield of **29c+27c** based on $n\text{-BuZnBr}$. ^1H NMR signals in the crude were assigned by analogy with 5-trifluoromethyl-*m*-xylene.¹¹⁶

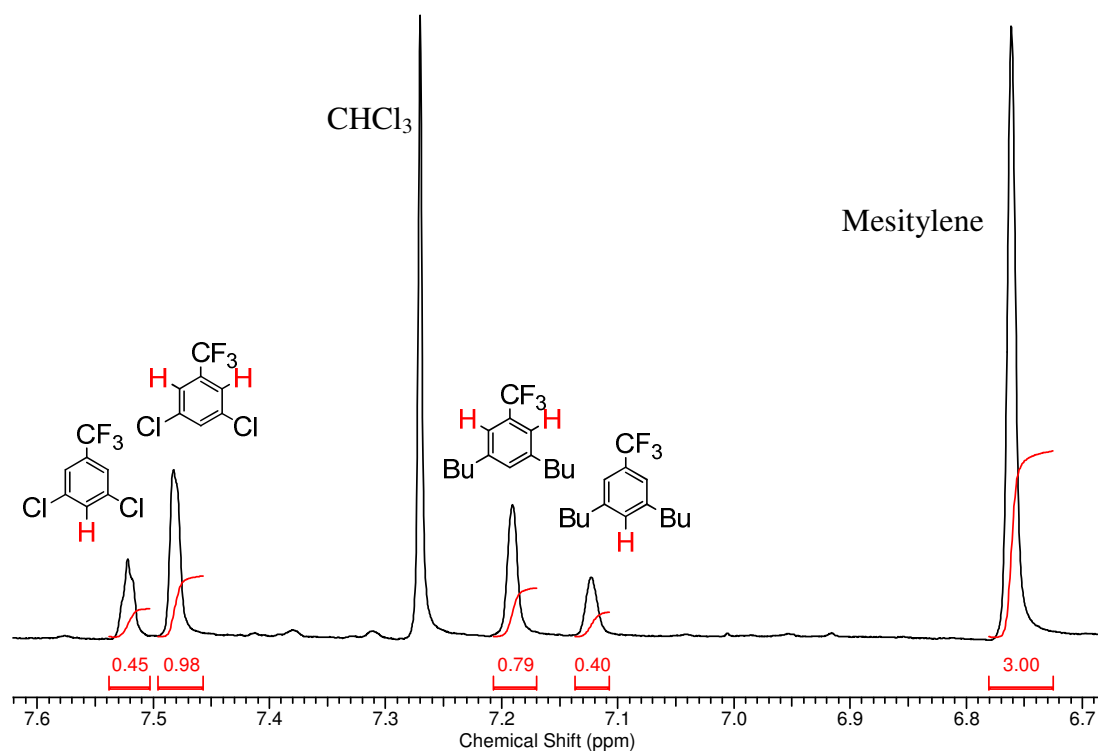
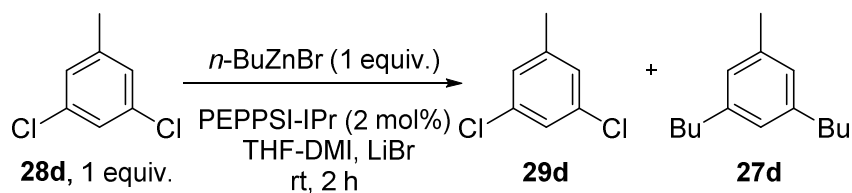


Table 3, Entry 4:



Using the general procedure for $\text{sp}^3\text{-sp}^2$ Negishi couplings employing 3,5-dichlorotoluene (40 mg, 0.25 mmol) a product mixture of **29d** and **27d** is obtained in a 6 : 94 ratio by GC-MS analysis and in a <5 : >95 ratio by ^1H NMR analysis. ^1H NMR analysis using mesitylene as internal standard indicated a 62% yield of **29d+27d** based on $n\text{-BuZnBr}$. ^1H NMR signals in the crude were assigned by analogy with 5-chloro-*m*-xylene¹¹⁰ and 1,3-di(*n*-butyl)toluene **27d**.¹¹¹

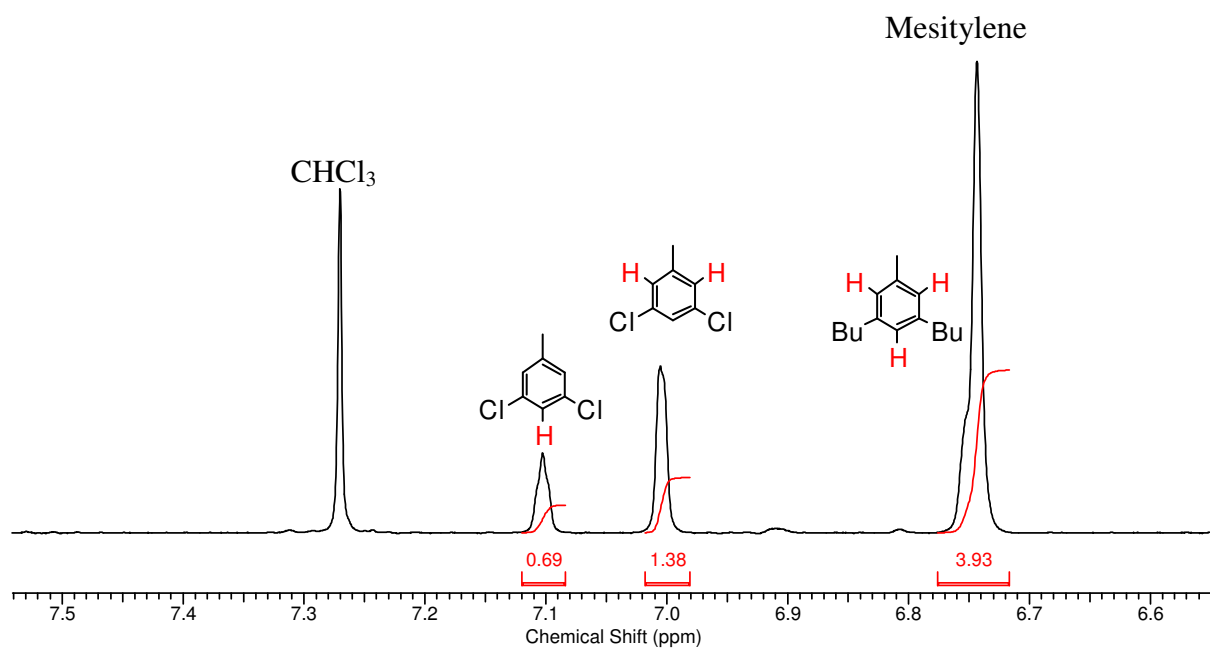
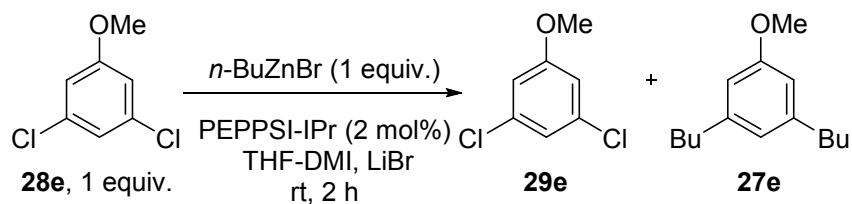


Table 3, Entry 5:



Using the general procedure for $\text{sp}^3\text{-sp}^2$ Negishi couplings employing 3,5-dichloroanisole (45 mg, 0.25 mmol) a product mixture of **29e** and **27e** is obtained in a 4 : 96 ratio by GC-MS analysis and in a <5 : >95 ratio by ^1H NMR analysis. ^1H NMR analysis using mesitylene as internal standard indicated a 92% yield of **29e+27e** based on $n\text{-BuZnBr}$. ^1H NMR signals in the crude were assigned by analogy with 3,5-dimethylanisole.¹¹³

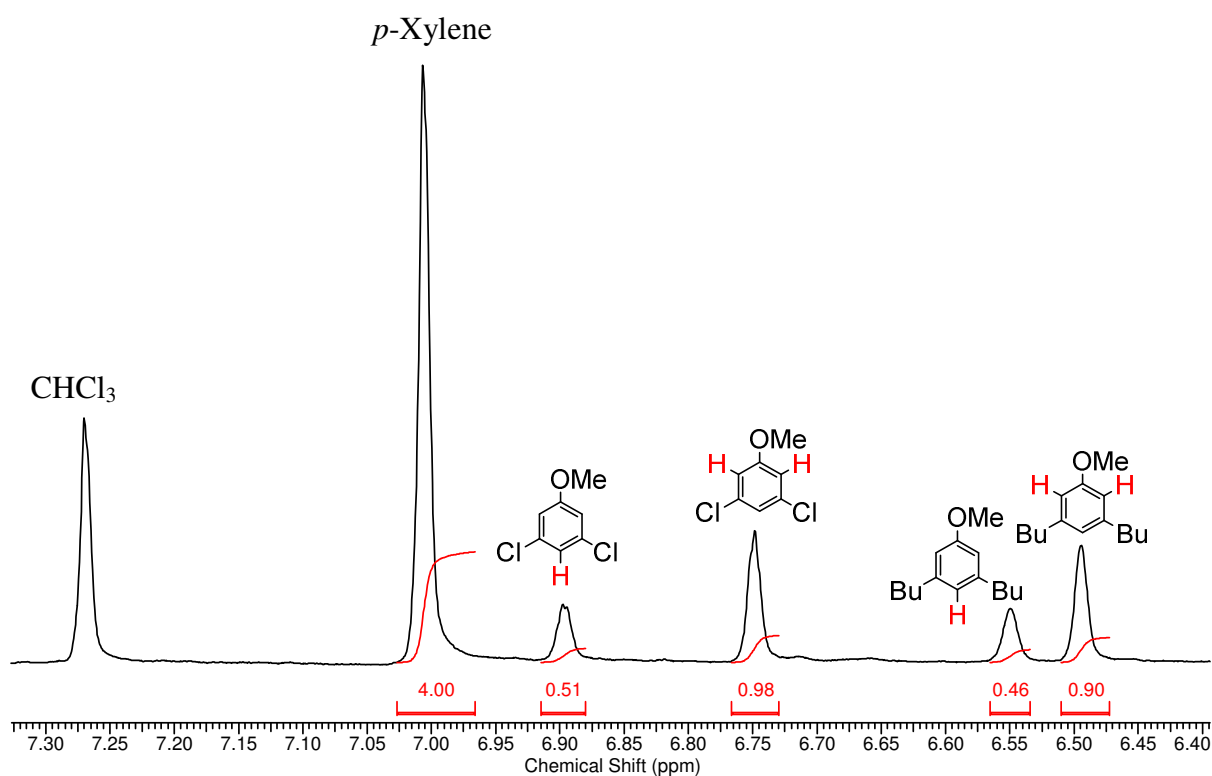
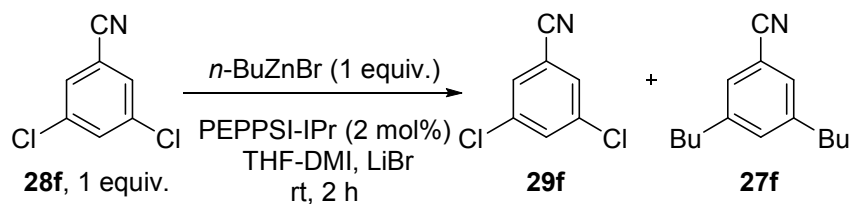


Table 3, Entry 6



Using the general procedure for $\text{sp}^3\text{-sp}^2$ Negishi couplings employing 3,5-dichlorobenzonitrile (43 mg, 0.25 mmol) a product mixture of **29f** and **27f** is obtained in a 76 : 34 ratio by GC-MS analysis and in a 91 : 9 ratio by ^1H NMR analysis. ^1H NMR analysis using mesitylene as internal standard indicated a 50% yield of **29f**+**27f** based on $n\text{-BuZnBr}$. ^1H NMR signals in the crude were assigned by analogy with 3-chloro-5-methylbenzonitrile¹¹⁰ and 3,5-dimethylbenzonitrile.¹¹⁷

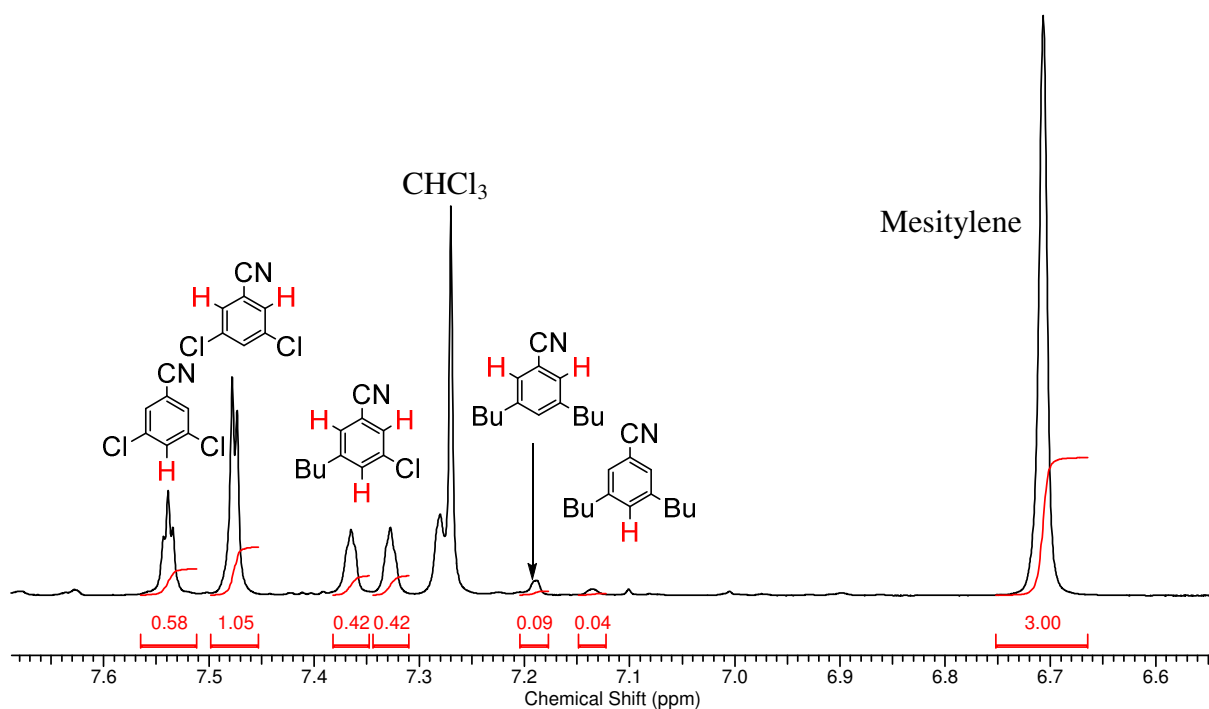
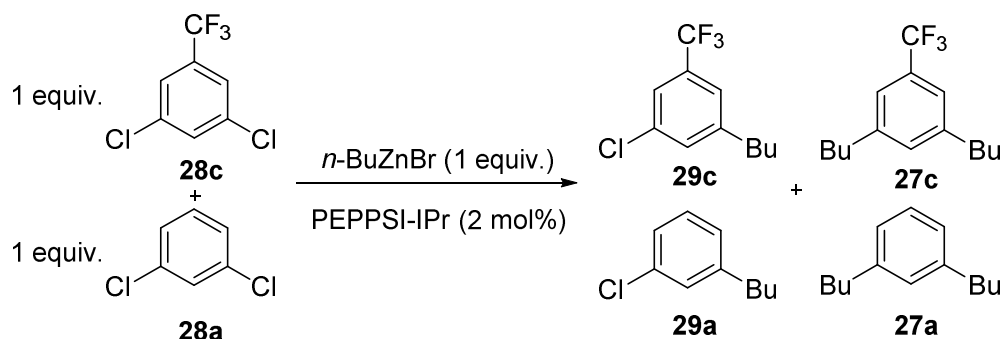


Table 4Table 4, Entry 1

Using the general procedure for $\text{sp}^3\text{-sp}^2$ Negishi competition couplings employing 1,3-dichloro-5-(trifluoromethyl)benzene (37 μL , 0.25 mmol) and 1,3-dichlorobenzene (29 μL , 0.25 mmol) a product mixture of **29c**, **27c**, **29a** and **27a** was obtained. A product mixture of **29c** and **27c** is obtained in a 12 : 88 ratio by GC-MS analysis and a ratio by ^1H NMR analysis could not be obtained due to overlapping peaks. ^1H NMR indicated a 67% yield of **29c**+**27c** using mesitylene as internal standard $n\text{-BuZnBr}$. A product mixture of **29a** and **27a** is obtained in a 73 : 27 ratio by GC-MS analysis and a ratio of 68 : 32 by ^1H NMR analysis. ^1H NMR analysis indicated a 33% yield of **29a**+**27a** using mesitylene as internal standard $n\text{-BuZnBr}$. Product ^1H NMR signals in the crude were assigned by analogy with 5-trifluoromethyl-*m*-xylene,¹¹⁶ 1-chloro-3-*n*-butylbenzene **29a**¹⁰⁹ and 1,3-di(*n*-butyl)benzene **27a**.¹⁰⁹

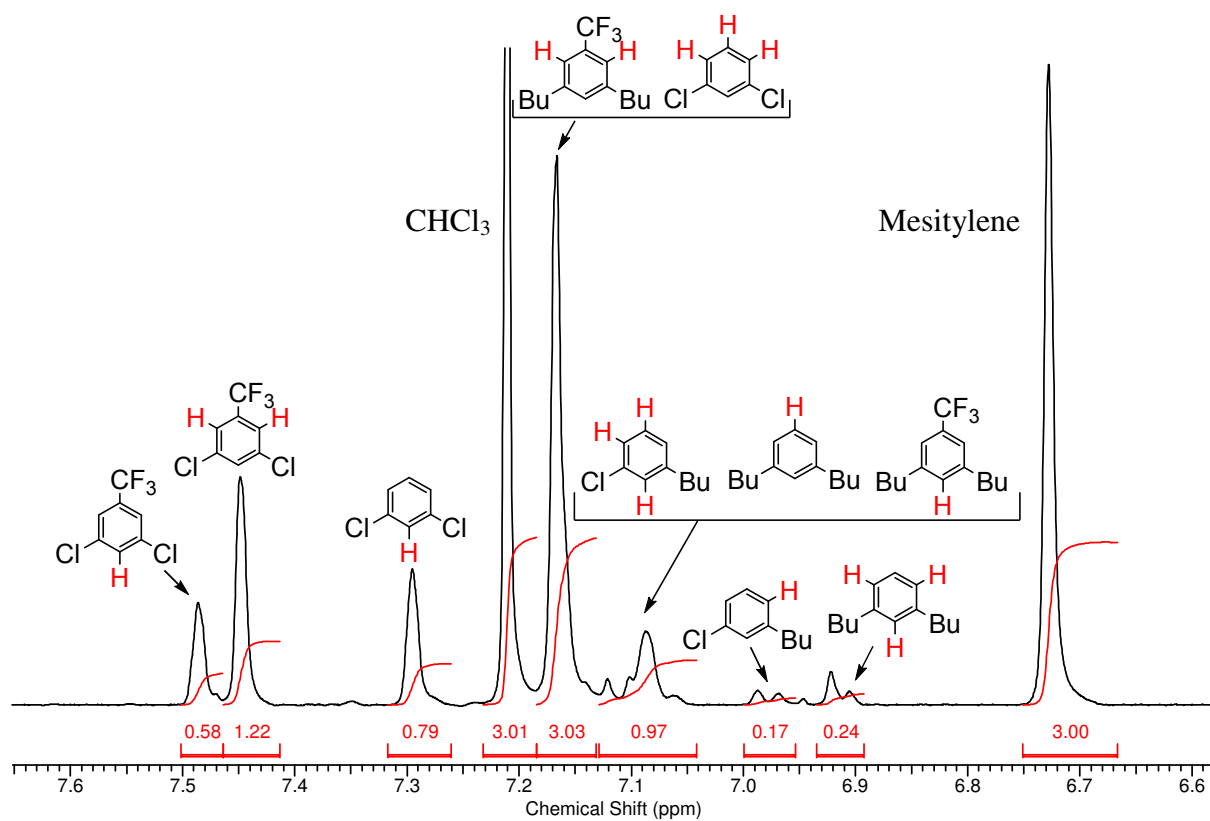
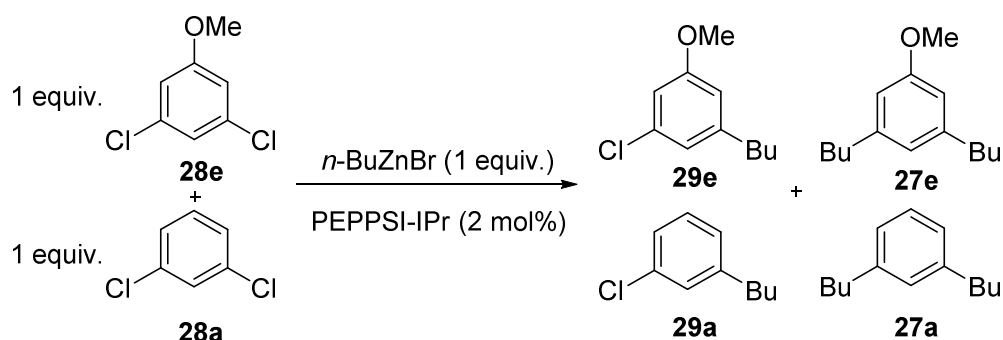


Table 4, Entry 2



Using the general procedure for $\text{sp}^3\text{-sp}^2$ Negishi competition couplings employing 3,5-dichloroanisole (45 mg, 0.25 mmol) and 1,3-dichlorobenzene (29 μL , 0.25 mmol) a product mixture of **29e**, **27e**, **29a** and **27a** was obtained. A product mixture of **29e** and **27e** is obtained in a 9 : 91 ratio by GC-MS analysis and a ratio of <5 : >95 by ^1H NMR analysis. ^1H NMR analysis indicated a 14% yield of **29e+27e** using mesitylene as internal standard *n*-BuZnBr. A product mixture of **29a** and **27a** is obtained in a 48 : 52 ratio by GC-MS analysis and a ratio of 57 : 43 by ^1H NMR analysis. ^1H NMR analysis indicated a 86% yield of **29a+27a** using mesitylene as internal standard *n*-BuZnBr. Product ^1H NMR signals in the crude were assigned by analogy with 3,5-dimethylanisole,¹¹³ 1-chloro-3-*n*-butylbenzene **29a**¹⁰⁹ and 1,3-di(*n*-butyl)benzene **27a**.¹⁰⁹

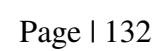
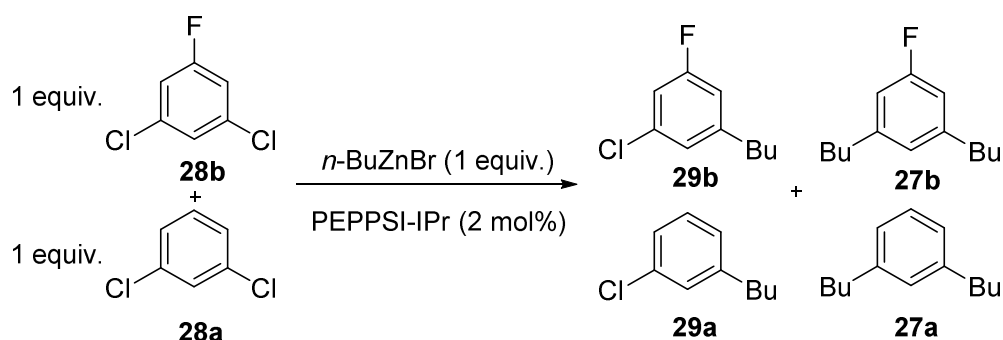


Table 4, Entry 3



Using the general procedure for $\text{sp}^3\text{-sp}^2$ Negishi competition couplings employing 3,5-dichloro-1-fluorobenzene (30 μL , 0.25 mmol) and 1,3-dichlorobenzene (29 mg, 0.25 mmol) a product mixture of **29b**, **27b**, **29a** and **27a** was obtained. A product mixture of **29b** and **27b** is obtained in a ratio of <5 : >95 by ^1H NMR analysis. ^1H NMR analysis indicated a 49% yield of **29b+27b** using mesitylene as internal standard *n*-BuZnBr. A product mixture of **29a** and **27a** is obtained in a ratio of 67 : 33 by ^1H NMR analysis. GC-MS ratios could not be obtained due to the overlap of peaks. ^1H NMR analysis indicated a 49% yield of **29a+27a** using mesitylene as internal standard *n*-BuZnBr. Product ^1H NMR signals in the crude were assigned by analogy with 5-fluoro-*m*-xylene,¹¹⁴ 1-chloro-3-*n*-butylbenzene **29a**¹⁰⁹ and 1,3-di(*n*-butyl)benzene **27a**.¹⁰⁹

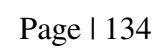
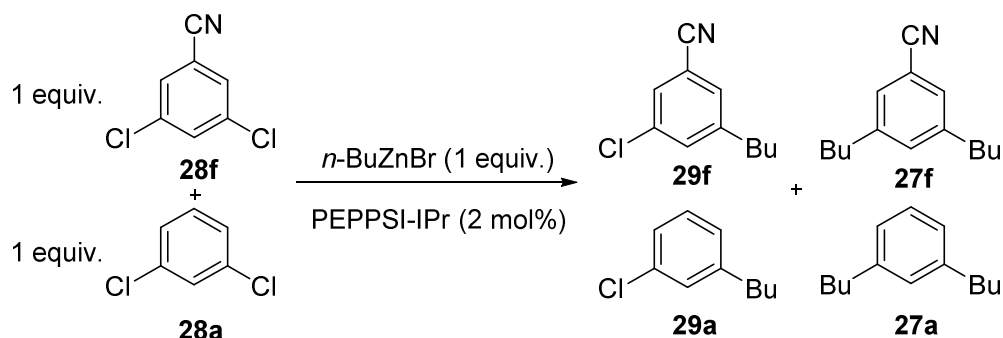


Table 4, Entry 4



Using the general procedure for $\text{sp}^3\text{-sp}^2$ Negishi competition couplings employing 3,5-dichlorobenzonitrile (43 mg, 0.25 mmol) and 1,3-dichlorobenzene (29 μL , 0.25 mmol) a product mixture of **29f**, and **27f** was obtained. A product mixture of **29f** and **27f** is obtained in a 90 : 10 ratio by GC-MS analysis and a ratio of 15 : 85 by ^1H NMR analysis. ^1H NMR analysis indicated a 55% yield of **29f**+**27f** using mesitylene as internal standard *n*-BuZnBr. No **29a** and **27a** were observed by ^1H NMR analysis. Product ^1H NMR signals in the crude were assigned by analogy with 3-chloro-5-methylbenzonitrile,¹¹⁰ 3,5-dimethylbenzonitrile,¹¹⁷ **29a**¹⁰⁹ and 1,3-di(*n*-butyl)benzene **27a**.¹⁰⁹

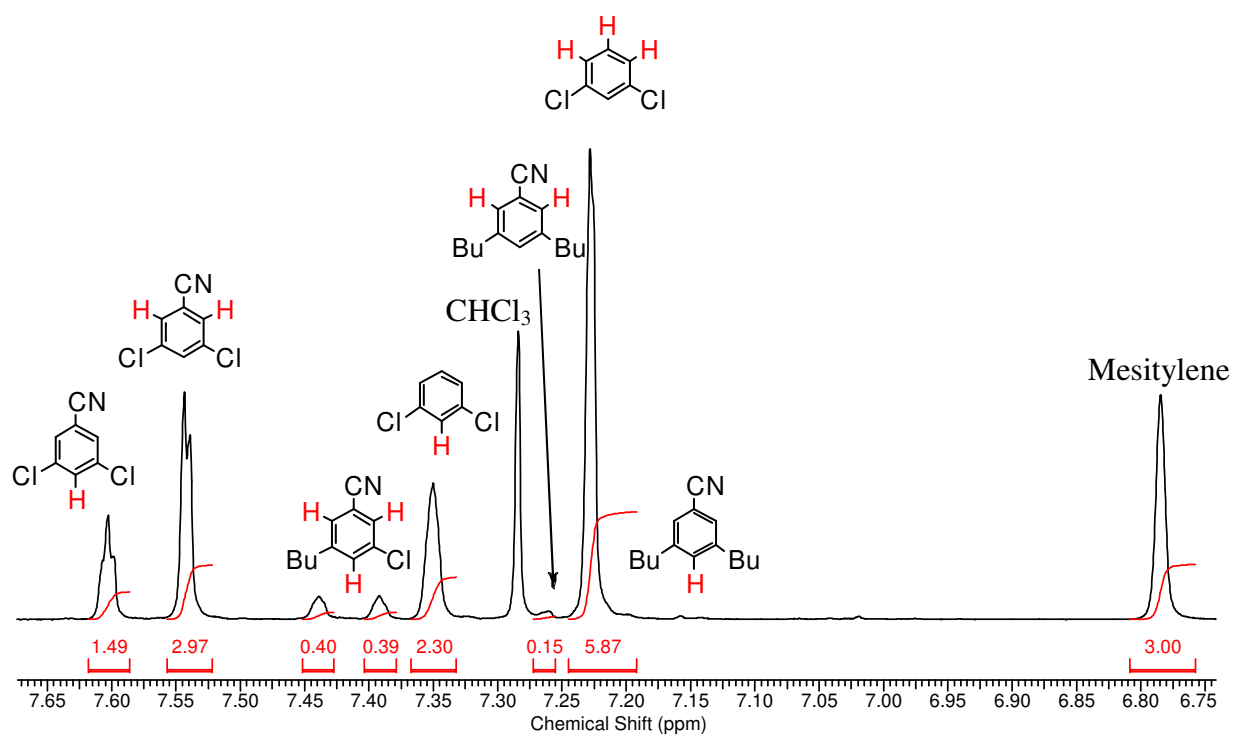
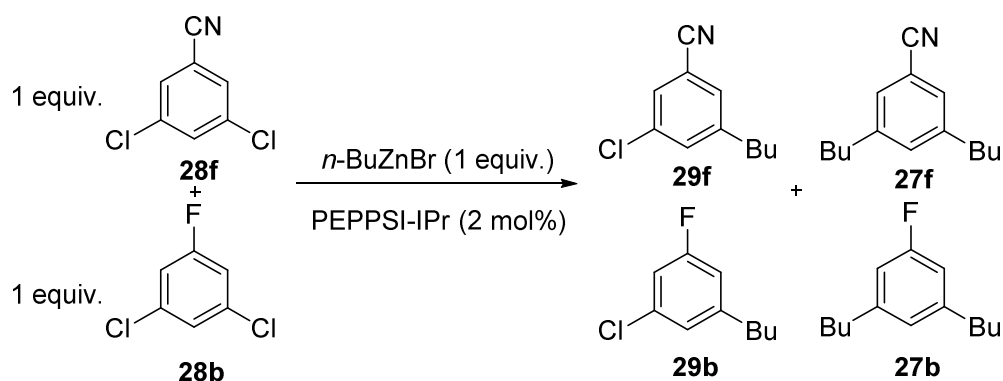
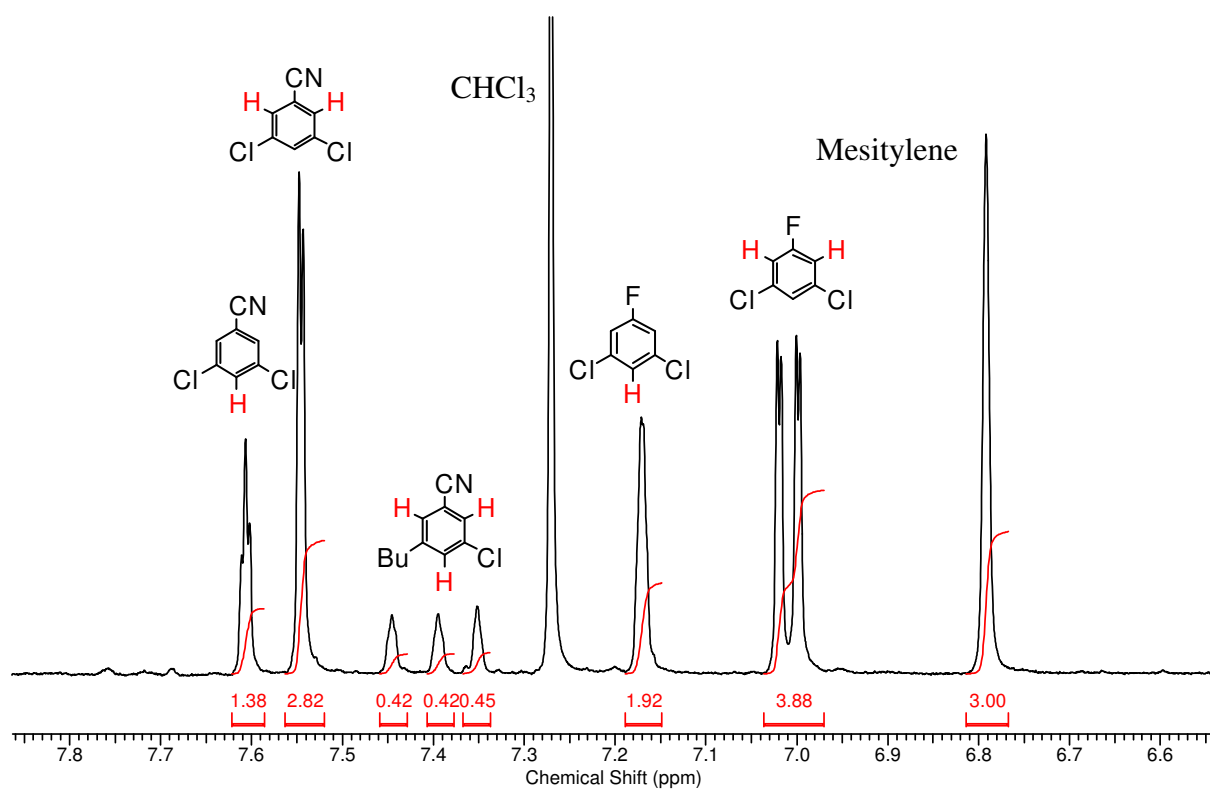


Table 4, Entry 5

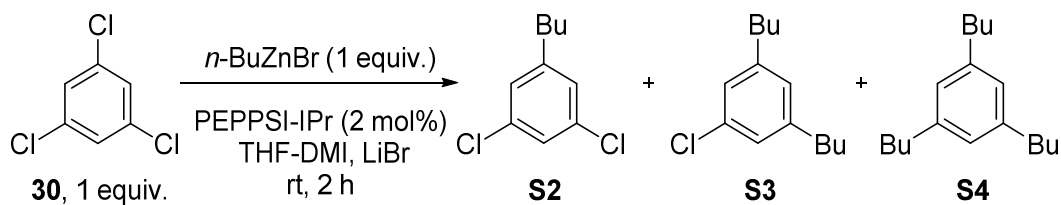


Using the general procedure for $\text{sp}^3\text{-sp}^2$ Negishi competition couplings employing 3,5-dichlorobenzonitrile (43 mg, 0.25 mmol) and 3,5-dichloro-1-fluorobenzene (30 μL , 0.25 mmol) a product mixture of **29f**, **27e**, **29b** and **27b** was obtained. A product mixture of **29e** and **27e** is obtained in a 88 : 12 ratio by GC-MS analysis and a ratio by ^1H NMR analysis could not be obtained. ^1H NMR analysis indicated a 42% yield of **29e+27e** using mesitylene as internal standard $n\text{-BuZnBr}$. No **29b** and **27b** were observed by ^1H NMR analysis. Product ^1H NMR signals in the crude were assigned by analogy with 3-chloro-5-methylbenzonitrile,¹¹⁰ 3,5-dimethylbenzonitrile¹¹⁷ and 3,5-fluoro-*m*-xylene.¹¹⁴

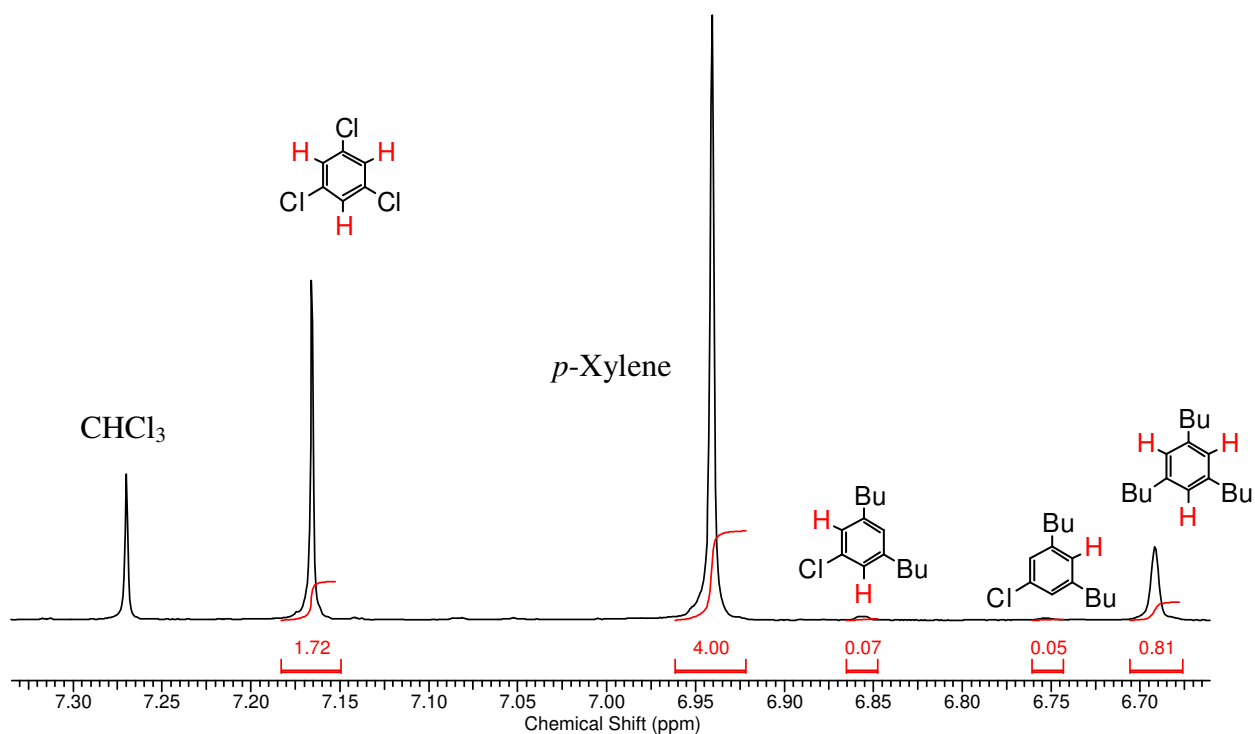


Scheme 29

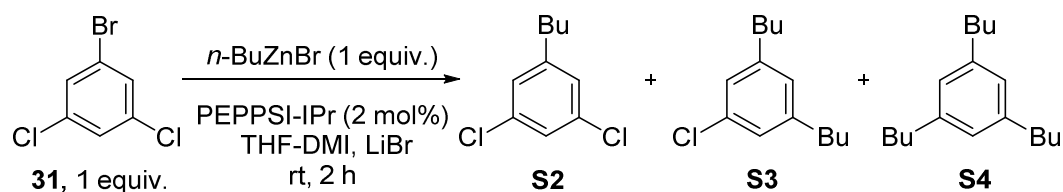
1,3,5-trichlorobenzene (30):



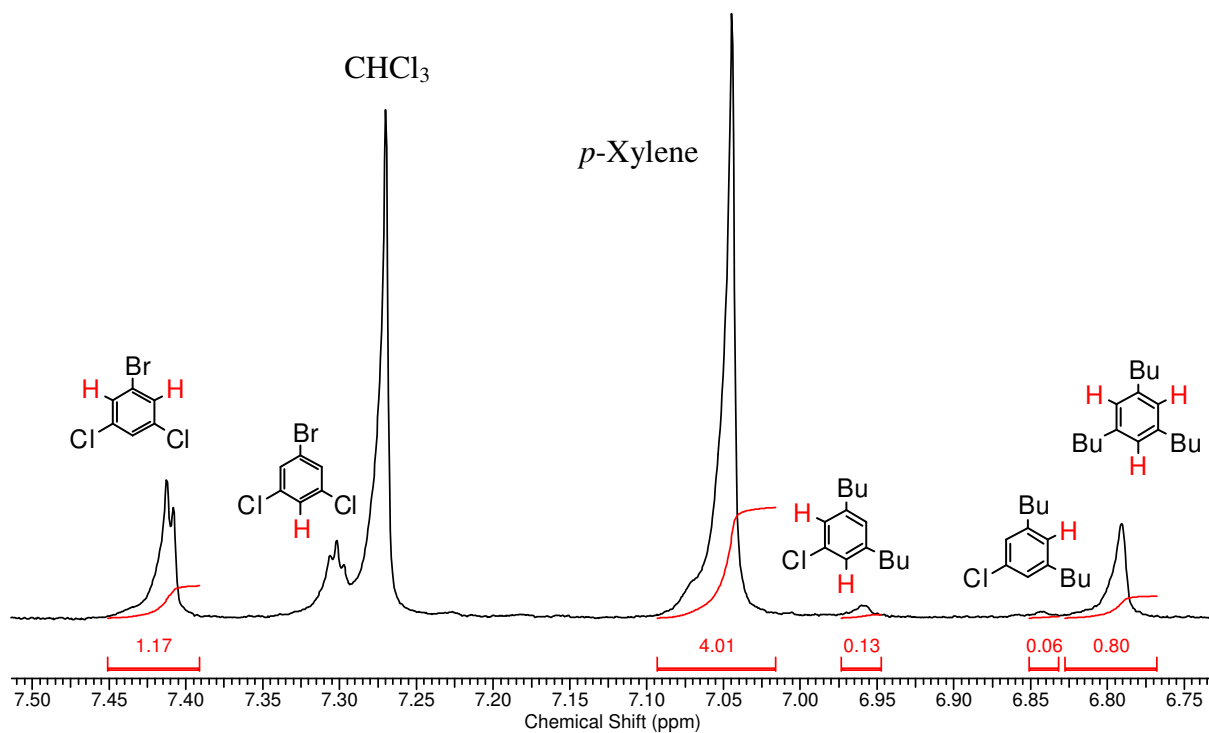
Using the general procedure for sp^3 - sp^2 Negishi couplings employing 1,3,5-trichlorobenzene (46 mg, 0.25 mmol) a product mixture of **S2**, **S3** and **S4** is obtained in a 5 : 7 : 88 ratio by GC-MS analysis and in a <5 : 12 : >83 ratio by ^1H NMR analysis. ^1H NMR analysis using mesitylene as internal standard indicated a 89% yield of **S3+S4** based on *n*-BuZnBr. Product ^1H NMR signals in the crude were assigned by analogy with **S3**¹¹⁰, **S4**¹¹⁸ and 3,5-dichlorotoluene (**28d**).



1-bromo-3,5-dichlorobenzene (**31**):

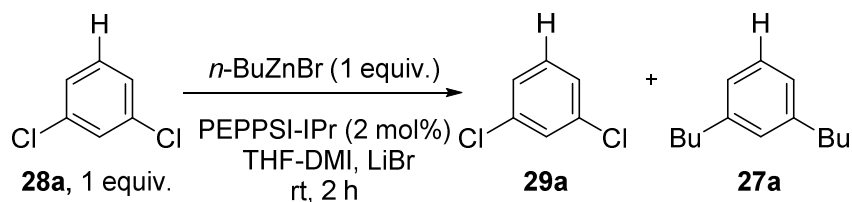


Using the general procedure for $\text{sp}^3\text{-sp}^2$ Negishi couplings employing 1-bromo-3,5-dichlorobenzene (57 mg, 0.25 mmol) a product mixture of **S2**, **S3** and **S4** is obtained in a 9 : 15 : 76 ratio by GC-MS analysis and in a <5 : 17 : >78 ratio by ^1H NMR analysis. ^1H NMR analysis using mesitylene as internal standard indicated a 93% yield of **S3+S4** based on *n*-BuZnBr. ^1H NMR signals in the crude were assigned by analogy with **S3**,¹¹⁰ **S4**¹¹⁸ and 3,5-dichlorotoluene (**28d**).

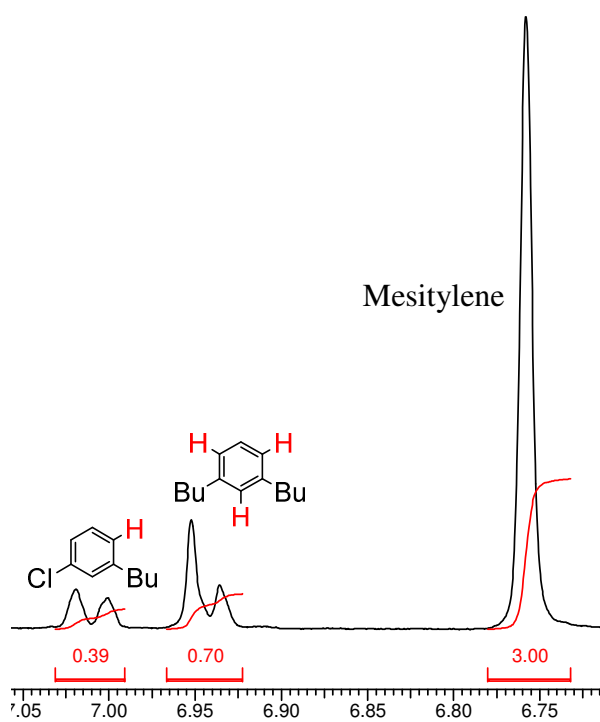


6.2.5 Variation in reaction conditions

All experiments from Tables 4 and 5 and Graphs 2-4 were performed using the general sp^3 - sp^2 Negishi coupling procedure for the coupling of 1,3-dichlorobenzene mediated by PEPPSI-IPr unless stated otherwise.

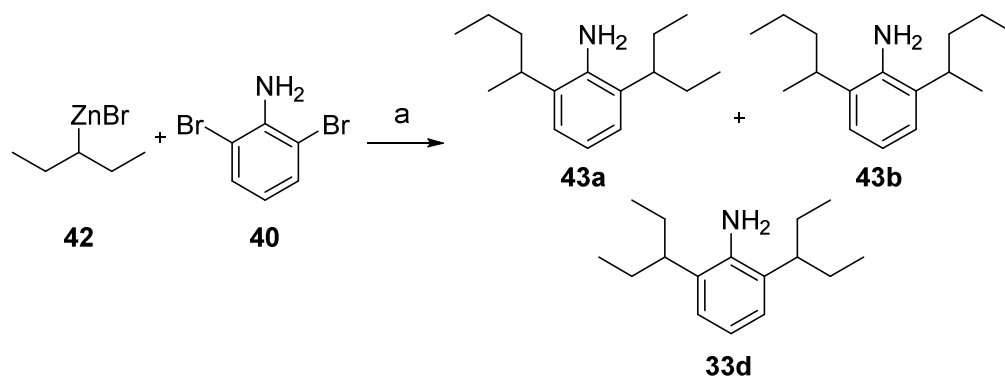


Key peaks in the crude ^1H NMR used to calculate the product ratios are shown, along with the internal standard (mesitylene).

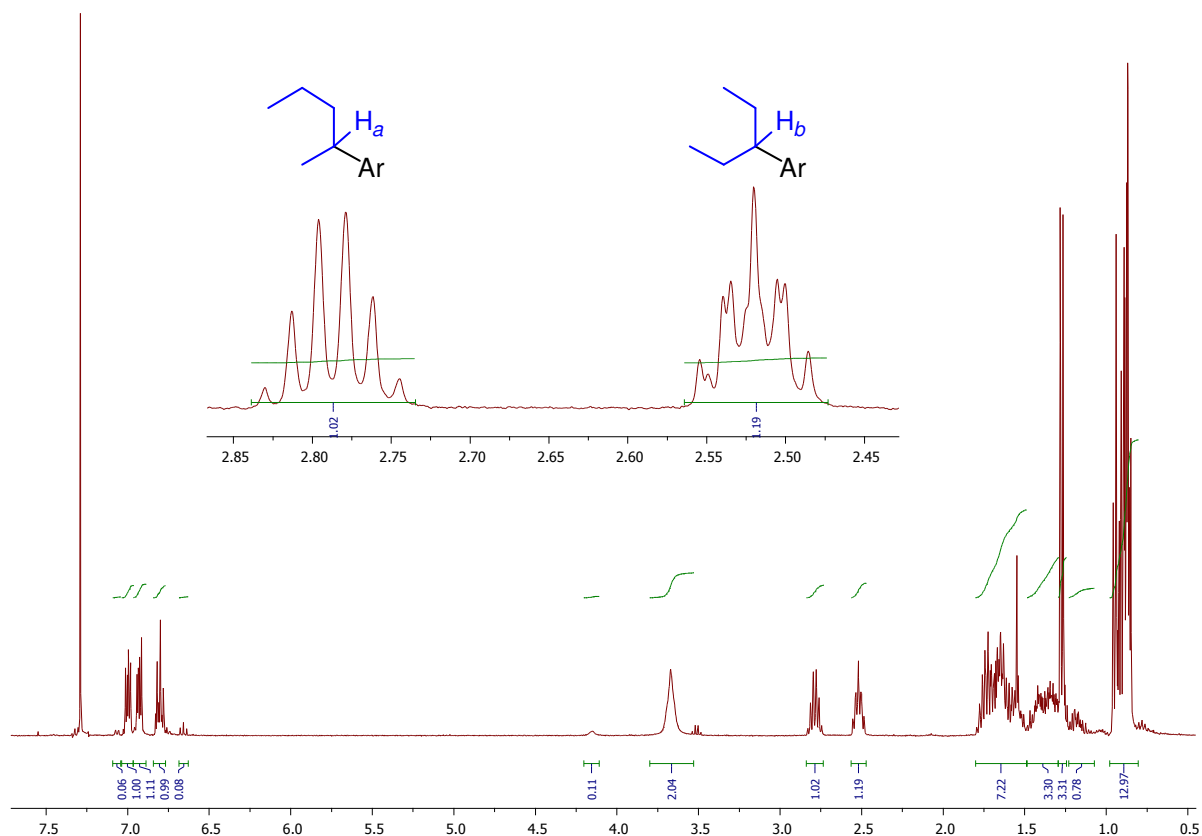


6.3 Chapter 3 Experimental

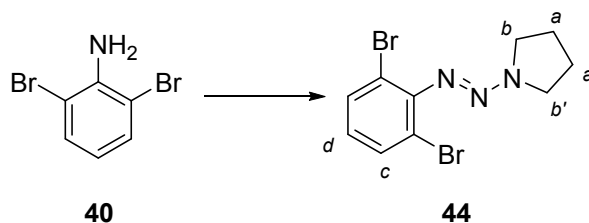
6.3.1 Attempted synthesis of 33d



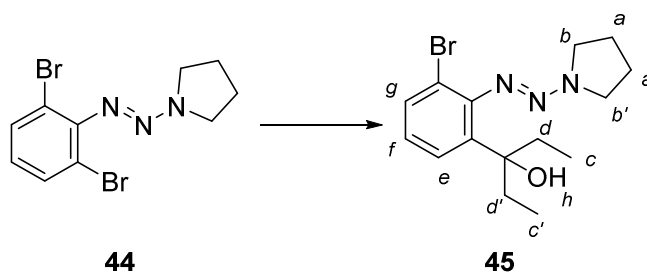
An oven-dried CEM vial equipped with a stirrer bar was charged with 2,6-dibromoaniline (**40**, 125 mg, 0.50 mmol) and PEPPSI-IPent (**35d**, 7.9 mg, 2 mol%). The vial was sealed, purged with nitrogen and anhydrous toluene (2.0 mL) added. The solution was cooled to 0 °C in an ice bath and 3-pentylzinc bromide (**42**, 4.0 mL, 2.0 mmol, 0.50 M in THF) was added slowly via syringe over 2 mins. The ice bath was removed after the addition and the reaction was stirred at rt for 3h. The reaction mixture was then quenched by addition of 1 M HCl (aq., 25 mL), extracted with AcOEt (3 × 25 mL), and the combined organic phases washed with brine (50 mL). The organic layer was dried over anhydrous MgSO₄, filtered, and concentrated *in vacuo*. The resulting residue was purified by flash column chromatography (0 – 67% Et₂O/Petrol) as an eluent to afford the product mixture. The ratio of the **33d** to its regioisomers could not be determined readily by ¹H NMR spectroscopic analysis. The ratio of 2-(2-pentyl)-6-(3-pentyl)aniline **43a** + 2,6-di(2-pentyl)aniline **43b** to 2,6-di(3-pentyl)aniline **33d** regioisomers appears to be 46 : 54, respectively, based on protons *a* and *b* displayed in the ¹H NMR below.



6.3.2 Route 1: Synthesis of aniline 33d



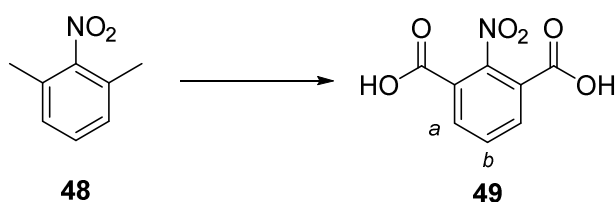
1-(2,6-dibromophenylazo)pyrrolidine (**44**):⁹⁹ A solution of 2,6-dibromoaniline (**40**, 5.0 g, 19.9 mmol) in conc. HCl (aq., 7.9 mL) was cooled in an ice bath. A solution of NaNO₂ (1.43 g, 20.9 mmol) in water (44 mL) was added dropwise. The resulting solution was stirred at 0 °C for 30 min and then added at once to a solution of pyrrolidine (2.86 g, 39.8 mmol) and K₂CO₃ (13.7 g, 99.5 mmol) in 1 : 2 MeCN / water (25 mL). The reaction mixture was stirred for 30 mins at 0 °C and extracted with CH₂Cl₂ (3 × 50 mL). The combined organic layers were washed with brine (2 × 100 mL), dried over anhydrous MgSO₄, filtered and concentrated *in vacuo*. The crude product was purified by flash column chromatography using CH₂Cl₂ : petrol (1 : 1) as an eluent to give 1-(2,6-dibromophenylazo)pyrrolidine (**44**) as a yellow liquid (3.03 g, 45% yield). ¹H NMR (400 MHz, CDCl₃) δ 7.53 (d, *J* = 8.0 Hz, 2H, Hd), 6.84 (t, *J* = 8.0 Hz, 1H, Hc), 3.96 (s, 2H, Hb), 3.73 (s, 2H, Hb), 2.08 (s, 4H, Ha).



1-(2-bromo-6-(3-hydroxy-3-pentyl)phenylazo)pyrrolidine (**45**): To a solution of 1-(2,6-dibromophenylazo)pyrrolidine (**44**) (2.0 g, 6.0 mmol) in anhydrous THF (1.5 mL) was slowly added *i*-PrMgCl·LiCl (3.3 mL, 6.6 mmol, 2.0 M in THF) at −40 °C. The reaction

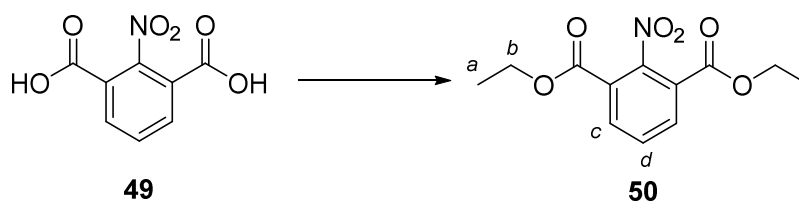
temperature was gradually increased to $-15\text{ }^{\circ}\text{C}$. After 2.5 h, a complete conversion to the Grignard reagent was observed as indicated by GC-analysis of hydrolyzed reaction aliquots. 3-Pentanone (1.27 mL, 12.0 mmol) in anhydrous THF (6.0 mL) was added and the reaction mixture was allowed to warm to rt then quenched with MeOH (5.0 mL). The reaction mixture was concentrated *in vacuo* and redissolved in CH_2Cl_2 . The organic phase was washed with 1M HCl (aq., $2 \times 50\text{ mL}$) and brine (50 mL), dried over anhydrous MgSO_4 , filtered and concentrated *in vacuo*. Purification by flash column chromatography using CH_2Cl_2 : AcOEt (3 : 7) rising to AcOEt as an eluent to give alcohol **45** as a brown solid (1.64 g, 80 % yield). **Melting point:** $42 - 44\text{ }^{\circ}\text{C}$; $^1\text{H NMR}$ (400 MHz, CDCl_3) δ 7.48 (dd, $J = 7.9, 1.1\text{ Hz}$, 1H, He), 7.17 (dd, $J = 7.9, 1.0\text{ Hz}$, 1H, Hg), 6.96 (t, $J = 7.9\text{ Hz}$, 1H, Hf), 5.89 (s, 1H, Hh), 3.99 (s, 2H, Hb), 3.69 (s, 2H, Hb), 2.08 (s, 4H, Ha), 1.87 (dq, $J = 14.7, 7.4\text{ Hz}$, 2H, Hd), 1.70 (dq, $J = 14.6, 7.4\text{ Hz}$, 2H, Hd), 0.79 (t, $J = 7.4\text{ Hz}$, 6H, Hc); $^{13}\text{C NMR}$ (101 MHz, CDCl_3) δ 147.9, 140.6, 132.7, 126.9, 125.6, 115.8, 79.4, 51.5, 46.8, 24.1, 23.8; **HRMS (ESI+)** m/z found: 340.1022 [M+H] Calc. ($\text{C}_{15}\text{H}_{22}\text{BrN}_3\text{O}$) 340.1019; **IR** (cm^{-1}) 3352, 2968, 2876, 1444, 1411, 1353, 1312, 970, 795, 781, 753, 733.

6.3.3 Route 2: Synthesis of aniline 33d

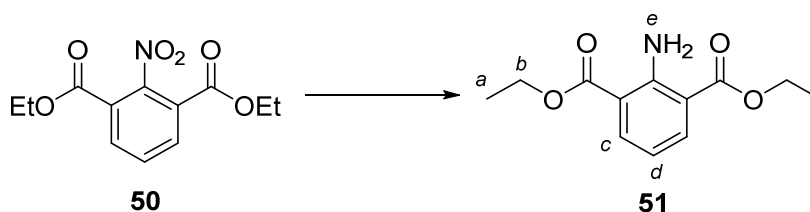


2-Nitroisophthalic acid (**48**):¹⁰⁰ 2-Nitro-*m*-xylene (**49**, 15.0 g, 99.2 mmol) and NaOH (6.0 g, 150 mmol) were added to water (750 mL) and heated to $95\text{ }^{\circ}\text{C}$. KMnO_4 (70 g, 443 mmol) was then added slowly for 2.5 hours before being refluxed for 20 hours. The reaction was cooled and then filtered. The filtrate was acidified with 2M HCl (aq.) to yield a white precipitate and filtered through a sinter funnel. The residue was washed

from the sintered funnel with acetone, and dried *in vacuo* to yield diacid **49** as a white precipitate (12.9 g, 61% yield). **Melting point:** >250 °C; ^1H NMR (400 MHz, DMSO) δ 8.18 (d, J = 7.8 Hz, 2H, H_b), 7.80 (t, J = 7.8 Hz, 1H, H_a); ^{13}C NMR (101 MHz, DMSO) δ 164.2, 148.8, 134.6, 131.2, 124.9.

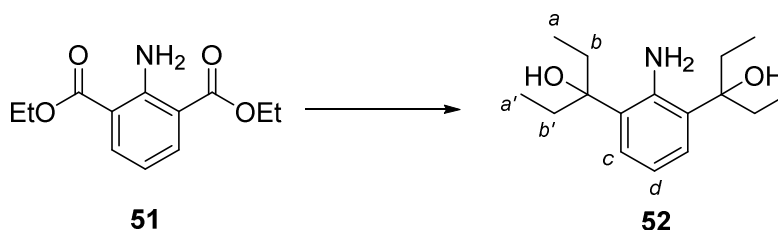


Diethyl 2-nitroisophthalate (**50**): Thionyl chloride (15.4 mL, 214 mmol) was added dropwise to a stirred solution of 2-nitroisophthalic acid (**49**, 11.3 g, 53.5 mmol) in EtOH (230 mL, dried over anhydrous MgSO_4) at 0 °C under nitrogen. The reaction mixture was stirred at 70 °C for 20 hours. The reaction mixture was concentrated *in vacuo* and dissolved in CH_2Cl_2 (250 mL). The organic mixture was washed with saturated NaHCO_3 (aq., 250 mL), dried over anhydrous MgSO_4 , filtered and concentrated *in vacuo* to give diethyl ester **50** as a white powder (11.5 g, 80% yield). **Melting point:** 85-87 °C; ^1H NMR (400 MHz, CDCl_3) δ 8.18 (d, J = 7.8 Hz, 2H, H_c), 7.64 (t, J = 7.8 Hz, 1H, H_d), 4.38 (q, J = 7.1 Hz, 4H, H_b), 1.36 (t, J = 7.1 Hz, 6H, H_a); ^{13}C NMR (101 MHz, CDCl_3) δ 162.9, 135.0, 130.2, 124.6, 62.9, 13.9; **HRMS (ESI+)** m/z found: 285.1081 $[\text{M}+\text{NH}_4]^+$, Calc. ($\text{C}_{12}\text{H}_{17}\text{N}_2\text{O}_6$) 285.1087; **IR** (cm^{-1}) 2991, 2910, 1734, 1721, 1608, 1548, 1367, 1262.

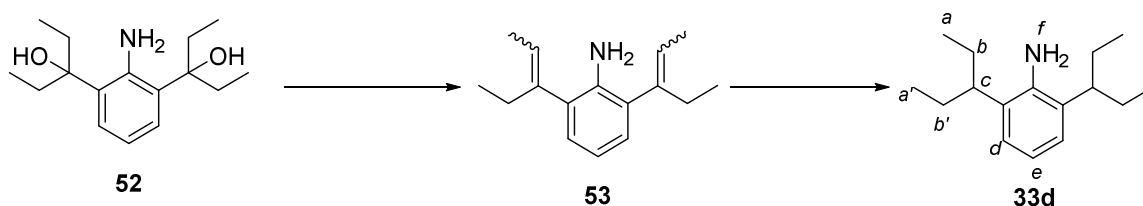


Diethyl 2-aminoisophthalate (**51**):¹¹⁹ A mixture of diester **50** (10.5 g, 39.3 mmol), 10% palladium on carbon (830 mg) and EtOH (250 mL) was stirred under an atmosphere of

hydrogen (1 atm) at rt for 6 hours. The mixture was filtered through a pad of Celite® washing through with MeOH and concentrated *in vacuo* to give aniline **51** as colourless crystals (8.90g, 87% yield). **Melting point:** 40-41 °C; **¹H NMR (400 MHz, CDCl₃)** δ 8.23 – 8.06 (m, 4H, H_c, H_e), 6.54 (t, *J* = 7.8 Hz, 1H, H_d), 4.33 (q, *J* = 7.1 Hz, 4H, H_b), 1.38 (t, *J* = 7.1 Hz, 6H, H_a); **¹³C NMR (101 MHz, CDCl₃)** δ 167.9, 153.4, 137.4, 113.6, 112.1, 60.6, 14.4.

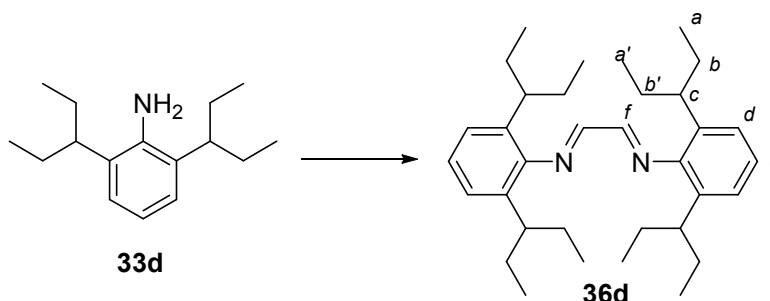


2,6-Di(pentan-3-ol)aniline (**52**):¹⁰² Ethylmagnesium bromide (100 mL, 200 mmol, 2M in THF) was added dropwise to a solution of aniline **51** (5.93 g, 25.0 mmol) in anhydrous THF (110 mL) at 0 °C. The mixture was stirred at rt for 3 h and neutralised with 1M HCl (aq., very carefully). The mixture was diluted with 1M HCl (aq., up to 500 mL) and extracted with Et₂O (2 × 500mL). The pH of the aqueous layer was adjusted to ~pH 9 with 1M NaOH (~300 mL) and the aqueous layer was then extracted with Et₂O (1 L). This organic layer was dried over anhydrous MgSO₄, filtered and concentrated *in vacuo* to give diol **52** as a clear oil (5.51 g, 83% yield). **¹H NMR (400 MHz, CDCl₃)** δ 6.91 (d, *J* = 7.8 Hz, 2H, H_c), 6.56 (t, *J* = 7.8 Hz, 1H, H_d), 2.14 – 1.98 (m, 4H, H_b), 1.99 – 1.83 (m, 4H, H_b), 0.85 (t, *J* = 7.4 Hz, 12H, H_a).; **¹³C NMR (101 MHz, CDCl₃)** δ 147.2, 128.1, 127.1, 115.3, 80.2, 31.0, 8.5.



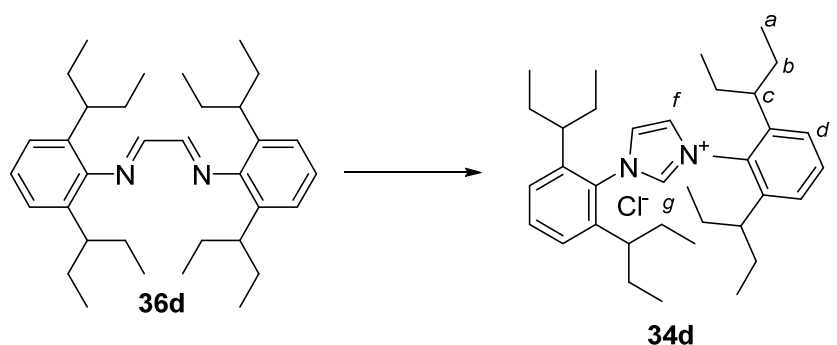
2,6-Di(3-pentyl)aniline (**33d**):¹⁰² Diol **52** (5.51 g, 20.1 mmol) and *p*-TsOH (385 mg, 2.01 mmol) were dissolved in anhydrous toluene (100 mL). The mixture was heated under reflux with Dean-Stark apparatus for 3 h. After cooling to room temperature, the reaction mixture was washed with saturated NaHCO₃ (aq., 100 mL) and brine (100 mL) solutions. The aqueous layer was extracted with AcOEt (200 mL). The combined organic layers were dried over anhydrous MgSO₄, filtered and concentrated *in vacuo* to give 2,6-di(pent-2-en-3-yl)aniline (**53**) as a yellow oil which was taken forward without purification (4.28 g, impure). The oil was dissolved in EtOH (100 mL), added to 10% palladium on carbon (852 mg) and was stirred under an atmosphere of hydrogen (1 atm) at rt for 12 hours. The mixture was filtered through a pad of Celite® washing through with MeOH and concentrated *in vacuo*. The residue was purified by flash column chromatography using CH₂Cl₂ : Petrol (1 : 4) as an eluent to give aniline **33d** as a colourless oil (3.43g, 59% yield over two steps). ¹H NMR (400 MHz, CDCl₃) δ 6.89 (d, *J* = 7.6 Hz, 2H, Hd), 6.81 – 6.71 (m, 1H, He), 3.62 (s, 2H, Hf), 2.55 – 2.42 (m, 2H, Hc), 1.79 – 1.49 (m, 8H, Hb), 0.83 (t, *J* = 7.4 Hz, 12H, Ha); ¹³C NMR (101 MHz, CDCl₃) δ 142.7, 130.2, 124.0, 118.6, 42.5, 28.2, 12.2.

6.3.4 PEPPSI-IPent synthesis



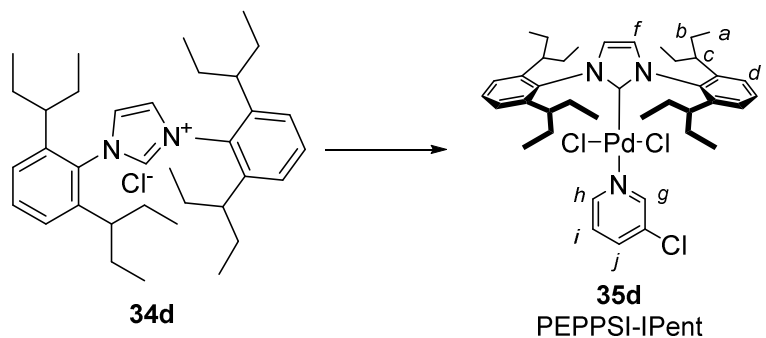
N,N'-Bis(di(3-pentyl))diazabutadiene (**36d**):¹⁰² Glyoxal (1.00 mL, 9.09 mmol, 40% in water) was added to a solution of aniline **33d** (3.43 g, 14.7 mmol) in MeOH (40 mL)

followed by addition of formic acid (86 μL , 2.28 mmol) at rt and was stirred for 4 h. The resulting precipitate was collected by filtration and the filtrate was concentrated *in vacuo* affording a brownish solid that was recrystallized from MeOH. Both solids were combined and dried under vacuum to give diimine **36d** as a bright yellow powder (3.14 g, 87% yield). **Melting point:** 66 - 67 $^{\circ}\text{C}$; ^1H NMR (400 MHz, CDCl_3) δ 8.01 (s, 2H, Hf), 7.18 – 7.09 (m, 2H, He), 7.09 – 7.03 (m, 4H, Hd), 2.56 – 2.44 (m, 4H, Hc), 1.72 – 1.46 (m, 16H, Hb), 0.80 (t, $J = 7.4$ Hz, 24H, Ha); ^{13}C NMR (101 MHz, CDCl_3) δ 164.0, 151.1, 134.0, 124.9, 124.0, 42.7, 29.1, 12.3.



IPent.HCl (**34d**):¹⁰² A solution of diimine **36d** (3.74 g, 7.65 mmol) in anhydrous THF (300 mL) was treated with anhydrous ZnCl_2 (1.04 g, 7.65 mmol) at 70 $^{\circ}\text{C}$ and stirred for 5 min. Paraformaldehyde (241 mg, 8.02 mmol) was subsequently added followed by the dropwise addition of anhydrous 4M HCl in dioxane (2.87 mL, 11.3 mmol). The reaction was stirred for 16 h at 70 $^{\circ}\text{C}$ and then concentrated *in vacuo*. The residue was dissolved in AcOEt (250 mL) and was washed with water (3×250 mL) and brine (250 mL). The combined aqueous phases were extracted with AcOEt (250 mL) and the organic phases were combined, dried over anhydrous MgSO_4 and filtered. The solvent was partially concentrated *in vacuo* until precipitation commenced and the resulting suspension was diluted with pentane (75 mL) and placed in the freezer for 20 min. The solid was isolated by filtration and washed with pentane to afford IPent.HCl **34d** as an off-white

microcrystalline powder (2.05 g, 50% yield). **Melting point:** >250 °C; ^1H NMR (400 MHz, CDCl_3) δ 8.95 (s, 1H, Ha), 8.30 (d, J = 1.5 Hz, 2H, Hf), 7.60 (t, J = 7.8 Hz, 2H, He), 7.28 (d, J = 7.8 Hz, 4H, Hd), 2.02 – 1.87 (m, 4H, Hc), 1.84 – 1.52 (m, 16H, Hb), 0.85 (t, J = 7.4 Hz, 12H, Ha), 0.78 (t, J = 7.4 Hz, 12H, Ha); ^{13}C NMR (101 MHz, CDCl_3) δ 142.7, 136.6, 132.9, 132.1, 128.4, 125.5, 43.7, 29.3, 28.6, 12.6, 12.5.



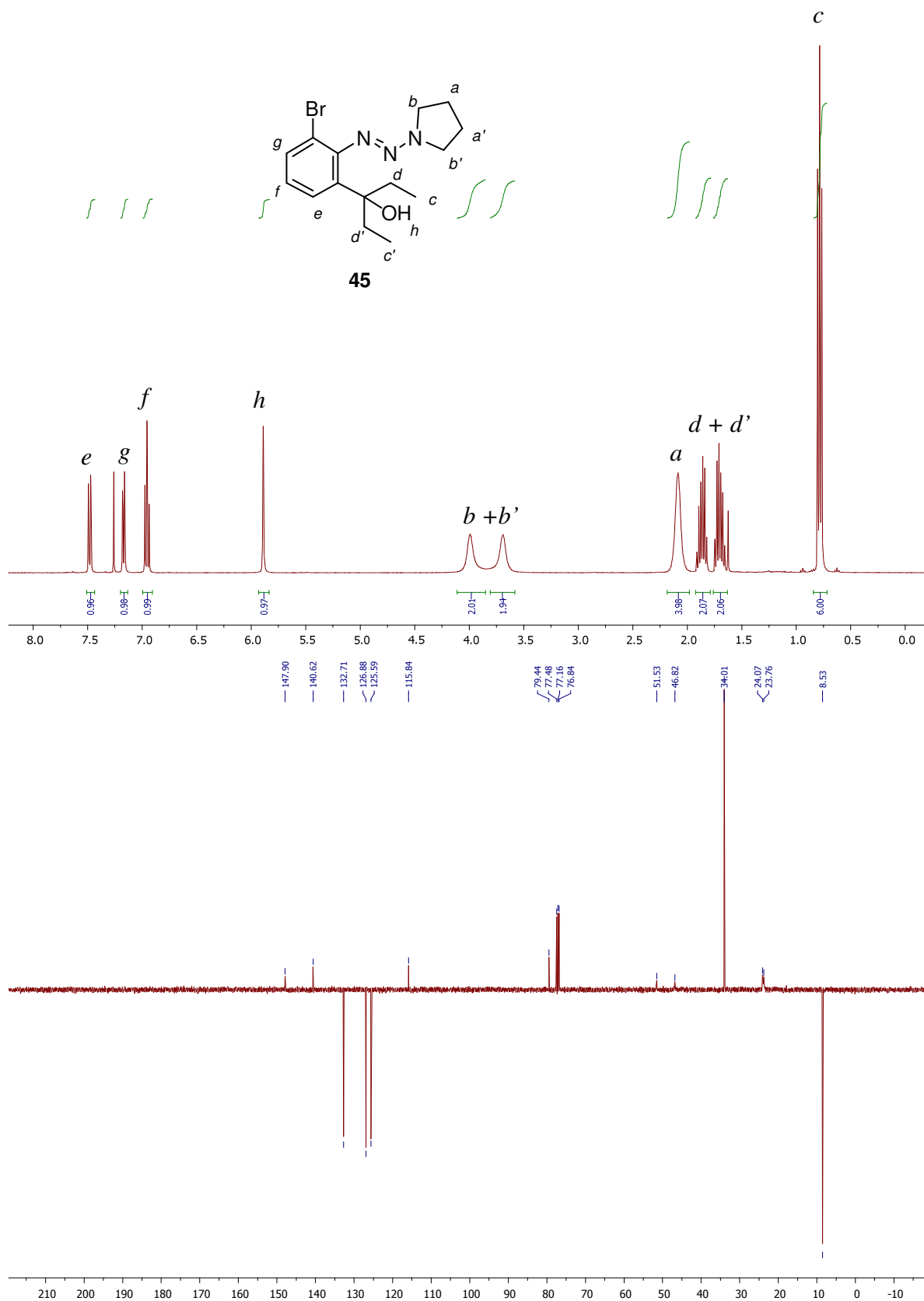
PEPPSI-IPent (**35d**):⁷⁹ In air, a 25 mL round bottomed flask was charged with PdCl_2 (177 mg, 1.0 mmol), IPent.HCl (**34d**, 590 mg, 1.1 mmol), K_2CO_3 (691 mg, 5.0 mmol) and a stirrer bar and flushed with nitrogen. 3-Chloropyridine (4.0 mL) was added and heated with vigorous stirring for 20 h at 80 °C. After cooling to rt, the reaction mixture was diluted with CH_2Cl_2 and passed through a short pad of silica gel covered with a pad of Celite® eluting with CH_2Cl_2 until the product was completely recovered and the solution concentrated *in vacuo*. To the residue was added *n*-hexane (50 mL) and removed *in vacuo*, this process was repeated three times. The crude was purified by flash column chromatography using CH_2Cl_2 : *n*-hexane (2 : 3) as an eluent, concentrated *in vacuo*, *n*-hexane (50 mL) was added and removed *in vacuo* to give PEPPSI-IPent (**35d**) as a pale yellow powder (633 mg, 80% yield). **Melting point:** >250 °C; ^1H NMR (400 MHz, CDCl_3) δ 8.64 (d, J = 2.3 Hz, 1H, Hg), 8.59 – 8.47 (m, 1H, Hi), 7.54 (ddd, J = 8.2, 2.3, 1.3 Hz, 1H, Hj), 7.44 (t, J = 7.8 Hz, 2H, He), 7.24 (d, J = 7.8 Hz, 4H, Hd), 7.11 – 6.99 (m, 3H, Hf, Hh), 2.87 – 2.68 (m, 4H, Hc), 2.22 – 2.02 (m, 4H, Hb), 1.98 – 1.75 (m, 4H,

Hb), 1.62 – 1.43 (m, 8H, Hb), 1.12 (t, $J = 7.3$ Hz, 12H, Ha), 0.79 (t, $J = 7.5$ Hz, 12H, Ha);

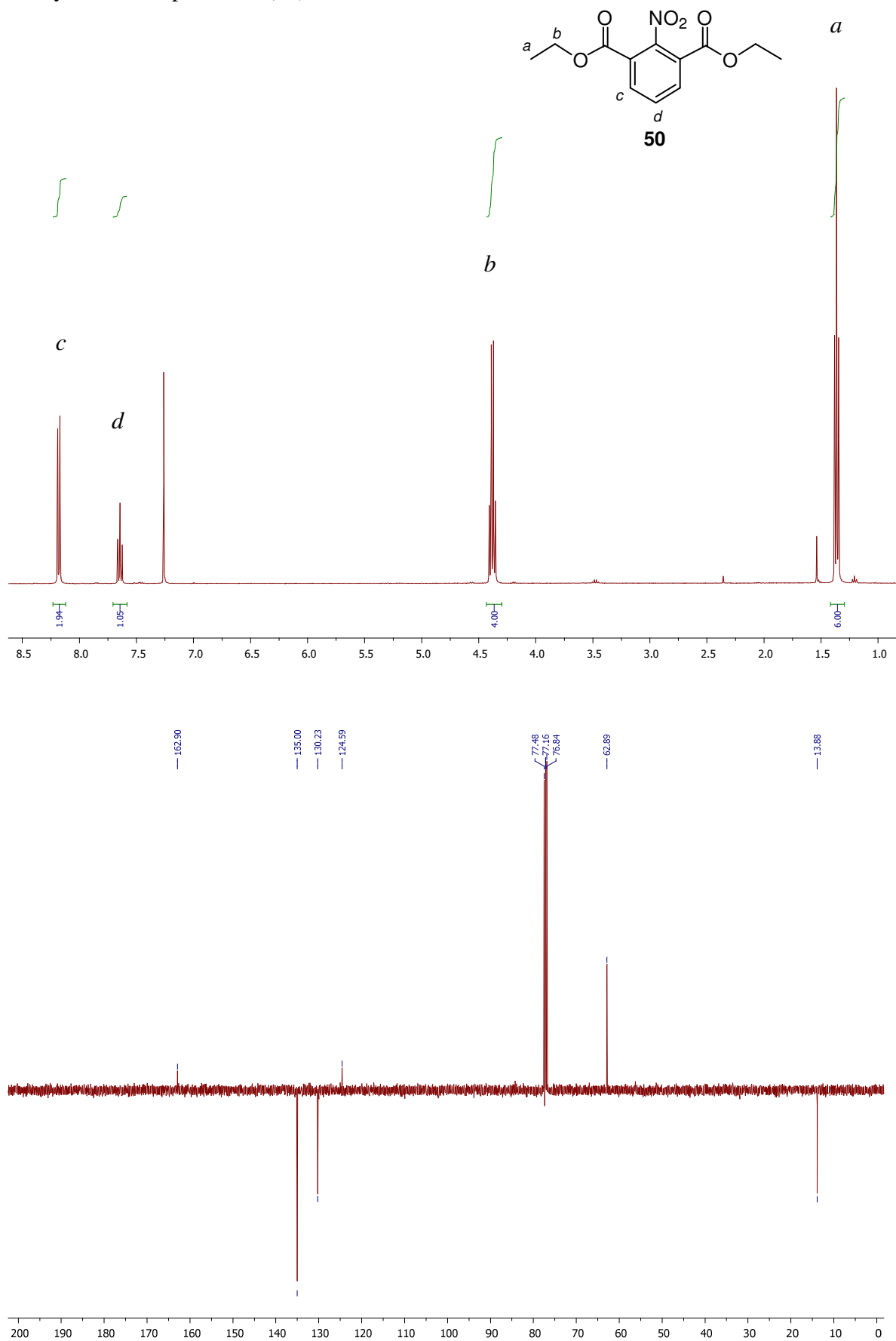
^{13}C NMR (101 MHz, CDCl_3) δ 152.4, 150.6, 149.6, 144.7, 137.4, 136.7, 132.0, 129.3, 125.5, 125.4, 124.4, 41.3, 28.9, 27.4, 13.0, 11.3.

6.3.5 Graphical NMR Data for all novel compounds

1-(2-bromo-6-(3-hydroxy-3-pentyl)phenylazo)pyrrolidine (**45**):



Diethyl 2-nitroisophthalate (**50**):



6.4 Chapter 4 Experimental

6.4.1 General Remarks

2,7-Dichlorofluorenone,¹²⁰ PEPPSI-IMes,⁹¹ PEPPSI-IEt⁹¹ and PEPPSI-IPr*¹²¹ were prepared according to reported procedures. The synthesis of PEPPSI-IPent was described previously. To facilitate the analysis of the outcome of cross coupling reactions the major product was isolated to confirm its identity and to verify the peaks of interest in the crude reaction mixture. All novel compounds were fully characterized. The characterization data for **69a**,¹²² **70a**,¹²³ **70b**,¹²⁴ **70c**,¹²⁵ **70f**,¹²⁶ **70h**,¹²⁷ **70j**,¹²⁸ **70k**,¹²⁹ **70n**,¹³⁰ **70o**,¹³¹ **70q**,¹³² **70r**,¹³³ **70s**,¹²² **69t**,¹³⁴ **70v**,¹³⁵ **70w**,¹³⁶ and **70x**¹³⁵ matched those of reported literature.

6.4.2 General Procedures

Preparation of ZnCl₂ (1M in THF): A flask equipped with a Young's tap was charged with ZnCl₂ (35.2 g, 251 mmol) and the solid dried under high vacuum at 160 °C for 16 h. The flask was cooled to rt and filled with N₂. THF (251 mL) was added and the mixture stirred for 24 h at rt until all solid had fully dissolved.

General procedure for Kumada couplings:⁷⁶ A CEM microwave vial was charged with PEPPSI-IPent (4.0 mg, 5.0 μmol), and, if solid at rt, the aryl halide (0.25 mmol). The vial was sealed, flushed with N₂, THF (0.88 mL) was added and the solution was stirred at 50 °C. If the aryl halide was a liquid at rt, it was added immediately after the addition of THF. PhMgBr (1.0 M in THF, 0.25 mL, 0.25 mmol) was added and the resultant solution was stirred for 3 h at 50 °C. Mesitylene was added as an internal standard (0.50 M in CDCl₃, 0.50 mL, 0.25 mmol), and the crude reaction mixture was analysed by GC-MS and ¹H NMR.

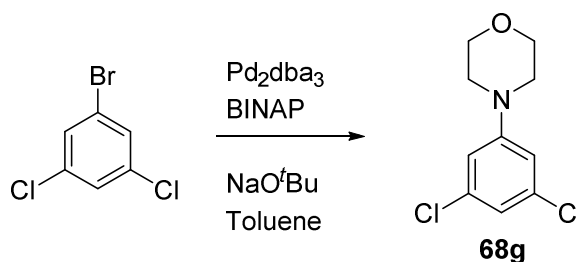
General procedure for Suzuki couplings:⁹¹ A CEM microwave vial was charged with PEPPSI-IPent (4.0 mg, 5.0 μmol), K₂CO₃ (105 mg, 0.75 mmol), PhB(OH)₂ (30 mg, 0.25

mmol) and, if solid at rt, the aryl halide (0.25 mmol). The vial was sealed, flushed with N₂, 1,4-dioxane (1.0 mL) was added and the resultant mixture was stirred at 60 °C for 12 h. If the aryl halide was a liquid at rt, it was added immediately after the addition of 1,4-dioxane. Mesitylene was added as an internal standard (0.50 M in CDCl₃, 0.50 mL, 0.25 mmol), and the crude reaction mixture was analysed by GC-MS and ¹H NMR.

General procedure for sp² Negishi couplings:⁸⁶ ZnCl₂ (1.0 M in THF, 2.0 mL, 2.0 mmol) and PhMgBr (1.0 M in THF, 2.0 mL, 2.0 mmol) were stirred vigorously under N₂ at rt for 30 min. NMP (4.0 mL) was added to the mixture and the resulting PhZnCl (1.0 mL, 0.25 mmol) was added by syringe to a CEM vial charged with PEPPSI-IPent (4.0 mg, 5.0 μmol), and the aryl halide (0.25 mmol) in NMP (0.50 mL). The reaction mixture was stirred at 30 °C for 2 h. Mesitylene was added as an internal standard (0.50 M in CDCl₃, 0.50 mL, 0.25 mmol), and the crude reaction mixture was analysed by GC-MS and ¹H NMR.

6.4.3 Synthesis of Starting Materials

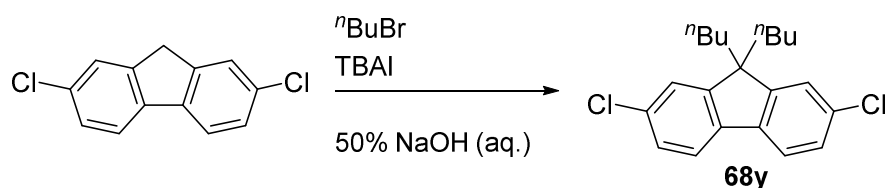
4-(3,5-dichlorophenyl)morpholine (68g):



A CEM vial was charged with Pd₂dba₃ (46 mg, 100 μmol), BINAP (93 mg, 150 μmol), NaO^tBu (231 mg, 2.4 mmol) and 1-bromo-3,5-dichlorobenzene (452 mg, 2.0 mmol). The vial was sealed and purged with N₂ before the addition of PhMe (5.0 mL) and morpholine (173 μL, 2.0 mmol). The mixture was stirred at 80 °C for 16 h. The reaction mixture was diluted with Et₂O (10 mL), filtered through a pad of Celite and concentrated *in vacuo*.

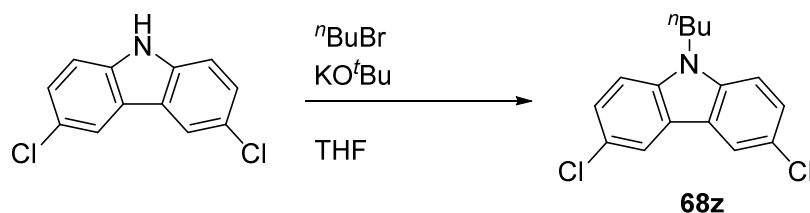
Chromatography (CH₂Cl₂) gave **68g** as a white solid (334 mg, 72%): **Melting point** 67 - 69 °C (lit.¹³⁷ 86 °C); **¹H NMR (400 MHz, CDCl₃)** δ 6.83 (t, *J* = 1.7, 1H) 6.73 (d, *J* = 1.7, 2H), 3.85 – 3.79 (m, 4H), 3.18 - 3.11 (m, 4H); **¹³C NMR (101 MHz, CDCl₃)** δ 152.8, 135.7, 119.4, 113.7, 66.7, 48.5.

2,7-Dichloro-9,9-dibutylfluorene (68y):



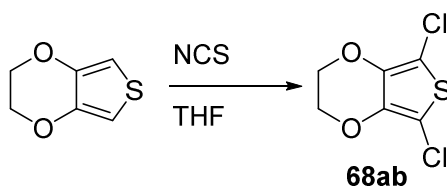
A CEM vial was charged with 2,7-dichlorofluorene (235 mg, 2.0 mmol), ⁿBu₄NI (73 mg, 200 μmol) and flushed with N₂. NaOH (50% w/w, degassed, 20 mL) was added and the mixture stirred for 5 minutes at rt. ⁿBuBr (1.51 mL, 14.0 mmol) was added and the reaction mixture heated at 70 °C for 12 h. The reaction mixture was cooled to rt and extracted with CHCl₃ (100 mL). The organic phase was washed with H₂O (100 mL), dried over MgSO₄, and concentrated *in vacuo*. Chromatography (9 : 1 petrol-CHCl₃) gave **68y** as a white solid (336 mg, 97%): **Melting point** 110 - 111 °C; **¹H NMR (400 MHz, CDCl₃)** δ 7.57 (dd, *J* = 7.8, 0.6, 2H), 7.33 – 7.27 (m, 4H), 1.97 – 1.87 (m, 4H), 1.15 – 1.03 (m, 4H), 0.69 (t, *J* = 7.4, 6H), 0.63 – 0.52 (m, 4H); **¹³C NMR (101 MHz, CDCl₃)** δ 152.5, 138.8, 133.3, 127.5, 123.4, 120.9, 55.7, 40.2, 26.0, 23.1, 13.9; **LRMS (ESI)** 346.3 [M]⁺; **HRMS (EI)** 346.1256 [M]⁺ (calc. for C₂₁H₂₄³⁵Cl₂ 346.1250 [M]⁺); **IR (cm⁻¹)** 2952, 2927, 2857, 1451, 1421, 1069, 807.

3,6-Dichloro-9-butylcarbazole (**68z**):



To a mixture of 3,6-dichlorocarbazole (472 mg, 2.0 mmol), KO^tBu (270 mg, 2.4 mmol) and THF (10 mL) was added $n\text{BuBr}$ (260 μL , 2.0 mmol) and the resulting mixture was stirred at 60 °C for 4 h. H_2O (50 mL) was added and the mixture extracted with CH_2Cl_2 (50 mL). The organic phase was dried over MgSO_4 , and concentrated *in vacuo*. Chromatography (petrol \rightarrow 3 : 1 petrol- CH_2Cl_2) gave **68z** as a white solid (519 mg, 89%): **Melting point** 68 – 70 °C; ^1H NMR (400 MHz, CDCl_3) δ 8.01 (d, J = 2.0, 2H), 7.45 (dd, J = 8.7, 2.0, 2H), 7.34 (d, J = 8.7, 2H), 4.28 (t, J = 7.2, 2H), 1.89 – 1.79 (m, 2H), 1.45 – 1.33 (m, 2H), 0.97 (t, J = 7.4, 3H); ^{13}C NMR (101 MHz, CDCl_3) δ 139.3, 126.5, 124.7, 123.1, 120.3, 110.1, 43.3, 31.2, 20.6, 14.0; **LRMS (ESI)** 291.1; **HRMS (EI)** 291.0573 $[\text{M}]^+$ (calc. for $\text{C}_{16}\text{H}_{15}^{35}\text{Cl}_2\text{N}$ 291.0576 $[\text{M}]^+$); **IR (cm^{-1})** 2959, 2935, 2917, 2876, 2857, 1473, 1439, 1076, 857, 794, 680.

2,5-Dichloro-3,4-ethylenedioxythiophene, **68ac**:



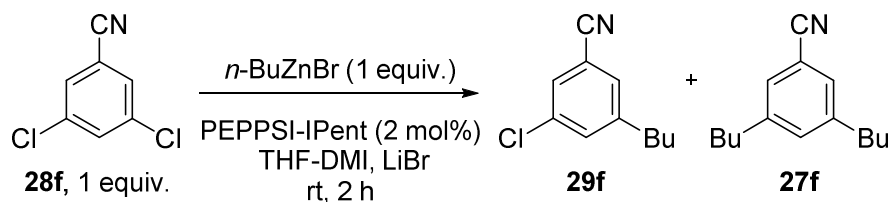
3,4-Ethylenedioxythiophene (1.41 g, 10 mmol) was dissolved in THF (50 mL) and cooled to 0 °C. *N*-Chlorosuccinimide (2.94 g, 22 mmol) was added and the resultant mixture was stirred at rt for 48 h. Na_2SO_3 (1.0 g, 7.9 mmol) was added, the suspension filtered and the filtrate concentrated *in vacuo*. The residue was dissolved in CH_2Cl_2 , filtered through a short plug of SiO_2 to remove the dark blue colour and concentrated *in vacuo*.

Chromatography (petrol \rightarrow 4:1 petrol-CH₂Cl₂) gave **68ac** as a white solid (1.21 g, 57%) which was stored under N₂ at $-18\text{ }^{\circ}\text{C}$: **Melting point** $59 - 60\text{ }^{\circ}\text{C}$ (lit.¹³⁸ $60 - 62\text{ }^{\circ}\text{C}$); ¹H NMR (400 MHz, CDCl₃) δ 4.26 (s, 4H); ¹³C NMR (101 MHz, CDCl₃) δ 137.4, 100.6, 65.1.

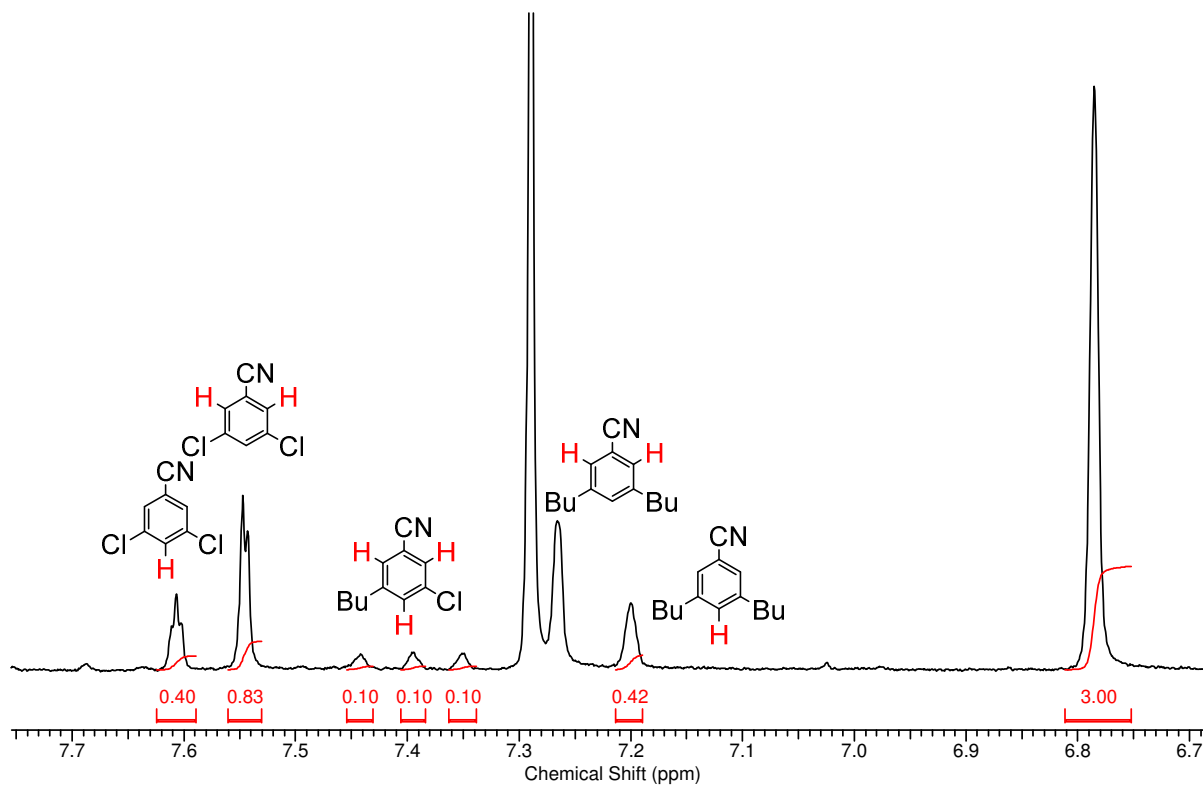
6.4.4 Experimental Data

Scheme 48

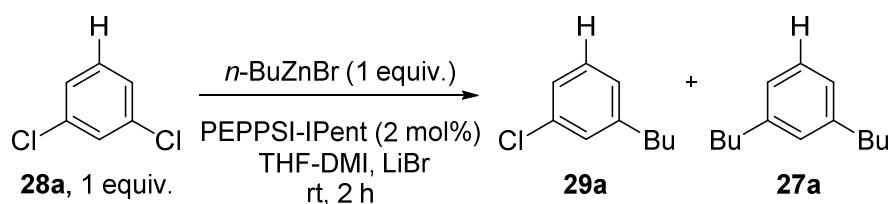
3,5-Dichlorobenzonitrile **28f**, PEPPSI-IPent



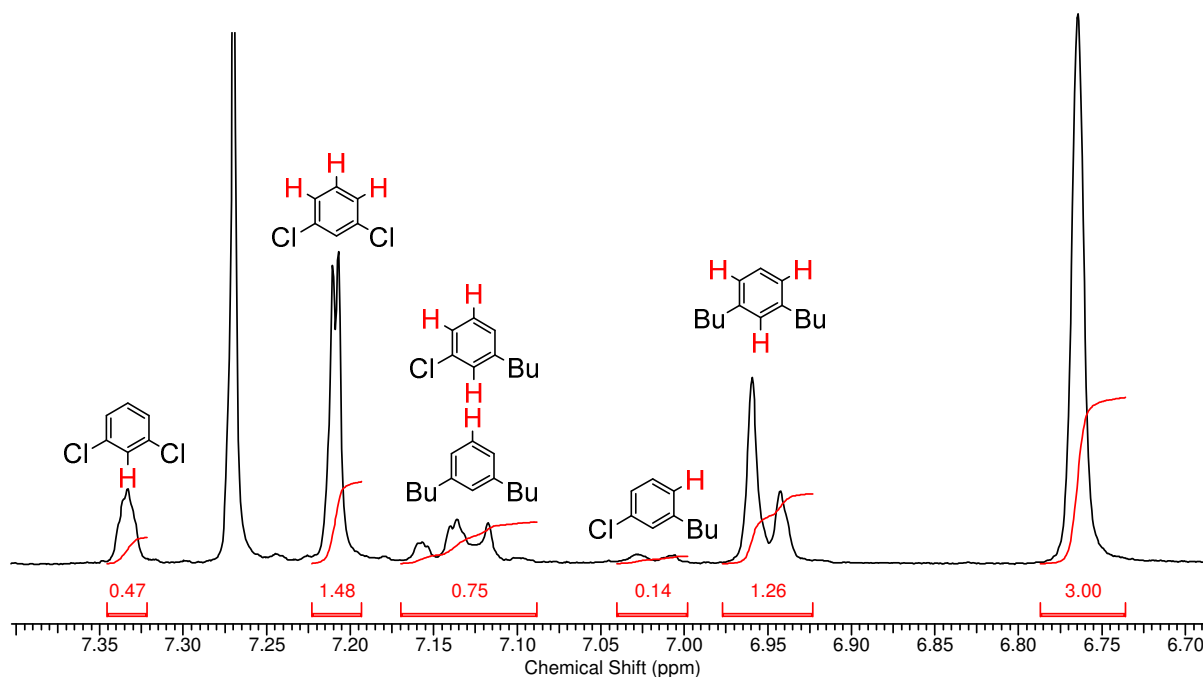
Using the general procedure for sp^3 - sp^2 Negishi couplings employing 3,5-dichlorobenzonitrile (43 mg, 0.25 mmol) a product mixture of **29f** and **27f** is obtained in a 24 : 76 ratio by GC-MS analysis and in a 19 : 81 ratio by ^1H NMR analysis. ^1H NMR analysis using mesitylene as internal standard indicated a 94% yield of **29f**+**27f** based on *n*-BuZnBr. Product ^1H NMR signals in the crude were assigned by analogy with 3-chloro-5-methylbenzonitrile¹¹⁰ and 3,5-dimethylbenzonitrile.¹¹⁷



1,3-Dichlorobenzene **28a**, PEPPSI-IPent

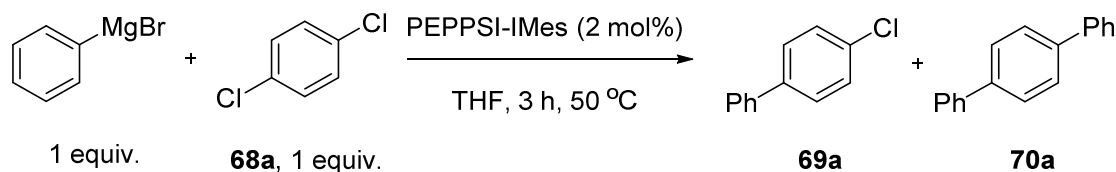


Using the general procedure for sp^3 - sp^2 Negishi couplings employing 1,3-dichlorobenzene (29 μ L, 0.25 mmol) a product mixture of **29a** and **27a** is obtained in a 15 : 85 ratio by GC-MS analysis and in a 25 : 75 ratio by ^1H NMR analysis. ^1H NMR analysis using mesitylene as internal standard indicated a 98% yield of **29a+27a** based on *n*-BuZnBr. Product ^1H NMR signals in the crude were assigned by analogy with 1-chloro-3-di(*n*-butyl)benzene **29a**¹⁰⁹ and 1,3-di(*n*-butyl)benzene **27a**.¹⁰⁹



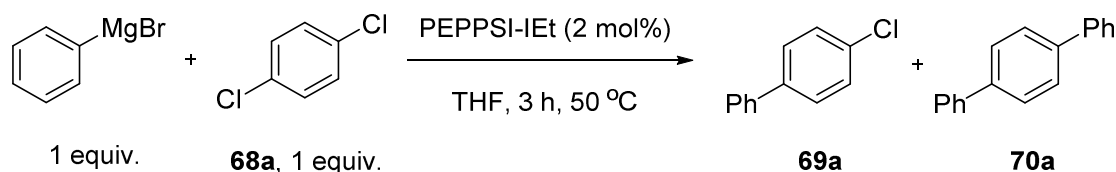
Scheme 50

PEPPSI-IMes:



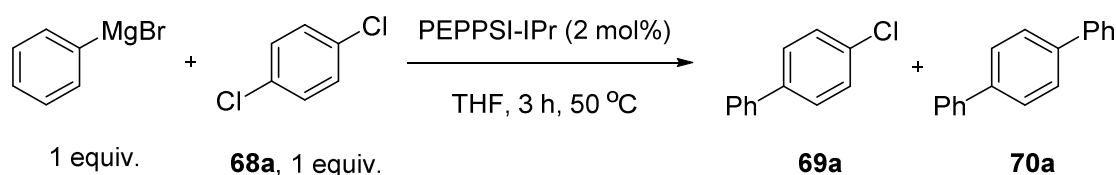
Using the general procedure for Kumada couplings employing PEPPSI-IMes (3.0 mg, 5.0 μmol) in place of PEPPSI-IPent a product mixture of **69a** and **70a** is obtained in a >99 : <1 ratio by GC-MS analysis. ^1H NMR analysis using mesitylene as internal standard indicated a 16% yield of **69a+70a** based on PhMgBr. The remaining reaction mixture was diluted in CH_2Cl_2 , filtered through a silica plug and reduced *in vacuo*. Automated flash chromatography (petrol raising to 1 : 9 CH_2Cl_2 : petrol) gave an analytical sample of major product 4-chloro-biphenyl **69a** as a white solid: [Melting point](#) 78 - 79 °C (lit.¹³⁹ 77-78); [\$^1\text{H}\$ NMR \(400 MHz, \$\text{CDCl}_3\$ \)](#) δ 7.59 – 7.49 (m, 4H), 7.48 – 7.39 (m, 4H), 7.39 – 7.33 (m, 1H). [\$^{13}\text{C}\$ NMR \(101 MHz, \$\text{CDCl}_3\$ \)](#) δ 140.2, 139.8, 133.5 129.1, 129.0, 128.5, 127.7, 127.1.

PEPPSI-IEt:



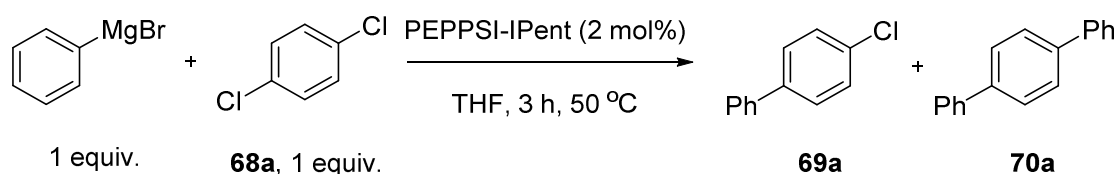
Using the general procedure for Kumada couplings, employing PEPPSI-IEt (3.1 mg, 5.0 μmol) in place of PEPPSI-IPent, a product mixture of **69a** and **70a** is obtained in a 70 : 30 ratio by GC-MS analysis. ^1H NMR analysis using mesitylene as internal standard indicated a 50% yield of **69a+70a** based on PhMgBr.

PEPPSI-IPr:



Using the general procedure for Kumada couplings, employing PEPPSI-IPr (3.4 mg, 5.0 μmol) in place of PEPPSI-IPent, a product mixture of **69a** and **70a** is obtained in a 45 : 55 ratio by GC-MS. ^1H NMR analysis using mesitylene as internal standard indicated an 83% yield of **69a+70a** based on PhMgBr. The remaining reaction mixture was diluted in CH_2Cl_2 , filtered through a silica plug and reduced *in vacuo*. Automated flash chromatography (petrol raising to 1 : 9 CH_2Cl_2 : petrol) gave an analytical sample of major product *p*-terphenyl **70a** as a white solid: **Melting point** 207 – 208 °C (lit.¹⁴⁰ 210 – 211 °C); ^1H NMR (400 MHz, CDCl_3) δ 7.69 (s, 4H), 7.65 (d, J = 7.3, 4H), 7.47 (t, J = 7.6, 4H), 7.37 (t, J = 7.4, 2H); ^{13}C NMR (101 MHz, CDCl_3) δ 140.9, 140.3, 129.0, 127.7, 127.5, 127.2.

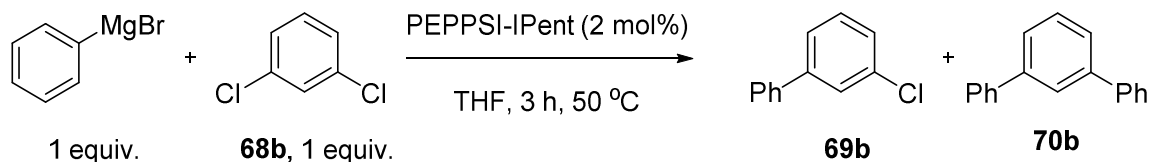
PEPPSI-IPent:



Using the general procedure for Kumada couplings a product mixture of **69a** and **70a** is obtained in a 6 : 94 ratio by GC-MS analysis. ^1H NMR analysis using mesitylene as internal standard indicated a 96% yield of **69a+70a** based on PhMgBr.

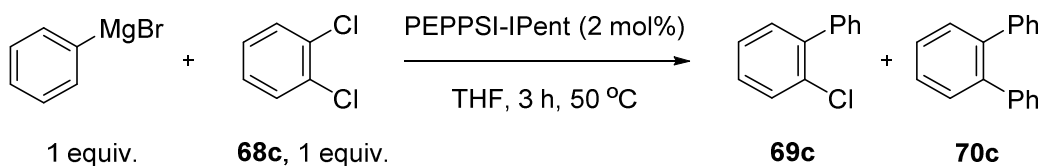
Scheme 51

m-Terphenyl **70b**:



Using the general procedure for Kumada couplings a product mixture of **69b** and **70b** is obtained in a 13 : 87 ratio by GC-MS analysis. ^1H NMR analysis using mesitylene as internal standard indicated an 80% yield of **69b**+**70b** based on PhMgBr. The remaining reaction mixture was diluted in CH_2Cl_2 , filtered through a silica plug and reduced *in vacuo*. Automated flash chromatography (petrol raising to 1 : 9 CH_2Cl_2 : petrol) gave an analytical sample of major product *m*-terphenyl **70b** as a white solid: [Melting point](#) 86 - 88 °C (lit.¹⁴¹ 84 - 85); [\$^1\text{H}\$ NMR \(400 MHz, \$\text{CDCl}_3\$ \)](#) δ 7.82 (s, 1H), 7.65 (d, J = 7.4, 4H), 7.59 (d, J = 7.5, 2H), 7.55 – 7.43 (m, 5H), 7.41 – 7.34 (m, 2H); [\$^{13}\text{C}\$ NMR \(101 MHz, \$\text{CDCl}_3\$ \)](#) δ 142.0, 141.4, 129.3, 129.0, 127.6, 127.4, 126.3, 126.3.

o-Terphenyl **70c**:

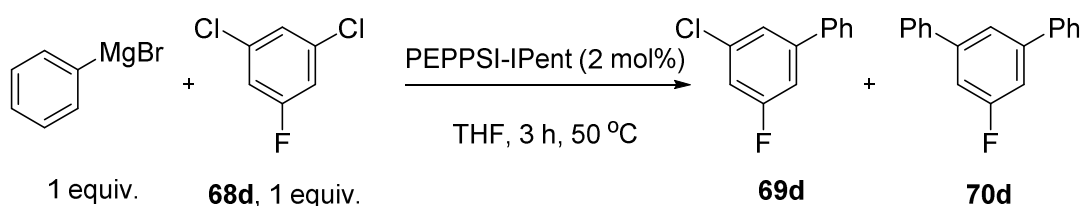


Using the general procedure for Kumada couplings a product mixture of **69c** and **70c** is obtained in a 84 : 16 ratio by GC-MS analysis. ^1H NMR analysis using mesitylene as internal standard indicated a 66% yield of **69c**+**70c** based on PhMgBr. The remaining reaction mixture was diluted in CH_2Cl_2 , filtered through a silica plug and reduced *in vacuo*. Automated flash chromatography (petrol raising to 1 : 9 CH_2Cl_2 : petrol) gave an

analytical sample of major product *o*-terphenyl **70c** as a white solid: **Melting point** 55 – 58 °C (lit.¹⁴⁰ 56 – 57 °C); **¹H NMR (400 MHz, CDCl₃)** δ 7.47 – 7.40 (m, 4H), 7.25 – 7.12 (m, 10H); **¹³C NMR (101 MHz, CDCl₃)** δ 141.7, 140.7, 130.7, 130.0, 128.0, 127.6, 126.6.

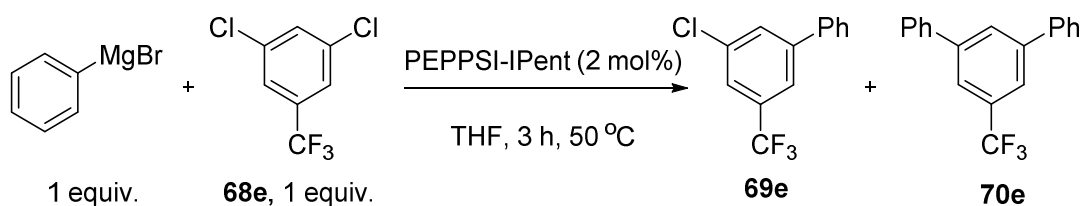
Scheme 52

1-Fluoro-3,5-diphenylbenzene 70d:



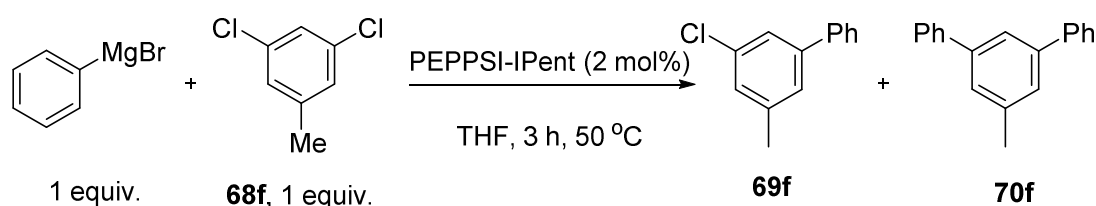
Using the general procedure for Kumada couplings a product mixture of **69d** and **70d** is obtained in a 3 : 97 ratio by GC-MS analysis. ¹H NMR analysis using mesitylene as internal standard indicated a 91% yield of **69d+70d** based on PhMgBr. The remaining reaction mixture was diluted in CH₂Cl₂, filtered through a silica plug and reduced *in vacuo*. Automated flash chromatography (petrol raising to 1 : 9 CH₂Cl₂ : petrol) gave an analytical sample of major product 1-fluoro-3,5-diphenylbenzene **70d** as a white solid: **Melting point** 70 – 71 °C; **¹H NMR (400 MHz, CDCl₃)** δ 7.66 – 7.58 (m, 5H), 7.51 – 7.45 (m, 4H), 7.43 – 7.37 (m, 2H), 7.31 – 7.26 (m, 2H); **¹³C NMR (101 MHz, CDCl₃)** δ 163.7 (d, *J* = 245.3 Hz), 144.0 (d, *J* = 8.3 Hz), 140.2 (d, *J* = 2.3 Hz), 129.1, 128.1, 127.3, 121.9 (d, *J* = 2.4 Hz), 112.95 (d, *J* = 22.2 Hz); **LRMS (ESI)** 248.6 [M]⁺; **IR (cm⁻¹)** 3064, 3037, 2925, 1594, 1575, 1408, 1336, 1165, 866, 756, 695, 689.

1,3-Diphenyl-5-trifluoromethylbenzene 70e:



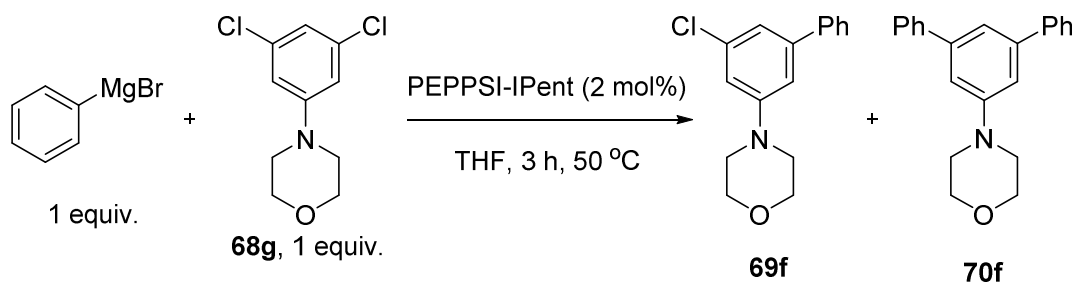
Using the general procedure for Kumada couplings a product mixture of **69e** and **70e** is obtained in a 5 : 95 ratio by GC-MS analysis. ^1H NMR analysis using mesitylene as internal standard indicated a 94% yield of **69e+70e** based on PhMgBr . The remaining reaction mixture was diluted in CH_2Cl_2 , filtered through a silica plug and reduced *in vacuo*. Automated flash chromatography (petrol) gave an analytical sample of major product 1,3-diphenyl-5-trifluoromethylbenzene **70e** as a white solid: **Melting point** 75 - 76 °C; ^1H NMR (400 MHz, CDCl_3) δ 8.02 – 7.98 (m, 1H), 7.88 – 7.83 (m, 2H), 7.72 - 7.66 (m, 4H), 7.56 – 7.50 (m, 4H), 7.49 - 7.43 (m, 2H); ^{13}C NMR (101 MHz, CDCl_3) δ 142.8, 140.0, 131.9 (q, J = 32.1 Hz), 129.4, 129.2, 128.3, 127.5, 124.4 (q, J = 272.7 Hz), 122.9 (q, J = 3.7 Hz); **LRMS (ESI)** 298.2 [M^+]; **HRMS (EI)** 298.0965 [M^+] (calc. for $\text{C}_{19}\text{H}_{13}\text{F}_3$ 298.0964 [M^+]); **IR** (cm^{-1}) 3036, 1363, 1264, 1167, 1110, 758, 694.

3,5-Diphenyltoluene **70f**:



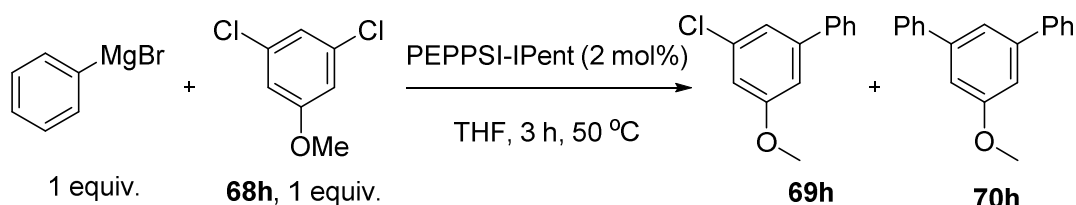
Using the general procedure for Kumada couplings a product mixture of **69f** and **70f** is obtained in a 2 : 98 ratio by GC-MS analysis. ^1H NMR analysis using mesitylene as internal standard indicated a 84% yield of **69h+70h** based on PhMgBr . The remaining reaction mixture was diluted in CH_2Cl_2 , filtered through a silica plug and reduced *in vacuo*. Automated flash chromatography (petrol raising to 1 : 9 CH_2Cl_2 : petrol) gave an analytical sample of major product 3,5-diphenyltoluene **70f** as a white solid: **Melting point** 137 - 140 °C (lit.¹⁴² 135 – 138 °C); ^1H NMR (400 MHz, CDCl_3) δ 7.67 (m, 5H), 7.48 (t, J = 7.6, 4H), 7.43 (d, J = 0.7, 2H), 7.41 - 7.36 (m, 2H), 2.52 (s, 3H); ^{13}C NMR (101 MHz, CDCl_3) δ 142.0, 141.5, 138.9, 128.9, 127.5, 127.4, 127.1, 123.6, 21.8.

1-Morpholino-3,5-diphenylbenzene **70g**:



Using the general procedure for Kumada couplings a product mixture of **69g** and **70g** is obtained in a <1 : >99 ratio by GC-MS analysis. ^1H NMR analysis using mesitylene as internal standard indicated a 71% yield of **69g**+**70g** based on PhMgBr . The remaining reaction mixture was diluted in CH_2Cl_2 , filtered through a silica plug and reduced *in vacuo*. Automated flash chromatography (1 : 9 petrol : CH_2Cl_2 raising to CH_2Cl_2) gave an analytical sample of major product 1-morpholino-3,5-diphenylbenzene **70g** as a white solid: **Melting point** 100 - 102 $^\circ\text{C}$; ^1H NMR (400 MHz, CDCl_3) δ 7.63 (dq, J = 2.6, 1.7, 4H), 7.48 – 7.42 (m, 4H), 7.40 – 7.34 (m, 2H), 7.32 (t, J = 1.5, 1H), 7.11 (d, J = 1.5, 2H), 3.94 – 3.88 (m, 4H), 3.33 – 3.27 (m, 4H); ^{13}C NMR (101 MHz, CDCl_3) δ 143.0, 141.9, 128.9, 127.6, 127.5, 118.7, 114.0, 67.1, 49.8; **LRMS (ESI)** 315.3 $[\text{M}]^+$; **HRMS (EI)** 315.1617 $[\text{M}]^+$ (calc. for $\text{C}_{22}\text{H}_{21}\text{ON}$ 315.1618 $[\text{M}]^+$); **IR** (cm^{-1}) 2967, 2849, 1592, 1419, 1448, 118, 955, 753, 695.

3,5-Diphenylanisole **70h**:

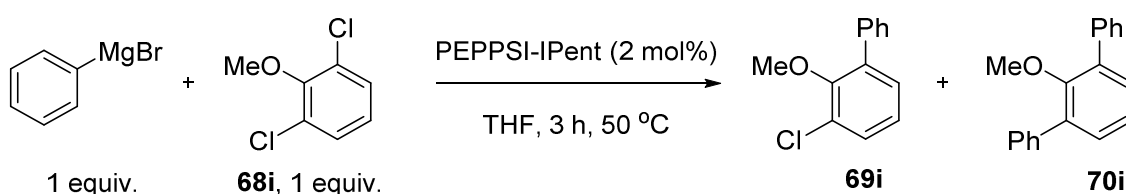


Using the general procedure for Kumada couplings a product mixture of **69h** and **70h** is obtained in a <1: >99 ratio by GC-MS analysis. ^1H NMR analysis using mesitylene as

internal standard indicated a 82% yield of **69h**+**70h** based on PhMgBr. The remaining reaction mixture was diluted in CH₂Cl₂, filtered through a silica plug and reduced *in vacuo*. Automated flash chromatography (petrol raising to 3 : 7 CH₂Cl₂ : petrol) gave an analytical sample of major product 3,5-diphenylanisole **70h** as a white solid: **Melting point** 91 - 93 °C (lit.¹²⁷ 91 – 92 °C); **¹H NMR (400 MHz, CDCl₃)** δ 7.69 – 7.62 (m, 4H), 7.51 – 7.43 (m, 4H), 7.43 – 7.35 (m, 3H), 7.15 – 7.10 (m, 2H), 3.93 (s, 3H); **¹³C NMR (101 MHz, CDCl₃)** δ 160.5, 143.3, 141.3, 128.9, 127.7, 127.4, 119.1, 111.9, 55.6.

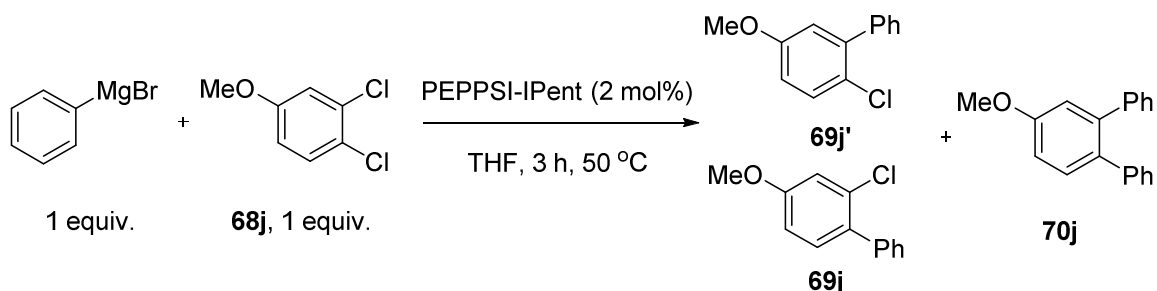
Scheme 53

2,6-Diphenylanisole 70i:



Using the general procedure for Kumada couplings a product mixture of **69i** and **70i** is obtained in a 8 : 92 ratio by GC-MS analysis. **¹H NMR** analysis using mesitylene as internal standard indicated a 85% yield of **69i**+**70i** based on PhMgBr. The remaining reaction mixture was diluted in CH₂Cl₂, filtered through a silica plug and reduced *in vacuo*. Automated flash chromatography (petrol raising to 3 : 7 CH₂Cl₂ : petrol) gave an analytical sample of major product 2,6-diphenylanisole **70i** as a colourless oil: **¹H NMR (400 MHz, CDCl₃)** δ 7.65 – 7.60 (m, 4H), 7.48 – 7.41 (m, 4H), 7.40 – 7.33 (m, 4H), 7.26 – 7.22 (m, 1H), 3.18 (s, 3H); **¹³C NMR (101 MHz, CDCl₃)** δ 155.1, 138.9, 135.9, 130.5, 129.5, 128.3, 127.3, 124.4, 60.6; **LRMS (ESI)** 260.2 [M⁺]; **HRMS (EI)** 260.1198 [M]⁺ (calc. for C₁₉H₁₆O 260.1196 [M]⁺); **IR (cm⁻¹)** 3060, 3025, 2929, 1462, 1407, 1226, 1005, 749, 697.

3,4-Diphenylanisole **70j** :



Using the general procedure for Kumada couplings a product mixture of **69j** or **69j'** and **70j** is obtained in a 12 : 0 : 88 ratio by GC-MS analysis. ^1H NMR analysis using mesitylene as internal standard indicated an 81% yield of **69j**+**70j** based on PhMgBr . The remaining reaction mixture was diluted in CH_2Cl_2 , filtered through a silica plug and reduced *in vacuo*. Automated flash chromatography (petrol raising to 3 : 7 CH_2Cl_2 : petrol) gave an analytical sample of major product 3,4-diphenylanisole **70j** as a white solid: **Melting point** 116-117 $^\circ\text{C}$ (lit.¹²⁸ 113 – 115 $^\circ\text{C}$); ^1H NMR (400 MHz, CDCl_3) δ 7.39 – 7.34 (m, 1H), 7.26 – 7.13 (m, 8H), 7.13 – 7.08 (m, 2H), 7.00 – 6.96 (m, 2H), 3.89 (s, 3H); ^{13}C NMR (101 MHz, CDCl_3) δ 158.9, 141.8, 141.5, 141.2, 133.3, 131.7, 130.0, 129.8, 127.9, 127.8, 126.6, 126.1, 115.9, 113.1, 55.4.

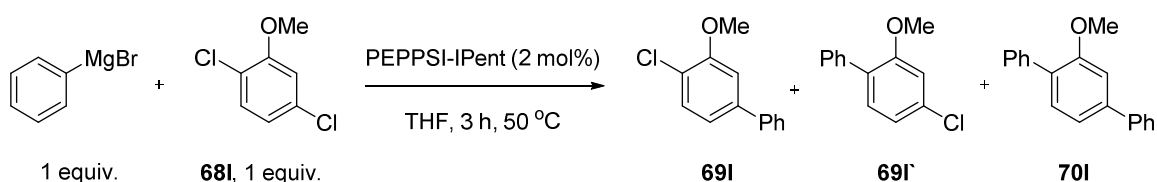
2,4-Diphenylanisole **70k**:



Using the general procedure for Kumada couplings a product mixture of **69k**, **69k'** and **70k** is obtained in a 29 : 1 : 70 ratio by GC-MS analysis. ^1H NMR analysis using mesitylene as internal standard indicated a 94% yield of **69k**+**69k'**+**70k** based on PhMgBr . The remaining reaction mixture was diluted in CH_2Cl_2 , filtered through a silica

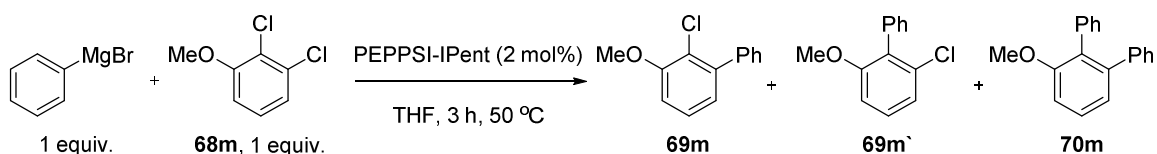
plug and reduced *in vacuo*. Automated flash chromatography (petrol raising to 3 : 7 CH₂Cl₂ : petrol) gave an analytical sample of major product 2,4-diphenylanisole **70k** as a white solid: **Melting point** 99 - 100 °C (lit.¹⁴³ 93 – 94 °C); **¹H NMR (400 MHz, CDCl₃)** δ 7.63 – 7.54 (m, 6H), 7.46 – 7.40 (m, 4H), 7.38 – 7.29 (m, 2H), 7.10 – 7.04 (m, 1H), 3.86 (s, 3H); **¹³C NMR (101 MHz, CDCl₃)** δ 156.2, 140.9, 138.6, 134.1, 131.2, 129.9, 129.7, 128.9, 128.2, 127.2, 127.2, 126.9, 126.9, 111.7, 55.9.

2,5-Diphenylanisole **70l**:



Using the general procedure for Kumada couplings a product mixture of **69l**, **69l'** and **70l** is obtained in a 21 : 0 : 79 ratio by GC-MS analysis. ¹H NMR analysis using mesitylene as internal standard indicated a 99% yield of **69l+70l** based on PhMgBr. The remaining reaction mixture was diluted in CH₂Cl₂, filtered through a silica plug and reduced *in vacuo*. Automated flash chromatography (petrol raising to 3 : 7 CH₂Cl₂ : petrol) gave an analytical sample of major product 2,5-diphenylanisole **70l** as a white solid: **Melting point** 96 - 100 °C; **¹H NMR (400 MHz, CDCl₃)** δ 7.70 – 7.64 (m, 2H), 7.63 – 7.58 (m, 2H), 7.52 – 7.33 (m, 7H), 7.31 – 7.27 (m, 1H), 7.22 (d, *J* = 1.5, 1H), 3.90 (s, 3H); **¹³C NMR (101 MHz, CDCl₃)** δ 156.9, 142.1, 141.2, 138.4, 131.3, 129.9, 129.7, 128.9, 128.2, 127.6, 127.3, 127.1, 119.9, 110.4, 55.8.; **LRMS (ESI)** 260.2 [M]⁺; **HRMS (EI)** 260.1200 [M]⁺ (calc. for C₁₉H₁₆O 260.1196 [M]⁺); **IR (cm⁻¹)** 3033, 2956, 2932, 1215, 753, 694.

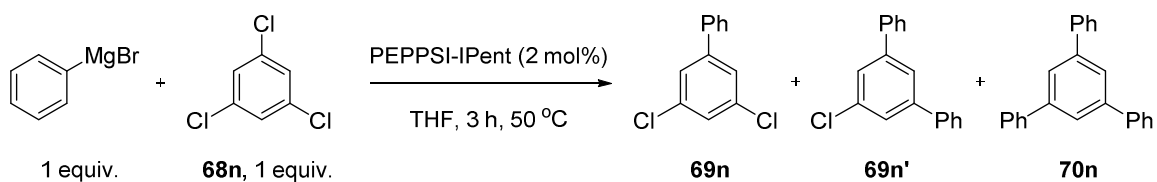
2,3-Diphenylanisole **70m**:



Using the general procedure for Kumada couplings a product mixture of **69m**, **69m'** and **70m** is obtained in a 70 : 0 : 30 ratio by GC-MS analysis. ^1H NMR analysis using mesitylene as internal standard indicated an 85% yield of **69m**+**70m** based on PhMgBr . The remaining reaction mixture was diluted in CH_2Cl_2 , filtered through a silica plug and reduced *in vacuo*. Automated flash chromatography (petrol raising to 3 : 7 CH_2Cl_2 : petrol) gave analytical samples of 2-chloro-3-phenylanisole **69m** and 2,3-diphenylanisole **70m**. **69m** (colourless oil): ^1H NMR (600 MHz, CDCl_3) δ 7.45 – 7.42 (m, 4H), 7.41 – 7.36 (m, 1H), 7.30 – 7.26 (m, 1H), 6.97 – 6.94 (m, 2H), 3.96 (s, 3H); ^{13}C NMR (101 MHz, CDCl_3) δ 155.6, 142.4, 139.6, 129.6, 128.1, 127.7, 127.1, 123.4, 121.3, 110.9, 56.5; LRMS (ESI) 218.3 $[\text{M}]^+$; HRMS (APCI) 219.0571 $[\text{M}+\text{H}]^+$ (calc. for $\text{C}_{13}\text{H}_{12}\text{O}^{35}\text{Cl}$ 219.0571 $[\text{M}+\text{H}]^+$); IR (cm^{-1}) 3060, 2939, 2839, 1568, 1465, 1422, 1262, 1218, 757, 698. **70m** (white solid): Melting point 108 – 109 $^\circ\text{C}$ ^1H NMR (400 MHz, CDCl_3) δ 7.39 (t, J = 8.0 Hz, 1H), 7.24 – 7.03 (m, 11H), 7.01 (dd, J = 8.3, 0.8 Hz, 1H), 3.79 (s, 3H); ^{13}C NMR (101 MHz, CDCl_3) δ 157.1, 143.0, 141.6, 137.0, 131.4, 130.0, 129.9, 128.4, 127.7, 127.5, 126.5, 126.4, 122.9, 110.2, 56.1.

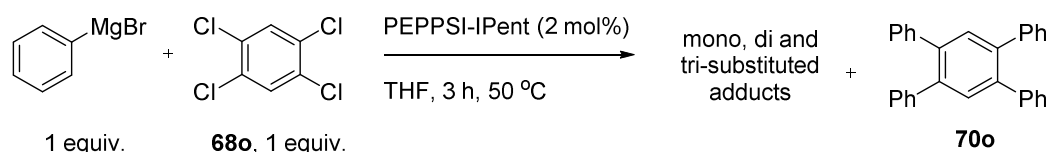
Scheme 54

1,3,5-Triphenylbenzene **70n**:



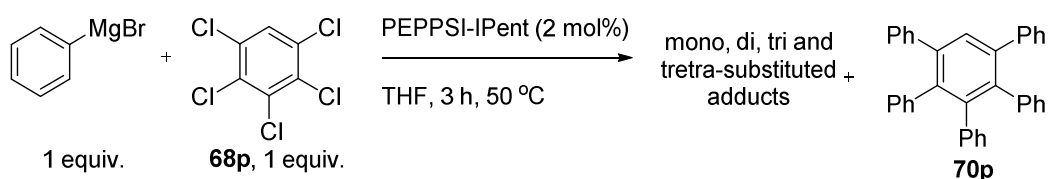
Using the general procedure for Kumada couplings a product mixture of **69n**, **69n'** and **70n** is obtained in a 2 : 5 : 93 ratio by GC-MS. ^1H NMR analysis using mesitylene as internal standard indicated an 75% yield of **69n+69n'+70n** based on PhMgBr . The remaining reaction mixture was diluted in CH_2Cl_2 , filtered through a silica plug and reduced *in vacuo*. Automated flash chromatography (petrol raising to 4 : 6 CH_2Cl_2 : petrol) gave an analytical sample of major product 1,3,5-triphenylbenzene **70n** as a white solid: **Melting point** 172 °C (lit.¹³⁰ 173 – 174 °C); ^1H NMR (400 MHz, CDCl_3) δ 7.79 (s, 3H), 7.74 – 7.68 (m, 6H), 7.52 – 7.45 (m, 6H), 7.43 – 7.36 (m, 3H); ^{13}C NMR (101 MHz, CDCl_3) δ 142.5, 141.3, 129.0, 127.7, 127.5, 125.3.

1,2,4,5-tetraphenylbenzene **70o**:



Using the general procedure for Kumada couplings a product mixture of mono, di and tri-coupled products and **70o** is obtained in a 19 : 1 : 2 : 78 ratio by GC-MS analysis. ^1H NMR analysis using mesitylene as internal standard indicated a combined 49% yield based on PhMgBr . The remaining reaction mixture was diluted in CH_2Cl_2 , filtered through a silica plug and reduced *in vacuo*. Automated flash chromatography (petrol raising to 6 : 4 CH_2Cl_2 : petrol) gave an analytical sample of major product 1,2,4,5-tetraphenylbenzene **70o** as a white solid: **Melting point** >250 °C (lit.¹⁴⁴ 274 – 275 °C); ^1H NMR (400 MHz, CDCl_3) δ 7.53 (s, 2H), 7.25 – 7.21 (m, 20H); ^{13}C NMR (101 MHz, CDCl_3) δ 141.1, 139.8, 133.1, 130.1, 128.1, 126.8.

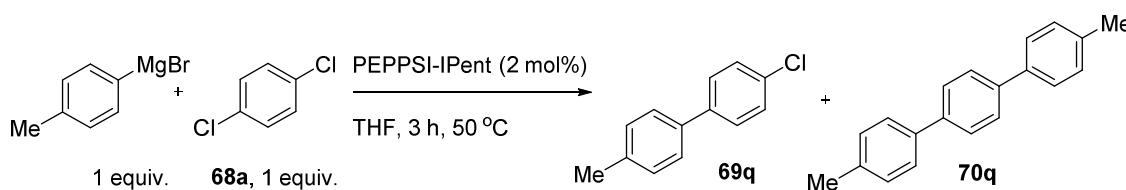
1,2,4,3,5-Pentaphenylbenzene **70p**:¹⁴⁵



Using the general procedure for Kumada couplings a product mixture of mono, di and tri and tetra-coupled products were obtained by GC-MS analysis. An accurate ratio of substituted products could not be obtained due to overlapping peaks in the GC-MS with protodeahalogenated species.

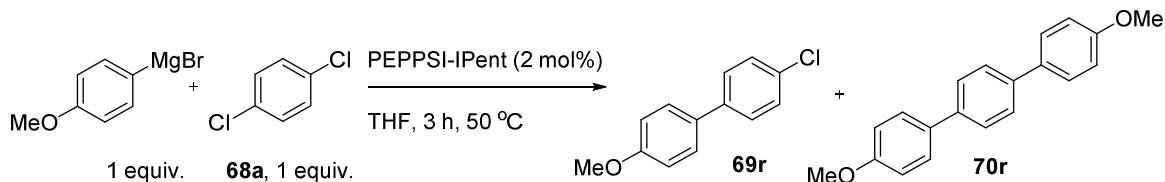
Scheme 55

1,4-Di(*p*-tolyl)benzene **70q**:



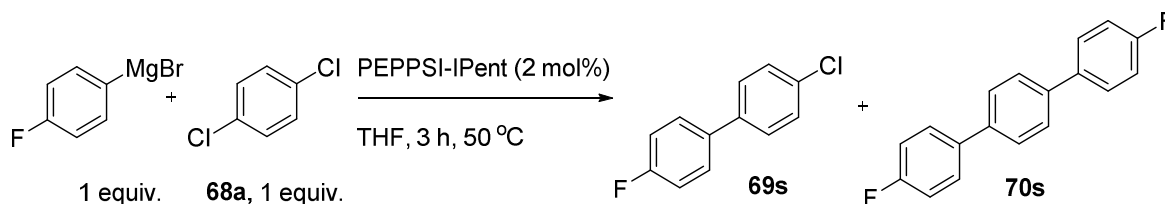
Using the general procedure for Kumada couplings a product mixture of **69q** and **70q** is obtained in a 11 : 89 ratio by GC-MS analysis. ¹H NMR analysis using mesitylene as internal standard indicated a 92% yield of **69q**+**70q** based on 4-MePhMgBr. The remaining reaction mixture was diluted in CH₂Cl₂, filtered through a silica plug and reduced *in vacuo*. Automated flash chromatography (petrol raising to 2 : 8 CH₂Cl₂ : petrol) gave an analytical sample of major product 1,4-di(*p*-tolyl)benzene **70q** as a white solid: **Melting point** >250 °C (lit.¹⁴⁶ 249 – 250 °C); ¹H NMR (400 MHz, CDCl₃) δ 7.57 (s, 4H), 7.49 – 7.44 (m, 4H), 7.22 – 7.17 (m, 4H), 2.33 (s, 6H); ¹³C NMR (101 MHz, CDCl₃) δ 139.9, 138.1, 137.2, 129.7, 127.4, 127.0, 21.3.

1,4-Di(*p*-anisole)benzene **70r**:



Using the general procedure for Kumada couplings a product mixture of **69r** and **70r** is obtained in a 10 : 90 ratio by GC-MS analysis. ¹H NMR analysis using mesitylene as internal standard indicated a 72% yield of **69r+70r** based on 4-MeOPhMgBr. The remaining reaction mixture was diluted in CH₂Cl₂, filtered through a silica plug and reduced *in vacuo*. Automated flash chromatography (petrol raising to 7 : 3 CH₂Cl₂ : petrol) gave an analytical sample of major product 1,4-di(*p*-anisole)benzene **70r** as a white solid: Melting point >250 °C (lit.¹⁴⁷ 270 – 271 °C); ¹H NMR (400 MHz, CDCl₃) δ 7.61 (s, 4H), 7.60 – 7.55 (m, 4H), 7.02 – 6.97 (m, 4H), 3.86 (s, 6H); ¹³C NMR (101 MHz, CDCl₃) δ 159.3, 139.3, 133.5, 128.2, 127.2, 114.4, 55.5.

4,4''-Difluoro-*p*-terphenyl **70s**:

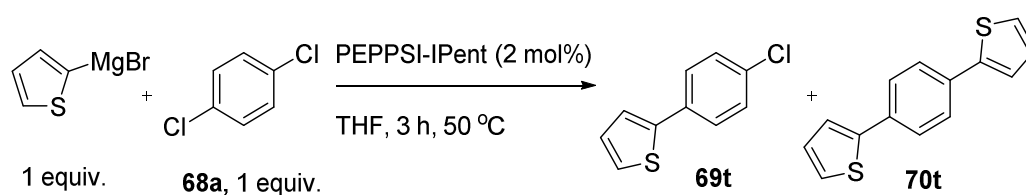


Using the general procedure for Kumada couplings a product mixture of **69r** and **70r** is obtained in a 4 : 96 ratio by GC-MS analysis. ¹H NMR analysis using mesitylene as internal standard indicated a 93% yield of **69s+70s** based on 4-FPhMgBr. The remaining reaction mixture was diluted in CH₂Cl₂, filtered through a silica plug and reduced *in vacuo*. Automated flash chromatography (petrol raising to 4 : 6 CH₂Cl₂ : petrol) gave an

analytical sample of major product 4,4''-difluoro-p-terphenyl **70s** as a white solid: [Melting point](#) 224 - 226 °C (lit.¹⁴⁸ 219 – 222 °C); [¹H NMR \(400 MHz, CDCl₃\)](#) δ 7.63 – 7.56 (m, 8H), 7.19 – 7.11 (m, 4H); [¹³C NMR \(101 MHz, CDCl₃\)](#) δ 162.7 (d, *J* = 246.7 Hz), 139.3, 136.9 (d, *J* = 3.2 Hz), 128.7 (d, *J* = 8.0 Hz), 127.6, 115.87 (d, *J* = 21.5 Hz).

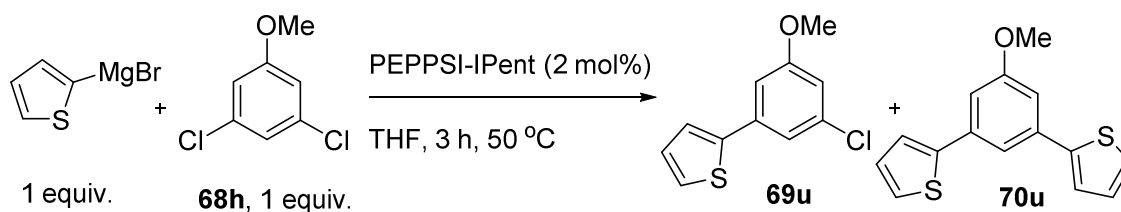
Scheme 56

1,4-Dithienylbenzene 70t:



Using the general procedure for Kumada couplings a product mixture of **69t** and **70t** is obtained in a 81 : 19 ratio by GC-MS analysis. ¹H NMR analysis using mesitylene as internal standard indicated a 92% yield of **69t**+**70t** based on 2-thienylMgBr. The remaining reaction mixture was diluted in CH₂Cl₂, filtered through a silica plug and reduced *in vacuo*. Automated flash chromatography (petrol) gave an analytical sample of major product 1-chloro-4-thienylbenzene **69t** as a white solid: [Melting point](#) 71 – 72 °C (lit.¹⁴⁹ 71 - 73 °C); [¹H NMR \(400 MHz, CDCl₃\)](#) δ 7.57 – 7.50 (m, 2H), 7.38 – 7.31 (m, 2H), 7.31 – 7.27 (m, 2H), 7.08 (dd, *J* = 4.9, 3.8 , 1H); [¹³C NMR \(101 MHz, CDCl₃\)](#) δ 143.3, 133.4, 133.1, 129.2, 128.3, 127.3, 125.3, 123.6.

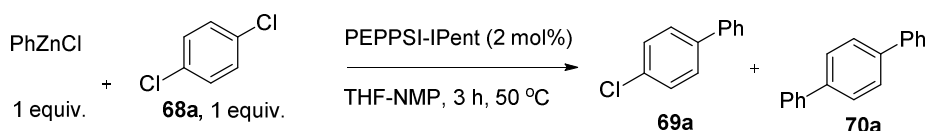
3,5-Dithienylanisole 70u:



Using the general procedure for Kumada couplings a product mixture of **69u** and **70u** is obtained in a 2 : 98 ratio by GC-MS analysis. ^1H NMR analysis using mesitylene as internal standard indicated a 77% yield of **69u+70u** based on 2-thienylMgBr. The remaining reaction mixture was diluted in CH_2Cl_2 , filtered through a silica plug and reduced *in vacuo*. Automated flash chromatography (petrol raising to 1 : 1 CH_2Cl_2 : petrol) gave an analytical sample of major product 3,5-dithienylanisole **70u** as a pale blue oil: ^1H NMR (400 MHz, CDCl_3) δ 7.46 (t, J = 1.4, 1H), 7.36 (dd, J = 3.6, 1.0, 2H), 7.31 (dd, J = 5.1, 1.0, 2H), 7.13 - 7.06 (m, 4H), 3.90 (s, 3H). ^{13}C NMR (101 MHz, CDCl_3) δ 160.5, 144.0, 136.4, 128.1, 125.3, 123.8, 116.7, 110.9, 55.6; LRMS (ESI) 272.2 $[\text{M}]^+$; HRMS (APCI) 273.0403 $[\text{M}+\text{H}]^+$ (calc. for $\text{C}_{15}\text{H}_{13}\text{OS}_2$ 273.0402 $[\text{M}+\text{H}]^+$); IR (cm^{-1}) 1587, 1222, 1170, 821, 694.

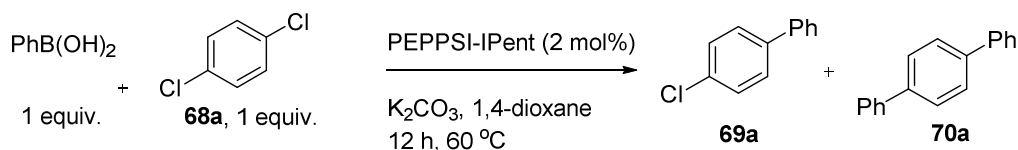
Scheme 57

p-Terphenyl 70a (Negishi coupling)



Using the general procedure for Negishi couplings a product mixture of **69a** and **70a** is obtained in a 11 : 89 ratio by GC-MS analysis. ^1H NMR analysis using mesitylene as internal standard indicated an 83% yield of **69a+70a** based on PhZnCl .

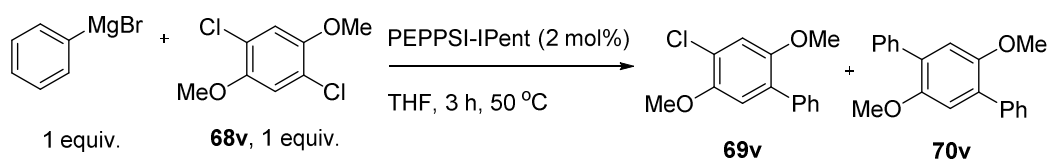
p-Terphenyl 70a (Suzuki coupling)



Using the general procedure for Negishi couplings a product mixture of **69a** and **70a** is obtained in a 3 : 97 ratio by GC-MS analysis. ¹H NMR analysis using mesitylene as internal standard indicated a 56% yield of **69a+70a** based on PhB(OH)₂.

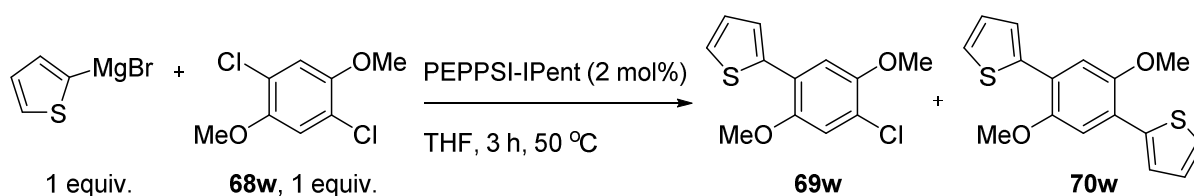
Scheme 58

1,4-Dimethoxy-2,5-diphenylbenzene 70v:



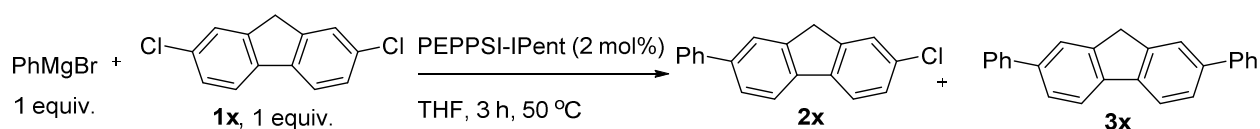
Using the general procedure for Kumada couplings a product mixture of **69v** and **70v** is obtained in a 3 : 97 ratio by GC-MS analysis. ¹H NMR analysis using mesitylene as internal standard indicated a 90% yield of **69v+70v** based on PhMgBr. The remaining reaction mixture was diluted in CH₂Cl₂, filtered through a silica plug and reduced *in vacuo*. The residue was recrystallized from EtOH to give an analytical sample of major product 1,4-dimethoxy-2,5-diphenylbenzene **70v** as a white solid: [Melting point](#) 146 - 148 °C (lit.¹⁵⁰ 149 – 150 °C); [¹H NMR \(400 MHz, CDCl₃\)](#) δ 7.62 – 7.57 (m, 4H), 7.48 – 7.41 (m, 4H), 7.39 – 7.32 (m, 2H), 7.02 – 6.94 (m, 2H), 3.79 (s, 3H); [¹³C NMR \(101 MHz, CDCl₃\)](#) δ 150.8, 138.5, 130.6, 129.6, 128.3, 127.3, 114.9, 56.6.

1,4-Dimethoxy-2,5-dithienylbenzene 70w:



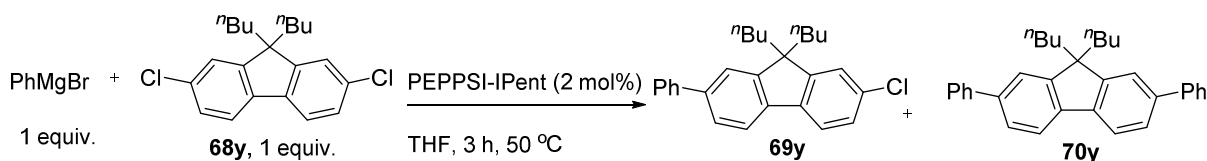
Using the general procedure for Kumada couplings a product mixture of **69w** and **70w** is obtained in a 10 : 90 ratio by GC-MS analysis. ^1H NMR analysis using mesitylene as internal standard indicated a 83% yield of **69w+70w** based on 2-thienylMgBr. The remaining reaction mixture was diluted in CH_2Cl_2 , filtered through a silica plug and reduced *in vacuo*. The residue was recrystallized from EtOH to give an analytical sample of major product 1,4-Dimethoxy-2,5-dithienylbenzene **70v** as a white solid: **Melting point** 134 - 136 °C (lit.¹³⁶ 135 – 136 °C); ^1H NMR (400 MHz, CDCl_3) δ 7.54 (dd, J = 3.7, 1.2, 2H), 7.35 (dd, J = 5.1, 1.1, 2H), 7.26 (s, 2H), 7.11 (dd, J = 5.1, 3.7, 2H), 3.95 (s, 6H); ^{13}C NMR (101 MHz, CDCl_3) δ 150.1, 139.2, 127.1, 125.9, 125.6, 123.2, 112.5, 56.6.

2,7-Diphenylfluorene **70x**:



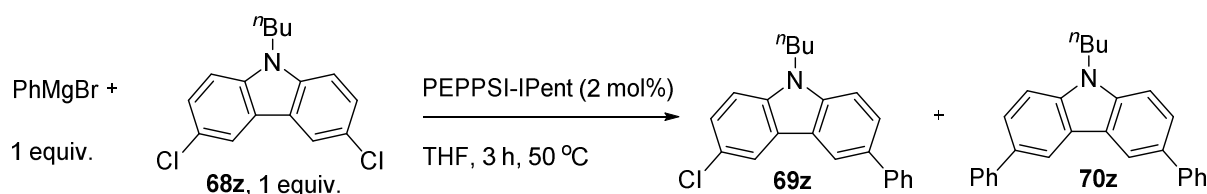
Using the general procedure for Kumada couplings a product mixture of **69x** and **70x** is obtained in a 8 : 92 ratio by GC-MS analysis. ^1H NMR analysis using mesitylene as internal standard indicated a 68% yield of **69x+70x** based on PhMgBr. The remaining reaction mixture was diluted in CH_2Cl_2 , filtered through a silica plug and reduced *in vacuo*. Automated flash chromatography (petrol raising to 1 : 1 CH_2Cl_2 : petrol) gave an analytical sample of major product 2,7-diphenylfluorene **70x** as a white solid: **Melting point** >250 °C (lit.¹⁵¹ 269 – 270 °C); ^1H NMR (400 MHz, CDCl_3) δ 7.91 – 7.83 (m, 2H), 7.83 – 7.76 (m, 2H), 7.70 – 7.62 (m, 6H), 7.50 – 7.43 (m, 4H), 7.39 – 7.33 (m, 2H), 4.03 (s, 2H); ^{13}C NMR (101 MHz, CDCl_3) δ 144.3, 141.6, 140.8, 140.1, 128.9, 127.3, 127.3, 126.3, 124.0, 120.4, 37.2.

2,7-Diphenyl-9,9-di(*n*-butyl)fluorene **70y**:



Using the general procedure for Kumada couplings a product mixture of **69y** and **70y** is obtained in a 11 : 89 ratio by GC-MS analysis. ^1H NMR analysis using mesitylene as internal standard indicated a 78% yield of **69y**+**70y** based on PhMgBr. The remaining reaction mixture was diluted in CH_2Cl_2 , filtered through a silica plug and reduced *in vacuo*. Automated flash chromatography (petrol raising to 1 : 1 CH_2Cl_2 : petrol) gave an analytical sample of major product 2,7-Diphenyl-9,9-di(*n*-butyl)fluorene **70y** as a white solid: **Melting point** 150-152 $^\circ\text{C}$; ^1H NMR (400 MHz, CDCl_3) δ 7.79 (d, J = 7.8, 2H), 7.74 – 7.68 (m, 4H), 7.64 – 7.57 (m, 4H), 7.53 – 7.45 (m, 4H), 7.41 – 7.34 (m, 2H), 2.06 (m, 4H), 1.18 – 1.05 (m, 4H), 0.79 – 0.66 (m, 10H); ^{13}C NMR (101 MHz, CDCl_3) δ 151.8, 141.8, 140.2, 128.9, 127.3, 127.3, 126.2, 121.7, 120.1, 55.3, 40.4, 26.2, 23.2, 14.0; **LRMS (ESI)** 430 $[\text{M}]^+$; **HRMS (ACPI)** 431.2731 $[\text{M}+\text{H}]^+$ (calc. for $\text{C}_{33}\text{H}_{35}$ 431.2733 $[\text{M}+\text{H}]^+$); **IR** (cm^{-1}) 2955, 2926, 2856, 2464, 822, 755, 695.

3,6-Diphenyl-9-*n*-butylcarbazole **70z**:

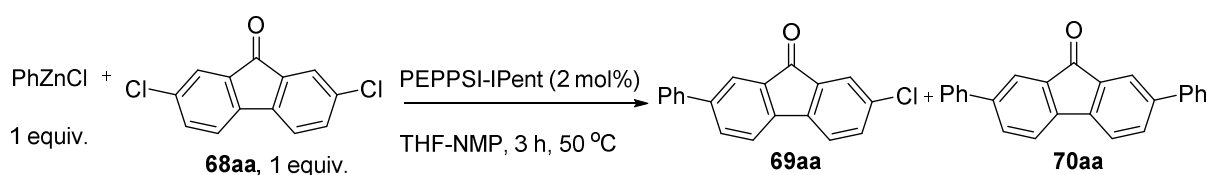


Using the general procedure for Kumada couplings a product mixture of **69z** and **70z** is obtained in a 15 : 85 ratio by GC-MS analysis. ^1H NMR analysis using mesitylene as internal standard indicated an 86% yield of **69z**+**70z** based on PhMgBr. The remaining

reaction mixture was diluted in CH₂Cl₂, filtered through a silica plug and reduced *in vacuo*. Automated flash chromatography (petrol raising to 1 : 1 CH₂Cl₂ : petrol) gave an analytical sample of major product 3,6-Diphenyl-9-*n*-butylcarbazole **70z** as a white solid: **Melting point** 157 - 158 °C; **¹H NMR (600 MHz, CDCl₃)** δ 8.36 (d, *J* = 1.4, 2H), 7.75 – 7.70 (m, 6H), 7.51 – 7.45 (m, 6H), 7.37 – 7.32 (m, 2H), 4.36 (t, *J* = 7.2, 2H), 1.95 – 1.88 (m, 2H), 1.49 – 1.41 (m, 2H), 0.98 (t, *J* = 7.4, 3H); **¹³C NMR (151 MHz, CDCl₃)** δ 142.3, 140.6, 132.6, 128.9, 127.4, 126.6, 125.5, 123.7, 119.1, 109.2, 43.3, 31.4, 20.8, 14.1; **LRMS (ESI)** 375 [M]⁺; **HRMS (APCI)** 376.2060 [M+H]⁺ (calc. for C₂₈H₂₆N 376.2060 [M+H]⁺); **IR (cm⁻¹)** 2956, 2927, 2871, 1600, 1475, 759, 696.

Scheme 59

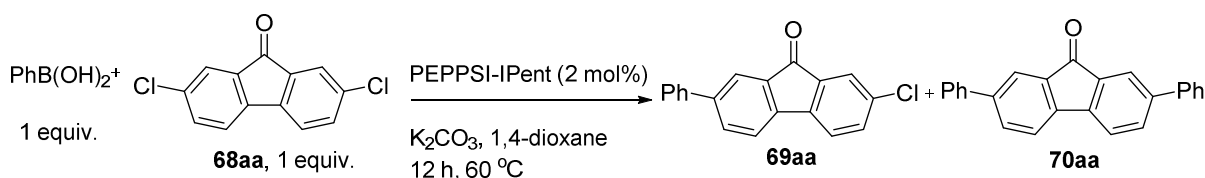
2,7-Diphenylflurenone 70aa (Negishi coupling):



Using the general procedure for sp² Negishi couplings a product mixture of **69aa** and **70aa** is obtained in a 57 : 43 ratio by GC-MS analysis. ¹H NMR analysis using mesitylene as internal standard indicated a 54% yield of **69aa**+**70aa** based on PhZnCl. The remaining reaction mixture was diluted in CH₂Cl₂, filtered through a silica plug and reduced *in vacuo*. Automated flash chromatography (petrol raising to CH₂Cl₂) gave an analytical sample of 2-chloro-7-phenylflurenone **69aa** and further recrystallization from EtOH gave an analytical sample of 2,7-diphenylflurenone **70aa**. **69aa** (orange solid): **Melting point** 206 – 210 °C; **¹H NMR (400 MHz, CDCl₃)** δ 7.91 (d, *J* = 1.3, 1H), 7.74 (dd, *J* = 7.8, 1.8, 1H), 7.66 – 7.55 (m, 4H), 7.52 – 7.44 (m, 4H), 7.42 – 7.36 (m, 1H); **¹³C NMR (151 MHz, CDCl₃)** δ 192.6, 142.7, 142.6, 142.6, 139.8, 136.1, 135.2, 134.9, 134.5,

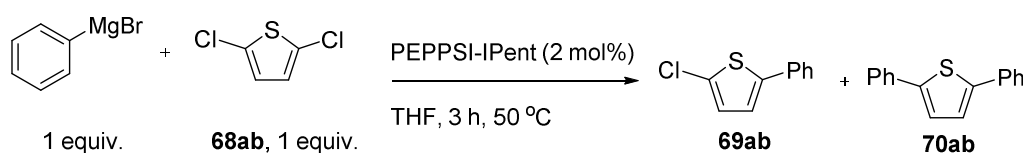
133.7, 129.1, 128.2, 127.0, 124.9, 123.4, 121.6, 121.0; **LRMS (ESI)** 290.3 [M]⁺; **HRMS (APCI)** 291.0574 [M+H]⁺ (calc. for C₁₉H₁₂O³⁵Cl 291.0571 [M+H]⁺); **IR (cm⁻¹)** 1708, 1599, 1451, 1184, 823, 763. **70z** (orange solid): **Melting point** 214 - 216 °C; **¹H NMR (400 MHz, CDCl₃)** δ 7.93 (d, *J* = 1.3, 2H), 7.75 (dd, *J* = 7.7, 1.7, 2H), 7.67 – 7.58 (m, 6H), 7.51 – 7.43 (m, 4H), 7.43 – 7.36 (m, 2H); **¹³C NMR (101 MHz, CDCl₃)** δ 193.9, 143.2, 142.4, 140.0, 135.4, 133.5, 129.1, 128.1, 127.0, 123.2, 120.9; **LRMS (ESI)** 332 [M]⁺; **HRMS (APCI)** 333.1274 [M+H]⁺ (calc. for C₂₅H₁₇O 333.1274 [M+H]⁺); **IR (cm⁻¹)** 3029, 1713, 1607, 1444, 840, 758, 736, 696.

2,7-Diphenylfluorenone **70aa** (Suzuki coupling):



Using the general procedure for Suzuki couplings a product mixture of **69aa** and **70aa** is obtained in a 51 : 49 ratio by GC-MS analysis. ¹H NMR analysis using mesitylene as internal standard indicated a 46% yield of **69aa+70aa** based on PhB(OH)₂.

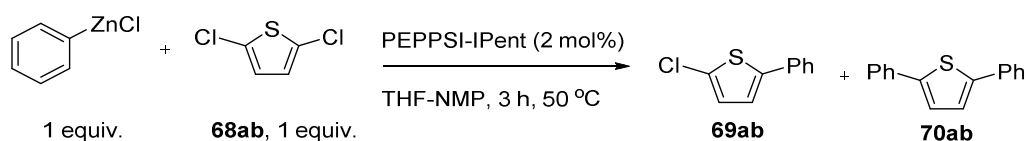
2,5-Diphenylthiophene **70ab** (Kumada coupling):



Using the general procedure for Kumada couplings a product mixture of **69ab** and **70ab** is obtained in a 85 : 15 ratio by GC-MS analysis. ¹H NMR analysis using mesitylene as internal standard indicated a 62% yield of **69ab+70ab** based on PhMgBr. The remaining reaction mixture was diluted in CH₂Cl₂, filtered through a silica plug and reduced *in vacuo*. The residue was recrystallized from EtOH to give an analytical sample of major

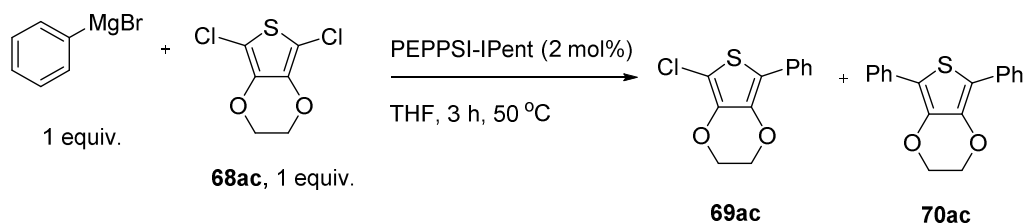
product **69ab** as a white solid: **Melting point** 64 - 66 °C; ^1H NMR (400 MHz, CDCl_3) δ 7.53 – 7.48 (m, 2H), 7.41 – 7.34 (m, 2H), 7.33 – 7.27 (m, 1H), 7.07 (d, J = 3.9, 1H), 6.89 (d, J = 3.9, 1H); ^{13}C NMR (101 MHz, CDCl_3) δ 143.1, 134.0, 129.3, 129.2, 128.0, 127.2, 125.7, 122.4; **LRMS (ESI)** 194.3 $[\text{M}]^+$; **HRMS (APCI)** 195.0029 $[\text{M}+\text{H}]^+$ (calc. for $\text{C}_{10}\text{H}_8^{35}\text{ClS}$ 195.0030 $[\text{M}+\text{H}]^+$); **IR** (cm^{-1}) 2952, 2918, 2847, 1448, 794, 147, 684.

2,5-Diphenylthiophene **70ab** (Negishi coupling):



Using the general procedure for sp^2 Negishi couplings a product mixture of **69ab** and **70ab** is obtained in a 97 : 3 ratio by GC-MS analysis. ^1H NMR analysis using mesitylene as internal standard indicated a 60% yield of **69ab+70ab** based on PhZnCl .

2,5-Diphenyl-3,4-ethylenedioxythiophene **70ac**:

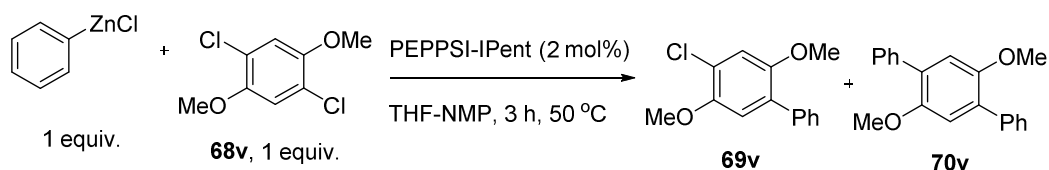


Using the general procedure for Kumada couplings a product mixture of **69ac** and **70ac** is obtained in an 81 : 19 ratio by GC-MS analysis. ^1H NMR analysis using mesitylene as internal standard indicated an 86% yield of **69ac+70ac** based on PhMgBr . The remaining reaction mixture was diluted in CH_2Cl_2 , filtered through a silica plug and reduced *in vacuo*. Automated flash chromatography (petrol raising to CH_2Cl_2) gave an analytical sample of 2,5-Diphenyl-3,4-ethylenedioxythiophene **70ac** as an off white solid. **Melting point** 105 - 106 °C (lit.¹⁵² 103 – 104 °C); ^1H NMR (CDCl_3 , 500 MHz) δ 7.80 (m, 4 H),

7.41 (m, 4 H), 7.25 (m, 2 H), 4.34 (s, 4 H); ^{13}C NMR (CDCl_3 , 125 MHz) δ 138.8, 133.1, 128.9, 126.7, 126.1, 115.6, 64.2

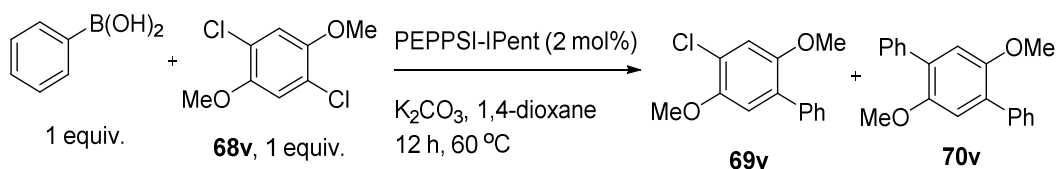
Scheme 60

1,4-Dimethoxy-2,5-diphenylbenzene 70v (Negishi coupling):



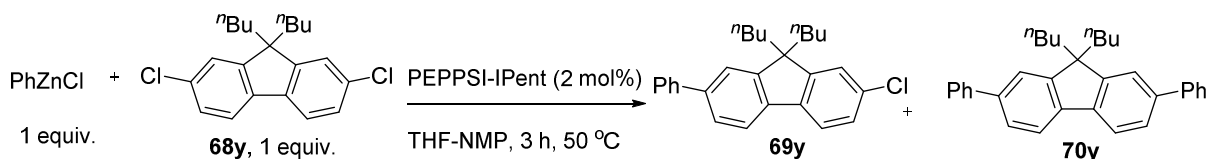
Using the general procedure for sp^2 Negishi couplings a product mixture of **69v** and **70v** is obtained in a 14 : 86 ratio by GC-MS analysis. ^1H NMR analysis using mesitylene as internal standard indicated a 67% yield of **69v**+**70v** based on PhZnCl .

1,4-Dimethoxy-2,5-diphenylbenzene 70v (Suzuki coupling):



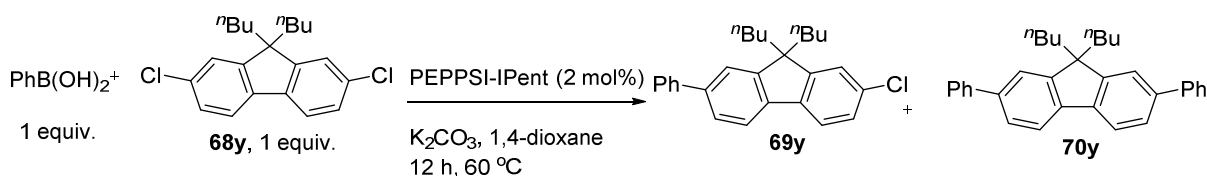
Using the general procedure for Negishi couplings a product mixture of **69v** and **70v** is obtained in a 15 : 85 ratio by GC-MS analysis. ^1H NMR analysis using mesitylene as internal standard indicated a 71% yield of **69v**+**70v** based on PhB(OH)_2 .

2,7-Diphenyl-9,9-di(*n*-butyl)fluorene 70y (Negishi coupling):



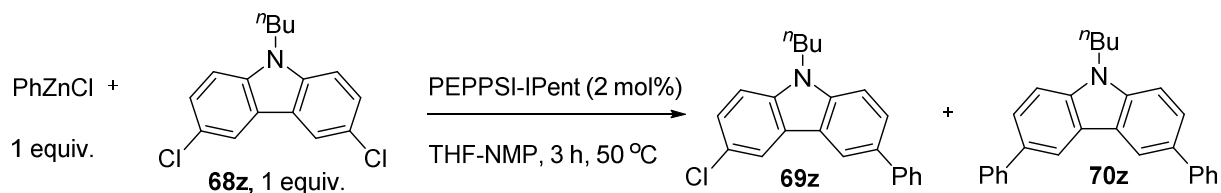
Using the general procedure for sp^2 Negishi couplings a product mixture of **69y** and **70y** is obtained in a 9 : 91 ratio by GC-MS analysis. ^1H NMR analysis using mesitylene as internal standard indicated a 79% yield of **69y**+**70y** based on PhZnCl .

2,7-Diphenyl-9,9-di(*n*-butyl)fluorene 70y (Suzuki coupling):



Using the general procedure for Suzuki couplings a product mixture of **69y** and **70y** is obtained in a 22 : 78 ratio by GC-MS analysis. ^1H NMR analysis using mesitylene as internal standard indicated a 44% yield of **69y**+**70y** based on PhB(OH)_2 .

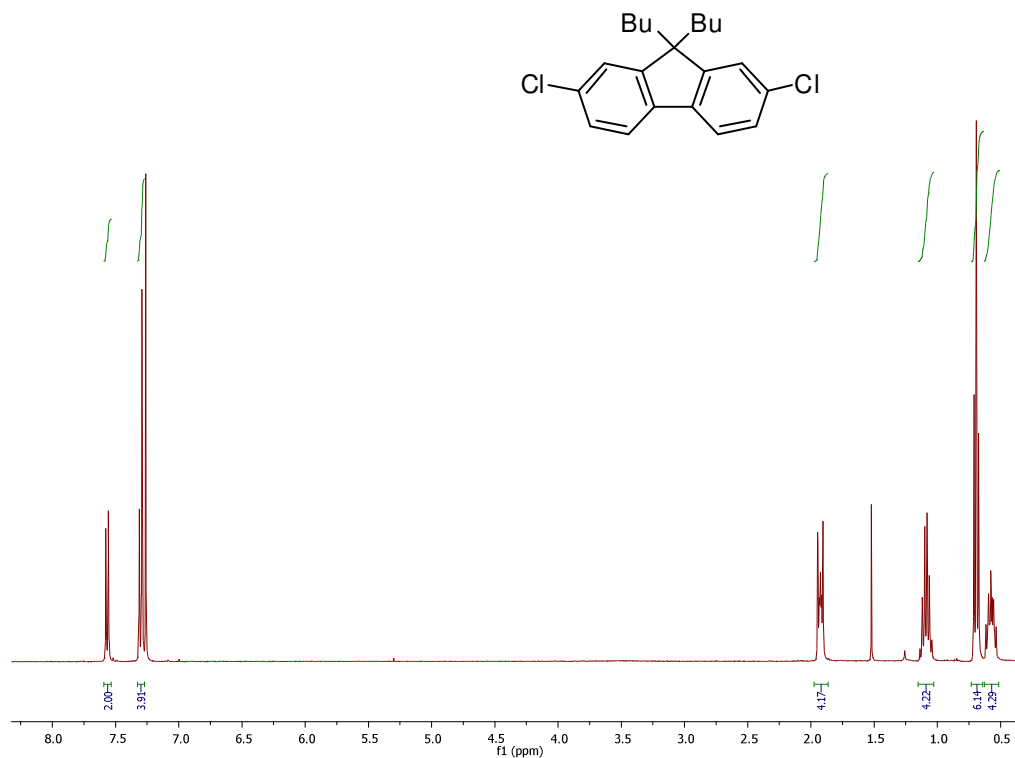
3,6-Diphenyl-9-*n*-butylcarbazole 70z (Negishi coupling):



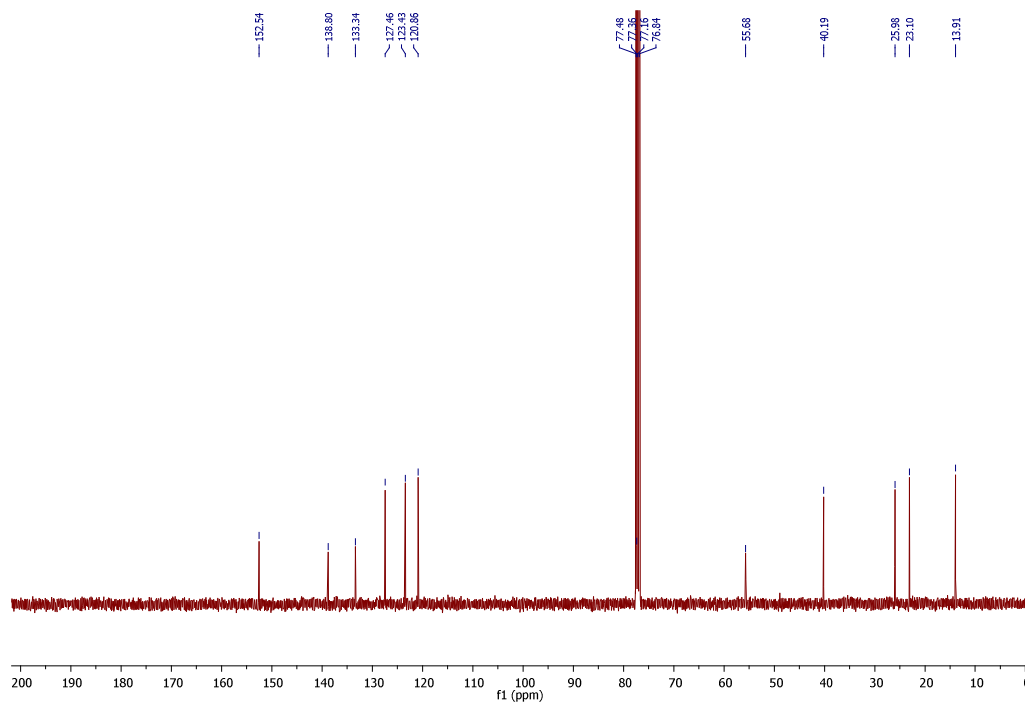
Using the general procedure for sp^2 Negishi couplings a product mixture of **69z** and **70z** is obtained in a 17 : 83 ratio by GC-MS analysis. ^1H NMR analysis using mesitylene as internal standard indicated a 51% yield of **69z**+**70z** based on PhZnCl .

6.4.5 Graphical NMR Data for all novel compounds

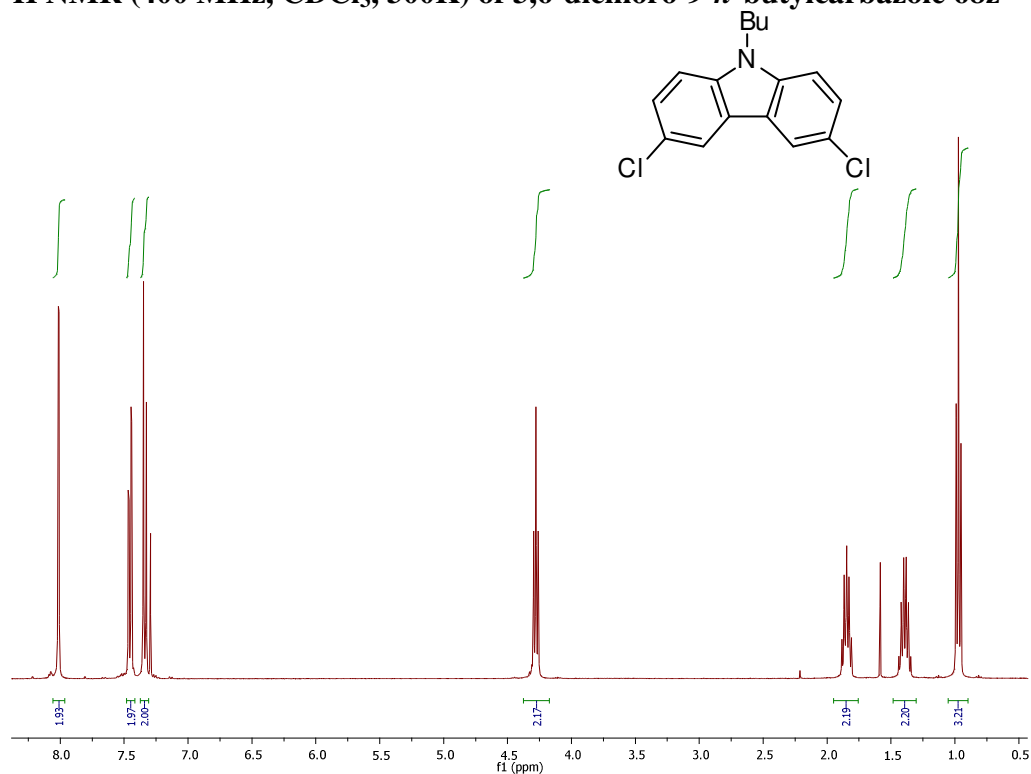
^1H NMR (400 MHz, CDCl_3 , 300K) of 2,7-dichloro-9,9-di(*n*-butyl)fluorene 68y



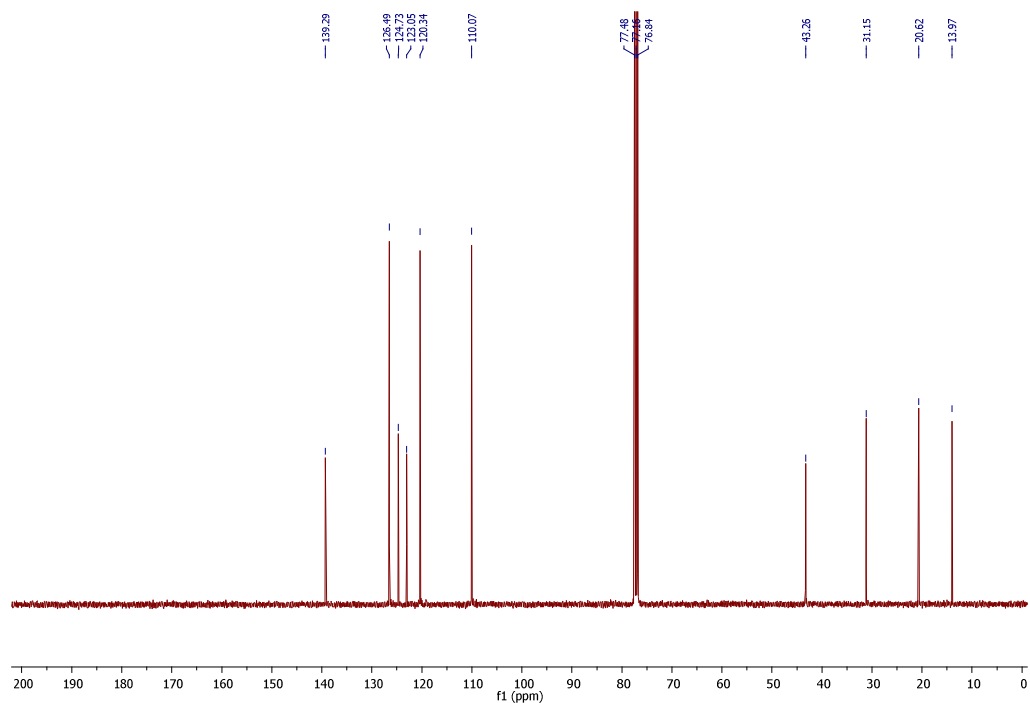
^{13}C NMR (100 MHz, CDCl_3 , 300K) of 2,7-dichloro-9,9-di(*n*-butyl)fluorene 68y



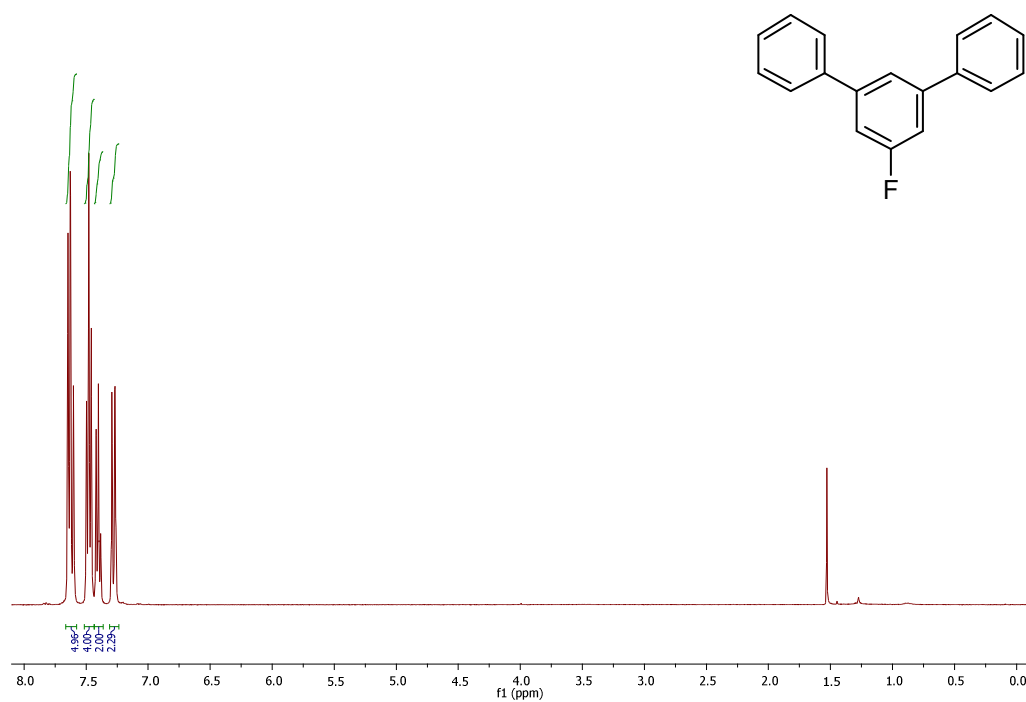
^1H NMR (400 MHz, CDCl_3 , 300K) of 3,6-dichloro-9-*n*-butylcarbazole 68z



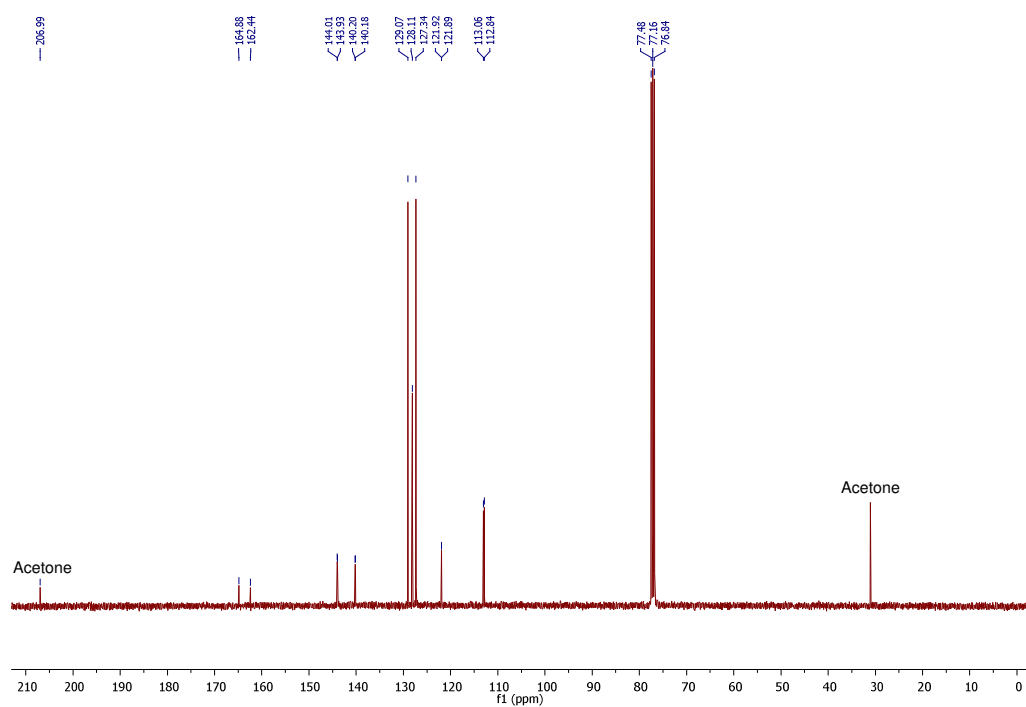
^{13}C NMR (100 MHz, CDCl_3 , 300K) of 3,6-dichloro-9-*n*-butylcarbazole 68z



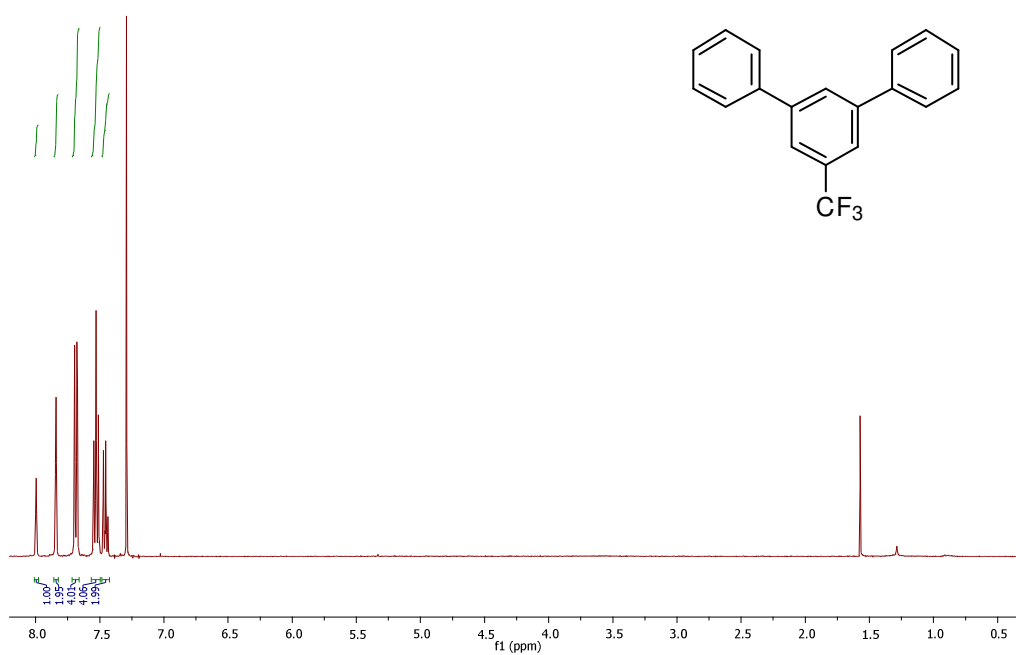
^1H NMR (400 MHz, CDCl_3 , 300K) of 1-fluoro-3,5-diphenylbenzene 70d



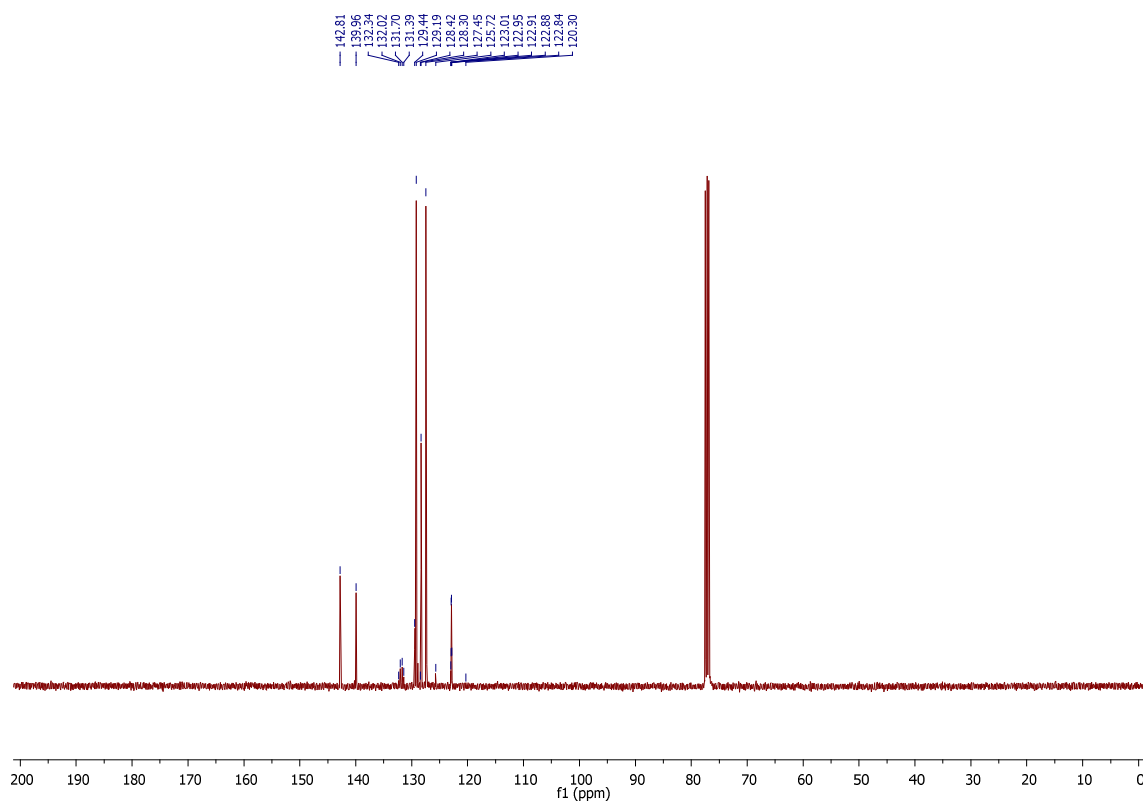
^{13}C NMR (101 MHz, CDCl_3 , 300K) of 1-fluoro-3,5-diphenylbenzene 70d



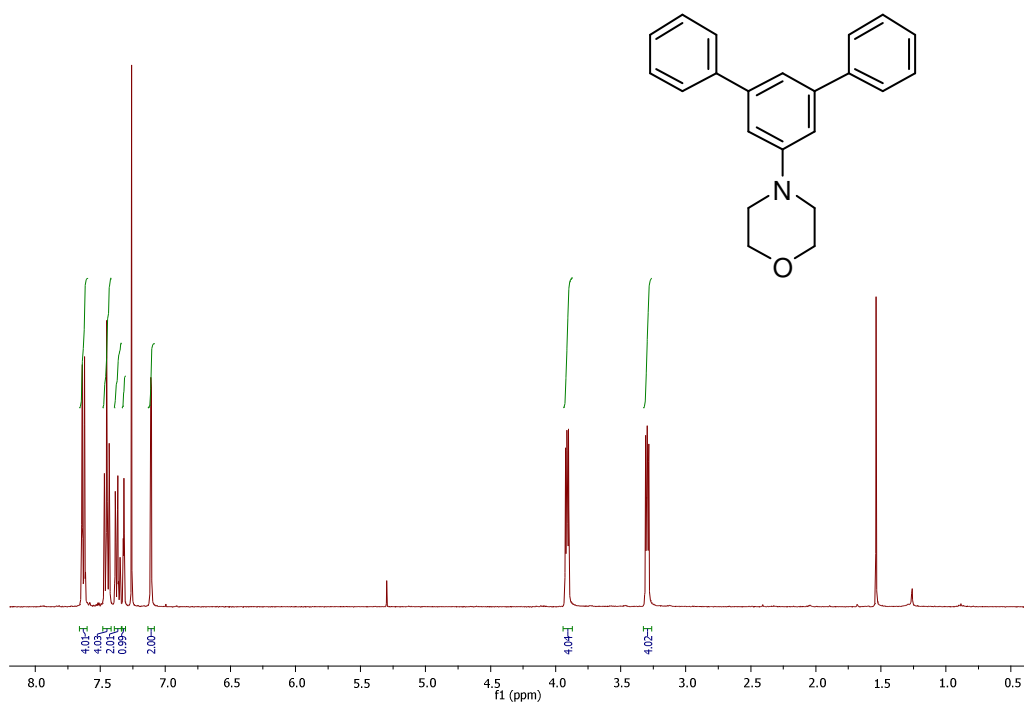
^1H NMR (400 MHz, CDCl_3 , 300K) of 1,3-diphenyl-5-trifluoromethylbenzene 70e



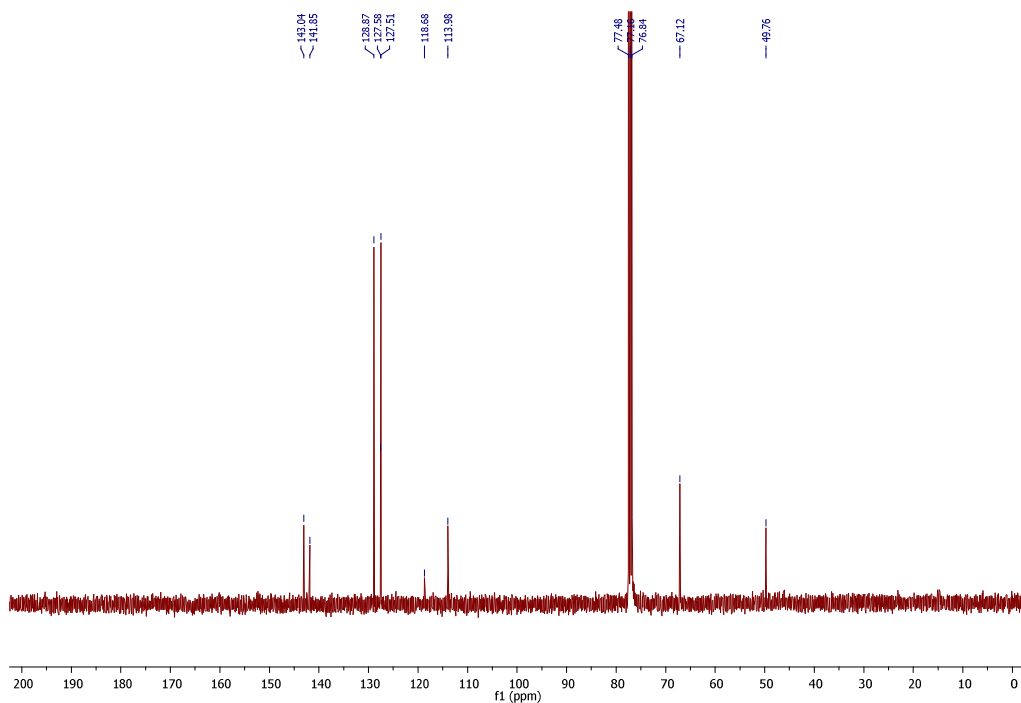
^{13}C NMR (100 MHz, CDCl_3 , 300K) of 1,3-diphenyl-5-trifluoromethylbenzene 70e



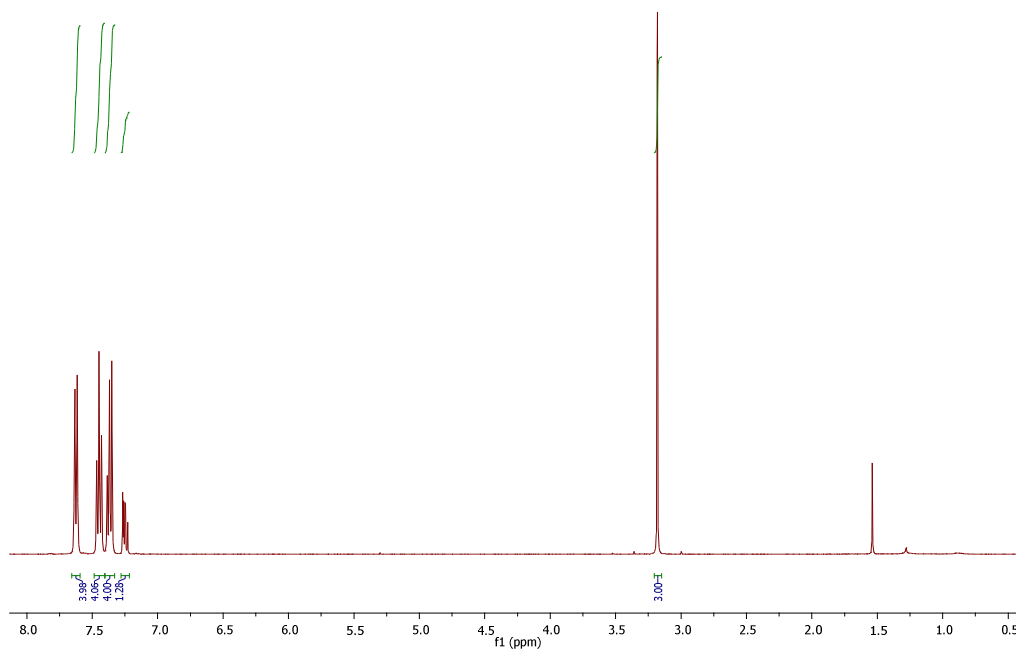
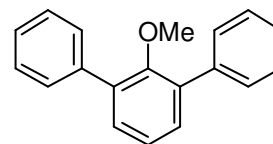
^1H NMR (400 MHz, CDCl_3 , 300K) of 1-morpholino-3,5-diphenylbenzene 70g



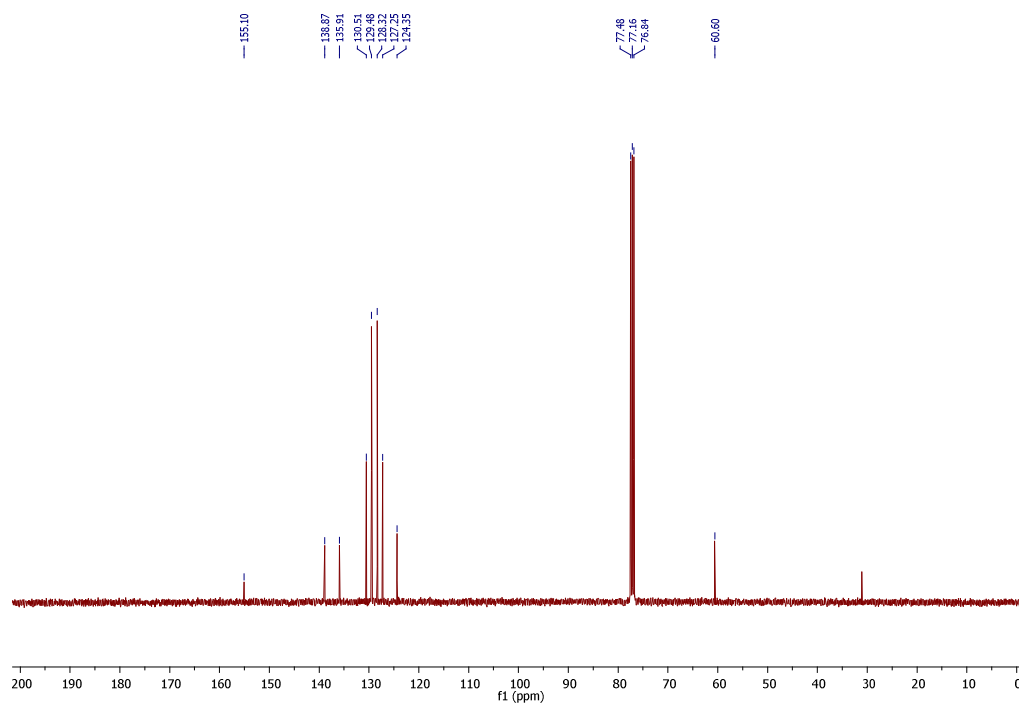
^{13}C NMR (100 MHz, CDCl_3 , 300K) of 1-morpholino-3,5-diphenylbenzene 70g



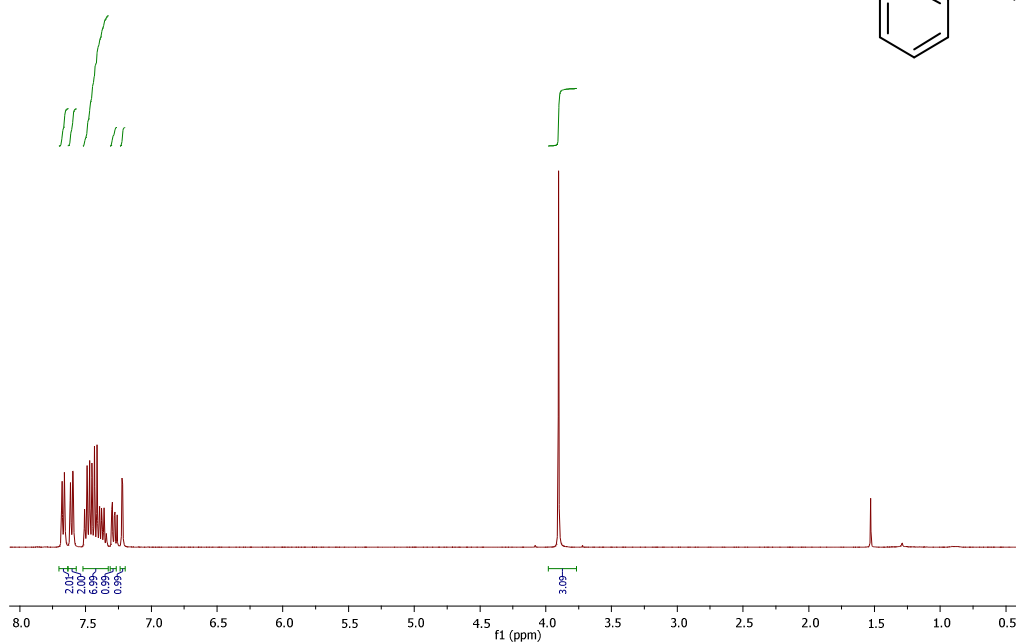
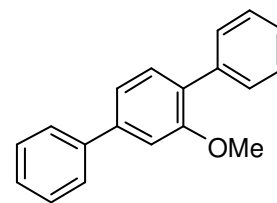
^1H NMR (400 MHz, CDCl_3 , 300K) of 2,6-diphenylanisole 70i



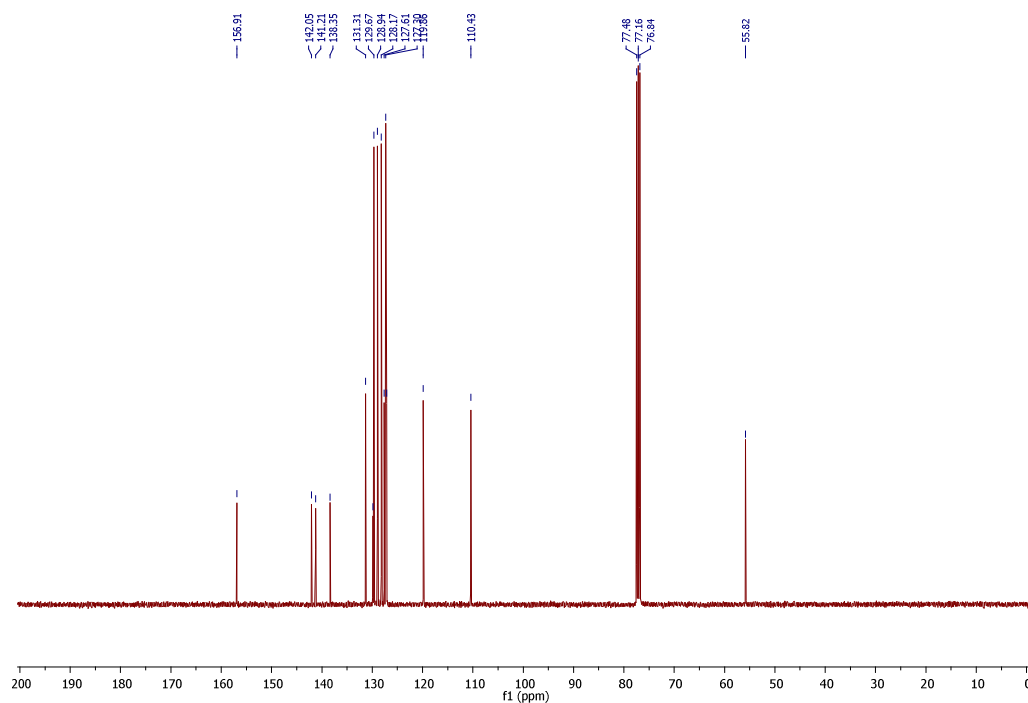
^{13}C NMR (100 MHz, CDCl_3 , 300K) of 2,6-diphenylanisole 70i



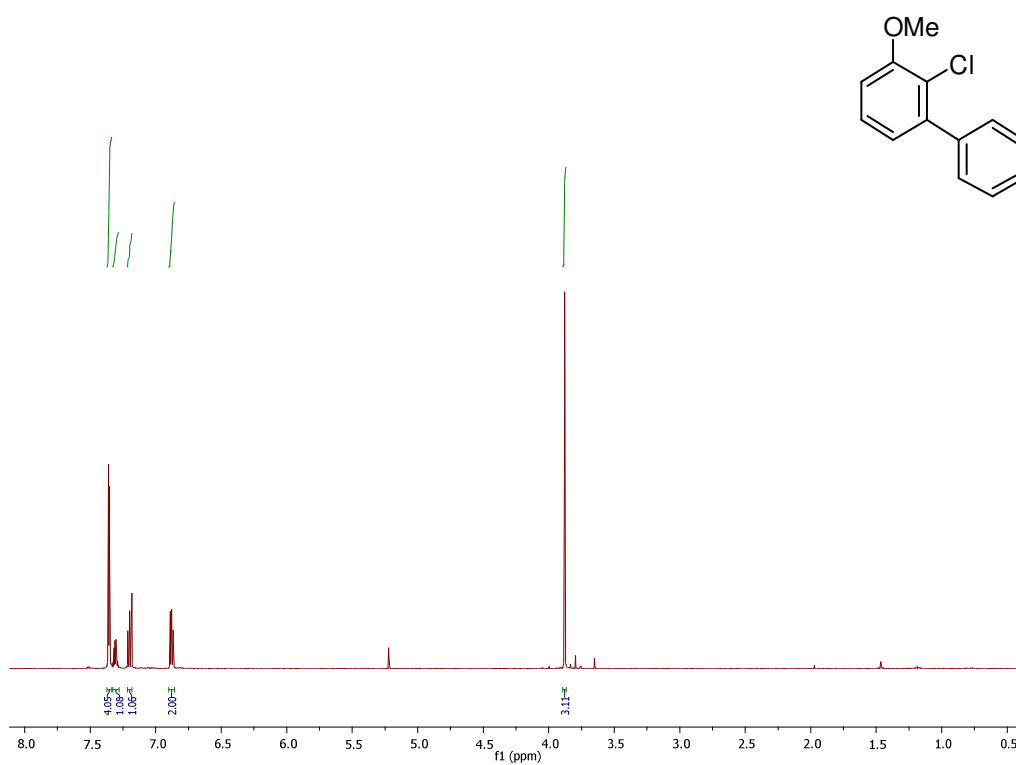
^1H NMR (400 MHz, CDCl_3 , 300K) of 2,5-diphenylanisole 70l



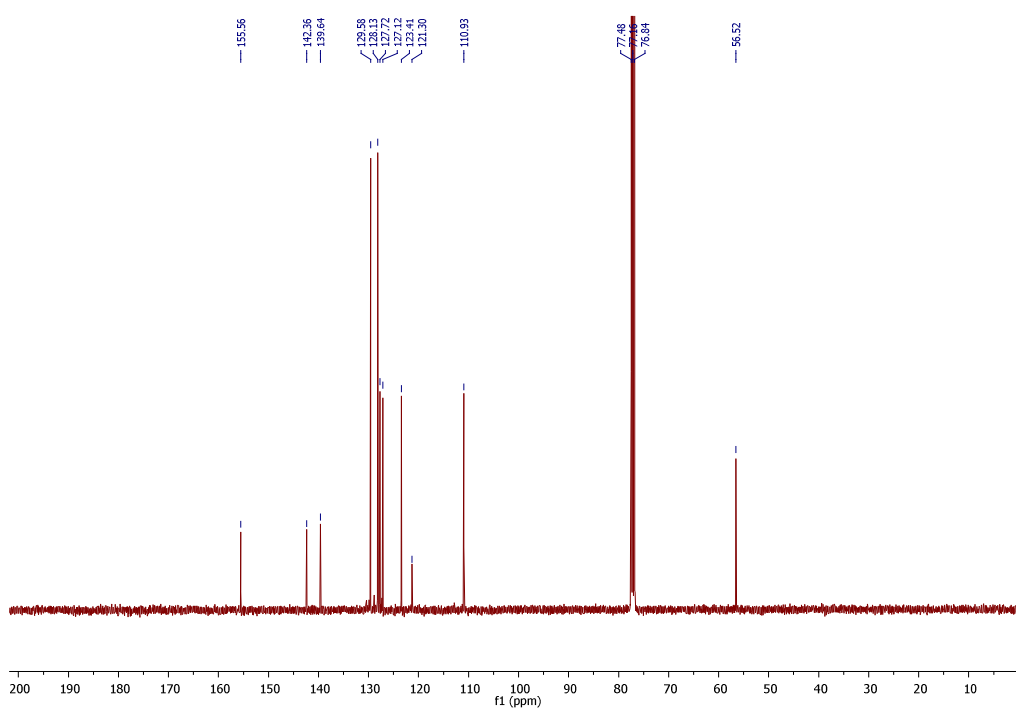
^{13}C NMR (100 MHz, CDCl_3 , 300K) of 2,5-diphenylanisole 70l



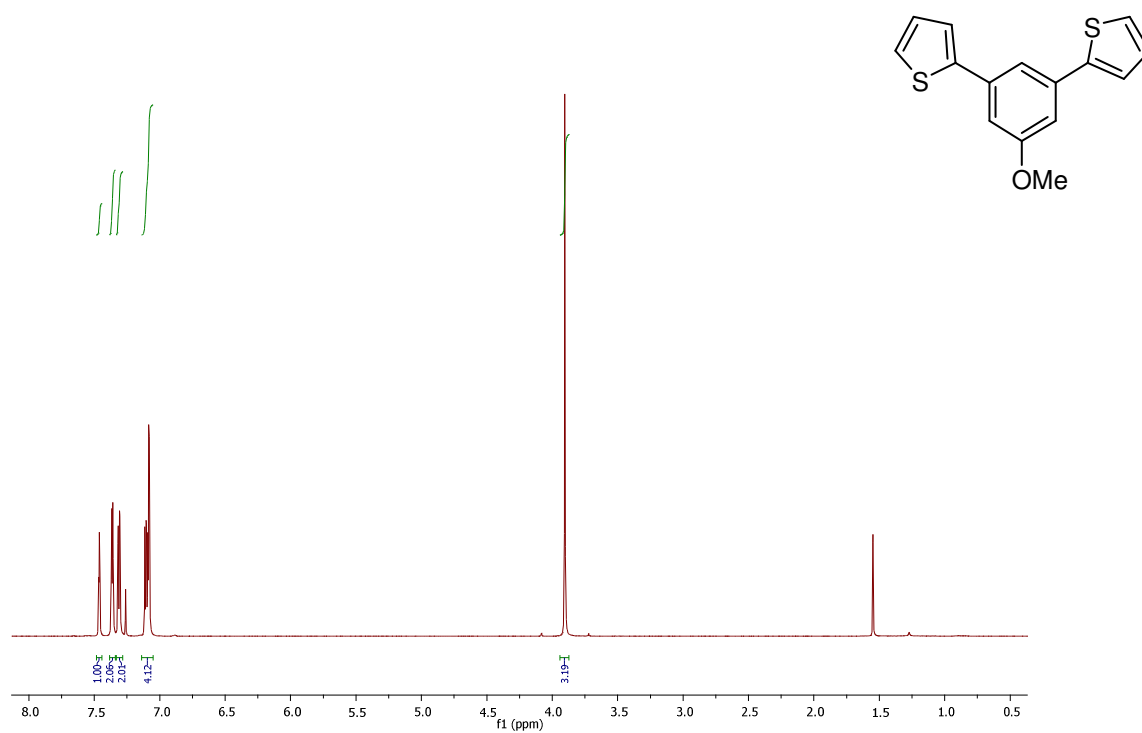
^1H NMR (400 MHz, CDCl_3 , 300K) of 2-chloro-3-methoxybiphenyl 69m



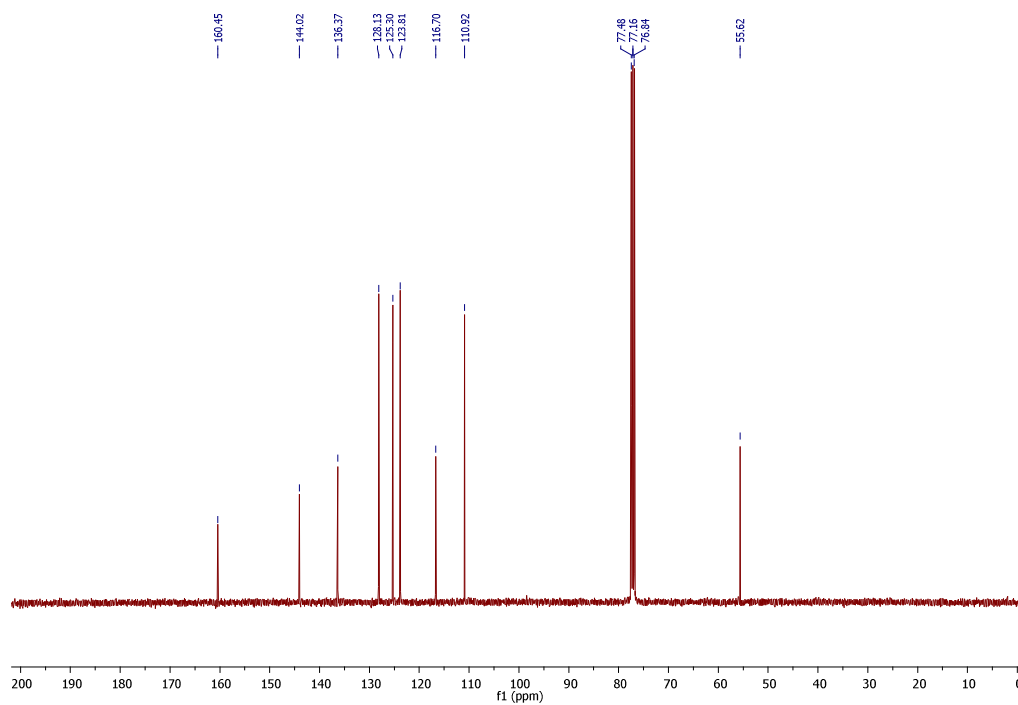
^{13}C NMR (100 MHz, CDCl_3 , 300K) of 2-chloro-3-methoxybiphenyl 69m



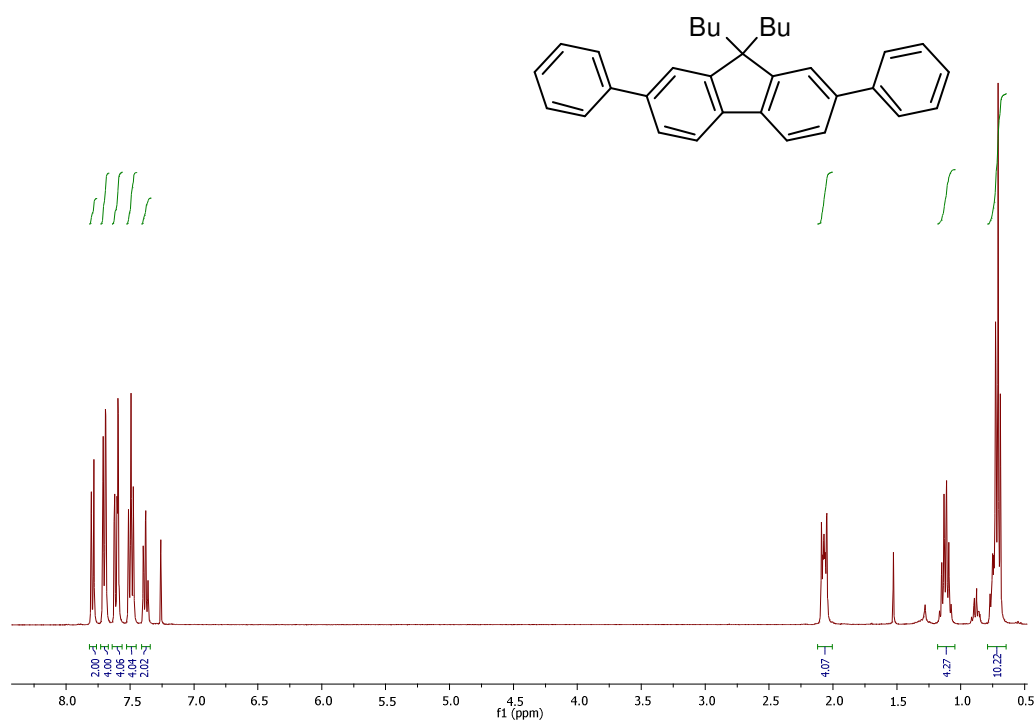
^1H NMR (400 MHz, CDCl_3 , 300K) of 3,5-di(2-thienyl)anisole 70t



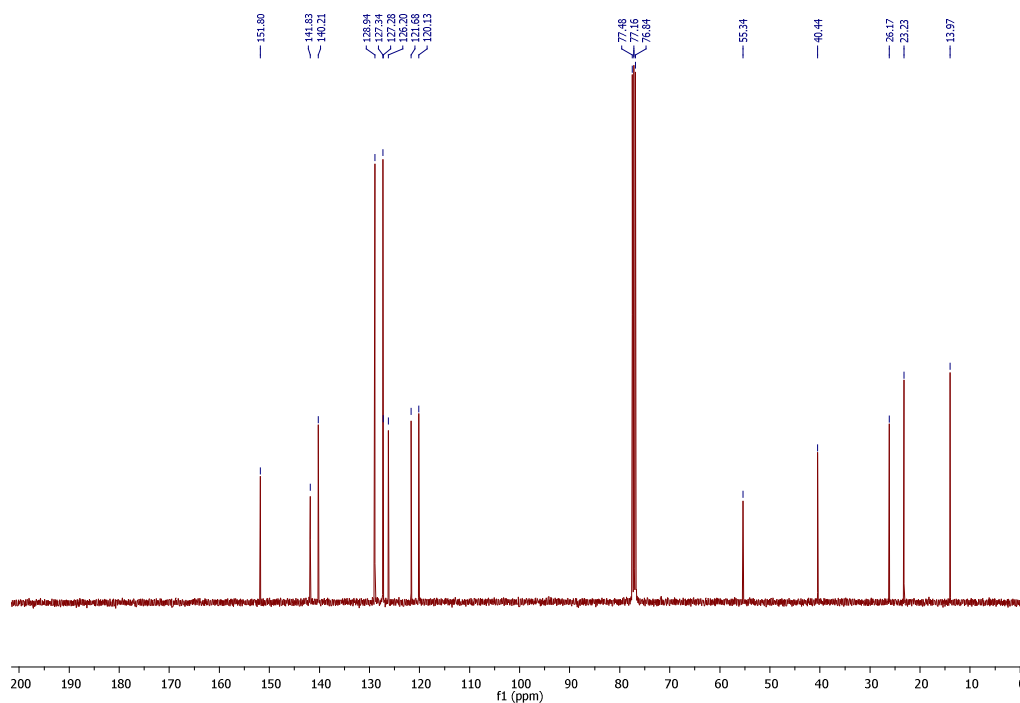
^{13}C NMR (100 MHz, CDCl_3 , 300K) of 3,5-di(2-thienyl)anisole 70t



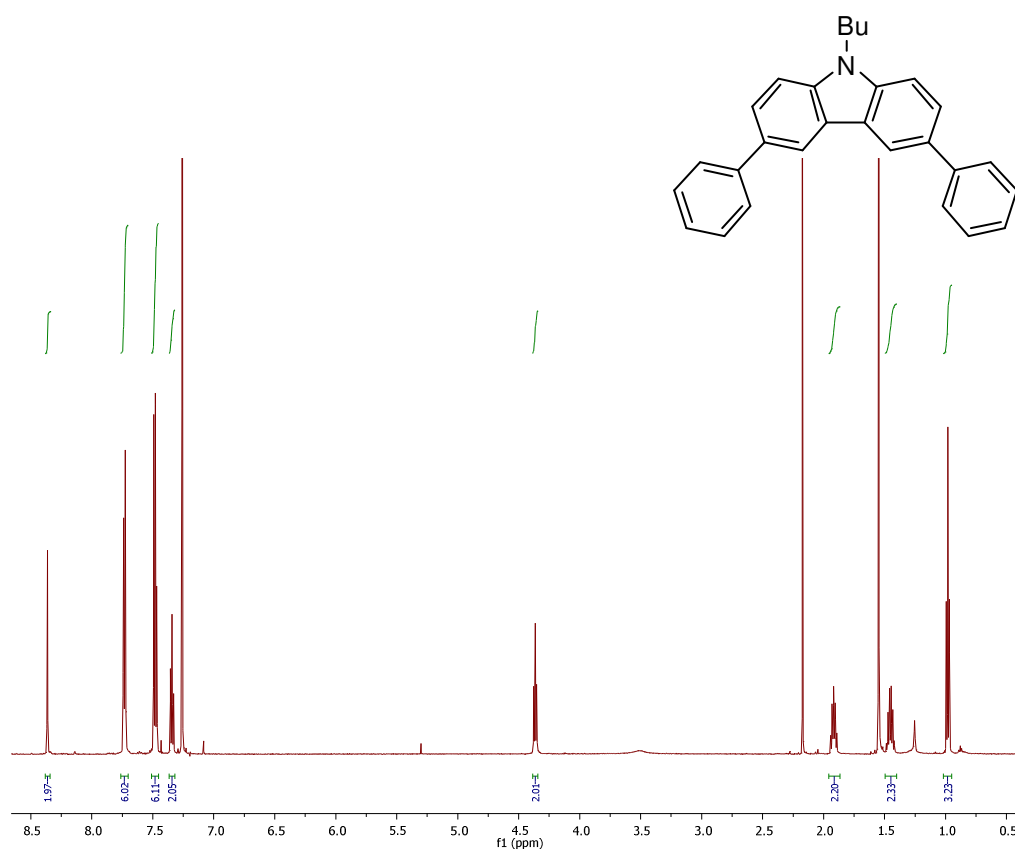
^1H NMR (400 MHz, CDCl_3 , 300K) of 2,7-bis(phenylene)-9,9-dibutylfluorene70x



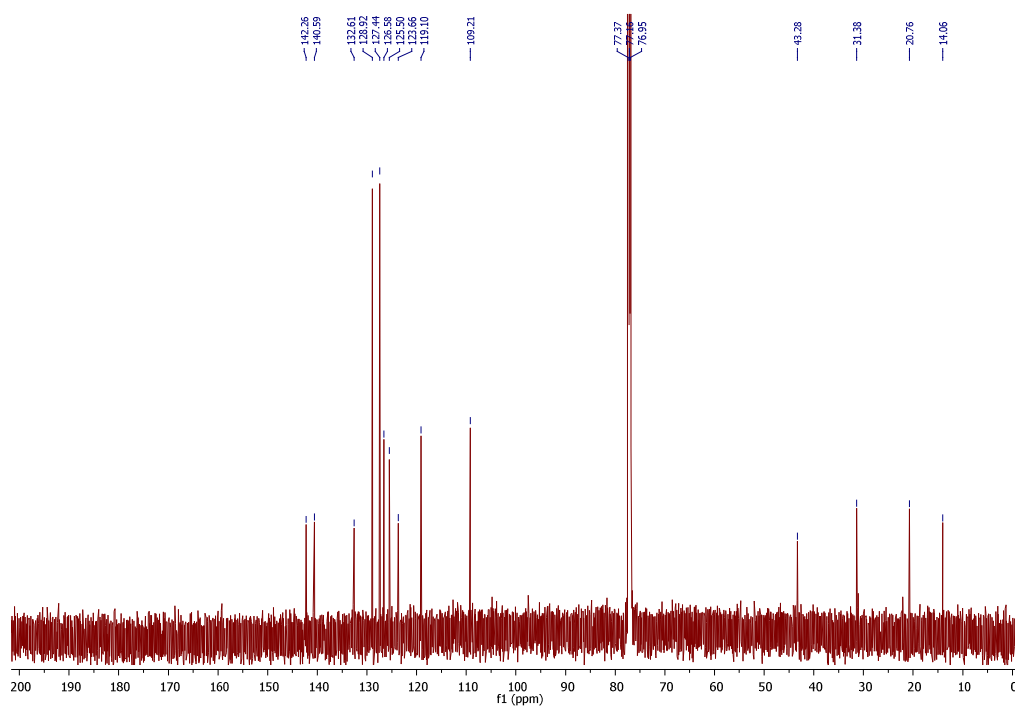
^{13}C NMR (100 MHz, CDCl_3 , 300K) of 2,7-bis(phenylene)-9,9-dibutylfluorene 70x



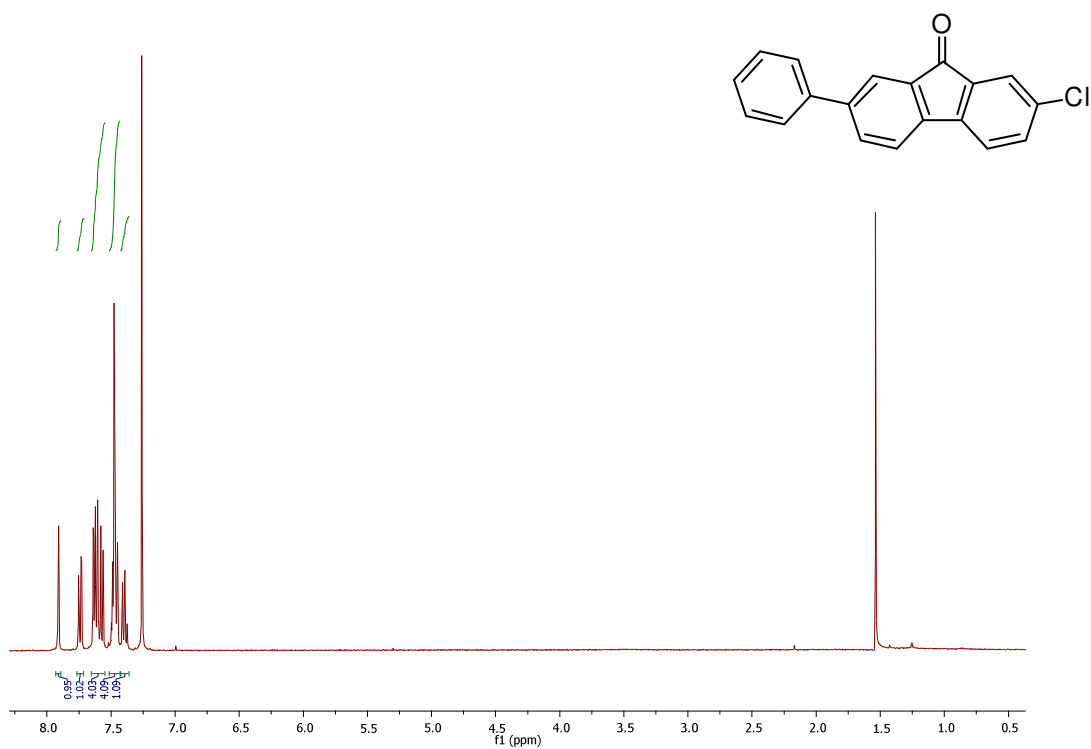
^1H NMR (400 MHz, CDCl_3 , 300K) of 3,6-diphenyl-9-butylcarbazole 70y



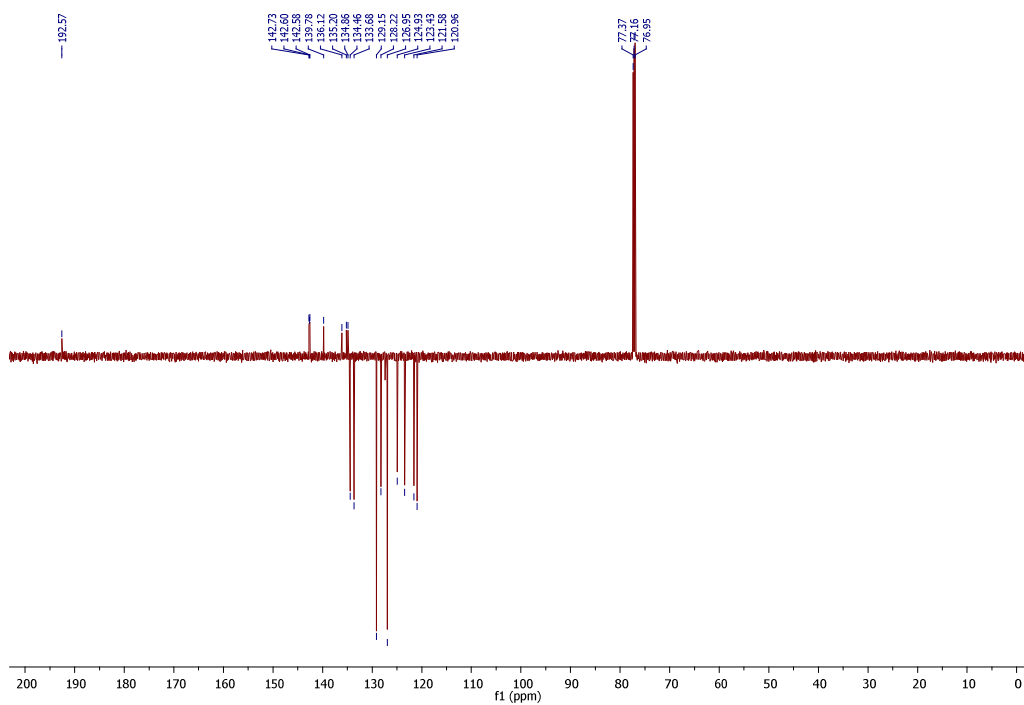
^{13}C NMR (100 MHz, CDCl_3 , 300K) of 3,6-diphenyl-9-butylcarbazole 70y



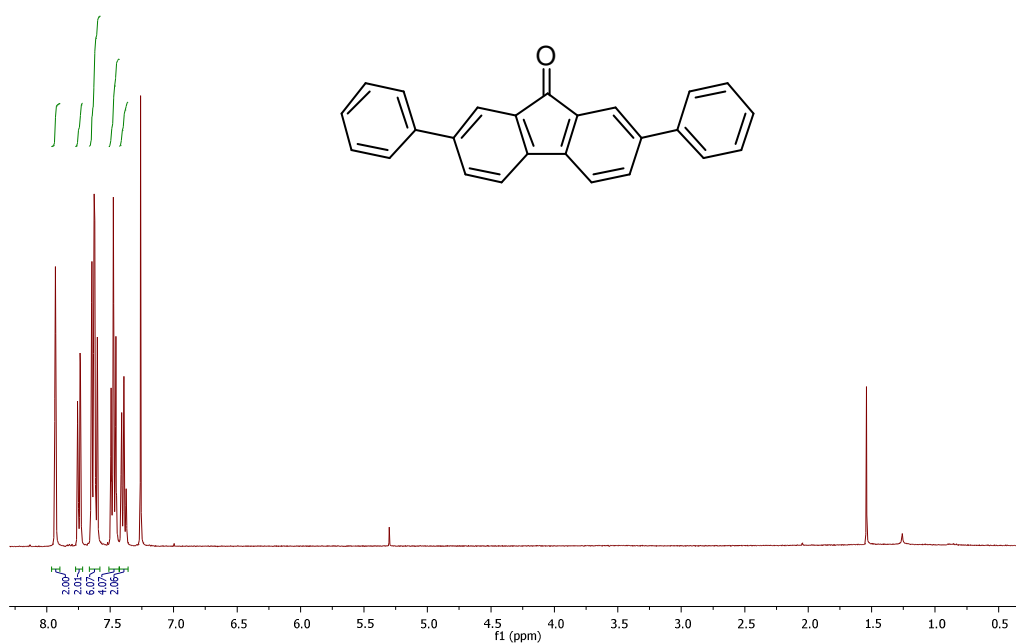
^1H NMR (400 MHz, CDCl_3 , 300K) of 2-chloro-7-phenylfluorone 69z



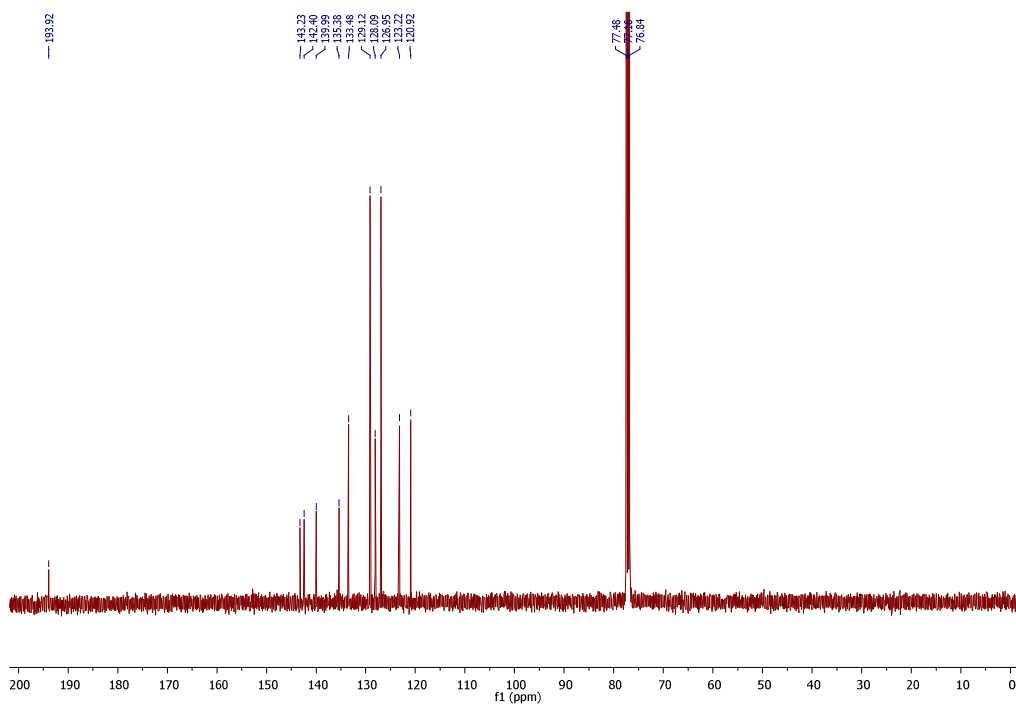
^{13}C NMR (100 MHz, CDCl_3 , 300K) of 2-chloro-7-phenylfluorone 69z



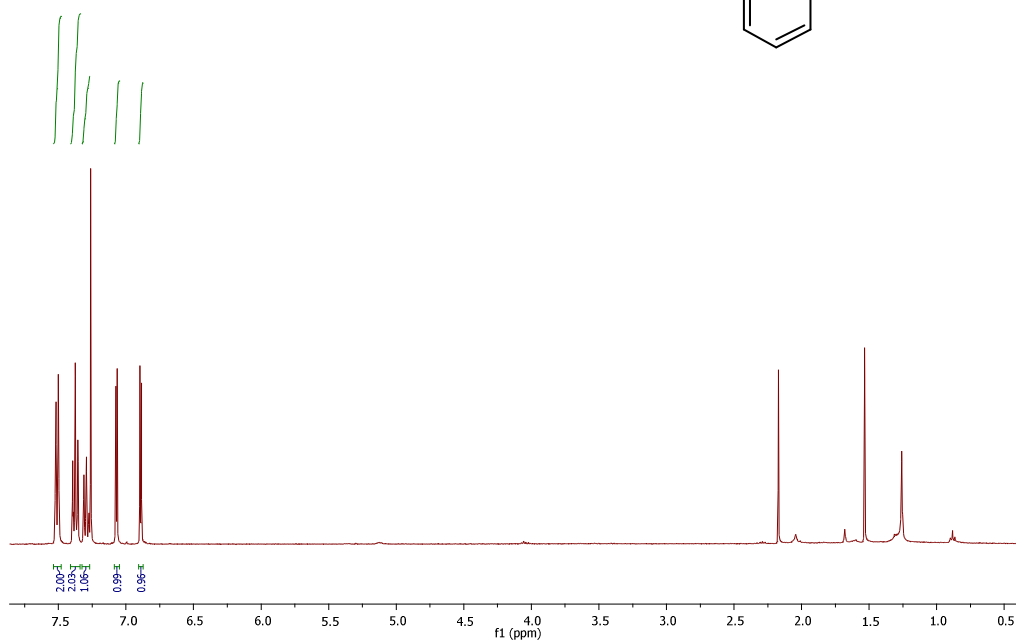
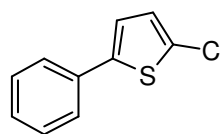
^1H NMR (400 MHz, CDCl_3 , 300K) of 2,7-diphenylfluornone 70z



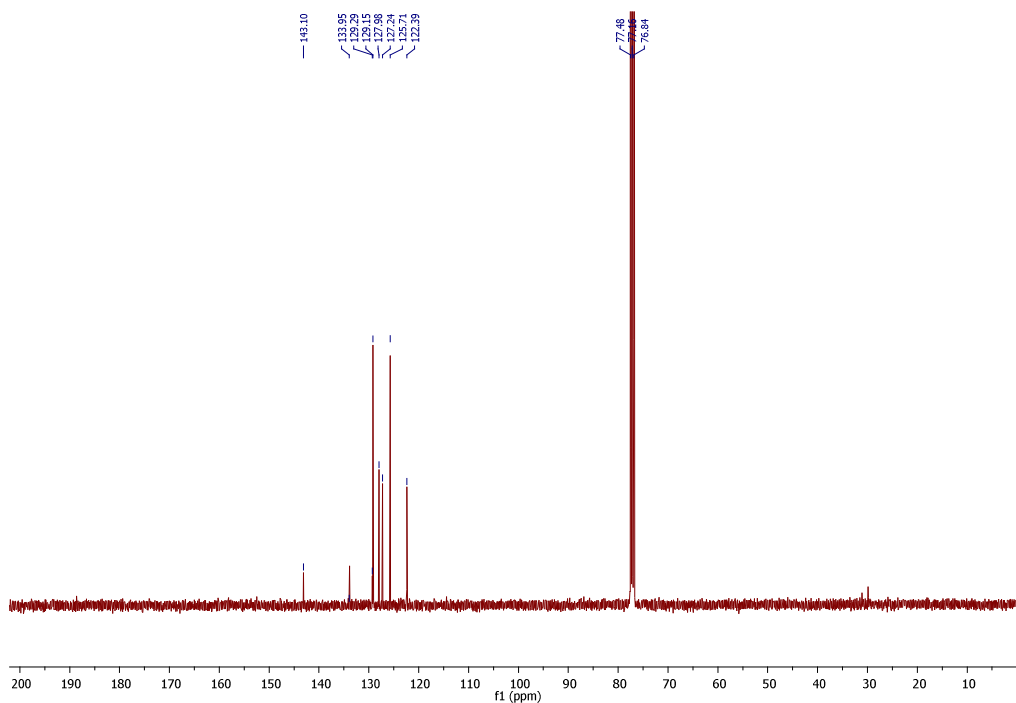
^{13}C NMR (100 MHz, CDCl_3 , 300K) of 2,7-diphenylfluornone 70z



^1H NMR (400 MHz, CDCl_3 , 300K) of 2-chloro-5-phenylthiophene 70aa



^{13}C NMR (100 MHz, CDCl_3 , 300K) of 2-chloro-5-phenylthiophene 70aa

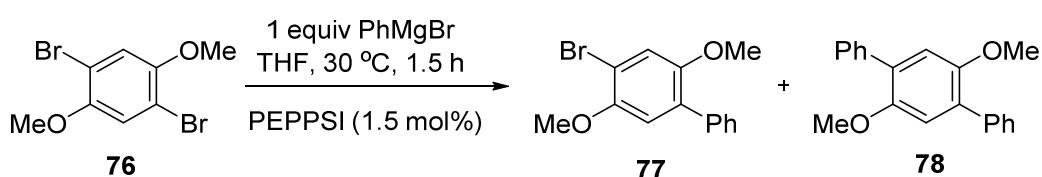


6.5 Chapter 5 Experimental

6.5.1 General Remarks

Compounds 1,4-dibromo-2,5-dihexyloxybenzene **73**, 1-bromo-2,5-dihexyloxybenzene **75**, and (4-bromo-2,5-dihexyloxyphenyl)boronic acid **79** were all synthesized in accordance with the literature.¹⁵³

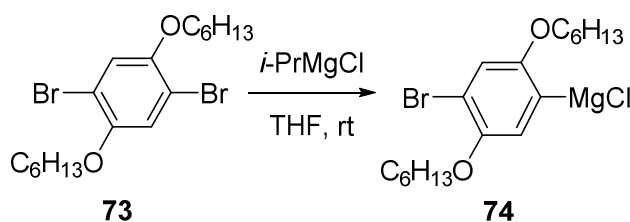
6.5.2. Coupling of PhMgBr and di bromide **76** mediated by PEPPSI precatalysts



A CEM microwave vial was charged with the desired PEPPSI precatalyst (3.75 μmol) and 1,4-dibromo-2,5-bis(methoxy)benzene (**76**, 74 mg, 0.25 mmol). The vial was sealed, flushed with N_2 , THF (2.25 mL) was added and the solution was stirred at 30 °C. PhMgBr (1.0 M in THF, 0.25 mL, 0.25 mmol) was added and the resultant solution was stirred for 1.5 h at 30 °C. Mesitylene was added as an internal standard (0.50 M in CDCl_3 , 0.50 mL, 0.25 mmol), and the crude reaction mixture was analyzed by GC-MS and ^1H NMR.

6.5.3 Kumada polymerization procedures

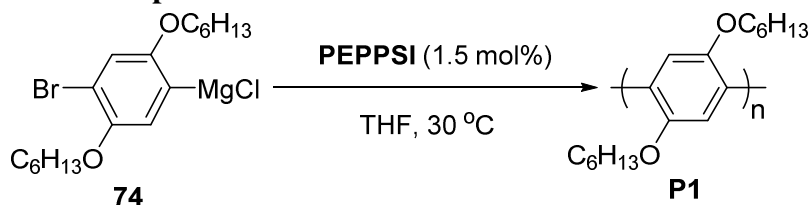
6.5.3.1. Monomer synthesis procedures



McNeil's procedure:⁸⁸ 1,4-dibromo-2,5-bis(hexyloxy)benzene (**73**, 1.025 g, 2.350 mmol) was dissolved in THF (2.4 mL) in a CEM microwave vial with a stir bar under N₂. Then, *i*-PrMgCl (1.82 M, 1.17 mL, 2.12 mmol) was added via syringe and was stirred for 16 h at rt.

Optimized procedure: Under N₂, *i*-PrMgCl (1.77 M, 3.60 mL, 6.36 mmol) was added via syringe to 1,4-dibromo-2,5-bis(hexyloxy)benzene (**73**, 3.075 g, 7.05 mmol) in a CEM microwave vial with a stir bar and was stirred for 16 h at rt. Then, THF (7.1 mL) was added via syringe and was stirred for 4 h at rt.

6.5.3.2. Polymerization procedure⁸⁸



A CEM microwave vial was charged with PEPPSI-IPr (5.1 mg, 7.5 μmol), and a stir bar. The vial was sealed, flushed with N₂, and THF (3.8 mL) was added. Monomer **74** (0.430 M in THF, 1.16 mL, 0.5 mmol) was then added via syringe and stirred for 1.5 h at 30 °C. The reaction was quenched with aq. HCl (5.0 M, 10 mL), extracted with CH₂Cl₂ (3 x 10 mL), dried over MgSO₄, filtered, and the solvent was removed *in vacuo*. The resulting solid was washed with MeOH, and dried *in vacuo*. ~1 mg of the residue was dissolved in THF passed through 0.2 μm PTFE filter prior to GPC analysis.

If the whole polymerization was not quenched an aliquot (~0.25 mL) was quenched with aq. HCl (12 M, 1 mL), extracted with CH₂Cl₂ (3 x 1 mL) with gentle heating, dried over MgSO₄, filtered, and the solvent was removed *in vacuo*. The residue was redissolved in THF and passed through 0.2 μm PTFE filter for GPC analysis.

6.5.3 Kumada polymerization experiments

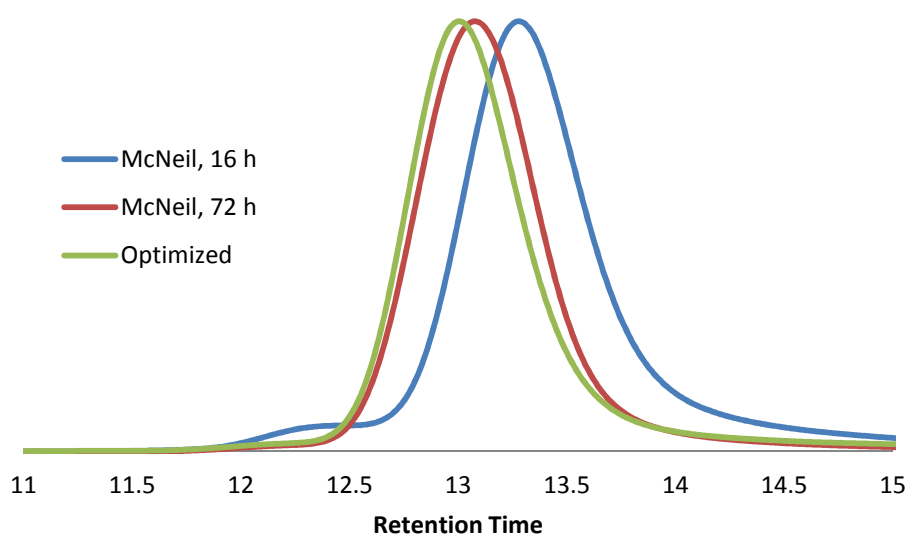
6.5.3.1 Catalyst loading scan

Using the McNeil conditions for monomer synthesis the amount of PEPPSI-IPr was varied keeping the monomer concentration constant. Monomer **74** was polymerized using the Kumada polymerization procedure.

Catalyst loading	Equiv. Monomer	M _n / kDa	PDI	Mass	Yield
1.5%	67	28.4	1.18	101 mg	73%
3.0%	34	13.3	1.13	101 mg	73%
6.0%	17	5.5	1.12	102 mg	73%

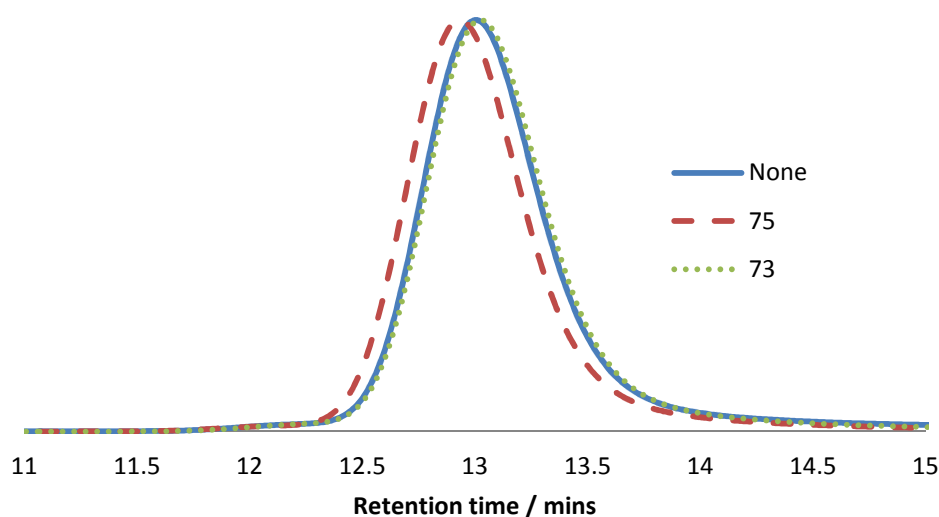
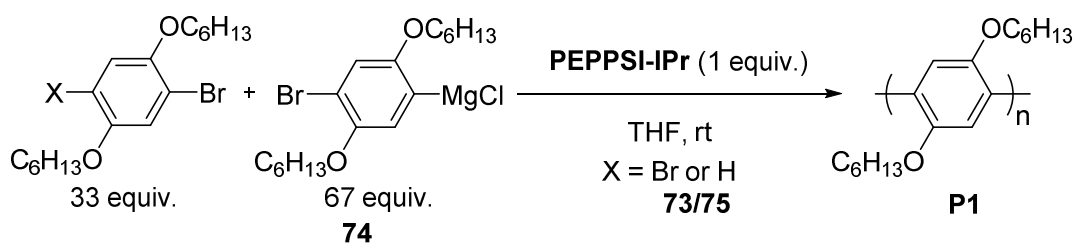
6.5.3.2 Polymerization of different monomer synthesis procedures

Using the different conditions for monomer synthesis, monomer **74** was polymerized using the Kumada polymerization procedure.



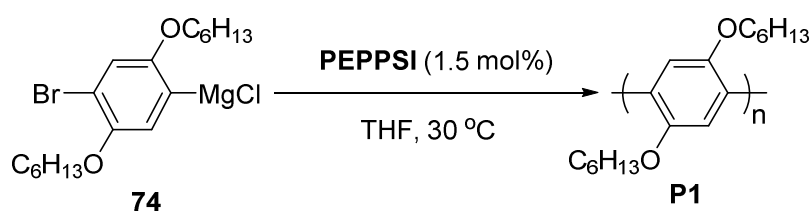
6.5.4.3 Addition of additives

Using the optimized conditions for monomer synthesis an additional 33 equivalents of dibromide **73** or impurity **75** was added to the CEM microwave vial with PEPPSI-IPr before the addition of monomer **74**.



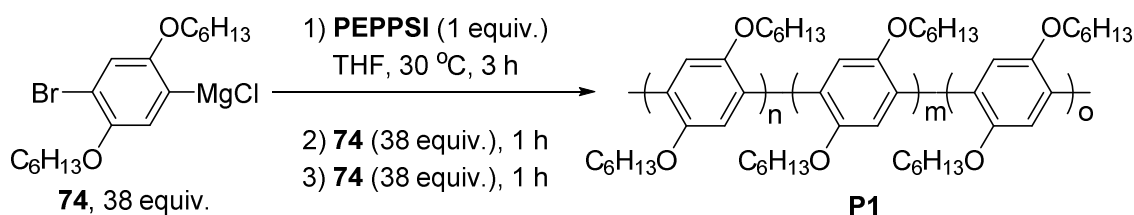
6.5.3.4 Polymerization of monomer **74** mediated by PEPPSI precatalysts

Using the optimized conditions for monomer synthesis the PEPPSI precatalysts -IMes, -IEt, -IPr and -IPent were polymerized using the Kumada polymerization procedure.



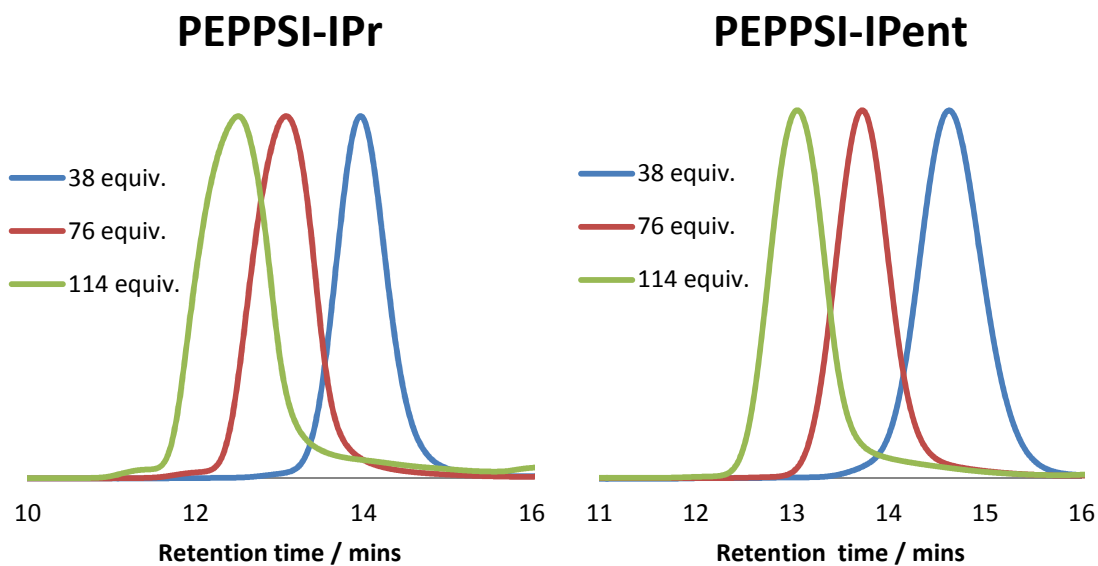
Entry	PEPPSI-	M _n / kDa	PDI	Yield
1	IMes	39.9	1.80	95%
2	IEt	40.8	1.28	96%
3	IPr	37.7	1.10	95%
4	IPent	20.2	1.08	59%

6.5.4.5 Block homo-polymerizations

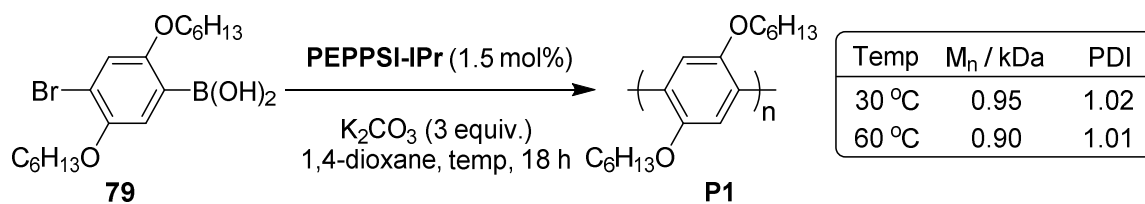


A CEM microwave vial was charged with PEPPSI-IPr (5.1 mg, 7.5 μ mol), and a stir bar. The vial was sealed, flushed with N₂, and THF (3.0 mL) was added. Monomer **74** (0.422 M in THF, 0.675 mL, 0.285 mmol, 38 equiv.) was then added via syringe and stirred for 3 h at 30 °C. After 3 h, an aliquot was withdrawn via syringe and immediately quenched with aq. HCl (12 M, 1 mL). Then, monomer **74** (0.422 M in THF, 0.675 mL, 0.285 mmol, 38 equiv.) was then added via syringe and stirred for 1 h at 30 °C. After 1 h, an aliquot was withdrawn via syringe and immediately quenched with aq. HCl (12 M, 1 mL). Then, Monomer **74** (0.422 M in THF, 0.675 mL, 0.285 mmol, 38 equiv.) was then added via syringe and stirred for 1 h at 30 °C. After 1 h, an aliquot was withdrawn via syringe and immediately quenched with aq. HCl (12 M, 1 mL). Each aliquot was then extracted with CH₂Cl₂ (3 x 1 mL) with gentle heating, dried over MgSO₄, filtered, and concentrated *in vacuo*. The residue was then dissolved in THF (~1.5 mL) with mild heating and passed through a 0.2 μ m PTFE filter for GPC analysis.

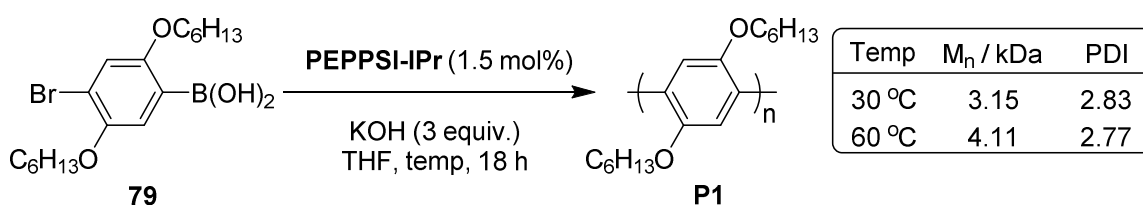
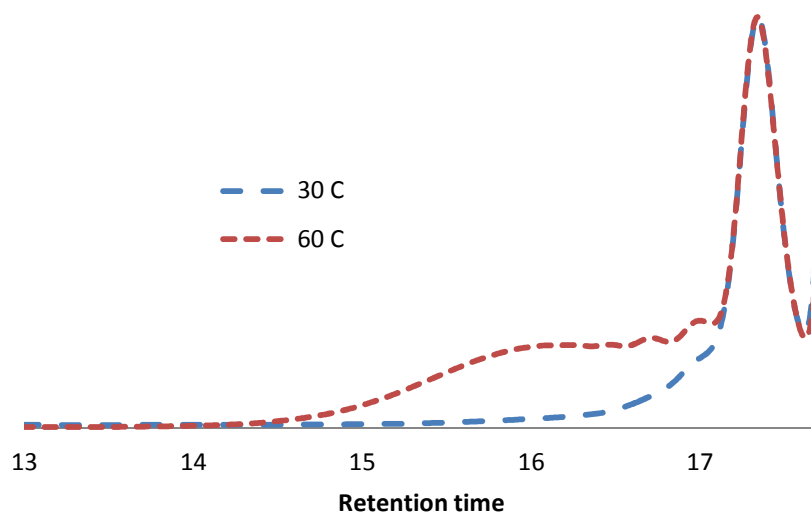
PEPPSI	Addition	Equiv. Of Monomer	M _n / kDa	M _w / kDa	PDI
IPr	1	38	17.1	18.5	1.09
IPr	2	76	38.0	42.6	1.12
IPr	3	114	57.6	70.9	1.23
IPent	1	38	9.55	10.4	1.09
IPent	2	76	21.0	22.7	1.08
IPent	3	114	35.9	40.3	1.12



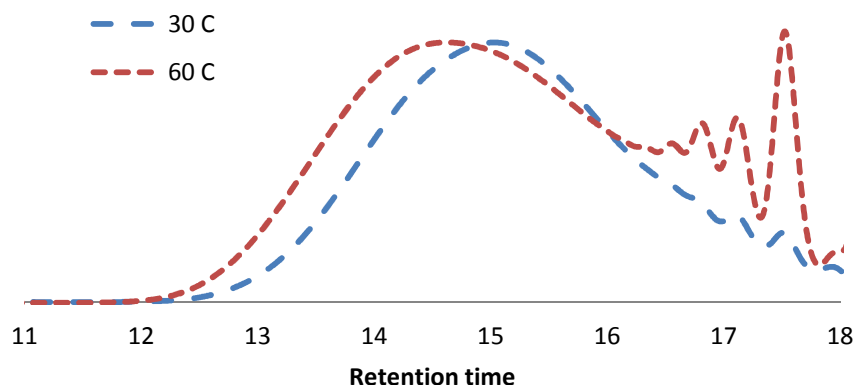
6.5.4 Suzuki polymerization procedures



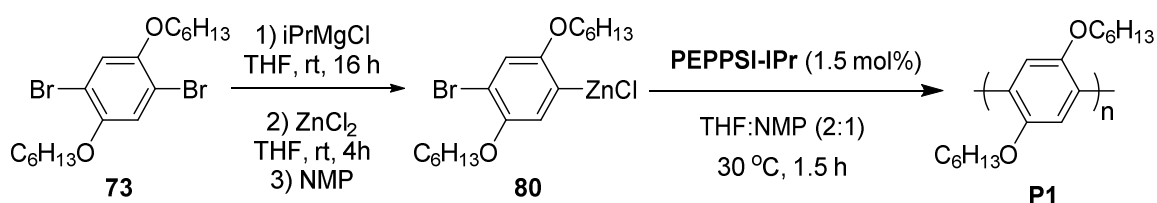
Suzuki polymerization 1: A CEM microwave vial was charged with PEPPSI-IPr (5.1 mg, 7.5 μmol), K_2CO_3 (207 mg, 1.5 mmol), monomer **79** (200 mg, 0.50 mmol) and a stir bar. The vial was sealed, flushed with N_2 , and dioxane (5.0 mL) was added and stirred for 6 h at 30 or 60°C. An aliquot (~0.25 mL) was quenched with aq. HCl (12 M, 1 mL), extracted with CH_2Cl_2 (3 x 1 mL) with mild heating, dried over MgSO_4 , filtered, and the solvent was removed *in vacuo*. The residue was redissolved in THF and passed through 0.2 μm PTFE filter for GPC analysis.



Suzuki polymerization 2: A CEM microwave vial was charged with PEPPSI-IPr (5.1 mg, 7.5 μmol), KOH (84 mg, 1.5 mmol), monomer **79** (200 mg, 0.50 mmol) and a stir bar. The vial was sealed, flushed with N_2 , and THF (5.0 mL) was added and stirred for 3 h at 30 or 60°C. An aliquot (~0.25 mL) was quenched with aq. HCl (12 M, 1 mL), extracted with CH_2Cl_2 (3 x 1 mL) with mild heating, dried over MgSO_4 , filtered, and the solvent was removed *in vacuo*. The residue was redissolved in THF and passed through 0.2 μm PTFE filter for GPC analysis.



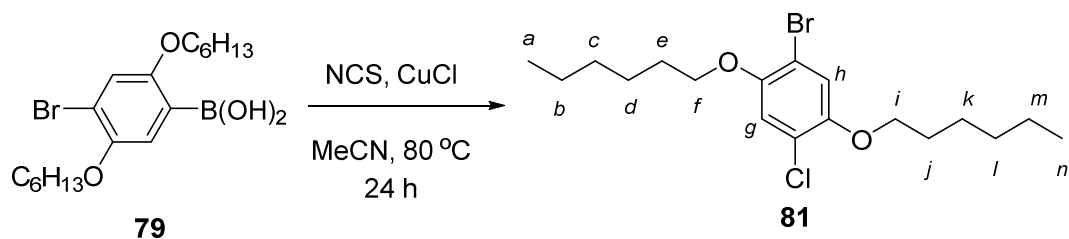
6.5.5 Negishi polymerization procedure



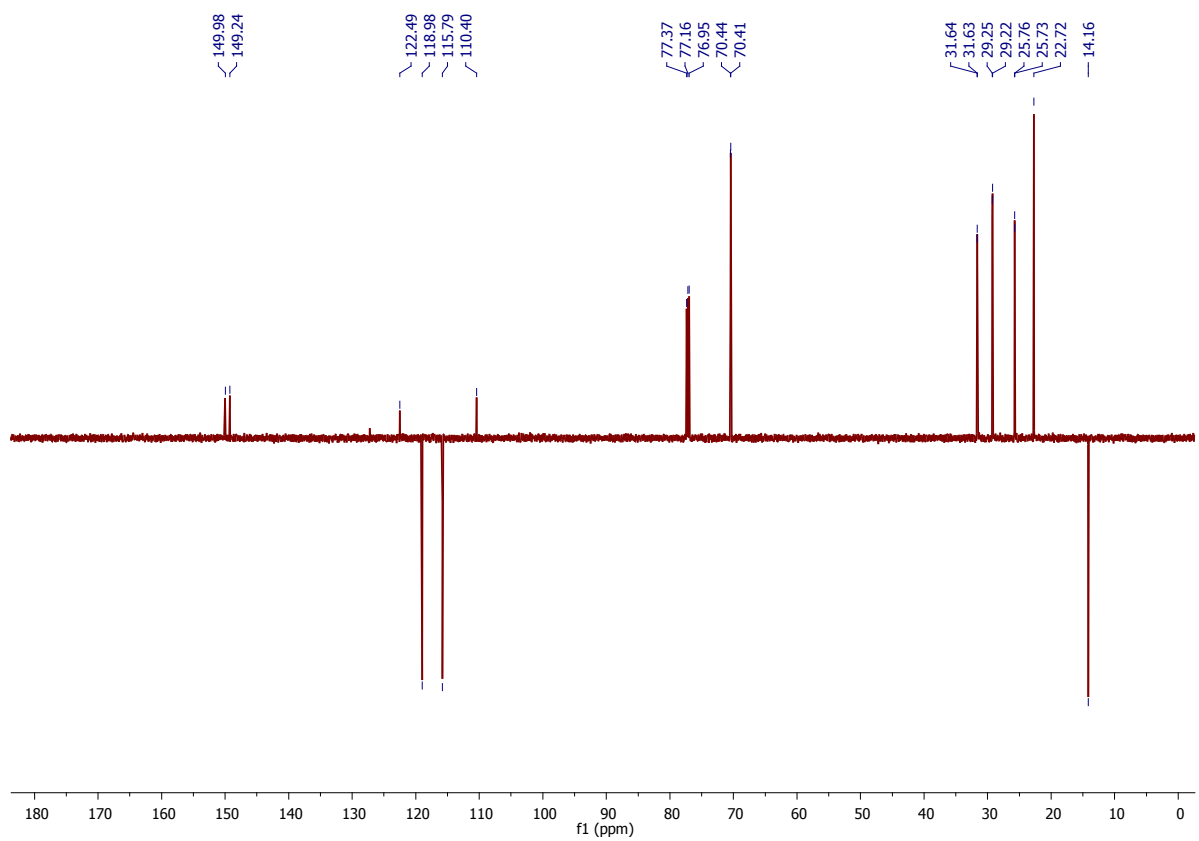
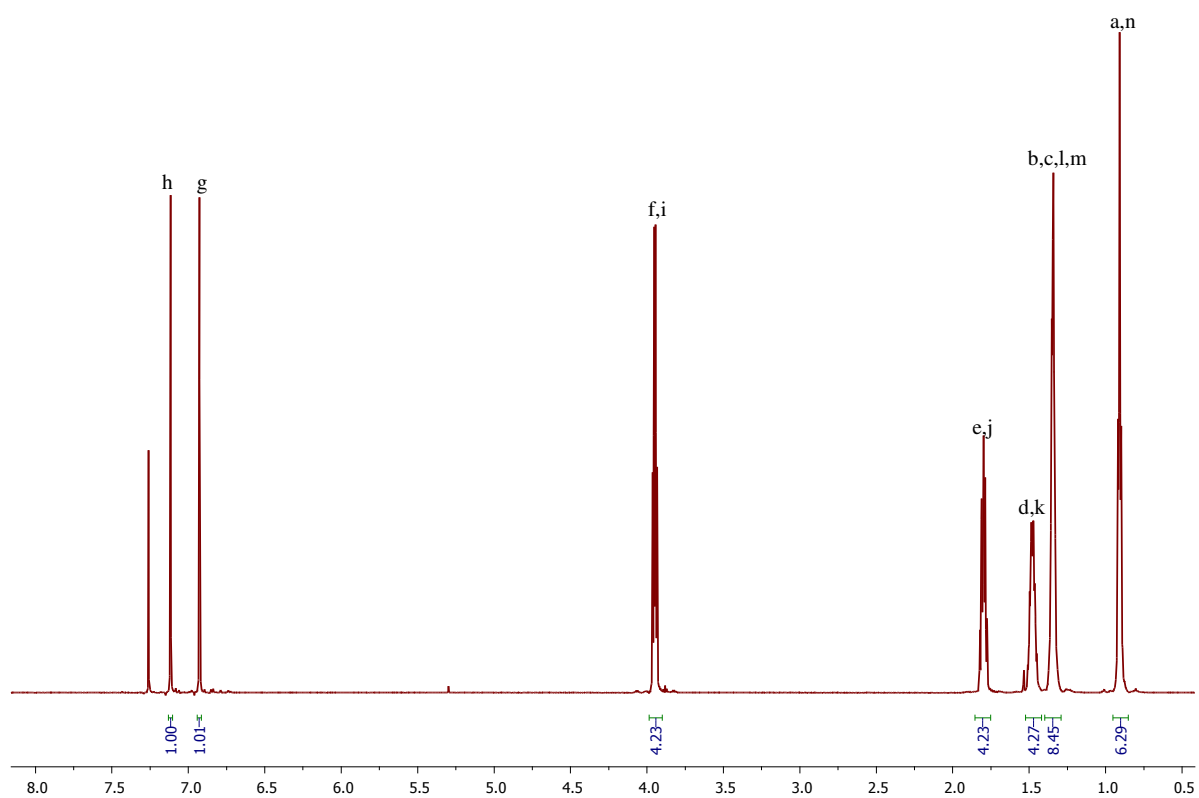
Monomer formation: *i*-PrMgCl (1.17 mL, 2.12 mmol) was added via syringe to 1,4-dibromo-2,5-bis(hexyloxy)benzene (**73**, 1.025 g, 2.35 mmol) in a CEM microwave vial with a stir bar and was stirred for 16 h at rt. ZnCl₂ (1 M in THF, 2.35 mL, 2.35 mmol) was added via syringe and was stirred for 4 h at rt. Then, NMP (3.5 mL) was added.

General procedure for Negishi couplings: A CEM microwave vial was charged with PEPPSI-IPr (5.1 mg, 7.5 μmol), and a stir bar. The vial was sealed, flushed with N₂, and THF (2.55 mL) was added. Monomer **80** (0.204 M in THF:NMP 1:1, 2.45 mL, 0.5 mmol, 67 equiv.) was then added via syringe and stirred for 1.5 h at 30 °C. An aliquot (~0.25 mL) was quenched with aq. HCl (12 M, 1 mL), extracted with CH₂Cl₂ (3 x 1 mL) with mild heating, dried over MgSO₄, filtered, and the solvent was removed *in vacuo*. The residue was redissolved in THF and passed through 0.2 μm PTFE filter for GPC analysis.

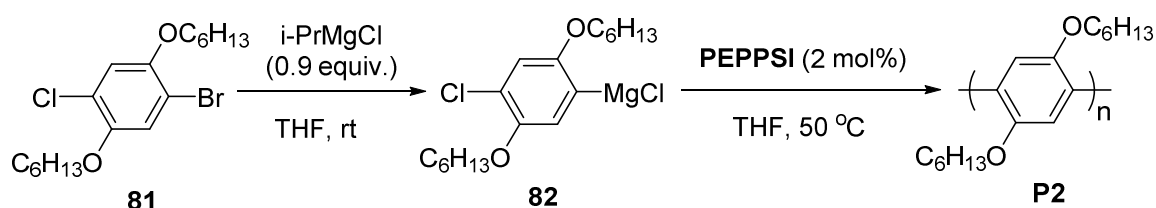
6.5.6 Synthesis of novel starting material



To a solution of 4-bromo-2,5-bis(hexyloxy)phenylboronic acid (**79**, 4.0 g, 10.0 mmol) in acetonitrile (5.0 mL) was added CuCl (0.99 g, 10.0 mmol) and *n*-chlorosuccinimide (1.34 g, 10.0 mmol). The reaction was heated at 80 °C for 24 h and then cooled to room temperature and diluted with Et₂O. The organic layer was washed with aq. HCl (1 M), aq. NaOH (1 M), and brine. The organic layer was dried over MgSO₄, filtered, and concentrated *in vacuo*. The crude product was purified by flash column chromatography using CH₂Cl₂ : petrol (1 : 1) as an eluent to give 1-bromo-4-chloro-2,5-bis(hexyloxy)benzene (**81**) as a yellow solid (3.86 g, 78% yield). **Melting point** 39-41 °C; ¹H NMR (600 MHz, CDCl₃) δ 7.12 (s, 1H, H_h), 6.93 (s, 1H, H_g), 3.95 (td, *J* = 6.5, 4.3 Hz, 4H, H_{f,i}), 1.86 – 1.75 (m, 4H, H_{e,j}), 1.55 – 1.42 (m, 4H, H_{d,k}), 1.41 – 1.27 (m, 8H, H_{b,m} and H_{c,l}), 0.93 – 0.87 (m, 6H, H_{a,n}); ¹³C NMR (151 MHz, CDCl₃) δ 150.0, 149.2, 122.5, 119.0, 115.8, 110.4, 70.4, 70.4, 31.6, 31.6, 29.3, 29.2, 25.8, 25.7, 22.7, 14.16; **HRMS (EI)** 390.0947 [M]⁺ (calc. for C₁₈H₂₈BrClO₂ 390.0961 [M]⁺).



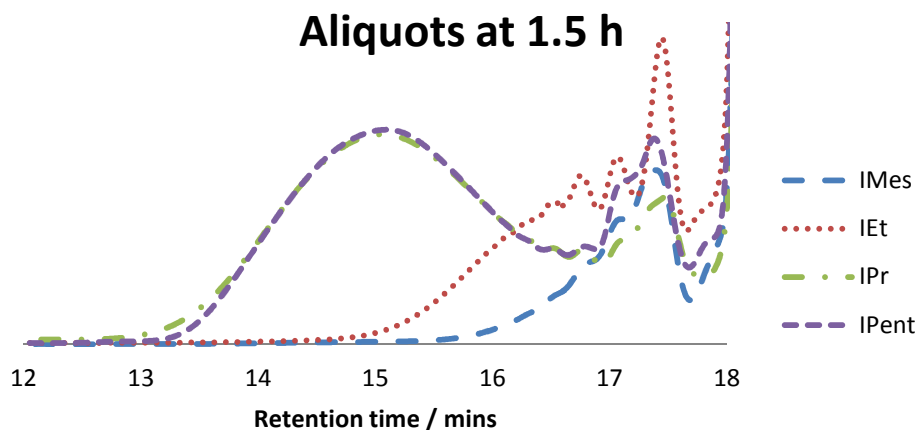
6.5.7 Chloride monomer polymerization procedure



Monomer synthesis: *i*-PrMgCl (1.17 mL, 6.36 mmol) was added via syringe to 1-bromo-4-chloro-2,5-bis(hexyloxy)benzene (**81**, 2.76 g, 7.05 mmol) in a CEM microwave vial with a stir bar and was stirred for 16 h at rt. Then, THF (7.1 mL) was added via syringe and was stirred for 4 h at rt.

Kumada polymerizations: A CEM microwave vial was charged with PEPPSI-IPr (6.8 mg, 10.0 μ mol), and a stir bar. The vial was sealed, flushed with N₂, and THF (3.8 mL) was added. Monomer **82** (0.428 M in THF, 0.5 mmol, 67 equiv.) was then added via syringe and stirred for 1.5 h at 30 °C. An aliquot at either 1.5 h or 18 h (~0.25 mL) was quenched with aq. HCl (12 M, 1 mL), extracted with CH₂Cl₂ (3 x 1 mL) with mild heating, dried over MgSO₄, filtered, and the solvent was removed *in vacuo*. The residue was redissolved in THF and passed through 0.2 μ m PTFE filter for GPC analysis.

PEPPSI	Time	M _n / Da	M _w / Da	PDI
IMes	1.5 h	1102	1271	1.15
IEt	1.5 h	1337	1810	1.35
IPr	1.5 h	4721	8902	1.89
IPr	18 h	4785	8608	1.80
IPent	1.5 h	4651	7787	1.67
IPent	18 h	4982	8822	1.77



6.6 References

- (76) Organ, M. G.; Abdel-Hadi, M.; Avola, S.; Hadei, N.; Nasielski, J.; O'Brien, C. J.; Valente, C. *Chem. Eur. J.* **2007**, *13*, 150.
- (79) Organ, M. G.; Calimsiz, S.; Sayah, M.; Hoi, K. H.; Lough, A. J. *Angew. Chemie Int. Ed.* **2009**, *48*, 2383.
- (86) Organ, M. G.; Avola, S.; Dubovyk, I.; Hadei, N.; Kantchev, E. A. B.; O'Brien, C. J.; Valente, C. *Chem. Eur. J.* **2006**, *12*, 4749.
- (91) O'Brien, C. J.; Kantchev, E. A. B.; Valente, C.; Hadei, N.; Chass, G. A.; Lough, A.; Hopkinson, A. C.; Organ, M. G. *Chem. Eur. J.* **2006**, *12*, 4743.
- (99) Liu, C.-Y.; Knochel, P. *Org. Lett.* **2005**, *7*, 2543.
- (100) Wang, Q.; Qu, D.-H.; Ren, J.; Chen, K.; Tian, H. *Angew. Chemie Int. Ed.* **2004**, *43*, 2661.
- (102) Meiries, S.; Le Duc, G.; Chartoire, A.; Collado, A.; Speck, K.; Athukorala Arachchige, K. S.; Slawin, A. M. Z.; Nolan, S. P. *Chem. Eur. J.* **2013**, *19*, 17358.
- (104) Wu, H.; Hynes, J. *Org. Lett.* **2010**, *12*, 1192.
- (105) Huo, S. *Org. Lett.* **2003**, *5*, 423.
- (106) Krasovskiy, A.; Knochel, P. *Synthesis* **2006**, 0890.
- (107) Marvel, C. S.; Overberger, C. G.; Allen, R. E.; Johnston, H. W.; Saunders, J. H.; Young, J. D. *J. Am. Chem. Soc.* **1946**, *68*, 861.

- (108) Bolli, M. H.; Marfurt, J.; Grisostomi, C.; Boss, C.; Binkert, C.; Hess, P.; Treiber, A.; Thorin, E.; Morrison, K.; Buchmann, S.; Bur, D.; Ramuz, H.; Clozel, M.; Fischli, W.; Weller, T. *J. Med. Chem.* **2004**, *47*, 2776.
- (109) Tamao, K.; Sumitani, K.; Kiso, Y.; Zembayashi, M.; Fujioka, A.; Kodama, S.; Nakajima, I.; Minato, A.; Kumada, M. *Bull. Chem. Soc. Jpn.* **1976**, *49*, 1958.
- (110) Murphy, J. M.; Liao, X.; Hartwig, J. F. *J. Am. Chem. Soc.* **2007**, *129*, 15434.
- (111) Day, G. M.; Howell, O. T.; Metzler, M. R.; Woodgate, P. D. *Aust. J. Chem.* **1997**, *50*, 425.
- (112) Trost, B. M.; Pissot-Soldermann, C.; Chen, I. *Chem. Eur. J.* **2005**, *11*, 951.
- (113) Bugarin, A.; Connell, B. T. *Chem. Commun.* **2011**, *47*, 7218.
- (114) Yu, Z.; Lv, Y.; Yu, C.; Su, W. *Tetrahedron Lett.* **2013**, *54*, 1261.
- (115) Onodera, G.; Matsuzawa, M.; Aizawa, T.; Kitahara, T.; Shimizu, Y.; Kezuka, S.; Takeuchi, R. *Synlett* **2008**, 755.
- (116) DeCosta, D.; Pincock, J. *J. Org. Chem.* **2002**, *67*, 9484.
- (117) Shu, Z.; Ye, Y.; Deng, Y.; Zhang, Y.; Wang, J. *Angew. Chemie Int. Ed.* **2013**, *52*, 10573.
- (118) Cadierno, V.; García-Garrido, S. E.; Gimeno, J. *J. Am. Chem. Soc.* **2006**, *128*, 15094.
- (119) Cadogan, J. I. G.; Kulik, S. *J. Chem. Soc. C Org.* **1971**, 2621.
- (120) Nakamura, H.; Tomonaga, Y.; Miyata, K.; Uchida, M.; Terao, Y. *Environ. Sci. Technol.* **2007**, *41*, 2190.
- (121) Chartoire, A.; Frogneux, X.; Boreux, A.; Slawin, A. M. Z.; Nolan, S. P. *Organometallics* **2012**, *31*, 6947.
- (122) Li, J.-H.; Liu, W.-J. *Org. Lett.* **2004**, *6*, 2809.
- (123) Basak, S.; Hui, P.; Boodida, S.; Chandrasekar, R. *J. Org. Chem.* **2012**, *77*, 3620.
- (124) Jin, Z.; Li, Y.-J.; Ma, Y.-Q.; Qiu, L.-L.; Fang, J.-X. *Chem. Eur. J.* **2012**, *18*, 446.
- (125) Antoft-Finch, A.; Blackburn, T.; Snieckus, V. *J. Am. Chem. Soc.* **2009**, *131*, 17750.
- (126) Dötz, F.; Brand, J. D.; Ito, S.; Gherghel, L.; Müllen, K. *J. Am. Chem. Soc.* **2000**, *122*, 7707.
- (127) Naka, K.; Sadownik, A.; Regen, S. L. *J. Am. Chem. Soc.* **1993**, *115*, 2278.

- (128) Kuchurov, I. V.; Vasil'ev, A. A.; Zlotin, S. G. *Mendeleev Commun.* **2010**, 20, 140.
- (129) Deckert-Gaudig, T.; Hünig, S.; Dormann, E.; Kelemen, M. T. *Euro. J. Org. Chem.* **2001**, 1563.
- (130) Xu, X.-H.; Azuma, A.; Kusuda, A.; Tokunaga, E.; Shibata, N. *Euro. J. Org. Chem.* **2012**, 1504.
- (131) Hatakeyama, T.; Hashimoto, S.; Ishizuka, K.; Nakamura, M. *J. Am. Chem. Soc.* **2009**, 131, 11949.
- (132) Xie, L.-G.; Wang, Z.-X. *Angew. Chemie Int. Ed.* **2011**, 50, 4901.
- (133) Chaumeil, H.; Drian, C. Le; Defoin, A. *Synthesis* **2002**, 757.
- (134) Kuhl, N.; Hopkinson, M. N.; Glorius, F. *Angew. Chemie Int. Ed.* **2012**, 51, 8230.
- (135) Bolliger, J. L.; Frech, C. M. *Adv. Synth. Catal.* **2010**, 352, 1075.
- (136) Lois, S.; Florès, J.-C.; Lère-Porte, J.-P.; Serein-Spirau, F.; Moreau, J. J. E.; Miqueu, K.; Sotiropoulos, J.-M.; Baylère, P.; Tillard, M.; Belin, C. *Euro. J. Org. Chem.* **2007**, 4019.
- (137) Desmarets, C.; Schneider, R.; Fort, Y. *Tetrahedron* **2001**, 57, 7657.
- (138) Meng, H.; Perepichka, D. F.; Bendikov, M.; Wudl, F.; Pan, G. Z.; Yu, W.; Dong, W.; Brown, S. *J. Am. Chem. Soc.* **2003**, 125, 15151.
- (139) Ullah, E.; McNulty, J.; Robertson, A. *Euro. J. Org. Chem.* **2012**, 2127.
- (140) Fan, X.-H.; Yang, L.-M. *Euro. J. Org. Chem.* **2011**, 1467.
- (141) Fan, X.-H.; Yang, L.-M. *Euro. J. Org. Chem.* **2010**, 2457.
- (142) Rajakumar, P.; Ganesan, K. *Synth. Commun.* **2004**, 34, 2009.
- (143) Basu, B.; Das, S.; Das, P.; Mandal, B.; Banerjee, D.; Almqvist, F. *Synthesis* **2009**, 1137.
- (144) Ishibe, N.; Hashimoto, K.; Sunami, M. *J. Org. Chem.* **1974**, 39, 103.
- (145) Xie, L.-G.; Wang, Z.-X. *Chem. Eur. J.* **2011**, 17, 4972.
- (146) Mejías, N.; Pleixats, R.; Shafir, A.; Medio-Simón, M.; Asensio, G. *Euro. J. Org. Chem.* **2010**, 5090.
- (147) Kamata, M.; Satoh, C.; Kim, H.-S.; Wataya, Y. *Tetrahedron Lett.* **2002**, 43, 8313.
- (148) Rao, M.; Banerjee, D.; Dhanorkar, R. *Synlett* **2011**, 1324.

- (149) Nakabayashi, K.; Higashihara, T.; Ueda, M. *Macromolecules* **2011**, *44*, 1603.
- (150) Alt, H. G.; Zenk, R. *J. Organomet. Chem.* **1996**, *522*, 39.
- (151) Moy, C. L.; Kaliappan, R.; McNeil, A. J. *J. Org. Chem.* **2011**, *76*, 8501.